Archaeological and Anthropological Sciences (2022) 14:17
https://doi.org/10.1007/s12520-021-01407-z

REVIEW

Pigments—Lead-based whites, reds, yellows and oranges and their alteration phases

Elisabetta Gliozzo[1] · Corina Ionescu[2]

Received: 31 January 2021 / Accepted: 30 June 2021

Abstract

This review summarises the state-of-the-art of lead-based pigment studies, addressing their production, trade, use and possible alteration. Other issues, such as those related to the investigation and protection of artworks bearing lead-based pigments are also presented. The focus is mineralogical, as both raw materials and degradation products are mineral phases occurring in nature (except for very few cases). The minerals described are abellaite, anglesite, blixite, caledonite, challacolloite, cerussite, cotunnite, crocoite, galena, grootfonteinite, hydrocerussite, laurionite, leadhillite, litharge, macphersonite, massicot, mimetite, minium, palmierite, phosgenite, plattnerite, plumbonacrite, schulténite, scrutinyite, somersetite, susannite, vanadinite and an unnamed phase ($PbMg(CO_3)_2$). The pigments discussed are lead white, red lead, litharge, massicot, lead-tin yellow, lead-tin-antimony yellow, lead-chromate yellow and Naples yellow. An attempt is made to describe the history, technology and alteration of these pigments in the most complete manner possible, despite the topic's evident breadth. Finally, an insight into the analytical methods that can (and should) be used for accurate archaeometric investigations and a summary of key concepts conclude this review, along with a further list of references for use as a starting point for further research.

Keywords Lead-based pigments · Cerussite-hydrocerussite-minium · Lead-tin and Naples yellow · Lead chromates · Pigments and degradation products · Archaeometry and archaeology

Premise

This Topical Collection (TC) covers several topics in the field of study, in which ancient architecture, art history, archaeology and material analyses intersect. The chosen perspective is that of a multidisciplinary scenario, capable of combining, integrating and solving the research issues raised by the study of mortars, plasters and pigments (Gliozzo et al. 2021).

The first group of contributions explains how mortars have been made and used through the ages (Arizzi and Cultrone 2021, Ergenç et al. 2021, Lancaster 2021, Vitti 2021). An insight into their production, transport and on-site organisation is further provided by DeLaine (2021). Furthermore, several issues concerning the degradation and conservation of mortars and plasters are addressed from practical and technical standpoints (La Russa and Ruffolo 2021, Caroselli et al. 2021).

The second group of contributions is focused on pigments, starting from a philological essay on terminology (Becker 2021). Three archaeological reviews on prehistoric (Domingo Sanz and Chieli 2021), Roman (Salvadori and Sbrolli 2021) and Medieval (Murat 2021) wall paintings clarify the archaeological and historical/cultural framework. A series of archaeometric reviews illustrate the state of the art of the studies carried out on Fe-based red, yellow and brown ochres (Mastrotheodoros et al. 2021); Cu-based greens and blues (Švarcová et al. 2021); As-based yellows and reds (Gliozzo and Burgio 2021); Pb-based whites, reds, yellows and oranges (this paper); Hg-based red and white (Gliozzo 2021); and organic pigments (Aceto 2021). An overview of the use of inks, pigments and dyes in manuscripts, their scientific examination and analysis protocol

This article is part of the Topical Collection on *Mortars, plasters and pigments: Research questions and answers*

✉ Elisabetta Gliozzo
elisabetta.gliozzo@uniba.it; elisabetta.gliozzo@gmail.com

Corina Ionescu
corina.ionescu@ubbcluj.ro

[1] Department of Humanities, University of Bari, Bari, Italy

[2] Electron Microscopy Center, Babeș-Bolyai University, Cluj-Napoca, Romania

Published online: 29 December 2021

(Burgio 2021) as well as an overview of glass-based pigments (Cavallo and Riccardi 2021) are also presented. Furthermore, two papers on cosmetic (Pérez Arantegui 2021) and bioactive (antibacterial) pigments (Knapp et al. 2021) provide insights into the variety and different uses of these materials.

Introduction

The average abundance of lead in the Earth's crust is 14 ppm (Lide 2008).

Lead is a chalcophile and amphoteric element, which can be attacked by alkalis and acids. While it is rarely found as a native element (included in the copper group), Pb-bearing minerals are rather widespread. These minerals are mostly oxides, sulfides/sulfates/sulfites and hydroxides, but several other types, such as carbonates, chlorides/chlorates, chromates, oxalates and acetates, may also be abundant. Galena is the most common Pb mineral, followed by its secondary phases, anglesite and cerussite. Lead-based minerals have been used for multiple purposes, from colouring to protective/isolating coating, cosmetics and pharmaceutics (Gunn 1973; Walter et al. 1999, 2003; Welcomme et al. 2006; Tapsoba et al. 2010; Vidale et al. 2016; Baraldi et al. 2020; Photos-Jones et al. 2020; Wang et al. 2020a).

This review intends to take stock of lead-based pigments, focusing on the various mineral phases that can be found during the investigation of paintings. This perspective facilitates the reader and implies an indication of the methods used in this field (*i.e.* identifying minerals as the primary objective of research aimed at characterising inorganic pigments).

With this aim in mind, this review is broken down into seven parts.

The first part deals with the main lead-based pigments, *i.e.* the mineral phases used as pigments or raw materials for their production. In each subsection, the macroscopic characteristics, structural parameters and production cycles are described. Although most of these pigments have resulted from a technological process, it is not yet possible to completely exclude that, in some cases, the painters also used natural correspondents. Therefore, some brief information on the formation and diffusion areas in nature[1] is provided to stimulate research dealing with the supply of raw materials. After describing the main characteristics of the mineral(s) and the corresponding pigment, alteration is addressed. Finally, in each subsection, an overview of the use and occurrence of the pigment/s in certain artworks is also provided.

The second part deals with the lead-based minerals found in paintings, as alteration phases of the pigments outlined in the first part. For each phase, mineralogical information is provided, and its occurrence in works of art is reviewed. Here, in addition to the most common or most used minerals, we also present some lesser-known phases which could be found in natural association with the former, sometimes with macroscopically indistinguishable colours or *habiti*. Other minor and/or rarer phases, such as rickturnerite ($Pb_7O_4[Mg(OH)_4](OH)Cl_3$; Rumsey et al. 2012b), shannonite (Pb_2OCO_3; Roberts et al. 1995) and fassinaite ($Pb_2^{2+}(S_2O_3)(CO_3)$; Bindi et al. 2011) have been omitted, as their structural parameters can hardly induce the analyst to confuse them with other phases; furthermore, their presence in artworks has not yet been documented. However, it is worth noting that shannonite may be present in cerussite-based compounds and, analogously to hydrocerussite, transforms to cerussite in water (Kotulanová et al. 2009). For space reasons, only those studies directly connected with the characterisation of pigments were considered; however, it is worth emphasising that a conspicuous body of literature exists on the alteration processes (especially for lead soaps[2]). The reader is invited to deepen this topic, as the outstanding information achieved so far on the modality and kinetics of the saponification processes represents critical knowledge for evaluating degradation and developing appropriate conservation strategies (Meilunas et al. 1990; Lazzari and Chiantore 1999; Erhardt et al. 2000; Higgitt et al. 2003; Plater et al. 2003; Saunders and Kirby 2004; Keune 2005; Van der Weerd et al. 2005; Boon and Ferreira 2006; Cotte et al. 2006, 2007; Doménech-Carbó et al. 2006; Dietemann et al. 2009; Manzano et al. 2009; van den Brink et al. 2009; Catalano et al. 2014; Hermans 2017; Baij et al. 2018; Casadio et al. 2019; Poli et al. 2019; Garrappa et al. 2020).

The third part deals with the production centres of the pigments outlined in the first part. In this brief chapter, the little information available to date is summarised.

The fourth part deals with lead-based pigments in which lead is combined with tin and/or antimony and chromium (except for natural crocoite, which is discussed in the first part). This section details the mineralogical description, production process and occurrence in artworks of lead-tin yellow I–II, lead-antimony yellow (Naples yellow), lead-tin-antimony yellow and lead chromates. Terminological issues are also addressed. Conversely, the intensive study of these materials as colouring agents in the field of glass and ceramic coatings has created such a body of literature that it would not

[1] DMS coordinates of natural occurrences are listed in Supplementary Materials, Table S1).

[2] Broadly speaking, lead soaps are lead carboxylates, viz. complexes of metal ions and fatty acids (from hydrolysed triglycerides of oils) which can deeply affect the visual appearance and integrity of a painting. Although they can play a stabilising role during drying (reducing the risks of swelling and fracturing; see, *e.g.*, Cotte et al. 2017), their formation, aggregation and migration (mostly driven by levels of moisture and temperature) may cause colour changes (*e.g.*, transparencies), protrusions, crusts and an overall weakening of the pictorial film.

have been possible to discuss it properly here. Therefore, the reader is referred to a short list of references that any researcher should read before approaching the archaeometric study of lead-containing glass and ceramic coatings, as follows: Turner and Rooksby (1959), Hedges and Moorey (1975), Hedges (1976), Henderson and Warren (1983), Mass et al. (1996, 2002), Mason and Tite (1997), Freestone and Stapleton (1998), Pernicka et al. (1998), Tite et al. (1998, 2008), Molera et al. (1999), Heck and Hoffmann (2000), Shortland (2002), Rosi et al. (2011) and Matin (2018).

The fifth part provides some brief notes, first on binding media and then on the diffusion of pigments. For this purpose, a literature review was performed and the list of consulted references is provided in the Supplementary Materials, Appendix 1. The geographic distribution and the association of lead-based pigments with other inorganic and organic materials are schematically described.

Based on the literature review, the sixth part provides an overview of the analytical methods used to investigate paintings. The advantages and disadvantages, with respect to the research questions, are highlighted for each technique.

The final part summarises the key points that should be known and considered in the study of lead-based pigments and their alteration phases.

Before delving into the matter, it is necessary to add an essential clarification on the chemical reaction equations reported for the various phases. The processes occurring in nature, the production cycles that lead to the creation of a pigment and the alterations arising in paintings can only take place under certain conditions. In nature, the pressure, temperature, oxygen fugacity and fluid circulation are some of the determining factors. For the production and alteration of pigments, the temperatures, relative humidity, lighting conditions, presence of carbon dioxide, water and sulfides and interactions with the binding media are the principal factors to be considered. Therefore, a reaction that may occur in nature does not necessarily happen in a painting and vice versa. For use of the reactions provided, the researcher must verify whether the reaction conditions are satisfied. A pressure of 1 atm represents the only constant for the reactions provided throughout this paper.

Main lead-based minerals, pigments and dryers

Lead white—cerussite ($PbCO_3$) and hydrocerussite ($2PbCO_3{\cdot}Pb(OH)_2$)

Mineralogical phases, structure and occurrence

Named after the Latin *cerussa* (Table 1), cerussite is a colourless to white (sometimes with grey, blue or green hues) carbonate (Table 2; Figure 1A). It is a member of the aragonite ($CaCO_3$) group, together with strontianite ($SrCO_3$) and witherite ($BaCO_3$). The type locality is in the Vicenza province in Italy (Boscardin et al. 2016), and it is typically found in the oxidised zone of lead deposits (Table 3).

Hydrocerussite is a white or light grey carbonate containing a hydroxyl group (Table 2; Figure 1B), named in 1877 by Nils Adolf Erik Nordenskiöld (Nordenskiöld 1877). Its type locality is Långban Mine in Sweden (Siidra et al. 2018b). The structure of hydrocerussite and its related phases (chiefly abellaite and grootfonteinite) is characterised by "electroneutral $[PbCO_3]^0$ cerussite type layers or sheets (...) separated by the stereochemically active $6s^2$ lone electron pairs on Pb^{2+} cations" (Siidra et al. 2018b).

Both cerussite and hydrocerussite are relatively abundant in nature (Anthony et al. 1990; Mindat.org) and are mostly found in the oxidised zone of lead deposits (Table 3). Notable occurrences are the Tsumeb and Kombat Mines in Namibia, the Monteponi and Montevecchio Mines in Sardinia (Italy), Příbram (Czech Republic), Friedrichssegen Mine in Rhineland-Pfalz (Germany), Merehead Quarry in Somerset (UK), Leadhills in Lanarkshire (Scotland, UK), Nerchinsk lead deposit in Zabaykalsky Krai (Siberia, Russia), Seh-Changi Mine near Neyband in Khorassan (Iran), Mont Saint-Hilaire (Quebec, Canada), Touissit Mine in Morocco, Broken Hill in New South Wales (Australia), Bunker Hill Mine (Idaho, USA), Leadville in Colorado (USA) and the Mammoth-St. Anthony Mine (Arizona, USA).

Most research has focused on the chemical and thermodynamical equilibria between these two phases and other lead carbonates (Figure 1), and experimental tests have been systematically performed in varying conditions (Bilinski and Schindler 1982; Flemming et al. 1984; Taylor and Lopata 1984; Petushkova and Lyalikova 1986; Mercy et al. 1998; Sánchez-Navas et al. 2013; Mendoza-Flores et al. 2017). Indeed, a conspicuous number of studies has also aimed to understand the speciation of lead in soils, groundwater and streams and to find remediation technologies (Basta and McGowen 2004). The results achieved may help to better understand the behaviour of these phases in nature (*i.e.* supply areas) and artworks, as well as to recover essential clues on the production technology of lead white (*psimythion/psimithium - cerussa*; Table 2, P3).

Of utmost importance is the fact that this pigment can be made up of a single component (*i.e.* cerussite or hydrocerussite), but it often includes varying amounts of both components (sometimes even including lead acetate).

The production of lead white

Not much is known about the possible exploitation of natural minerals. *Plinius* reported that 'native' cerussite was found at the estate of *Theodotus*'s at Smyrna (Table 1, P4), but he did

Table 1 Literary sources (the texts in the original language are provided in Supplementary Materials, Table S2). Translations: Rackham (1952) for *Plinius*; Osbaldeston and Wood (2000) for *Dioscorides*; Caley and Richards (1956) for *Theophrastus*; Morgan (1914) for *Vitruvius*. Other texts, personal translation. The text of *(H)Eraclius* is from Heraclius (1873)

In text	*Reference*	Translation
P1	*Plinius, Naturalis Historia,* 33, 31, 95	It cannot be smelted except when combined with lead or with the vein of lead, called galena and lead ore, which is usually found running near veins of silver ore. Also when submitted to the same process of firing, part of the ore precipitates as lead while the silver floats on the surface, like oil on water.
P2	*Plinius, Naturalis Historia,* 33, 35, 106-109	The same mines also produce the mineral called scum of silver. Of this there are three kinds, with Greek names meaning respectively golden, silvery and leaden; and for the most part, all these colours are found in the same ingots. The Attic kind is the most approved, next the Spanish. The golden scum is obtained from the actual vein, the silvery from silver, and the leaden from smelting the actual lead, which is done at Puteoli, from which place it takes its name. Each kind however is made by heating its raw material till it melts, when it flows down from an upper vessel into a lower one and is lifted out of that with small iron spits and then twisted round on a spit in the actual flame, in order to make it of moderate weight. Really, as may be inferred from its name, it is the scum of a substance in a state of fusion and in process of production. It differs from dross in the way in which the scum of a liquid may differ from the lees, one being a blemish excreted by the material when purifying itself and the other a blemish in the metal when purified. Some people make two classes of scum of silver which they call 'scirerytis' and 'peumene,' and a third, leaden scum which we shall speak of under the head of lead. To make the scum available for use, it is boiled a second time after the ingots have been broken up into pieces the size of finger-rings. Thus after being heated up with the bellows to separate the cinders and ashes from it it is washed with vinegar or wine, and cooled down in the process. In the case of the silvery kind, in order to give it brilliance, the instructions are to break it into pieces the size of a bean and boil it in water in an earthenware pot with the addition of wheat and barley wrapped in new linen cloths, until the silvery scum is cleaned of impurities. Afterwards, they grind it in mortars for 6 days, three times daily washing it with cold water and, when they have ceased operations, with hot, and adding salt from a salt-mine, an obol weight to a pound of scum. Then on the last day, they store it in a lead vessel. Some boil it with white beans and pearl-barley and dry it in the sun, and others boil it with beans in a white woolen cloth till it ceases to discolour the wool; and then they add salt from a salt-mine, changing the water from time to time, and put it out to dry on the 40 hottest days of summer. They also boil it in a sow's paunch in water, and when they take it out, rub it with soda, and grind it in mortars with salt as above. In some cases, people do not boil it but grind it up with salt and then add water and rinse it.
P3	*Plinius, Naturalis Historia,* 34, 54, 175-176	Psimithium also, that is cerussa, is produced at lead-works. The most highly spoken of is in Rhodes. It is made from very fine shavings of lead placed over a vessel of very sour vinegar and so made to drip down. What falls from the lead into the actual vinegar is dried and then ground and sifted, and then again mixed with vinegar and divided into tablets and dried in the sun, in summertime. There is also another way of making it, by putting the lead into jars of vinegar kept sealed up for 10 days and then scraping off the sort of decayed metal on it and putting it back in the vinegar, till the whole of it is used up. The stuff scraped off is ground up and sifted and heated in shallow vessels and stirred with small rods till it turns red and becomes like sandarach, realgar. Then, it is washed with fresh water till all the cloudy impurities have been removed. Afterwards, it is dried in a similar way and divided into tablets. Its properties are the same as those of the substances mentioned above, only it is the mildest of them all, and besides that, it is useful for giving women a fair complexion; but like scum of silver, it is a deadly poison. The cerussa itself if afterwards melted becomes red.
P4	*Plinius, Naturalis Historia,* 35, 19, 37	The third of the white pigments is ceruse or lead acetate, the nature of which we have stated in speaking of the ores of lead. There was also once a native ceruse found on the estate of Theodotus at Smyrna, which was employed in old days for painting ships. At the present time, all ceruse is manufactured from lead and vinegar, as we said.
P5	*Plinius, Naturalis Historia,* 35, 20, 38	Burnt ceruse was discovered by accident, when some were burnt up in jars in a fire at Piraeus. It was first employed by Nicias above-mentioned. Asiatic ceruse is now thought the best; it is also called purple ceruse and it costs 6 denarii per pound. It is also made in Rome by calcining yellow ochre which is as hard as marble and quenching it with vinegar. Burnt ceruse is indispensable for representing shadows.
D1	Dioscorides, *De Materia Medica (*Περὶ ὕλης ἰατρικῆς*), 5, 87 vel 102*	Some spuma argenti or froth of silver is made from sand called molibditis [molybdenite—disulfide of molybdenum] blown in a furnace until perfectly fired. Some are made from silver and some from lead. The Attican is best, next to this is the Spanish, after these that from Dicaearchia in Campania and from Sicily, for much of it is made in these various places from lead plates [2] that are fired. The best is a yellow glittering sort called chrysitis; that from Sicily is called argyritis [silver], and that from silver is called calabritis. It is astringent and softening, filling up hollownesses, repressing abnormal growths of flesh and forming new skins, as well as being cooling, and closing the pores. [3] You should burn it as follows. Divide it into pieces the size of carya, place them on burning coals and blow on them until thoroughly fired. Then, wipe away the filth that has formed on it and put it in jars. Some quench it three times with vinegar or wine then burn it again, and having done these things, put it in jars. It is washed like cadmia. [4] It is made white as follows. Take as much as an Athenian choenix [two pints] of that which is called argyritis [silver] (and if not, then one of the others) broken into pieces the size of beans, and throw it into a new ceramic jar. [5] Pour on water and throw in two pints of white wheat as well. Take a handful of barley, bind it in a thin clean linen cloth, hang it from the handle of the ceramic jar, and boil it until the barley is broken. Then, pour it all out into a clean broad-mouthed plate, separate the wheat, and throw it away. Pour on water to wash the sediment, rubbing it strongly at the same time with your hands. Then, take it out, dry it and beat it in a Thebaean mortar, pouring on warm water until it has dissolved. Straining out the water, pound it again for a whole day, and in the evening pour on hot water then leave it alone. In the

Table 1 (continued)

In text	*Reference*	Translation
		morning, strain out that water, pour in more and repeat this procedure [6] three times a day. Do this for 7 days. Then mix to a pound of lithargyrum five teaspoonfuls of mineral salt, pour on warm water and beat it three times a day, straining out the old water and mixing in new water each time. Even if it turns white, pour on warm water until it contains no saltiness. Dry it in a very hot [7] sun (first throwing away the liquid) then put it in jars. Alternatively, take one pound of argyritis [silver], beat it into small pieces carefully, and mix in three times as much mineral salt, also pounded into small pieces. Put it into a new ceramic jar, and add water until it is covered. Stir it every day, morning and evening, pouring in more water as needed, but pouring out none of the original water. Do this for 30 days for if it is not stirred it becomes as hard as a shell. [8] Afterwards (having poured out the saltwater), gently beat the sediment finely in a Thebaean mortar. Put it into a ceramic jar, pour in water, and stir it diligently with your hands, pouring out the first water and pouring on more until it has no saltiness. Then, pour out the white lithargyrum into another jar, make lozenges with it, and keep them in a lead [9] box.
D2	*Dioscorides, De Materia Medica (*Περὶ ὕλης ἰατρικῆς*), 5, 88 vel 103*	[103] Cerussa is made as follows. Pour the sharpest vinegar into a broad-mouthed jar or ceramic urn, and fasten a lead plate to the mouth of the jar with a little reed mat placed underneath. On the top of it put covers so that the vinegar cannot evaporate before it is dissolved, and falls down distilled. Strain out the pure liquid on top. Pour the viscous stuff out into a jar and dry it in the sun. Then, it must be ground in a hand mill, or finely pounded some other way and sarced [scraped]. Repeat this pounding and scraping three or four times. That which is sarced [scraped] first is the best, to be used in eye medicines, and the next best follows next, and so on. Some use a bullrush mat, fastening it towards the middle of the jar so that it touches the vinegar. Then, they cork the mouth of it, seal it all up and leave it alone. After some days, they take off the cover to look in, and when it is all dissolved, they repeat the procedures previously described. To form it into lozenges, it must be kneaded with sharp vinegar, shaped and dried in the sun. The things mentioned here must be done in the summer for then it becomes white and effective. It is also made in the winter, the ceramic pots set over furnaces, baths, or chimneys. The warmth is carried from above, the same as the sun. That which is made in Rhodes, Corinth or Lacedaemonia is considered the best. The next is that which comes from Puteoli. It is roasted as follows: place a new Ostracean jar (especially an Athenian) over light burning coals, sprinkle on cerussa pounded into small pieces, and stir it continuously. When it is ashy in colour take it out, cool it and use it. If you want to burn it put the pounded small pieces into a hollow platter set it over live coals, and stir it with a stick of ferula until it is similar in colour to sandarac then take it out and use it. If cerussa is washed the same way as cadmia, some call this sacyx. Mixed with stiff ointments, plasters called lipara, and with lozenges [tablets, but not to take internally] it is cooling, pore-closing, softening, filling, reduces the intensity of symptoms; and furthermore gently represses abnormal growths, and forms new skins; it is among those things which taken internally kill.
T1	*Theophrastus,* Περὶ λίθων (*De Lapidibus*), 55-57	These are prepared artificially, and so is white lead. Lead about the size of a brick is placed in jars over vinegar, and when this acquires a thick mass, which it generally does in 10 days, then the jars are opened and a kind of mold is scraped off the lead, and this is done again until it is all used up. The part that is scraped off is ground in a mortar and decanted frequently, and what is finally left at the bottom is white lead. Verdigris is made in much the same way. Red copper is placed over grape-residues and the matter that collects on it is scraped off; for it is verdigris that appears there.
V1	*Vitruvius, De Architectura* 7, 12, 1-2	It is now in place to describe the preparation of white lead and of verdigris, which with us is called "aeruca." In Rhodes, they put shavings in jars, pour vinegar over them and lay pieces of lead on the shavings; then, they cover the jars with lids to prevent evaporation. After a definite time, they open them and find that the pieces of lead have become white lead. In the same way, they put in plates of copper and make verdigris, which is called 'aeruca'. White lead on being heated in an oven changes its colour on the fire and becomes sandarach. This was discovered as the result of an accidental fire. It is much more serviceable than the natural sandarach dug up in mines.
E1	*(H)Eraclius, De coloribus et de artibus Romanorum,* 1, 36	How lead is made and from this the red lead. If you want to prepare red lead, or also the white, which is called cerusa, take pieces of lead, put them in a new pot and fill it with the strongest vinegar; cover it up, put it in a warm place and leave it for a month. Then, open the pot and put what you find around the lead sheets in another vessel, put it on the fire and keep stirring the paint until it becomes white as snow; remove it now from the fire, take as much colour as you like; and that is called cerusa. Put the rest on the fire again and continue stirring until it turns into red minium. For this reason, I warn you to stir because, if you do not stir it, it would turn white again, and in this way, take it off the fire and let the vessel cool down.
BM1	Bologna Manuscript 2861 (15th century)	Remove lead sheets and place them in a jar, over the vapour of very strong vinegar. Cover it well with mud and put it under the manure for 2 months. Then, scrape off the white matter that you will find above the sheets and repeat the aforementioned process until they are worn out.
BM2	*Segreti per colori*	M272. To make yellow glass for rosaries or beads Take 1 lb. of lead, 2 lb of tin and melt and calcine them to make glass for rosaries. M273. To make zallolino to paint. Take 2 lb of tin and calcined lead, 2 lb of rosary glass, 2.5 lb of minium and 0.5 l of finely ground Valdarno sand. Put them into the kiln and let it refine. It will be perfect.

Table 1 (continued)

In text	*Reference*	Translation
PZ1	Andrea Pozzo, *Prospettiva de pittori e architetti*	Giallolino di fornace In Rome, it is called giallolino of Naples. I used it as a fresco, and it is preserved: but I have never tried to expose it to the air. Colours incompatible with lime, and which cannot be used in fresco paints White lead, minium, Venetia lacquer, fine lacquer, copper green, blue-green, leek green, cane green, holy yellow, Flanders giallolino, orpiment, indigo, bone black, biadetto
MA1	Marcucci 1816	[Naples yellow] the method to obtain it is to take 12 parts of Plaiter's white lead, and diaphoretic antimony (or antimony oxide [turned] white due to nitro), two parts of burnt alum (namely alumina sulphate; deprived of a portion of crystallization water), half part of ammonia salt (or ammonium chloride). Make it into powder in a stone mortar and, once stored in an earthen jar, place it in a furnace for 3 h to calcinate. Once the jar is cold, grind the yellow to keep it for use.
VA1	Vauquelin 1809	The process for dceomposing iron chromate is shown in detail and mainly consists of using only half a part of nitre against one of chromate. To obtain a very pure chromium oxide with a very beautiful colour, it is necessary to heat strongly in a beaker, with an appropriate colour, the chromate of pure mercury, until no more oxygen is released and to keep the fire longer if you want to get a less dark shade.
NO1	*Nouveau dictionnaire d'histoire naturelle appliquée aux arts. Tome XXVII*	Chromic acid and lead oxide exist together in nature. The native lead chromate is crystalline and of the brightest red-orange colour. Artificial chromate is a beautiful yellow, and is used in painting on canvas, porcelain and wood. It is obtained by decomposing the chromate of potash by the acetate of lead.
NO2		[---] Lead chromate, commonly called Siberian red lead, is an elegant mineral, remarkable for its beautiful orange-red or dawn colour; its dust, however, is lemon yellow or greenish, and sometimes reddish. It almost always crystallises in brilliant prisms, elongated at the top, and whose shapes are extremely difficult to grasp; sometimes, it occurs in small masses, veins and encrustations; it is brilliant. Its fracture is laminated along the longitudinal direction of the prisms, and glassy in the transverse direction. It is translucent and even semi-transparent, or very rarely transparent. It is not hard and breaks easily. Its specific gravity is 6.026, according to Brisson, and 5.750, according to Bindheim. Exposed to a torch, it decays(?) and melts into a gray slag, and colours the borax glass green. It is partially reduced by means of this salt. Not effervescent with acids. According to MM. Vauquelin and Thénard, derives from: [Figure in Supplementary materials, Table S2]

not specify who the painters that employed it "*in old days for painting ships*" were. In the same paragraph, he also drew a distinction between the artificially produced variety, used in his time, and the natural one, which was in disuse by that time.

As for white lead recipes, *Theophrastus* suggested leaving a piece of lead the size of a brick in jars over vinegar for about 10 days, then to scrape off the "*kind of mold*" that formed, repeating the operation until the total conversion of the piece of lead initially introduced had taken place (Table 1, T1). *Plinius* added that production took place at the same time/place as that of lead and mentioned two different methods: suspension over vinegar and immersion in vinegar (Table 1, P3).

Similar procedures were also described by *Vitruvius* (Table 1, V1), *Dioscorides* (Table 1, D2) and *(H)Eraclius*. This last author described both the immersion and heating procedures in his *De coloribus et de artibus Romanorum* between the 7th and 12th centuries (Table 1, E1). He also provided some technical advice for the diversification of white and red lead production.

In summary, two main methods have been described in the literature for producing lead white: (1)suspensions—in open or sealed vessels—and immersion. The two procedures inevitably led to the formation of different compounds (due to different carbon dioxide circulation and availability and bacterial activity) and it must also be considered that the immersion procedure has not yet been experimentally tested. Simplifying matter, only lead acetate may form if only acetic acid vapours rising from the vinegar can reach the lead. The decomposition of organic matter (*e.g.*, horse manure, tanbark, urine) described by the ancient authors (as well as by more recent documentary sources and experimental tests) could then produce both the carbon dioxide and the heating required to trigger the reaction transforming lead acetate into lead carbonates.

Photos-Jones et al. (2020) clarified that the activity of aerobic/anaerobic bacteria is crucial for the production/consumption of CO_2/O_2—*i.e.* the bulk of the gases within the pot—and showed that in closed systems (sealed vessels), the composition of the oxos/vinegar is fundamental. They carefully examined the recipe handed down by Theophrastus, in order to verify to what extent it is possible to obtain a *psimythion* of pure cerussite, as well as the role of the *oxos* (spoiled wine) when used in place of vinegar. Starting from the analysis of pellets from the 5th to 4th centuries BC, the authors performed DNA sequencing (which did not reveal the presence of microorganisms) and proposed to recognise the key driver of *psimythion* synthesis in the reactions between

abiotic (lead phases) and biotic (*e.g.*, *Acetobacter* in spoiled wine) components.

Taking a considerable leap in time, in the 15th century, Venice was the main producer of the lead white variety named 'Venetian white' (Beck et al. 2020; Hendriks et al. 2020). However, according to the contemporary recipe handed down by an anonymous author in the Bologna Manuscript named *Segreti per colori*, the process does not seem remarkably different from that adopted in antiquity (Table 1, BM), including scraps of lead, vinegar steam and a jar cover with mud (*luto*) put under manure. The recipe has also been reported by Merrifield (1849) but with a slightly different translation.

During the 16th and 17th centuries, another method was developed for industrial applications: the 'Dutch' or 'stack' process. This procedure is similar to the ancient ones, as it involves the exposure of lead strips or 'buckles' to vinegar for 1 to 3 months (Gettens et al. 1967). The main differences, compared to the ancient procedures, seem to lie in the following:

(a) the type of clay pot used[3]—although we do not know the exact shape (nor porosity) of the ancient vessels, except that they were (broad-mouthed)jar-shaped and may have had a lid (Table 1, D2, P3, P5, T1, V1);
(b) the stacking of some hundreds or thousands of these pots in rows and their embedding in fermenting tanbark or dung (*i.e.* external source of CO_2), which could produce both heat and carbon dioxide (Thompson 1971).

Development of the stack process led to the widespread commercialisation of lead white. Between the 17th and 18th centuries, The Netherlands were the major producer, as attested by the "*over 35 lead white factories*" present by the end of the 18th century (Hendriks et al. 2020 quoting Homburg and De Vlieger 1996). The development of England's production is also to be placed shortly after (Rowe 2017). From this moment on, the method remained essentially unchanged in principle; however, thanks to the discovery of carbon dioxide in the late 18th century, it was better understood and adapted to increase its productivity.

For example, the 'chamber method'—generally attributed to a patent awarded to James Creed in 1749—exploited heat flowing into a chamber (see Stols-Witlox 2014 on the possibility that this reconstruction is not entirely true). The 'German method', implemented by Franz von Herbert at the end of the 18th century, represents the development of the 'chamber method' and sure proof of its use in the industrial field. It was developed following the innovations introduced by Herbert, who used fruit must vinegar produced by his own orchard in Wolfsberg (Austria) and, successively, wine lees from his Klagenfurt factory to make the famous 'Krems white' (Stols-Witlox et al. 2012, 2014; Hendricks et al. 2019). There is no agreement in the literature on the denomination and attribution of the various methods; however, the 'philological' problem does not significantly change the overall reconstruction.

In the 19th century, white lead found a valuable competitor in zinc oxide (Roy 1993; see also Spennemann 2020), but its use did not cease.

For example, the reports compiled by Jussen—general consul of the United States in Austria (Jussen 1887; see Supplementary Materials, Appendix 2)—informed of the existence of the varieties named K*remserweiss* (also *Cremnitz White* and *Kremnitz White*) and *Venetianerweiss* (whose history was lost in the past). He also listed several methods used to produce lead white (*i.e.* Lothman, Gannal, Fourmetier, Pattinson and Chenot, along with the method employed in the lead white factory of Theodor Lefebre & Co.). Over the centuries, the process was thus refined, where some treatments conducted before and/or after the synthesis, such as grinding, washing (in water or acids) and further heating (also in water), led to the production of numerous varieties of lead white (see, *e.g.*, Stols-Witlox 2011; Stols-Witlox et al. 2012; Gonzalez et al. 2017a). Modern chemistry has also substantially modified the production process, using precipitation and hydrolysis to obtain lead white from metallic lead (both in a dry environment and by water immersion).

Excluding carbonate-based whites, white lead remained "*the most important of all white pigments*" (Gettens et al. 1967) until the early 20th century, when titanium whites became predominant (Eastaugh et al. 2004).

At the beginning of the 21st century, lead white was banned from the market, due to its toxicity (but not in all countries; since 2015 in Europe).

Archaeometric investigations have confirmed the information handed down by the authors and have clarified both the processes and the nature of the resulting products (Figure 2). Gonzalez et al. (2019b) reproduced the 'stack' process—although "*not faithfully*" as claimed by the authors—and clearly reconstructed the reaction path leading to the formation of plumbonacrite, hydrocerussite and cerussite. These authors also demonstrated that, during the 'Dutch Golden Age', the 'classic ratio' between cerussite and hydrocerussite was 30:70. On the same topic, the chemical reactions for hydrocerussite formation have also been reported by Sánchez-Navas et al. (2013; derived from previous literature). These authors used the 'stack' process to investigate crystal growth features that can be affected by the medium in which the precipitation occurs. They found that cerussite and hydrocerussite crystals showed different morphology and crystallinity depending on the medium in which the precipitation occurred.

For example, cerussite crystals formed from gels showed dendritic or acicular habitus (or aggregates with pseudocubic

[3] *A specially made clay pots which had a separate compartment in the bottom to hold a weak solution of vinegar*(Thompson 1971, p. 91)

Table 2 Chemical formulae, space groups and structural parameters of Pb-based minerals mentioned in the text [Pb content from Webmineral database (n.d.), if not differently specified; N/S, natural/synthetic]

Name	Formula	Pb (wt%)	N/S	Crystal system	Space group	*a* (Å)	*b* (Å)	*c* (Å)	β (°)	Vol. (Å^3)	*Z*	Reference
Abellaite	$NaPb_2(CO_3)_2$ (OH)	72.0	N	Hexagonal	$P6_3mc$	5.254 (2)	=	13.450 (5)	-	321.5 (2)	2	Ibáñez-Insa et al. 2017
	$NaPb_2(CO_3)_2$ (OH)		S	Hexagonal	$P6_3mc$[1]	5.276 (1)	=	13.474 (4)	-	324.8 (1)	2	Krivovichev and Burns 2000
	$NaPb_2(CO_3)_2$ (OH)		S	Hexagonal	$P31c$[2]	5.268 (4)	=	13.48 (1)	-	324.0 (7)	-	Belokoneva et al. 2002
	$NaOH{\cdot}2PbCO_3$		S	Hexagonal	-	5.273 (2)		13.448 (5)	-	-	2	Brooker et al. 1983
Anglesite	$PbSO_4$	68.3	N	Orthorhombic	*Pbnm*	6.95802 (1)	8.48024 (3)	5.39754 (1)	-	318.486 (1)	4	Antao 2012
Blixite	$Pb_8O(OH)_2Cl_4$	86.3	S	Monoclinic	*C*2/*c*	26.069 (5)	5.8354 (11)	22.736 (4)	β = 102.61 (6)	3375.3 (11)	8	Krivovichev and Burns 2006
Cerussite	$PbCO_3$	77.5	[3]	Orthorhombic	*Pmcn*	5.1820 (4)	8.4953 (9)	6.1436 (5)	-	270.46 (4)	-	Ye et al. 2012
			S	Orthorhombic	*Pmcn*	5.18324 (2)	8.49920 (3)	6.14746 (3)	-	270.817	4	Antao and Hassan 2009
			N	Orthorhombic	*Pmcn*	5.179 (1)	8.492 (3)	6.141 (2)	-	-	4	Chevrier et al. 1992
Caledonite	$Pb_5Cu_2(CO_3)(SO_4)_3(OH)_6$	64.2	N	Orthorhombic	$Pmn2_1$	7.146 (3)	20.089 (7)	6.560 (5)	-	941.73	2	Giacovazzo et al. 1973
Challacolloite	KPb_2Cl_5	65.7	N	Monoclinic	$P2_1/c$	8.864 (8)	7.932 (8)	12.491 (11)	β =90.153 (5)	878.2 (1)	4	Schlüter et al. 2005
			N	Monoclinic	$P2_1/c$	8.8989 (4)	7.9717 (5)	12.5624 (8)	β =90.022 (4)	891.2 (1)	4	Mitolo et al. 2009
Cotunnite	$PbCl_2$	74.5	S	Orthorhombic	*Pnam*	7.6222 (5)	9.0448 (7)	4.5348 (4)	-	312.63	4	Sass et al. 1963
Crocoite	$Pb(CrO_4)$	64.1	N	Monoclinic	$P2_1/n$	7.127 (2)	7.438 (2)	6.799 (2)	β=102.43 (2)	350.90	4	Effenberger and Pertlik 1986
Galena	PbS	86.6	N	Isometric	*Fm*-3*m*	5.9237 (3)	5.9237 (3)	5.9237 (3)	-	207.864 (2)	4	Noda et al. 1987
Grootfonteinite	$Pb_3O(CO_3)_2$	88.4[4]	N	Hexagonal	$P6_3/mmc$	5.303 (1)	=	13.770 (3)	-	335.3 (1)	2	Siidra et al. 2018a
Hydrocerussite	$Pb_3(OH)_2$ $(CO_3)_2$	86.3[4]	N	Trigonal	*R*-3*m*	5.2475 (1)	=	23.6795 (7)	-	564.69 (1)	3	Siidra et al. 2018b
			S	Trigonal	*R*-3*m*	5.257 (3)	=	23.636 (15)	-	565.7 (8)	3	Siidra et al. 2018b
			S	Trigonal	*R*-3*m*	5.247	=	23.702	-	565.01 (12)	3	Martinetto et al. 2002
Laurionite	Pb(OH)Cl	79.8	N	Orthorhombic	*Pcmn*	9.6987	4.0203	7.1110	-	277.27	4	Palache 1934
Leadhillite	$Pb_4(SO_4)(CO_3)_2(OH)_2$	76.8	N	Monoclinic	$P2_1/a$	9.110 (2)	20.820 (4)	11.590 (3)	β=90.46 (2)	2198.21 (1)	8	Giuseppetti et al. 1990
			N	Monoclinic	$P2_1/a$	9.104 (2)	20.792 (6)	11.577 (3)	β=90.50 (2)	2191.3 (9)	8	Bindi and Menchetti 2005
Lead-tin yellow I	Pb_2SnO_4	-	S	Tetragonal	P_42/mbc	8.7371	=	6.307	-	481.46	4	Byström and Westgren 1943; Swanson et al. 1972
			S	Tetragonal	P_42/mbc	8.7276 (2)	=	6.2970 (2)	-	479.65 (2)	-	Spahr et al. 2020

Table 2 (continued)

Name	Formula	Pb (wt%)	N/S	Crystal system	Space group	*a* (Å)	*b* (Å)	*c* (Å)	β (°)	Vol. (Å^3)	*Z*	Reference
			S	Orthorhombic	*Pbam*	8.7215 (3)	8.7090 (3)	6.2919 (3)	-	477.90 (4)	-	Gavarri et al. 1981
			S	Orthorhombic	*Pbam*	8.7288 (3)	8.7263 (3)	6.2969 (2)	-	479.64 (3)	-	Spahr et al. 2020
Lead-tin yellow II	$PbSnO_3$	-	S	Cubic	*Fd-3m*	10.719	=	=	-	1231.4	4	Morgenstern Badarau and Michel 1971
	$PbSn_{0.76}Si_{0.24}O_3$	-	S	Cubic	*Fd-3m*	10.715 (4)	=	=	-	-	-	Clark et al. 1995
Litharge	α-PbO	92.8	S	Tetragonal	*P4/nmm*	3.975	=	5.023	-	79.37	2	Wyckoff 1963
			S [5]	Tetragonal	*P4/nmm*	3.9744	=	5.0220	-	159.04	2	Boher et al. 1985
			S [6]	Tetragonal	*P4/nmm*	3.998	=	5.0654	-	81.038	-	Boher et al. 1985
			S [7]	Tetragonal	*P4/nmm*	4.0039	=	5.0712	-	81.297	-	Boher et al. 1985
Macphersonite	$Pb_4(SO_4)(CO_3)_2(OH)_2$	76.8	N	Orthorhombic	*Pbca*	9.242 (2)	23.050 (5)	10.383 (2)	-	2211.9 (8)	8	Steele et al. 1998
Massicot	β-PbO	92.8	S	Orthorhombic	*Pbcm*	5.8931 (1)	5.4904 (1)	4.7528 (1)	-	153.78 (1)	4	Hill 1985
Mimetite	$Pb_5(AsO_4)_3Cl$	69.6	N	Hexagonal	$P6_3/m$	10.250 (2)	=	7.454 (1)	-	678.214 (2)	2	Calos et al. 1990
Minium	Pb_3O_4	90.7	S	Tetragonal	*P-4b2*	8.86	=	6.66	-	522.81	-	Gross 1943
			S	Tetragonal	$P4_2/mbc$	8.811	=	6.563	-	509.51	4	Gavarri and Weigel 1975
	Pb_3O_4 [8]		S	Tetragonal	$P4_2/mbc$	8.815	=	6.53	-	-	4	Zyryanov and Gusev 2001
	Pb_3O_{4-x}		S [9]	Tetragonal	$P4_2/mbc$	8.79	=	7.65	-	-	4	Zyryanov and Gusev 2001
Naples Yellow	$Pb_2Sb_2O_7$ (bindheimite)	3.8	-	Cubic	*Fd-3m*	10.41	=	=	-	1124.86	8	Gasperin 1955
	$Pb_2Sb_2O_7$ (oxyplumboroméite)		N	Cubic	*Fd-3m*	10.3783 (6)	=	=	-	1117.84 (11)	8	Hålenius and Bosi 2013
Palmierite	$K_2Pb(SO_4)_2$	44.1	S	Trigonal/Hexagonal	*R-3m*	5.497 (1)	=	20.864 (2)	-	546.1 (5)	3	Tissot et al. 2001
Pb-Sn-Sb yellow	$Pb_2(MSb)O_{6.5}$ (M = Sn)[10]	-	S	Cubic	*Fd-3m*	10.5645 (2)	=	=	-	1179.11 (6)	8	Cascales et al. 1986
Phoenicochroite	$Pb_2O(CrO_4)$	80.9	-	Monoclinic	*C2/m*	14.001	5.675	7.137	β =115.22	513.021	4	Williams et al. 1970
Phosgenite	$Pb_2Cl_2(CO_3)$	76.0	N	Tetragonal	*P4/mbm*	8.1600	8.1600	8.8830	-	591.480	4	Köchlin 1887; Giuseppetti and Tadini 1974
Plattnerite	β-PbO_2	86.6	S?	Tetragonal	-	4.955 (3)	=	3.383 (2)	-	-	-	Leciejewicz and Padlo 1962
			N	Tetragonal	*P4/mnm*	9.9525 (4)	=	3.3863 (4)	-	83.06 (1)	2	White 1970
			S	Tetragonal	$P4_2/mnm$	4.9578 (2)	=	3.3878 (2)	-	-	2	D'Antonio and Santoro 1980
			N	Tetragonal	$P4_2/mnm$	4.9581 (10)	=	3.3866 (7)	-	83.3	2	Paulsen et al. 2019
Plumbonacrite ("a")	$Pb_5O(OH)_2(CO_3)_3$	88.1 [4]	S	Trigonal	*P-3c1*	9.0891 (7)	=	24.832 (3)	-	1776.6 (3)	6	Krivovichev and Burns 2000

Table 2 (continued)

Name	Formula	Pb (wt%)	N/S	Crystal system	Space group	*a* (Å)	*b* (Å)	*c* (Å)	β (°)	Vol. (Å^3)	*Z*	Reference
Plumbonacrite ("b")	$Pb_5O(OH)_2(CO_3)_3$		N	Trigonal	$P6_3cm$	9.0921 (7)	=	24.923 (3)	-	1784.3 (3)	6	Rumsey et al. 2012a
Schulténite	$Pb(AsO_3OH)$	59.7	N	Monoclinic	*Pa*	5.83	6.76	4.85	β = 84.35[11]	190.4	2	Claringbull 1950
Scrutinyite	α-PbO_2	86.6	S	Orthorhombic	*Pbcn*	4.948	5.951	5.497	-	161.862	4	Zaslavskii et al. 1950
			N	Orthorhombic	*Pbcn*	4.971 (2)	5.956 (2)	5.438 (3)	-	161.00 (9)	4	Taggart et al. 1988
Somersetite	$Pb_8O(OH)_4(CO_3)_5$	87.5 [4]	N	Hexagonal	$P6_3/mmc$	5.2427 (7)	=	40.2624 (6)	-	967.0 (3)	2	Siidra et al. 2018c
Susannite	Heated leadhillite (82°C)		S	Trigonal	*P*3	9.077 (8)		11.611 (9)	-	828 (1)	3	Bindi and Menchetti 2005
	$Pb_4(SO_4)(CO_3)_2(OH)_2$		N	Trigonal	*P*3	9.0718 (7)		11.570 (1)	-	824.6 (1)	3	Steele et al. 1999
Vanadinite	$Pb_5(VO_4)_3Cl$	73.1	N	Hexagonal	$P6_3/m$	10.3174	=	7.3378	β = 90.03 (3)	676.45	2	Dai and Hughes 1989
(Slag - seawater)	$NaPb_5(CO_3)_4(OH)_3$[12]	73.0	A	Hexagonal	$P6_3/mmc$	5.2533 (11)	=	29.425 (6)	-	703.3 (3)	2	Siidra et al. 2018d
Unnamed phase	$PbMg(CO_3)_2$	-	S	Trigonal	*R*32	4.924	=	16.56	-	-	-	Lippmann 1966

[1] Symmetry assignment later revised as $P6_3/mmc$ by Siidra et al. (2018a) and Bette et al. (2017); [2] Symmetry assignments later revised as $P6_3/mmc$ by Bette et al. (2017) and Siidra et al. (2018a); [3] $Ca_{0.001}Pb_{0.999}CO_3$; [4] PbO wt% in Siidra et al. (2018);[5] At 295°K=~22 °C; [6] At 673°K=~400 °C; [7] At 723°K=~450°C; [8] Pb_3O_4 prepared by mechanical processing; [9] *Y*-PbO + PbO_2 sample after 10 min of processing at .33 MJ/kg (red-brown colour); [10] Pyrochlore; [11] Spencer and Mountain (1926); [12] $Na_{0.51}Ca_{0.49})Pb_5(OH)_{2.51}O_{0.49}(CO_3)_4$

Table 3 Occurrences and associations of the phases mentioned in the text (alphabetical order). Data from publications quoted in the dedicated sections (esp. Ibáñez-Insa et al. 2017; Siidra et al. 2018c. In addition: Spencer and Mountain 1926; Embrey and Hicks 1977; Pinch and Wilson 1977; Turner 2006) and from Anthony et al. (1990) (http://www.handbookofmineralogy.org/). Mineral names are given according to the list provided by International Mineralogical Association (2020)

Phase	Occurrence	Association
Abellaite	'As sparse coatings on the surface of the primary mineralization'	Andersonite, aragonite, As-rich vanadinite, čejkaite, chalcopyrite, coffinite, covellite, devilline, galena, gordaite, hydrozincite, malachite, nickeloan cobaltite, pyrite, roscoelite, sphalerite, tennantite and uraninite
Anglesite	Oxidized zone of lead deposits	Brochantite, caledonite, cerussite, galena, gypsum, lanarkite, leadhillite, linarite, macphersonite, malachite, massicot, mimetite, pyromorphite, sulfur, susannite and wulfenite
Blixite	Secondary, in oxidized zone of lead-bearing ore (in particular galena)	Mendipite, laurionite, paralaurionite, mereheadite, symesite, parkinsonite, hausmannite, brucite, hydrocerussite, calcite, dolomite, cerussite and anglesite
Caledonite	Secondary mineral in oxidized zone of Pb-Cu ore	Cerussite, anglesite, azurite, malachite, brochantite, linarite and leadhillite
Cerussite	Oxidized zone of lead deposits; low-temperature hydrothermal or supergene environments	Anglesite, azurite, galena, malachite, phosgenite, pyromorphite and smithsonite
Challacolloite	Hydrothermal phase and product of fumarole activities	Anglesite, chubarovite, cotunnite, hephaistosite, hematite, hollandite, jakobssonite, leonardsenite, olsacherite, saltonseaite, sofiite, flinteite and xincomenite
Cotunnite	Primary (sublimates from hot volcanic gases, including fumaroles) Secondary, in oxidized zone of lead-bearing ore (in particular galena)	Primary: burnsite, flinteite, sellaite, fluorite, halite, anhydrite, sofiite, flinteite, chubarovite, anglesite, saltonseaite, hollandite, jakobssonite, olsacherite and many others Secondary: galena (relic), anglesite, cerussite, hydrocerussite, mendipite, blixite, laurionite, paralaurionite, matlokite, phosgenite, barstowite, challacolloite, tenorite, halite and burnsite
Crocoite	Secondary mineral in the oxidized areas of lead ore associated to Cr-rich rocks	Cerussite, wulfenite, anglesite, embreyite, pyromorphite, vanadinite, dundasite and several Pb, Cu and Ag ore minerals
Galena	Hydrothermal veins; contact metamorphic deposits, rarely in pegmatites; frequently hosted in limestones and dolostones	Barite, calcite, chalcopyrite, dolomite, marcasite, pyrite, quartz, siderite, silver minerals, sphalerite and tetrahedrite
Grootfonteinite	Regional metamorphism in 'a primary, Pb-Mn-(As-Ba)-rich, chemically heterogeneous, volcanic-hydrothermal assemblage'	Barite, cerussite, clinochlore, dolomite, hausmannite, jacobsite, melanotekite, rhodochrosite and sahlinite
Hydrocerussite	Oxidised zones of lead deposits	Cerussite, diaboleite, galena, lead, leadhillite, matlockite and paralaurionite
Laurionite	Secondary, in oxidized zone of lead-bearing ore (in particular galena) and by reaction of lead minerals with the seawater	Anglesite, cotunnite, cerussite, phosgenite, blixite, mendipite, paralaurionite and dolomite
Leadhillite	Oxidised zones of lead deposits	Anglesite, boleite, brochantite, caledonite, cerussite, diaboleite, lanarkite, linarite, paralaurionite and wherryite
Litharge	Oxidised zones of lead deposits	Galena, hydrocerussite, lead, massicot and plattnerite
Macphersonite	Oxidised zones of lead deposits	Caledonite, cerussite, galena, leadhillite, mattheddleite, pyromorphite, quartz, scotlandite and susannite
Massicot	Oxidised zones of lead deposits	Cerussite, Fe-oxy/hydroxides, litharge, minium, Sb-oxides and wulfenite
Mimetite	Secondary mineral in oxidized zone of Pb-As ore	Fornacite, schulténite, anglesite, cerussite, smithsonite, pyromorphite and wulfenite
Minium	Oxidised zones of lead deposits	Cerussite, galena, lead, litharge, massicot, mimetite and wulfenite
Palmierite	Can be deposited directly from volcanic fumaroles	Jarosite, hematite, aphthitalite and ferronatrite
Phosgenite	Secondary, in oxidized zone of lead-bearing ore (in particular galena). Secondary, by reaction of lead minerals with the seawater	Barstowite, cerussite, anglesite and laurionite
Plattnerite	Oxidation product during hydrothermal mineralization [also from Cu-Fe-Pb oxysulfide precursors, see Kucha 1998]	Aurichalcite, calcite, cerussite, duftite, hemimorphite, leadhillite, hydrozincite, mimetite, murdochite, pyromorphite, quartz, rosasite, smithsonite and wulfenite
Plumbonacrite	Oxidized zone of hydrothermal polymetallic deposits	Anglesite, linarite, galena and somersetite
Scrutinyite	Oxidation product during hydrothermal mineralization	Fluorite, 'limonite' (Fe-oxy/hydroxides), murdochite, plattnerite, quartz and rosasite

Table 3 (continued)

Phase	Occurrence	Association
Schulténite	Secondary mineral in oxidized zone of Pb-As ore	Anglesite, barite, bayldonite, bornite, cerussite, cuproadamite, galena, arsenopyrite, olivenite, duftite, scorodite, mimetite, tsumebite and tennantite
Somersetite	Hydrothermal veins—remobilization of older, limestones hosted veins of galena, fluorite, calcite and baryte. 'Manganese pods'. Forms very thin intergrowths with plumbonacrite	Aragonite, baryte. calcite, cerussite, diaboleite, hydrocerussite, manganese oxide, mereheadite, mimetite, plumbonacrite. quartz and symesite
Susannite	Rare in oxidized zones of hydrothermal lead-bearing deposits (forms from leadhillite at 82 °C)	Anglesite, caledonite, cerussite, lanarkite, leadhillite and macphersonite
Syngenite	In marine salt deposits, as diagenetic product. Can be deposited directly from volcanic gas or hydrothermal fluids	Halite, monetite, whitlockite, gypsum and brushite
Vanadinite	Secondary mineral, in the oxidized zones of lead-bearing deposits	Cerussite, anglesite, galena, mimetite, pyromorphite, barite, iron oxides, calcite, wulfenite and crocoite

forms), while hydrocerussite formed in a biomediated experiment was poorly crystalline.

A possible differentiation in the type of raw materials used for production has been suggested by Niknejad and Karimy (2019). These authors provided an in-depth analysis on the production of Persian lead white (*sefidāb-i-sorb*), starting from the analysis of three technical treatises: the *Bayān al-sanāāt* (second half of the 12th century), the *Gowhar-nāmeh* (15th century) and the *Qānoun al-sovar* (1533–1608). The reconstruction of the process allowed for the observation that the raw material (*Murdārsanj*, *i.e.* PbO) mixed with salt (NaCl) led to the formation of laurionite (Pb(OH)Cl), blixite ($Pb_8O_5(OH)_2Cl_4$) and phosgenite ($Pb_2Cl_2(CO)_3$), thus also providing a possibly discriminating element between European and Persian productions[4].

Lead white in artwork

Between the 4th century BC and the 4th century AD, attestations of the use of lead white, regarding the Mediterranean area, are few and limited to coffin cartonnage, earthenware, wall paintings and wood portraits found in Egypt, Italy and, possibly, Ukraine (*e.g.*, Sack et al. 1981; Smith and Barbet 1999; Scott et al. 2003; Aliatis et al. 2010; Salvant et al. 2018; de Ferri et al. 2019; Abdallah et al. 2020; Tarquini et al. 2020).

According to *Plinius*, white lead was indispensable, in the Roman period, for representing shadows (Table 1, P5); however, the identification of this pigment in the waterproofing caulking of the 1st BC to the 1st AD San Rossore shipwrecks (Pisa, Italy) testifies to its further use, beyond decorative purposes (Colombini et al. 2003).

Between the 4th and 7th centuries, such attestations are even fewer. Some hydrocerussite occurrences have been reported in the wall paintings of Coptic monasteries and on Sutra parchment both from Wadi El Natrun in Egypt (Moussa et al. 2009) and China (Liu et al. 2016, 2019).

Conversely, starting from the 8th century AD, there was an increase in its use, culminating in a real boom in the 17th century (Figure 3A). Although this reconstruction is affected by the 'state-of-the-art effect', it can be considered true, in general terms.

Lead white has been found on sculptures in alabaster, limestone, sandstone, ceramic and wood, as well as on earthenware (*e.g.*, 'campana' reliefs), wall paintings, oil paintings on canvas, glass and wood icons, paper (*e.g.*, 'lajan'), wallpaper and parchment in illuminated manuscripts and even on wooden musical instruments (*e.g.*, a harpsichord).

The painters were perfectly aware of the instability of lead pigments in fresh lime plasters (*e.g.*, alkaline and humid environments); therefore, they used the *a secco* technique for them selectively (see, *e.g.*, Cavallo et al. 2012; Liu et al. 2016; Levstik et al. 2019; Figures 4A, B). Consequently, the combination of *fresco* and *secco* techniques has been frequently reported in wall paintings (see also Gebremariam et al. 2013; Hradil et al. 2013; Malletzidou et al. 2019).

The distemper technique has also been found in early 3rd to 4th centuries AD Egyptian paintings on canvas (Sack et al. 1981), through to a 19th-century painted plafond of a house in St. Petersburg (Russia; Petrova et al. 2019; lead white uncertain). Egg-tempera (*e.g.*, Stanzani et al. 2016; Serafima et al. 2019a), oil tempera (Fiorillo et al. 2020), '*tempera grassa*' (Cardell et al. 2009; Bratu et al. 2015) and modified egg-tempera (*e.g.*, Lazidou et al. 2018) represent the most common techniques used for wood painting, especially for icons.

Typical uses of lead white also regard the preparation of the priming layers and grounds and for the application of thin foils. In the first case, the examples are very numerous between the 12th and 19th centuries. For example, priming layers constituted of lead white

[4] Blixite and laurionite have also been possibly found in Angkor Wat, Cambodia (Uchida et al. 2012)

Cerussite: $Pb + C + \frac{3}{2}O2 \rightarrow PbCO_3$

-1315.5 ΔfG°/kJ mol-1; -1315.5 ΔfG°/nPb/kJ mol Pb-1

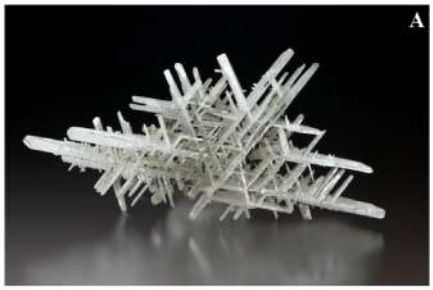

CERUSSITE

$3PbCO_3 + H_2O \rightarrow Pb(OH)_2 \cdot (PbCO_3)_2$ (hydrocerussite) $+ CO_2$ (Mercy et al. 1998)

$PbCO_3 + H_2O_2 \rightarrow PbO_2$ (plattnerite) $+ H_2CO_3$ (Petushkova & Lyalikova 1986)

Hydrocerussite: $3Pb + 2C + 2O_2 + H_2 \rightarrow 2PbCO_3 \cdot Pb(OH)_2$

-1699.8 ΔfG°/kJ mol-1; -566.6 ΔfG°/nPb/kJ mol Pb-1

HYDROCERUSSITE

$Pb_3(OH)_2(CO_3)_2 + CO_2 \rightarrow 3PbCO_3$ (cerussite) $+ H_2O(l)$ (Taylor and Lopata 1984)

$Pb_3(OH)_2(CO_3)_2 + CO_3^{2-}(aq) \rightarrow 3PbCO_3$ (cerussite) $+ 2OH^-_{(aq)}$ (Taylor and Lopata 1984)

$Pb_3(OH)_2(CO_3)_2 + 2H^+ \rightarrow 3Pb^{2+} + 2CO_3^{2-} + 2H_2O$ (Mendoza-Flores et al. 2017)

$Pb_3(CO_3)_2(OH)_2 \xrightarrow{300\text{-}400°C} *3PbO + 2CO_2 + H_2O$ (de la Roja 2008)

$2PbCO_3 \cdot Pb(OH)_2 + 2H_2S \rightarrow 2PbS$ (galena) $+ 2CO_2 + 6H_2O$ (Goltz et al. 2013)

$2PbCO_3 \cdot Pb(OH)_2 + 3H_2S \rightarrow 3PbS$ (galena) $+ 2CO_2 + 4H_2O$ (Franceschi et al. 2010)

$2PbCO_3 \cdot Pb(OH)_2 + H_2O_2 \rightarrow 2PbCO_3$ (cerussite) $+ PbO_2$ (plattnerite) $+ H_2O$ (Petushkova & Lyalikova 1986)

$2PbCO_3 \cdot Pb(OH)_2 + 3H_2O_2 \rightarrow 3PbO_2$(plattnerite) $+ 2H_2CO_3 + 2H_2O$ (Petushkova & Lyalikova 1986)

$4Pb(CO_3) \cdot 2Pb(OH)_2 + O_2 \rightarrow 2Pb_3O_4$ (red lead) $+ 2H_2O + 4CO_2$ (Kotulanová et al. 2009)

$2PbCO_3 \cdot Pb(OH)_2 + \frac{3}{2}O_2 \rightarrow 3PbO_2$ (plattnerite) $+ 2CO_2 + H_2O$ (Giovannoni et al. 1990)

$2PbCO_3 \cdot Pb(OH)_2 + 2O_2 \rightarrow 3PbO_2$ (plattnerite) $+ 2CO_2 + 2H_2O$ (Franceschi et al. 2010)

$5[2PbCO_3 \cdot Pb(OH)_2] + Ca(OH)_2 \rightarrow 3[Pb_5O(OH)_2(CO_3)_3$ (plumbonacrite)$] + CaCO_3 + 3H_2O$ (Aze 2005)

$2PbCO_3 \cdot Pb(OH)_2 + 2Ca(OH)_2 \rightarrow 3PbO \cdot H_2O + 2CaCO_3 + 2H_2O$ (Aze 2005)

$2[2PbCO_3 \cdot Pb(OH)_2] + Ca(OH)_2 \rightarrow Pb_5O(OH)_2(CO_3)_3$ (plumbonacrite) $+ \alpha$-PbO (litharge) $+ CaCO_3 + 2H_2O$ (Aze 2005)

Fig. 1 Cerussite (**A**) and hydrocerussite (**B**). Standard chemical reaction of formation (Franceschi et al. 2010 after Weast 1998), thermodynamic data and chemical reaction involving its transformation. Mineral photos: cerussite and hydrocerussite from the Tsumeb Mine, Namibia [Arkenstone specimens. Photo credits: Rob Lavinsky, irocks.com–Mindat.org Photo ID 18565 and 173886 – Copyrighted. Permission has been obtained for reproduction in this article]. The CC-BY licence does not supersede previously copyrighted material; therefore, these images remain under owner's copyright]

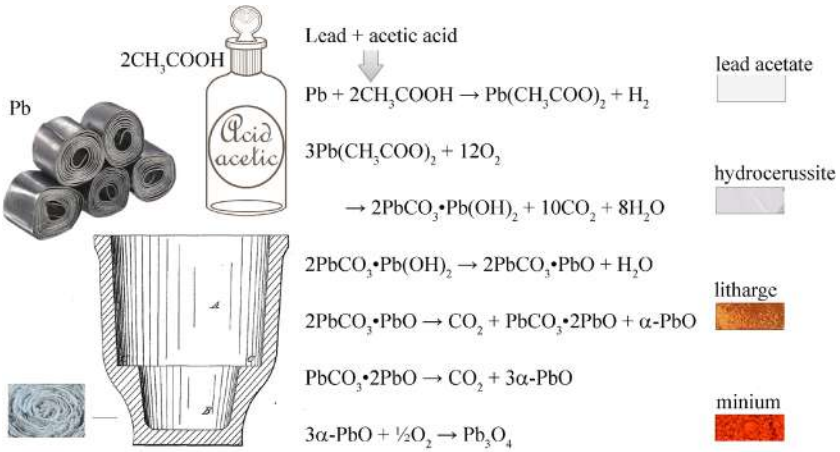

Fig. 2 The production of lead white and minium starting from lead sheets and acetic acid. The pot for corroding lead white was patented by J.H. Chadwick (US Patent #: US000051018) on 21 November 1865

has been found (a) in medieval (~12th – 13th centuries) polychrome sculptures and reliefs of the Ferrara Cathedral and Parma Baptistery (Pinna et al. 2020); (b) in several oil paintings on canvas, such as those by Carlo Bononi (*The Coronation of the Virgin*, Ferrara 1617; Impallaria et al. 2020), Jan de Bray (*Judith and Holofernes*, 1659 on oak panel; Albertson et al. 2019) and several Spanish painters of the 16th – 17th centuries (Doménech-Carbó et al. 2019); and (c) in a 16th-century Coptic icon, mixed with hemp fibres, animal glue and gypsum (Abdel-Maksoud et al. 2020). Two priming layers of lead white and oil (first) and lead white mixed with lead-tin yellow I (second) have even been found in the *Salvador Mundi*, allegedly painted by Leonardo da Vinci around 1500 (Gutman Rieppi et al. 2020).

The realisation of grounds with lead white is even more frequent. For example, (a) in oil paintings on canvas such as those by Bartolomé Esteban Murillo (linen canvas, 1618–1682, Seville; Križnar et al. 2019); (b) in the 17th-century *Martyrdom of Saint Sebastian*, painted by Cecco del Caravaggio (Jasiński 2019); (c) in the polychrome plasterworks of the Alhambra complex at Granada (Spain; Arjonilla et al. 2019b); (d) in late 19th-century paintings, such as *Exit from the Theater*, attributed to Honoré Daumier (1863; Smieska et al. 2019); and (e) in the 16th-century oil paintings on wood altarpiece by the Portuguese painter Garcia Fernandes (act. 1514–1565), kept in the Goa Cathedral in India (Antunes et al. 2018).

In this regard, the use of lead white for the coating of 17th to 20th century *Lajian* (wax-coated) paper has been investigated by Li et al. (2020c); for its use in manuscripts, the reader is referred to Burgio (2021), in this TC.

As for the use of lead white in gilding, the studies carried out by Sansonetti et al. (2010) have illustrated some possible stratigraphic sequences. The authors carried out extensive research on 17th- to 19th-century stuccoes in four different monuments in Lombardy (Italy) and found different sequences in the gilding preparation layer[5].

Further analytical evidence has been provided by (a)Blasco-López et al. (2016), who investigated the 14th- to 17th-century plasterwork of the Salón de Embajadores in the Royal Alcázar of Seville (Spain) and found cerussite and linseed oil as a preparation layer for gold foil (covering a gypsum layer); (b) Pinna et al. (2020), who investigated the medieval porch of the main portal of the Ferrara Cathedral (Italy) and found a mixture of white lead, lead-tin yellow I, red ochre and anatase in the preparation layer of gold gilding; and (c) Sansonetti et al. (2020), who investigated 17th-century stuccoes made by the Italian 'Artists of the Lakes' in Lombardia[6] (Italy) and found gold leaf applied over a '*missione*' made of chrome yellow or ochre mixed with lead white.

As for its association with other inorganic materials, gypsum (Armenini 1856) and, more frequently, calcite/chalk have been reported (see, *e.g.*, Coremans and Thissen 1962; Edwards et al. 2000; Castro et al. 2004a; Edwards et al. 2007 also with barite; Kotulanová et al. 2009; de Ferri et al. 2019 also with dolomite). The role of calcite in modifying pigments properties has been deepened by de Viguerie et al. (2018), who demonstrated that calcite addition increases the transparency, the elastic and viscous moduli and the yield stress of pure lead white. A mixture with chalk was also used by several 16th- to 17th-century Dutch painters, who called it '*lootwit*', as opposed to the '*schelpwit*'

[5] Artworks kept at Mantova in the Church of Sant' Andrea and at Milan in the Sanctuary of Rho, the Church of San Fedele and the Royal Palace. From the oldest to the most recent layers (separated by dashes): (a) yellow ochre - colophony + wax – Cu + Zn gilt - lead white, cinnabar, chrome yellow - siccative oil - lead white, cinnabar, chrome yellow and orange – Au + Cu gilt; (b) lead white, red ochre - Au gilt - lead white, minium, red ochre, calcite - Au gilt - colophony + wax - lead white, barium white, yellow ochre, chrome yellow - lead white, yellow ochre - Au + Cu gilt; (c) red ochre, minium – Au + Cu gilt - lead white, barium white - lead white, barium white, yellow ochre - Au gilt; and (d) lead white, minium, yellow ochre, oil - lead white, yellow ochre, oil - Au gilt - lead white, calcite, yellow ochre, oil - Au gilt - Prussian blue, lead white, oil (over painted).

[6] Artworks kept in the Church of S. Lorenzo in Laino, Church of S. Maria dei Ghirli in Campione d'Italia and Church of S. Maria Assunta in Puria.

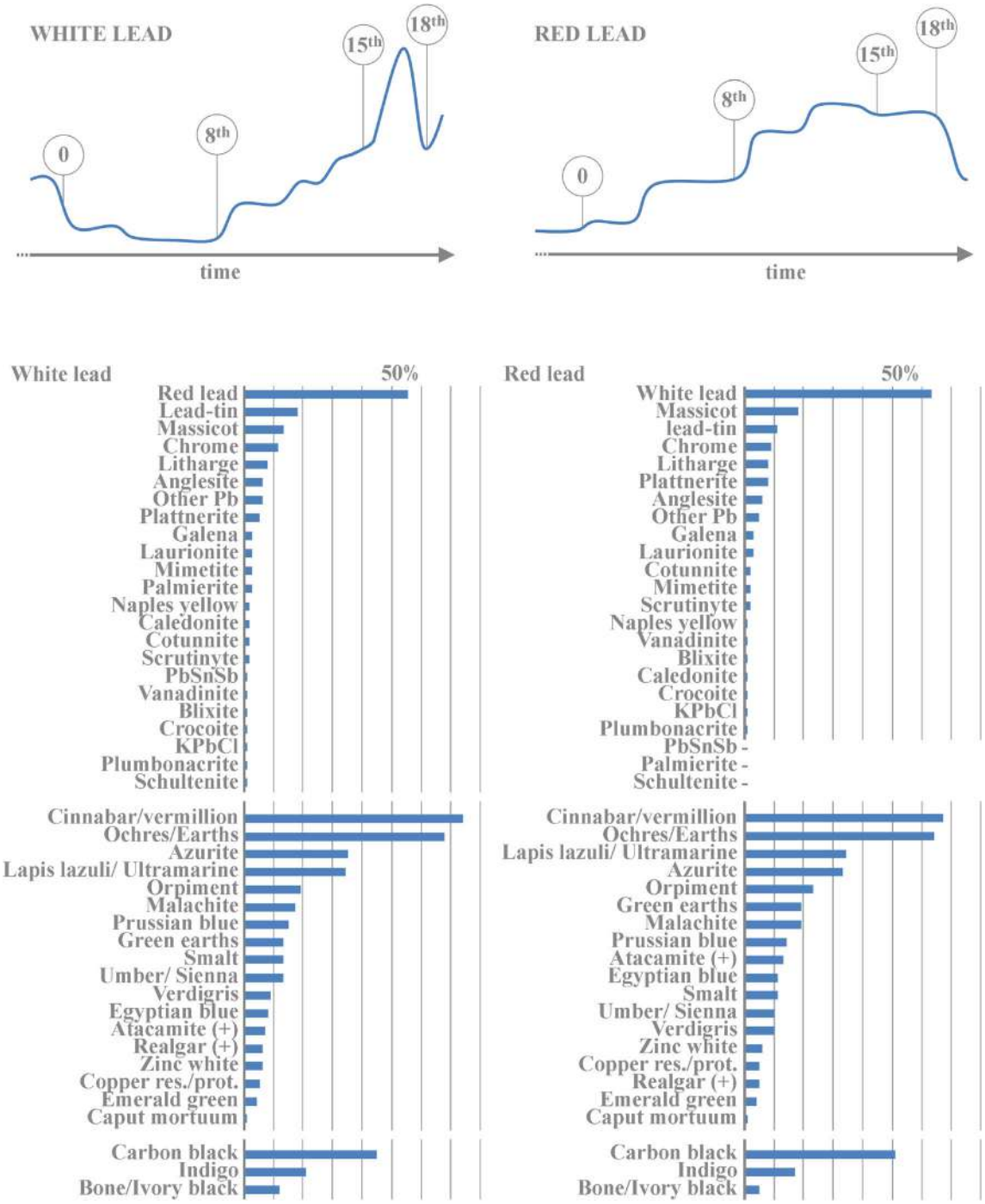

Fig. 3 A simplified overview of the use of lead white (**A**) and red lead (**B**) over the centuries. Information relating to the occurrences of the various phases in artworks was drawn from personal filing, using the references listed in Supplementary Materials, Appendix 1. The occurrences include, without distinction, all types of supports and techniques

made of pure white lead (Van der Graaf 1961). Among the other pigments, lead white has been frequently associated with most of them, to lighten their colours.

As for its combined use with organic pigments, it is interesting to note the associations with carbon black, indigo and red lakes; these latter seem primarily used when minium is absent, although this is not a rule.

Certified evidence helps us to understand the distribution and methods of use of the lead white; however, the most important aspect that can be deduced from the literature is

Fig. 4 Details of the 'Madonna and Child enthroned with Saints' painted by Ambrogio Lorenzetti in the first half of the 14th century AD (Damiani et al. 2014). The wall painting is preserved in the St. Augustine Church (Siena, Italy). **A** For the vest of the Child, white lead was painted *a secco*. **B** The vest of Saint Agatha was painted *a secco* using white lead. **C** The orange hues of the throne formed by the wings of the cherubim were painted with red lead. **D** Scanning electron microscope, backscattered electrons imagery, showing a colony of fungi formed on a layer of white lead. [The CC-BY licence does not supersede previously copyrighted material; therefore, these images remain under owner's copyright.]

linked to this pigment's characterisation, bearing an invitation to greater accuracy in determining the phases present in artworks. Indeed, cerussite and hydrocerussite have been found both individually and in combination (Prieto et al. 2005; Gonzalez et al. 2016, 2017a, b, 2019a, b; Vanmeert et al. 2018; De Meyer et al. 2019a; van Loon et al. 2019). Archaeometric studies have highlighted the importance of their qualitative and, possibly, quantitative determination, as they have different behaviours, especially in terms of reactivity.

In this regard, the experimental studies performed by Kotulanová et al. (2009) and Vagnini et al. (2020) represent a milestone, with regard to the characterisation of both pigments and the transformations that can occur to these two phases, considered individually or combined (see below). Applied studies, such as those performed by Gonzalez et al. (2019a), are further fundamental in understanding how painters used lead-based white mixtures and how to analyse them. These authors, for example, demonstrated that the *impasto* used by Rembrandt van Rijn (The Netherlands, 1606–1669) was made of a mixture of cerussite and hydrocerussite (with very high HC: C ratio) and that plumbonacrite, which is stable only in alkaline conditions (pH > 10), may have resulted from the carbonation of the PbO drier.

Transformation and alteration products

Several experimental tests have been devoted to investigating the transformation of lead white into litharge, massicot and red lead. For example, Senna and Kuno (1971) obtained massicot from lead white heated at ~600 °C. Ciomartan et al. (1996) studied the thermal decomposition of basic lead(II) carbonate (static air, atmospheric conditions) and found several intermediate products between 21 and 370 °C (Figure 5). De la Roja et al. (2008) investigated the chromatic variations of lead white roasted at 330 °C as a function of time.

Similarly, San Andrés et al. (2008) demonstrated how time and temperature transform lead white into different lead-based compounds as follows:

(1) a mixture of litharge, massicot and lead oxide carbonate ($Pb_3O_2(CO_3)$) is obtained by roasting lead white at 600 °C for 15 min;
(2) massicot, along with other lead oxides (Pb_2O_3 and Pb_5O_8), is obtained by roasting lead white at 600 °C for at least 45 min;
(3) litharge is obtained by using a lower temperature (~330 °C) for a longer time (~3–4 h);
(4) red lead is obtained after about 20 h (at ~330 °C).

As for alteration products, the darkening of lead white is a typical alteration issue resulting from its conversion into lead sulfide (PbS, galena) or lead dioxide (scrutinyite α-PbO_2 and plattnerite β-PbO_2). Several authors have reported on this alteration, especially in watercolours, manuscripts, canvas and wall paintings (Augusti 1949; Plenderleith 1956; Carlyle and Townsend 1990; Giovannoni et al. 1990; Roy 1993; Clark and Gibbs 1998; Burgio et al. 1999; Saunders 2000; Andalo et al. 2001; Clark 2002; Smith and Clark 2002a, b; Goltz et al. 2003; Saunders and Kirby 2004; Franceschi et al. 2010; Gutman et al. 2014; Melo et al. 2016; Coccato et al. 2017; Vagnini et al. 2020), as well as in out-door decorations, such as polychrome ceramic statues (Pérez Rodríguez et al. 1998).

From these studies, it becomes clear that many various factors can induce the darkening and blackening of white lead. These range from pollutants (*e.g.*, SO_2, SO_3, NO_x), alkali, salts, acids, hydrogen sulfide (H_2S) and oxidising agents to other environmental factors such as humidity, temperature and microbial activity.

In the literature, it has often been repeated that the darkening process of white lead is still not fully understood. Indeed, the basic problem is that the variables involved are so numerous and different from each other that any type of painting technique, pigment, binder and environmental condition can speed up, slow down and/or drive the transformations, in one sense or another. This aspect clearly emerged in some valuable experimental works, which are summarised below.

Goltz et al. (2003) performed a series of tests using basic lead carbonate mixed with various binders (linseed oil, gum Arabic, water and egg tempera) and evaluated their behaviour under exposure to $H_2S_{(g)}$. Darkening occurred after ~24 h at 20 °C and after only 2 h at 50 °C. Using the same time frame, (a) all of the different binding agents seemed to play protective roles and (b) the mixture containing lead white and other S-containing pigments, such as cinnabar, orpiment and realgar, did not result in darkening (experiment carried out in the darkness).

Kotulanová et al. (2009) tested the behaviour of several lead-based pigments (lead white, massicot and minium) in the presence of various types of inorganic salts, both those naturally present in the environment (Na_2SO_4, $MgSO_4$, $CaSO_4$, NaCl, $NaNO_3$, $Ca(NO_3)_2$, Na_2CO_3, K_2CO_3 and urea) and those synthetically prepared for restoration ($NaHCO_3$, $KHCO_3$, $(NH_4)_2CO_3$ and NH_4HCO_3). The treatment of cerussite (containing 68% cerussite, 6% hydrocerussite and 26% shannonite) left only cerussite, regardless of whether natural or synthetic salts were used. The times detected for the transformations were different, and the authors observed other products (potassium basic lead carbonate, laurionite and abellaite, using K_2CO_3, NaCl and Na_2CO_3/$NaHCO_3$, respectively) in only three cases. In one case (using $CaSO_4$), the hydrocerussite remained for over a year. The lead white (containing hydrocerussite, lead acetates, lead oxide sulfate hydrate and plumbonacrite)

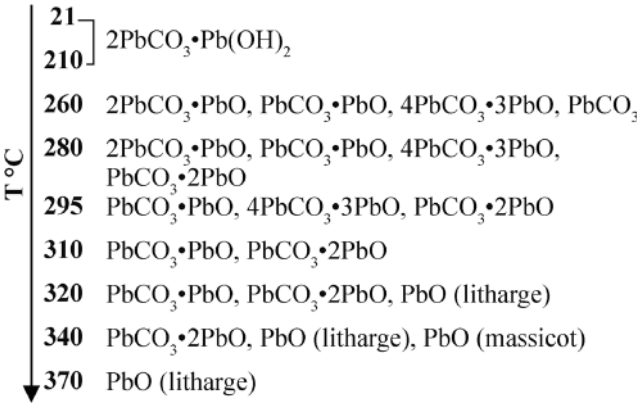

Fig. 5 The main steps following the exposure of lead to acetic acid (data from Ciomartan et al. 1996)

reacted with all the salts used providing different products[7]. Only when a strong oxidising agent such as NaClO was introduced into the water suspension was darkening observed, together with the formation of plattnerite and scrutinyite (along with remnants of the pre-existing phases and cerussite). Accordingly, the same experiment conducted with hydrogen peroxide (30%) did not show any colour change.

Vagnini et al. (2020) conducted a series of experiments, using cerussite and hydrocerussite taken individually. First, they experimentally reproduced two extreme RH conditions (*i.e.* at 93% and 8% RH, 25 °C), in order to study the transformation of cerussite and hydrocerussite during lime carbonation. Secondly, they tested the oxidation potential of sodium hypochlorite (NaClO) when applied to these two phases.

For the first series of experiments, both cerussite and hydrocerussite were mixed with two parts of lime (to partially simulate *fresco* conditions); for the second series, cerussite and hydrocerussite were applied with a proteinaceous binder on 'a secco' painting mock-ups and covered for about 2 h with a cotton pack embedded with NaClO.

Investigations conducted on the first series showed the following:

(a) at 93% RH, cerussite transformed into litharge in 18 days and disappeared after 370 days;
(b) at 8% RH, hydrocerussite transformed into litharge and massicot in 204 days and then released massicot and minor red lead as final products at 370 days;
(c) at 93% RH, hydrocerussite turned into massicot in 2 days, massicot and red lead formed in 98 days and, finally, only red lead and minor massicot were observed after 370 days.

Overall, the main achievements reached by these authors can be summarised as follows:

(1) the alkaline environment favoured the oxidation of hydrocerussite (hydrocerussite Pb(II) → red lead Pb(II) and Pb(IV)) but not that of cerussite (cerussite Pb(II) → litharge Pb(II)), the reaction being accelerated by high percentages of humidity;
(2) the alkaline environment was not sufficient to trigger the transformation of litharge into massicot in cerussite samples, while high RH percentages favoured the formation of red lead in hydrocerussite samples (maintaining a basic environment);
(3) even under high alkalinity, the formation of plattnerite or scrutinyite (Pb(IV)) is not a spontaneous process, as it requires strong oxidising agents. These phases were obtained only by the effect of a strong reducing agent such as sodium hypochlorite;
(4) the application of sodium hypochlorite confirmed the greater reactivity of hydrocerussite, compared to cerussite, and the preferential formation of plattnerite by cerussite and scrutinyite by hydrocerussite;
(5) while the oxidation process triggered by NaClO is completed using either cerussite or hydrocerussite, cerussite transformed into plattnerite and minor scrutinyite (+halite); conversely, hydrocerussite transformed into cerussite, scrutinyite and minor plattnerite (+halite).

Salvadó et al. (2009) demonstrated the formation of lead carboxylates in 15th-century oil and egg yolk tempera paintings and observed that lead and calcium carboxylates were "*more crystalline with the egg yolk than with the drying oil*".

Finally, Petushkova and Lyalikova (1986) investigated the role of microbial activity in the conversion of lead white to lead sulfide. They observed the formation of yellow (4 days) and brown (6 days) lead precipitates due to the growth of *Arthrobacter siderocapsulatus*. Petushkova and Lyalikova (1986) and Aze et al. (2008a) regarded plattnerite as an alteration product of lead white and massicot.

The few examples proposed above allow us to clarify that there is no single factor that can be deemed responsible for all cases (see also the section focused on lead soaps below). Moreover, while it is realistic that the variables to be identified as responsible for a specific case study are more than one, it can be even more difficult to 'quantify' the contribution of one variable over that of another.

To conclude this first part on lead white, it is also worth adding that the selective application of hydrogen peroxide can convert black lead sulfide (PbS) into white lead sulphate

[7] The products were only cerussite using $(NH_4)_2CO_3$ or NH_4HCO_3; only abellaite using Na_2CO_3; cerussite + abellaite using $NaHCO_3$; cerussite + hydrocerussite using $(NH_2)_2CO$; cerussite + potassium basic lead carbonate using $KHCO_3$; hydrocerussite + potassium basic lead carbonate using K_2CO_3; hydrocerussite + cerussite + leadhillite using Na_2SO_4 or $CaSO_4$; and same + lanarkite using $MgSO_4$.

($PbSO_4$), which is commonly used as a restoration technique (Carlyle and Townsend 1990; Daniels and Thickett 1992; McFarland 1997; Lussier 2008). As already described by Plenderleith (1956), the method was definitively tested by Giovannoni et al. (1990), using hydrogen peroxide (H_2O_2) and acetic acid (CH_3COOH), partially retracing how the lead white was originally produced. After Giovannoni and co-workers, this method was named the 'Florentine method' by Koller et al. (1990), who applied it to the painted vault (c. 1580 AD) of the Strechau castle in Styria (Austria). This technique is still in use, although not always successfully (see, *e.g.*, McFarland 1997).

Red lead—minium (Pb_3O_4)

Mineralogical phase, structure and occurrence

Minium is a red lead oxide (Table 2; Figure 6) that is mainly found in association with galena and cerussite (Table 3). On the origin of the name minium (μίνιο) and its relationship with cinnabar (κινναβαρι), see Trinquier (2013) and Becker (2021) in this TC.

The crystal structure of minium was first determined by Byström and Westgren (1943) and Gross (1943) and then deepened by Gavarri and Weigel (1975) and Gavarri et al. (1978). A significant number of papers have focused on the thermal behaviour of this phase and the effects of grinding (see, *e.g.*, Dachille and Roy 1960; White et al. 1961; Aleksandrov et al. 1978; Avvakumov et al. 1983; Bohér and Garnier 1984; Boher et al. 1984; Barriga et al. 1988; Zyryanov and Gusev 2001). More recently, Zhou et al. (2012), Vanmeert et al. (2015) and Ayalew et al. (2016) have investigated the photoactivity of minium. The mechanisms proposed in the former two papers are illustrated in Figure 6A. As for the third paper, the authors experimentally tested the photoactivity of minium both in the presence and absence of bicarbonate ions and demonstrated the importance of these processes (formation of PbO or hydrocerussite) in the degradation processes. Following the studies performed by Kang et al. (1988), Guo et al. (2016) simulated a depleting chlorine regime to investigate the dissolution of minium and proposed a rational model of the process (Figure 6B).

The natural mineral occurs in the oxidised part of lead ore deposits, where it is associated with several lead minerals (Table 2), particularly galena, cerussite, litharge and massicot. Minium can be found in many places but only in low amounts (Anthony et al. 1990). Notable occurrences are Mežica (Slovenia), Leadhills in Lanarkshire (Scotland, UK), Sarrabus in Sardinia (Italy), Tsumeb (Namibia), Långban Mine (Sweden), TchahMilleh Mine (Iran), Bleialf in Rheinland-Pfalz (Germany) and Leadville in Colorado (USA).

The production of red lead

In ancient texts, the production process was handed down by various authors. *Plinius* specified that the discovery was accidental, following the *Piraeus* fire (Table 1, P5); similarly, *Vitruvius* handed down that it "*was discovered as the result of an accidental fire*" (Table 1, V1). Among the manufactured products, *Plinius* also included two other varieties: (1) a high-quality variety, the *Asiatica* (Table 1, P5), characterised by purple shades, and (2) a variety manufactured in Roma, which was obtained from the calcination and subsequent quenching with vinegar of *sile marmoroso* (ochre hard as marble; Table 1, P5—in this latter case, however, the reference is unclear).

Dioscorides (Table 1, D2), *Vitruvius* (Table 1, V1) and *(H)Eraclius* (Table 1, E1) similarly describe lead white roasting as the production process of red lead and some compare its colour to that of *sandaraca*.

Based on archaeometric research and experimental work, the various steps leading to red lead production have been clearly described by Ciomartan et al. (1996), Aze (2005) and Aze et al. (2007). As schematised in Figure 2, after the formation of hydrocerussite from the acetate formed on the surface of lead sheets, subsequent roasting induces the decarbonisation and dehydration of hydrocerussite, which leads to the production of litharge. Finally, the oxidation of litharge leads to the formation of red lead.

Indeed, red lead was mainly produced by roasting lead white (hydrocerussite) or litharge (Saunders et al. 2002); however, the decomposition of hydrocerussite can trigger the formation of intermediate phases (*e.g.*, $4PbCO_3{\cdot}3PbO$ and $PbCO_3$) and final products (*e.g.*, only red lead or combined with other phases such as PbO), mainly depending on the temperature and oxygen fugacity conditions under which the process took place. Consequently, either litharge or (if using high temperatures) massicot may be present at the end of the process, due to incomplete reactions (Ciomartan et al. 1996; Boden 1998; Risold et al. 1998)

Considering the rarity of minium as a natural mineral and the information handed down by ancient texts, it seems appropriate to believe that almost all red lead used in antiquity was of artificial origin, although we cannot exclude the use of natural minium. In this latter case, it may also have been called by other names, considering that impurities of various types may vary the shade of the pigment. Moreover, the production of red lead may have represented a secondary product of silver smelting and, more specifically, of the waste litharge (Walton and Trentelman 2009).

Red lead in artwork

As with other lead-based pigments, red lead-based compounds were likely used first as drugs rather than as colouring

Minium: $3Pb + 2O_2 \rightarrow Pb_3O_4$

-601.2 ΔfG°/kJ mol-1; -200.4 ΔfG°/nPb/kJ mol Pb-1

MINIUM

$Pb_3O_4 + 4H^+ = PbO_2 + 2Pb^{2+} + 2H_2O$	(Kang et al. 1988)	[1]
$Pb_3O_4 + 4H_3O^+ \rightarrow \beta\text{-}PbO_2 + 2Pb^{2+} + 6H_2O$	(Aze et al. 2007)	[2]
$Pb_3O_4 + 2H_2SO_4 \rightarrow \beta\text{-}PbO_2 + 2PbSO_4 + 2H_2O$	(Aze et al. 2007)	[3]
$Pb_3O_4 + O_2 = 3PbO_2$	(Aze 2005)	[4]
$Pb_3O_4 + 4H^+ \rightarrow PbO_2$ (plattnerite) $+ 2Pb^{2+} + 2H_2O$	(Aze et al. 2008)	[5]
$Pb_3O_4 + 2H_2O_2 \rightarrow 3PbO_2 + 2H_2O$	(Aze 2005)	[6]
$Pb_3O_4 + 4[H^+, C_2H_3O_2^-] \rightarrow PbO_2 + 2[Pb^{2+}, (C_2H_3O_2^-)_2] + 2H_2O$	(Aze 2005)	[7]
$Pb_3O_4 + 2[2H^+, SO_4^{2-}] \rightarrow PbO_2 + 2PbSO_4 + 2H_2O$	(Aze 2005)	[8]

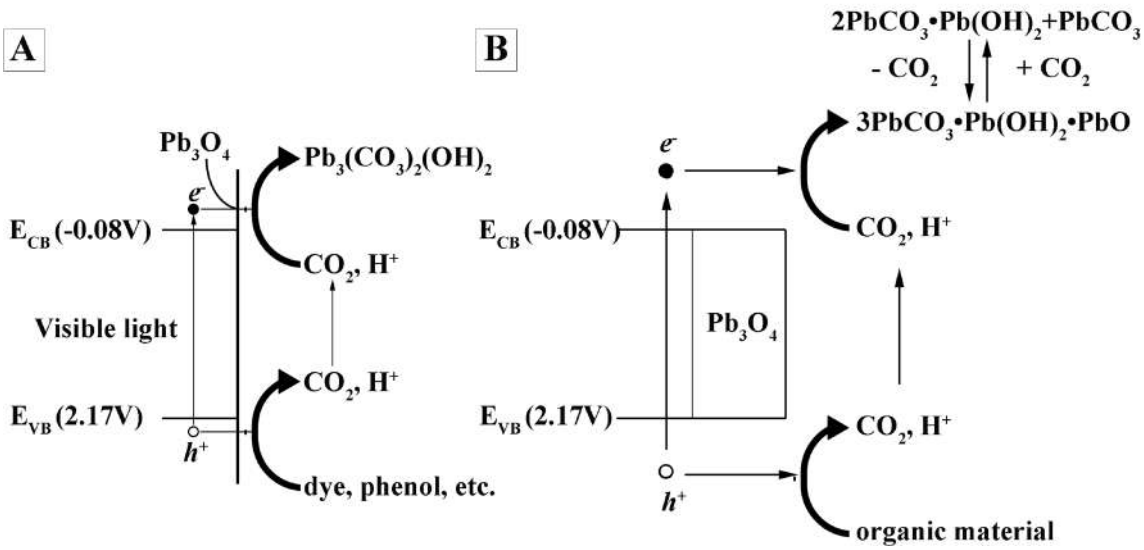

Fig. 6 Minium: standard chemical reaction of formation (Franceschi et al. 2010 after Weast 1998), thermodynamic data and chemical reaction involved in its transformation. The mineral shown is from Broken Hill, New South Wales, Australia [Arkenstone specimen. Photo credits: Rob Lavinsky, irocks.com–Mindat.org Photo ID 1013485 – Copyrighted. Permission has been obtained for reproduction in this article. The CC-BY licence does not supersede previously copyrighted material; therefore, these images remain under owner's copyright]. Mechanism of photochemical degradation of red lead, as proposed by (**A**) Zhou et al. (2012) and (**B**) Vanmeert et al. (2015).

pigments. It is not surprising that, in the Ebers Papyrus (~ 1550 BC), red lead is often indicated as a remedy to combat diseases such as *pterygium* (as well as other eye and vision problems), alopecia, tremor of the fingers and tapeworms (Bryan 1930). Its application to different types of paintings was rare from the 2nd century BC to the 1st century AD (Figure 3), while it recorded a very sharp and progressive increase along the following centuries (Figure 3). Conversely, its use as an anticorrosive paint, textile paint (for linen cloth; Walton and Trentelman 2009 and the references therein) and decorative paint seems to have never been interrupted, up until the modern age. At present, its toxicity has led to a sharp decline of its use, mainly being relegated to the production of batteries (exploiting its properties as an electrode material) and glass (Ayalew et al. 2016).

As far as supports and techniques are concerned, the same considerations made previously for lead white apply. However, it has some noteworthy aspects:

- it has also been used to decorate paper currencies (Shi and Li 2013), inlays (Zhao et al. 2020), lacquers (Bösiger 2019) and ancient manuscripts (Aceto et al. 2008);
- it has been less used for priming layers and grounds, although it was widely used in the Alhambra complex (Granada, Spain; Cardell et al. 2009; Arjonilla et al. 2019a);
- it has been similarly used as a substrate and mordant for gilding (Pereira-Pardo et al. 2019; Mounier et al. 2020; Zhou et al. 2020);
- it has been used, likely more frequently, in *fresco* painting (see, *e.g.*, Hein et al. 2009; Almaviva et al. 2018; Khramchenkova et al. 2019), although most occurrences relate to the *fresco-secco* technique (see also Daniilia et al. 2000, 2008; Figure 4C);
- in one case, the *encausto* technique has also been reported (Gehad et al. 2015).

As for its association with other pigments, mixtures are mostly reported with lead white, calcite/chalk, cinnabar (Gliozzo 2021), red ochre and red lake. Conversely, it is rarely found alone (*i.e.* without lead white) in paintings where organic pigments have also been used, except for carbon black.

Transformations and alteration products

Among the most common degradation effects described in the literature, both whitening and blackening have been observed.

The whitening is due to the carbonation of lead monoxide, which is present in red lead as an impurity due to an incomplete reaction (see above for the production process). Lead monoxide reacts to form lead carbonates ($PbCO_3$ and $Pb_3(CO_3)_2(OH)_2$; see Aze et al. 2007 and the references therein) through different paths, mostly determined by the presence of moisture, CO_2 and media (Saunders et al. 2002).

The blackening is due to the formation of plattnerite and lead sulfide ($PbSO_4$). In the presence of dilute sulfuric acid solutions (*i.e.* atmospheric pollutants), this process includes the sulfation of Pb(II) atoms present in PbO impurities (Figure 7, Eq. 5), followed by the 'solvolytic disproportionation'[8] of Pb_3O_4 into lead dioxide (PbO_2) (Kang et al. 1988, Figure 6, Eq. 1; Aze et al. 2007, Figure 6, Eqs. 2–3).

Aimed at unravelling the alteration path of red lead, Aze et al. (2007) carried out an experimental work on naturally aged wall paintings (built in 1977), which were exposed to different conditions (alkaline, oxidant and acidic media), environments (humid and thermo-hygrometric stressed) and lighting. Firstly, the authors observed the formation of plattnerite and anglesite (+ gypsum) in the "*outer part of the pictorial layer*" and validated the formation of these lead phases in dilutes sulfuric acid solutions. Secondly, they verified that light or hydrogen peroxide did not affect red lead while confirming the importance of humidity in the formation of carbonates.

Based on Ayalew et al. (2016), the presence of CO_2 is among the main factors responsible for the photodegradation of this pigment, as it is present in the atmosphere and can also be produced in the paint, through the oxidative decarboxylation of some binders. Moreover, the presence of PbO impurities (due to incomplete synthesis during production) can significantly modify the photoactivity of lead, with coexisting Pb (II) and Pb (IV) states.

The effects of applying different binding media, such as linseed, walnut, poppy-seed and stand oil to a mixture of minium, have been thoroughly investigated by Švarcová et al. (2020). These authors observed the crystallisation of lead formate ($Pb(HCOO)_2$), due to the evaporation of formic acid from the autoxidation of drying oils and its reaction with lead particles. This lead formate represents an intermediate phase that, while not leading to chromatic variations in the painting, contributes to the formation of lead carbonates or lead soaps; therefore, it cannot be identified in artworks.

Platania et al. (2020) have also ventured on a similar theme. Based on previous studies on the formation of carbonates, chlorides, oxides and sulfates in the aggregates of metal soaps (van der Weerd et al. 2002; Boon 2006; Boon et al. 2007), they investigated red lead formed by the mineralisation of the soaps.

Finally, Mazzeo et al. (2008) verified that red lead and litharge are likely to produce higher amounts of carboxylates than lead white, lead-tin yellow and Naples yellow.

Apart from light, temperature, humidity and binding media, other key factors in the degradation process of this pigment that have been recognised are chlorine salts (Daniilia and Minopoulou 2009), microorganisms (Petushkova and Lyalikova 1986; Giovannoni et al. 1990) and fungi (Feng et al. 1999; Figure 4D).

Litharge (α-PbO) and massicot (β-PbO)

Mineralogical phases, structure and occurrence

Litharge derives from the Greek term λιθάργνρος—meaning silver stone (from λίθος, stone and ἄργυρος, silver)—and its production was explained by both Dioscorides and *Plinius* (Table 1, D1 and P2). The etymology of massicot can be vaguely associated with the early Arabic *martak*, the Italian *marzacotto*, the Spanish *mazacote* and the late 15th-century French *massicot*.

Litharge and massicot are the red (tetragonal) α-phase and the yellow (orthorhombic) β-phases of PbO, respectively (Table 2, Figure 7).

[8] The solvolytic disproportionation studied by Kang et al. (1988) is reported in Figure 7, Eq. 1 and describes the dissolution of $Pb_2(II)Pb^{I}IV)O_4$ into two compounds, with higher $[Pb(IV)O_2]$ and lower [Pb(II)] oxidation states (*i.e.* disproportionation), respectively, in the presence of a solvent.

PbO: $Pb + ½O_2 \rightarrow PbO$

-187.9 ΔfG°/kJ mol-1; -187.9 ΔfG°/nPb/kJ mol Pb-1

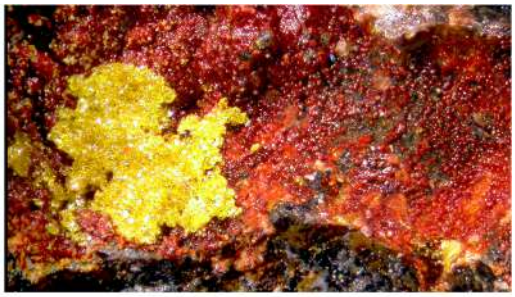

LITHARGE AND MASSICOT

$PbO + H_2O + NaCl \rightarrow Pb(OH)Cl + NaOH$	(Tapsoba et al. 2010)	[1]
$PbO + H_2O + NaCl + ½Na_2CO_3 \rightarrow ½Pb_2Cl_2CO_3 + 2NaOH$	(Tapsoba et al. 2010)	[2]
$PbO + H_2O_2 \rightarrow *PbO_2 + H_2O$	(Giovannoni et al. 1990)	[3]
$3PbO + 2HCO_3^- + H_2O \rightarrow Pb_3(CO_3)_2(OH)_2$ (hydrocerussite) $+ 2OH^-$	(Ayalew et al. 2016)	[4]
$PbO + H_2SO_4 \rightarrow PbSO_4$ (anglesite) $+ H_2O$	(Aze et al. 2007)	[5]
$3\alpha\text{-}PbO + 2CO_2 + H_2O \rightarrow 2PbCO_3 \cdot Pb(OH)_2$ (hydrocerussite)	(Aze 2005)	[6]
$5\alpha\text{-}PbO + 3CO_2 + H_2O \rightarrow Pb_5O(OH)_2(CO_3)_3$ (plumbonacrite)	(Aze 2005)	[7]
$⅗PbO + CO_3^{2-} + ⅗H_2O \rightarrow ⅙Pb_{10}O(OH)_6(CO_3)_6$ (plumbonacrite) $+ 2OH^-$	(Taylor and Lopata 1984)	[8]

Fig. 7 Litharge and massicot: standard chemical reaction of formation (Franceschi et al. 2010 after Weast 1998), thermodynamic data and chemical reactions involving their transformation. Mineral photo: litharge (red) and massicot (yellow) from the Thorikos Bay, Lavrion Mining District, Attica, Greece [Photo credits: Ko Jansen -Mindat.org Photo ID 997691–Copyrighted. Permission has been obtained for reproduction in this article. The CC-BY licence does not supersede previously copyrighted material; therefore, these images remain under owner's copyright] [*Scrutinyite or plattnerite]

Both polymorphs crystallise in a layered arrangement and their structure (Table 2; Trinquier and Hoffmann 1984) and properties have been extensively studied (see, *e.g.*, Radhakrishnan et al. 1983; Canepa et al. 2012). Both an α-phase (stable below 208 °K=−65 °C; Hédoux et al. 1989; Moreau et al. 1989) and a γ-phase are also known to occur along the litharge → massicot path (Adams et al. 1992).

Further studies have focused on their thermodynamic and mechanochemical phase transformations (Söderquist and Dickens 1967; Okuri and Ogo 1982; Trinquier and Hoffmann 1984; Baleva and Tuncheva 1994). The transition temperature between (low-temperature) litharge and (high-temperature) massicot (α→β) has been placed at 489 °C (Trinquier and Hoffmann 1984; Baleva and Tuncheva 1994), 540 °C (White et al. 1961) or 580 °C (Lin and Nadiv 1979) under atmospheric pressure. Conversely, the massicot→ litharge transformation (β→α) can be achieved at room temperature, upon mechanical treatment (*e.g.*, isothermal ball milling; see Senna and Kuno 1971, Lin and Niedzwiedz 1973; Criado et al. 1982).

Their multiple and various applications of industrial importance (*e.g.*, in photodetectors, lead–acid batteries, gasoline and integrated circuits) have chiefly stimulated recent research (see, *e.g.*, Cao et al. 2003; Perry and Wilkinson 2007; Bhagat et al. 2018); however, the occurrence of these two phases in nature is much rarer than that of galena, as they are mainly found as secondary minerals in oxidised zones of lead deposits and/or hydrothermal environments (Table 3), such as at Cucamonga Peak in California (USA), at Mežica in Slovenia, at Långban Mine (Sweden) and in the slags related to the Lavrion ancient mines in Attica (Greece) (Mindat.org).

Historically, litharge was a typical secondary product of lead cupellation during silver smelting and, from this practice, it derived the ancient denomination of *spuma argenti*. Its absence or presence at smelting sites has been variously interpreted, following Rehren et al. (1999). Either it was used as a product for medical or building purposes (*e.g.*, for waterproof lining), as a semi-finished product from which to gather residual silver, or as a tool to enhance the smelting process (added to the smelting charge). Its value was considered high enough to be worked and traded (see, *e.g.*, Negueruela et al. 2004; Renzi et al. 2009). Within the field of archaeometallurgy, other studies have regarded the occurrence of litharge in corrosion crusts after the weathering of ancient lead objects, such as lead pipes (see, *e.g.*, Essington et al. 2004), or as a tracer of ancient non-ferrous metallurgy processes (see, *e.g.*, Keim et al. 2017).

As for painting, it is a widely accepted opinion that litharge was used as a siccative (*i.e.* drying agent) rather than an art pigment (Toniolo et al. 1998). The use of litharge as a dryer

has been discussed in relation to both the palette of specific painters (*e.g.*, for Rembrandt's paintings, see Gonzalez et al. 2019a) and the formation of alteration products due to saponification (see below). The preparation of a lead medium using litharge cooked with linseed oil (in 1: 3/4 ratio) is commonly referred to Antonello da Messina (1430–1479) (Maroger 1948), but it has also been handed down by later authors (Gonzalez et al. 2019a).

Litharge and massicot in artwork

The correct assessment of the occurrence of these phases is affected by the relatively high number of cases in which the identification is not certain (see, *e.g.*, Edwards et al. 2000, 2001; Wang et al. 2004; Uchida et al. 2012; Blasco-López et al. 2016; Khramchenkova et al. 2019; Malletzidou et al. 2019).

In the cases where litharge has been identified with certainty, it appears decidedly rarer than massicot. Based on data from the literature (see Supplementary Appendix 1), it is possible to list five (perhaps six) occurrences, in which it was (a) sometimes associated with massicot, as well as lead white and red lead; (b) found in paintings ranging from the 11th to the 19th century in Europe and India; and (c) present on all types of common supports, such as wood ceilings, miniature paintings, manuscripts, wall frescoes, wooden panels and egg-tempera icons (Burgio et al. 1999; Edwards et al. 2001; López Cruz et al. 2011; Ravindran et al. 2011; Amadori et al. 2016; Stanzani et al. 2016; Arjonilla et al. 2019a; Serafima et al. 2019b).

Massicot was identified with a slightly higher frequency—18 occurrences—in which it was:

- associated with both lead white and red lead (9 cases), red lead (6), plattnerite (4), lead-tin yellow type I (3), scrutinyite (3), anglesite (2), galena (2), lead white (2), litharge (2), $PbMg(CO_3)_2$(2) and chrome orange and yellow (1):
- found in paintings ranging from the 1st to the 19th century, in Europe, India and Iran:
- present on all types of common supports, such as wood ceilings, glass icon as (fatty tempera), illuminated manuscripts and wall paintings (*fresco* and *secco*), as well as in powdered raw pigments and wood cupboards (Burgio et al. 1999; Bruni et al. 2002; Smith and Clark 2002a; Castro et al. 2008; Kotulanová et al. 2009; Aliatis et al. 2010; Ravindran et al. 2011; Hradil et al. 2013; Lukačević et al. 2013; Duran et al. 2014; Bratu et al. 2015; Holakooei and Karimy 2015; Felix et al. 2018; Kantoglu et al. 2018; Vanmeert et al. 2018; Arjonilla et al. 2019a; Khramchenkova et al. 2019; Costantini et al. 2020b; Fioretti et al. 2020).

From case to case, the presence of litharge and/or massicot can be interpreted as a deliberately used pigment, an impurity derived from red lead or, based on Vagnini et al. (2020), a secondary phase from lead white. In this regard, it may be useful to note that only massicot was identified among the powdered pigments found in Pompeii (Aliatis et al. 2010).

Crocoite ($PbCrO_4$) and mimetite ($Pb_5(AsO_4)_3Cl$)

Mineralogical phases, structure and occurrence

Crocoite is a monoclinic lead chromate (Tables 2 and 3). The transparent prismatic to acicular crystals display bright colours, ranging from red to hyacinth red, reddish orange, orange and yellow (Figure 8A). The structure of crocoite is monazite-type, with a tetrahedral anion group XO_4, where X = Cr (Quareni and De Pieri 1965; Effenberger and Pertlik 1986a). According to Loeffler and Burns (1976), the red-orange colour of crocoite is due to the oxygen (O^{2-}) to metal (Cr^{6+}) charge-transfer within the CrO_4^{2-} group, which determines a strong absorption of the visible light in the violet-green domain.

Crocoite is a rare secondary mineral, found in the oxidation zone of lead-bearing ore associated with Cr-rich rocks (also in abandoned mines). It is associated with both primary (*e.g.*, galena, chromite) and secondary (*e.g.*, pyromorphite, phosgenite, cerussite, anglesite, vanadinite, opal, chrysoprase, malachite; Table 3) minerals. The first mention of crocoite ('Siberian red lead') and chemical studies date back to the end of the 18th century, as related to the Tsvetnoi mine (Berezov ore deposit) in the Ural Mts., Russia (Macquart 1789; Beudant 1832b; Williams 1974). When crocoite replaces anglesite, it is closely associated with 'parent' galena. With advanced oxidation, crocoite will form along with cerussite, sometimes distant from galena.

In some old literary sources, this phase is incorrectly referred to as 'red ore of lead' instead of 'chrome yellow' (West FitzHugh 1986; see the section dedicated to lead chromates below).

Notable occurrences include the Dundas area in Tasmania (Australia); for example, at the Adelaide lead-silver mine and Red Lead Mine, numerous and extremely large vugs filled in with large, deep red-orange crystals of crocoite have been found (Bottrill et al. 2006; Moore and Wilson 2012). Adelaide Mine became the world's most famous producer of crocoite specimens. Other occurrences are those from the Happy Jack Mine (Lady Bee Mine) in the Comet Vale (Australia) and the Wadnaminga gold mines (South Australia). The Mindat.org database lists many occurrences distributed worldwide, such as Băiţa Bihor (Romania), Obercallenberg Quarry (Germany), Leadhills (Scotland, UK),

Nontron (France), Goiabeira (Brazil) and Darwin in California (USA).

Mimetite is lead chloroarsenate containing 69.61 wt% Pb. It forms an efflorescence of small crystals or botryoidal crusts (Figure 12D, E). Its structure has been investigated by Baker (1966), Calos et al. (1990) and Dai et al. (1991) (Table 2). Mimetite belongs to the apatite group, having the general formula $M_5(ZO_4)_3X$, where M = Ca, Sr, Pb or Na, Z = P, As, Si or V, and X = F, OH or Cl. In mimetite, Pb(1) bonds to nine O atoms, whereas Pb (2), which is larger, bonds to six oxygen and two chlorine atoms, to form irregular Pb(2)-O_6Cl_2 polyhedra. As bonds to four O, in a tetrahedral arrangement. The study performed by Bajda (2010) demonstrated that, between 5 and 55 °C, it is most stable at neutral to weakly alkaline pH.

Mimetite is a secondary mineral, which forms in the oxidation zone of Pb–As ore deposits, at the expense of galena and chalcopyrite (Table 3). Under the name of 'mimétès', Beudant (1832b, pp. 594–595) described crusts or fibres associated to Cu-Pb deposits, located near St Day in Cornwall (England), Johanngeorgenstadt (Germany) and Champallement (France). The name comes from Greek *mimethes* = imitator, due to its resemblance to pyromorphite. The fibrous mineral known as 'prixite' was only later recognised as 'mimetite' (Guillemin et al. 1955). A fibrous yellowish mimetite has been found to be associated with weathered galena at Les Molérats mine in the centre of France (Thiéry 2014). Mimetite also occurs as a weathering product on Zn-smelting slags deposited near Katowice in Poland (Bril et al. 2008). Its occurrences are numerous worldwide (Mindat.org), in locations such as Tsumeb (Namibia), Příbram (Czech Republic), several places in Cornwall (England), Leadhills (Scotland), Phoenixville (Pennsylvania, USA) and Broken Hill (New South Wales, Australia).

Crocoite and mimetite in artwork

Crocoite was likely used before the introduction of artificial lead chromates. Evidence supporting this hypothesis can be summarised as follows:

1. it is unlikely that it formed from the alteration of other phases based on the absence of other Cr-pigments;
2. its intentional production is unlikely, based on the lack of chromium metallurgy in the Middle Ages;
3. in the few cases where crocoite was found, no traces of any later interventions were observed[9].

The use of natural crocoite has been hypothesised in two cases only: (1) in 13th- century mural paintings in the Siena Cathedral in Italy (Mugnaini et al. 2006) and (2) in the 13th-century church of St. Gallus in Kuřívody (northern Bohemia), together with mimetite (Hradil et al. 2014). More doubtful is the discovery carried out in the 14th-century wall paintings of the Dagaoxuan Taoist Temple at Beijing in China (Lei et al. 2017). The authors did not seek to solve the concerns regarding whether it was natural crocoite or a pigment imported from Europe for subsequent repairs.

The occurrences of mimetite are relatively more numerous; however, in order to correctly interpret its presence in paintings, it is worth noting that this phase may be present as a pigment or as a phase of alteration. For example, the decay of realgar and orpiment may lead to the formation of mimetite and schulténite (Vanmeert et al. 2019). In the literature, the presence of mimetite as a primary pigment or as an alteration phase is not always clarified. Consequently, in the list of occurrences collected below, this aspect is outlined only when it has been discussed by the authors:

- in the 4th-century BC wall paintings of ancient Macedonian funerary monuments, together with vanadinite (Brekoulaki 2006);
- in the yellow-orange and green paint (mixed with Egyptian blue) of the 4th to 2nd century BC grave stelai from Alexandria (kept at Louvre Museum, Paris, France), Rouveret (1998), Rouveret and Walter (1998) and Kakoulli (2002) found mimetite and vanadinite. Rouveret and Walter (1998) suggested an Iranian provenance of mimetite[10];
- on a Greek-Ptolemaic grave stele (limestone) with a soldier and two girls, dated to the second half of the 3rd century BC (Leona 2009). The stele was found in 1884 in a tomb near Alexandria (Egypt) and kept at The Metropolitan Museum of Art in New York (USA), as a Gift from Darius Ogden Mills in 1904. Leona interpreted the presence of mimetite as a deliberately used yellow pigment and, hypothesising the Laurion provenance of the pigment, inferred the Athenian provenance of the painter as well;
- in the wall paintings of the 2nd century AD tomb of Palmyra in Syria, investigated by Buisson et al. (2015);
- in the 9th- to 10th-century wall decorations of Masjid-iJame at Fahraj (Holakooei and Karimy 2015), whose provenance was related to the Pb-Zn deposit at Darreh Zanjir (Iran);
- on the painted decoration of the sandstone sculptures (Vairocana Buddha) in the Dazu Rock Carvings at Chongqing (China), dated to the late 12th to mid-13th centuries but having been retouched since the 1850s (Li

[9] These considerations were agreed upon with the help of an anonymous reviewer.

[10] We do not know what the arguments were in favour of this hypothesis; however, mimetite occurs in several Iranian provinces (*e.g.*, Isfahan, South Khorasan, West Azerbaijan, Yazd and Zanjan; source mindat.org). See also below, Holakooei and Karimy (2015);

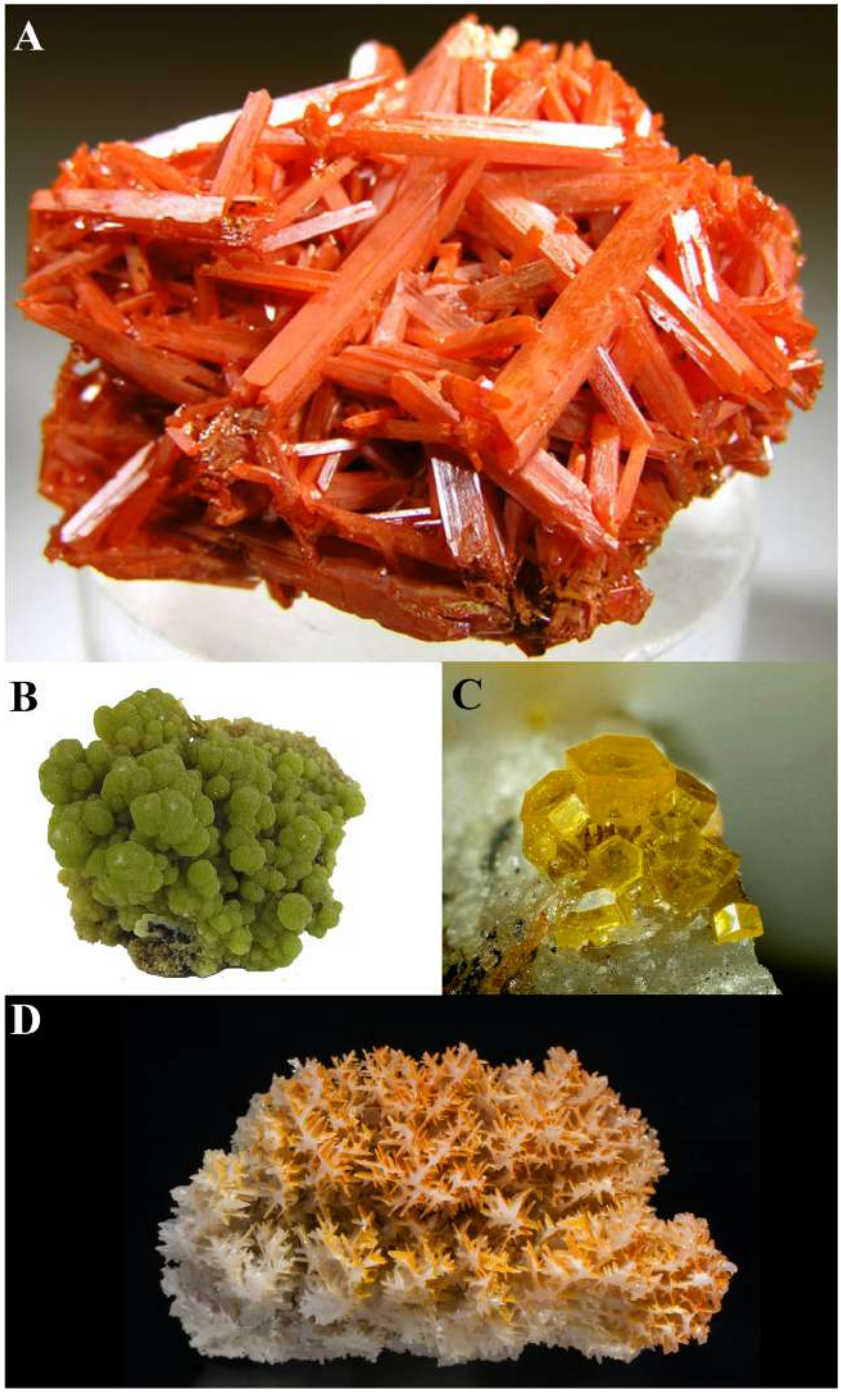

Fig. 8 **A** Crocoite from Adelaide Mine, Tasmania, Australia [Arkenstone specimen. Photo credits: Rob Lavinsky, irocks.com- Photo ID: 40436]. **B** Mimetite from the Ojuela Mine near Mapimí, Mexico [Arkenstone specimen. Photo credits: Rob Lavinsky, irocks.com-Mindat.org Photo ID: 151580]. **C** Mimetite from the Guatomo Mine, Bannang Sata District, Thailand [photo credits: Enrico Bonacina –Mindat.org Photo ID: 268267]. **D**Chromium-rich mimetite on cerussite from Nakhlak (Madan-e Nakhlak) Mine, Isfahan, Iran [specimen and photo: fabreminerals.com-Mindat.org Photo ID: 709680] [All images are subject to copyright owned by the photographers indicated above. The CC-BY licence does not supersede previously copyrighted material. Permission has been obtained for reproduction in this article]

et al. 2020b). These authors described in detail the spontaneous formation of mimetite + lavendulan ($NaCaCu_5(AsO_4)_4Cl{\cdot}5H_2O$) from emerald green ($Cu(C_2H_3O_2)_2{\cdot}3Cu(AsO_2)_2$) + cerussite;

– in the 13th-century Church of St. Gallus in Kuřívody (northern Bohemia), where it was interpreted as a degradation product formed by the alteration of orpiment mixed with lead-based pigments (Hradil et al. 2014);
– in a 17th-century oil on canvas (still life painting) by Jan Davidsz de Heem (1606–1684; De Keyser et al. 2017; Vanmeert et al. 2019), where schulténite (alteration product) was also found.

Lead-based minerals mainly found as alteration phases of the previous pigments

Galena (PbS)

Mineralogical phase, structure and occurrence

Named by *Plinius* (Table 1, P1), galena is a lead-grey (Figure 9), isometric sulfide (Table 2). In galena [MIIS-II], the M site can be substituted by several metallic trace elements, in particular, by those with I, II or III oxidation states (based on Goldschmidt's second rule), through different types of substitutions (*e.g.*, simple and coupled; see Chutas et al. 2008; Renock and Becker 2011; George et al. 2015, 2016).

Common trace elements are Mn, Fe, Co, Cu, Zn, Ga, As, Se, Ag, Cd, In, Sn, Sb, Te, Tl, Bi and minor Au and Hg (Blackburn and Schwendeman 1977; Foord and Shawe 1989; George et al. 2015, 2016). Their partition into galena depends on several factors, such as their oxidation state, ionic radius and availability. However, the co-existence of other phases (Table 3)—chiefly sphalerite, chalcopyrite (George et al. 2016) and wurtzite (Bethke and Barton 1971)—can influence their distribution across different deposits, within a single deposit, as well as in the grains of a single specimen (George et al. 2015).

The oxidation reactions and dissolutions mechanisms of galena have been studied in detail. The dissolution of galena plays a key role in several environmental and geochemical processes; therefore, its mobility (acid rock drainage) and potential toxicity have been experimentally investigated under varying conditions (*e.g.*, in solutions with different pH and dissolved oxygen at different temperatures) (Hsieh and Huang 1989; Ruby et al. 1994; Basta and McGowen 2004; De Giudici et al. 2005; Acero et al. 2007; Goryachev and Nikolaev 2012; Gutiérrez et al. 2016; Johnson et al. 2016; Chen et al. 2017; Zha et al. 2020 and the references therein).

Various factors, such as the pH value, the activities of both sulfur and lead and the CO_2 partial pressure of the fluid, affect the stability of these phases. The weathering of galena leads to the formation of lead and several secondary phases such as cerussite ($PbCO_3$), anglesite ($PbSO_4$), pyromorphite group minerals (*e.g.*, pyromorphite [$Pb_5(PO_4)_3Cl$], mimetite [$Pb_5(AsO_4)_3Cl$] and vanadinite [$Pb_5(VO_4)_3Cl$]) and other minor phases.

Regarding the occurrence of lead-bearing minerals (Table 3), galena is undoubtedly the most common species; it is also one of the most common among overall metallic sulfides. It occurs in both terrestrial and seafloor sulfide deposits (Fallon et al. 2017) and represents the most abundant primary lead phase in lead-bearing ore deposits. The sites are so numerous that they cannot be listed exhaustively; however, galena sources which have been certainly exploited in the different periods of the past and valuable compositional information (chemistry and isotope values) for ore deposits can be gained from archaeometallurgical studies and databases (*e.g.*, the Oxford archaeological lead isotope database OXALID from the Isotrace Laboratory, http://oxalid.arch.ox.ac.uk; and the Lead isotope ratios for Mediterranean ores, available in open document format from: http://www.brettscaife.net/lead/data/index.html, Scaife et al. 1999). However, it is worth mentioning at least a few significant galena deposits, such as Leadville in Colorado (USA), Freiberg in Saxony (Germany), Laurion (Lavrion) mines in the Lavrion Mining District (Attica, Greece), Baia Mare Mining District (Romania), Mendip Hills in Somerset (UK), Leadhills in Lanarkshire (Scotland, UK) and the ancient mines in Sardinia, at Monteponi and Montevecchio (data from Mindat.org). Moreover, a large body of useful literature also falls within the field of acid mine drainage studies, along with geological studies aimed at evaluating the mining potential of specific deposits.

Finally, it is important to note that galena can be found in cerussite aggregates (see, *e.g.*, Mondillo et al. 2018) and could therefore be combined with lead white, if the natural mineral had been used, instead of the artificial pigment.

Galena in artwork

Galena is rarely found in artwork and is generally interpreted as an alteration product of lead white (Smith and Clark 2002b; Smith et al. 2002):

- Carlyle and Towsend (1990) found lead sulfide in a 19th-century unvarnished oil sketch by J.M.W. Turner;
- Burgio et al. (1999) found galena in 18th-century Javanese and Thai manuscripts;
- Smith et al. (2002) found lead sulfide in a 16th-century manuscript illumination of the Jamnitzer manuscript;
- Franquelo et al. (2015) hypothesised the formation of PbS (due to alteration) on the 16th-century polychrome gothic-renaissance altarpiece at Santiago Church in Écija (Spain) by Alejo Fernandez Aleman;
- Tarquini et al. (2020) found galena (degradation) on the Campana reliefs found at the Palatine Hill in Rome (Italy; before the second half of the 2nd century);
- Costa et al. (2016) claimed that galena was present on the *Trompetender Putto* painting by Gustav Klimt (early 1880s), but the analyses were carried out using scanning electron microscopy.

Furthermore, Holakooei and Karimy (2015) found galena to be associated with red lead, plattnerite, mimetite and hemimorphite in the 9th- 10th century AD wall paintings of Masjid-i Jame in Fahraj (Yazd province, Iran).

Finally, Colombini et al. (2003) identified galena in paints applied to the 1st BC – 1st AD 'Ship C' found at the ancient

$Pb + \frac{1}{8}S_8 \rightarrow PbS$

-98.7 ΔfG°/kJ mol-1; -98.7 ΔfG°/nPb/kJ mol Pb-1

GALENA

$PbS + 4H_2O \rightarrow PbSO_4$ (anglesite) $+ 8H^+ + 8e^-$

$PbS + 2O_2 \rightarrow Pb^{2+} + SO_4$ (Hsieh and Huang 1989)

$PbS + 2O_2 \rightarrow PbSO_4$ (anglesite) (Keim and Markl 2015)

$PbS + 2OH^- \rightarrow Pb(OH)_2$ (hydroxide) $+ S^0 + 2e$ (Goryachev and Nikolaev 2012)

$PbS + CO_3 \rightarrow PbCO_3$ (cerussite) $+ S^0 + 2e$ (Goryachev and Nikolaev 2012)

$PbS + CO_2 + H_2O + 2O_2 \rightarrow PbCO_3$ (cerussite) $+ H_2SO_4$ (Keim and Markl 2015)

$2PbS + SO_4^{2-} + 2O_2 + H_2O \rightarrow PbSO_4$ (anglesite) $+ PbOH^+ + OH^- + S_2O_3^{2-}$ (Lara et al. 2011)

$PbS + 2Fe^{3+} \rightarrow Pb^{2+} + S^0 + 2Fe^{2+}$ (Szczerba and Sawłowicz 2009)

$PbS + 2Fe^{3+} + 3SO_4^{2-} + 3/2O_2 + H_2O \rightarrow PbSO_4$ (anglesite) $+ 2Fe^{2+} + 2H^+ + 3SO_4^{2-}$ (Park and MacDiarmid 1975)

Fig. 9 Galena: standard chemical reaction of formation (Franceschi et al. 2010 after Weast 1998), thermodynamic data and chemical reaction involving its transformation. Mineral photo: galena from the Borieva Mine in the Madan ore field, Bulgaria. [Arkenstone specimen. Photo credits: Rob Lavinsky, irocks.com-Mindat.org Photo ID: 157198 – Copyrighted. Permission has been obtained for reproduction in this article. The CC-BY licence does not supersede previously copyrighted material; therefore, these images remain under owner's copyright]

harbour of San Rossore (Pisa, Italy). They indicated galena as being responsible for the blackening of the pictorial surface. The authors did not put forward any hypothesis about its presence; however, cerussite was the only lead-based pigment individuated in the association.

Anglesite ($PbSO_4$), palmierite ($K_2Pb(SO_4)_2$) and associated phases

Mineralogical phases, structure and occurrence

Anglesite is a colourless to white (sometimes with grey, yellow, green or blue hues) sulphate (Figure 10A, B), which is a member of the barite group (Tables 2 and 3). It was named in 1832 by Francois Sulpice Beudant who individuated it at the Parys Mine (Island of Anglesey, Wales, UK; corresponding to the type locality) (Beudant 1832a). Anglesite (and cerussite) occurs in lead-bearing ore oxidation zones, "*either as in situ replacement of galena and/or as euhedral crystals in cavities of former, partially dissolved galena*" (Keim and Markl 2015), mainly in low-temperature hydrothermal areas (Hazen et al. 2013) (Table 3). In nature, anglesite is relatively frequent (Mindat.org; Anthony et al. 1990), such as at the Tsumeb and Kombat mines in Namibia, Mežica in Slovenia, Cromford and Matlock in Derbyshire (UK), Leadhills in Lanarkshire (Scotland, UK), Bleiberg in Carinthia (Austria), Genna Zinkhütte in Nordrhein-Westfalen (Germany), Nerchinsk in Siberia (Russia), Bunker Hill Mine in Idaho (USA) and Dundas in Tasmania (Australia).

Palmierite is a colourless to white, trigonal sulfate (Tables 2 and 3; Figure 10C). Its observations are rare and include only eight countries, including Russia (the Tolbachich volcano in Kamtcheatka), Spain (La Cruz lead smelter slag locality in Linares) and Germany (Genna Zinkhütte in Nordrhein-Westfalen Land and Oberhütte in Sachsen). The type locality is Mt. Vesuvius (Naples, Italy), where it occurs as a fumarolic sublimate. Recognised in the early twentieth century, it has been structurally studied by various authors since the middle of the century (Bellanca 1946; Tissot et al. 2001).

As, for both these phases, their use as a pigment has not been definitively excluded, it should be added that, in nature, they are frequently associated with leadhillite, macphersonite

and susannite. These are common to rare Pb hydroxide sulfate carbonates that constitute the leadhillite group (Tables 2 and 3; Figure 10D–F).

Leadhillite is typically colourless to white but may also be grey, yellowish, pale green or blue. Susannite is colourless to yellowish or greenish, while macphersonite is colourless to white but also pale amber. The type locality is the same for all three phases, that is, the Susanna Mine (Leadhills in Scotland, UK). The crystal structures have been provided by Giuseppetti et al. (1990) for leadhillite, by Steele et al. (1999) for susannite and by Steele et al. (1998) for macphersonite (the rarest of the three phases). Leadhillite pseudomorphically replaces galena and transforms into susannite at 82 °C. The structural changes accompanying this transformation have been studied by Bindi and Menchetti (2005). Leadhillite, macphersonite and susannite are very rare and can be found in small amounts, in the oxidised zone of lead ore deposits, such as at Tsumeb (Namibia), Dundas (Tasmania, Australia), Bleiberg in Carinthia (Austria) and Caldbeck Fells (Cumbria, UK). Finally, it is worth mentioning that leadhillite has been found in weathered dumps of the medieval mining district at Altemannfels in Germany by Keim et al. (2017).

Anglesite and palmierite in artwork

The use of anglesite as a white pigment is extremely rare (Eastaugh et al. 2004) and, for this reason, it was chosen to be listed in this section, instead of the previous one on the main lead-basedminerals and pigments. The numerous studies focused on the mechanisms of anglesite and cerussite formation performed by Aze et al. (2006, 2007, 2008a) have clearly demonstrated the secondary nature of this phase. As such, it has been found in the following:

- Cambodia—wall paintings (11th/17th century?) of the Cruciform gallery, Angkor Wat complex (Uchida et al. 2012)
- China—(a) walls, reliefs and Buddha statues (618–907 AD) in caves no. 512 and 689 at the Guangyuan Thousand-Buddha Grotto, near Guagyuan (Sichuan, China; He et al. 2012); (b) Qing dynasty (1644–1912) wall paintings of the Imperial Taidong Tomb (Hebei, China; Fu et al. 2020); and (c) 907–960 AD wall paintings of the Feng Hui Tomb in the Bin County (Shaanxi, China; Wang et al. 2004)
- Italy—Late Medieval (~15th century) wall paintings of the St. Stephen's Chapel, near Bolzano (Costantini et al. 2020b)
- Slovakia—wall paintings (Marian cycle; ~1000 AD) of the St George Church at Kostol'any pod Tríbečom (Hradil et al. 2013)
- Spain—(a) 16th-century(?) ceramic statues in the Seville Cathedral (Pérez-Rodríguez et al. 1998) and (b) 19th-century redecoration of the wall paintings of the Room of the Beds (Royal Bath of Comares), Alhambra, Granada (Arjonilla et al. 2019b)

Further occurrences of anglesite, regarding oils on canvas, include the Girl with a Pearl Earring (c. 1665) by Johannes Vermeer (kept at the Mauritshuis museum in The Netherlands; De Meyer et al. 2019a, b) and two artworks by Vincent van Gogh: the *Flowers in a blue vase* (June 1887) and the *Wheat stack under a cloudy sky* (October 1889) (both kept at the Kröller-Müller Museum in Otterlo, The Netherlands; Van Der Snickt et al. 2012 and Vanmeert et al. 2015, respectively). To these, it may be possible to add Şerifaki et al. (2009), who claimed to have found anglesite, used as a priming white layer in the decorations of the 19th-century Taxiarhis Church on Alibei-Adasi Island (Ayvalık) in Turkey.

Finally, it is worth adding that Hradil et al. (2007) found anglesite mixed with lanarkite in three 18th to 19th-century oil paintings on canvas, painted with Pb-Sb-Sn yellow. The authors interpreted the presence of these phases (as well as that of rosiaite) as by-products of Pb-Sb-Sn yellow production using the raw material Sb_2S_3 (see Figure 14, Eqs. 6–7).

The occurrences of palmierite are rare and limited to 17th-century paintings on canvas (De Keyser et al. 2017; De Meyer et al. 2019a, b; Vanmeert et al. 2019) and oak wood panels (Albertson et al. 2019; Simoen et al. 2019). A further occurrence, with regard to the Voynich manuscript, has been investigated by a private company[11].

Scrutinyite (α-PbO_2) and plattnerite (β-PbO_2)

Mineralogical phases, structure and occurrence

Scrutinyite (Tables 2 and 3) is a red-brown mineral, first known as a synthetic material (Kameyama and Fukumoto 1946; Zaslavskii et al. 1950; Zaslavskii and Tolkachev 1952). The natural mineral was later discovered at the Sunshine#1 adit of the Blanchard Mine at Bingham in New Mexico (USA) by Taggart et al. (1988)[12]. It occurs, together with plattnerite, in the oxidised parts of lead ore deposits. The name derives from the necessity of a close 'scrutiny' to distinguish it from plattnerite (Webmineral.com).

[11] https://web.archive.org/web/20160304091449/http://beinecke.library.yale.edu/sites/default/files/voynich_analysis.pdf

[12] An earlier note on the discovery was provided in an abstract presented in 1984 at the Joint FM-MSA-TGMS Mineralogical Symposium "Minerals of Mexico" (Tucson, Arizona), which we could not find.

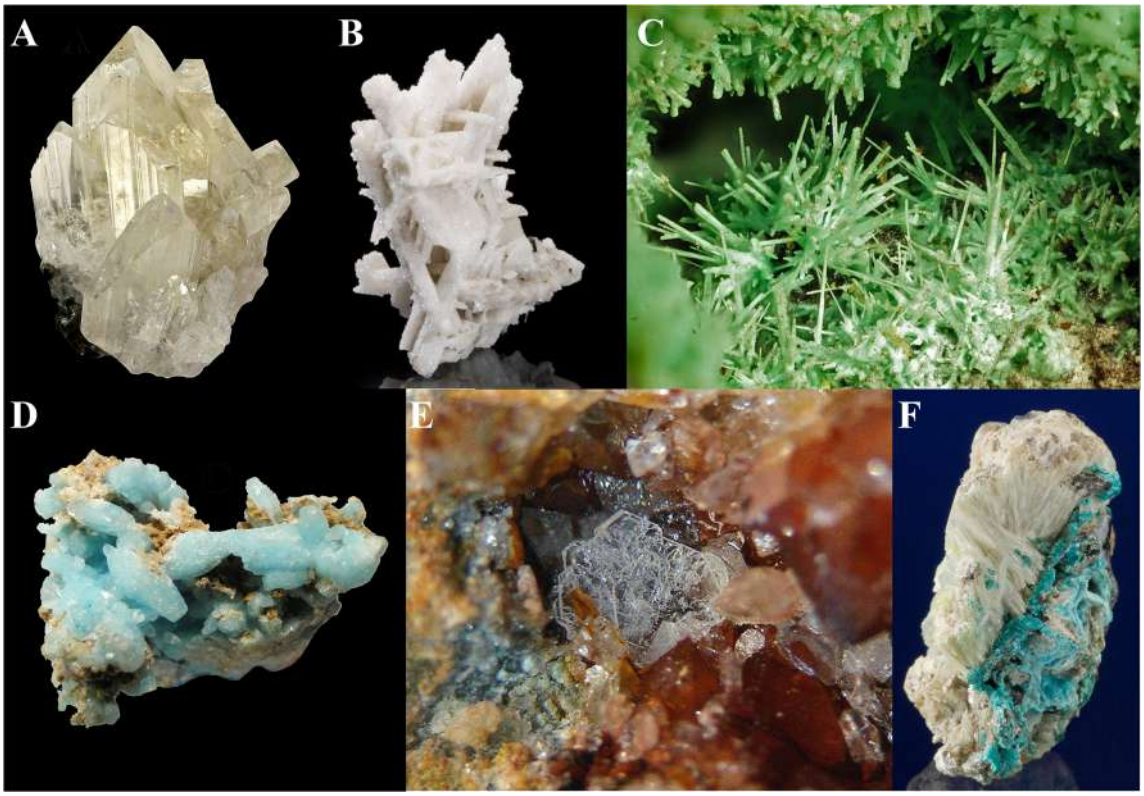

Fig. 10 **A** Anglesite from the Touissit Mine, Morocco [Arkenstone specimens. Photo credits: Rob Lavinsky, irocks.com- Mindat.org Photo ID: 181543]. **B** Anglesite from Broken Hill South Mine, New South Wales, Australia [Arkenstone specimens. Photo credits: Rob Lavinsky, irocks.com- Mindat.org Photo ID: 393034]. **C** Palmierite from Monte Somma, Somma-Vesuvius complex, Italy [Photo credits: Enrico Bonacina -Mindat.org Photo ID: 898863]. **D** Leadhillite from the Mammoth-Saint Anthony Mine, Arizona, USA [Arkenstone specimens. Photo credits: Rob Lavinsky, irocks.com-Mindat.org Photo ID: 37761]. **E** Macphersonite from the Tiny-Arenas Mine, Sardinia, Italy [photo credits: Antonio Gamboni - Mindat.org Photo ID: 80093]. **F** Susannite and lanarkite from the Susanna Mine, Leadhills, South Lanarkshire, Strathclyde (Lanarkshire), Scotland, UK [By Rob Lavinsky, iRocks.com– CC-BY-SA-3.0, CC BY-SA 3.0]. [All images are subject to copyright owned by the photographers indicated above. The CC-BY licence does not supersede previously copyrighted material. Permission has been obtained for reproduction in this article]

Plattnerite has a brownish to dark greyish black colour and a rutile-type structure (Tables 2 and 3; Figure 11A). Crystallographic studies have been performed on both natural (Paulsen et al. 2019) and synthetic (Leciejewicz and Padlo 1962; D'Antonio and Santoro 1980; Harada et al. 1981) materials, as well as under different pressure conditions (*e.g.*, 23–140 GPa in Grocholski et al. 2014).

Apart from the Blanchart Mine, scrutinyite and plattnerite have been found to occur at few sites in Greece (Lavrion mining district), Mexico (Durango), Namibia (Kunene) and the USA (Nevada and New Mexico) (Mindat.org).

Scrutinyite and plattnerite in artwork

Although they generally represent alteration products (Kotulanová et al. 2009), the use of plattnerite as an art pigment has been suggested by Holakooei and Karimy (2015). The hypothesis advanced by these authors was based on the prevalence of plattnerite in black paint and, on the other hand, due to the natural availability of this phase close to Fahraj (Darreh Zanjir mine, 35 km far). This is the only case in which this hypothesis has been formulated to the best of our knowledge.

Overall, these phases are fundamental in the study of paintings, as they represent alteration indicators. However, while plattnerite has been partially studied and frequently observed in wall paintings (Daniilia et al. 2008; Daniilia and Minopoulou 2009; Kotulanová et al. 2009; Hradil et al. 2013, 2014; Gutman et al. 2014; Liu et al. 2016; de Ferri et al. 2019; Costantini et al. 2020b), scrutinyite has rarely received attention (Kotulanová et al. 2009; Lytle et al. 2009; Costantini et al. 2020a; Vagnini et al. 2020).

The formation of plattnerite from lead white has been verified through experimental tests using hydrogen peroxide (H_2O_2) at high RHs (Aze 2005), ozone (Aibeo et al. 2008) and NaClO. In the last case, the experiments performed by Kotulanová et al. (2009) demonstrated that, in the presence of NaClO, lead white reacts very quickly, turning black–brown. Similarly, the experiments carried out by Vagnini et al. (2020) assessed the formation of plattnerite and minor scrutinyite (+ halite) when the starting material was cerussite, as well as the formation of scrutinyite and minor plattnerite (+ cerussite and

halite) when the starting material was hydrocerussite (see above). The practical implications of these results also lie in the fact that scrutinyite is easier to remove during restoration operations due to its higher solubility than plattnerite. A mixture of both plattnerite and scrutinyite can also form in 8 days in a chlorinated water solution with pH = 8.1 (Lytle et al. 2009).

The secondary products of plattnerite are minium, litharge, massicot and another lead phase (lead oxide $PbO_{1.55}$). The transformation of βPbO_2 into Pb_3O_4 occurs spontaneously in air at T>375 °C (Clark et al. 1937); in more detail, the reaction path described by Greenwood and Earnshaw (1997) is as follows: βPbO_2 → (290 °C) $Pb_{12}O_{19}$ → (350 °C) $Pb_{12}O_{17}$ → (375 °C) Pb_3O_4 → (600 °C) PbO. The thermal treatment of plattnerite performed by Aze et al. (2008b) provided similar transformation temperatures: βPbO_2 → (300 °C) Pb_2O_3 → (375 °C) Pb_3O_4 → (589 °C) αPbO → (>589 °C) βPbO.

The degradation and conversion of plattnerite using Ar+ lasers (*e.g.*, with a power higher than 30 mW) are crucial aspects to be taken into due account during the investigation (see the section on analytical methods below; Burgio et al. 2001; Aze et al. 2008c).

Plumbonacrite ($Pb_5O(OH)_2(CO_3)_3$) and associated phases

Mineralogical phases, structure and occurrence

Plumbonacrite is a lead oxide–hydroxide carbonate that, together with abellaite, grootfonteinite and somersetite (Tables 2 and 3), is related to hydrocerussite. These phases can be naturally found to be associated and, therefore, are of interest in the study of lead white.

Plumbonacrite is a lead-based ('plumbo') mineral with a pearly lustre ('nacre') (Figure 11B), individuated at the type locality Torr Works (Merehead) Quarry (East Cranmore, Somerset, UK) (Williams et al. 2012). It was first investigated by Krivovichev and Burns (2000) (Table 2 'a'), then revalidated in 2012 (Table 2 'b') (Rumsey et al. 2012a).

Abellaite is a colourless to white (Tables 2 and 3; Figure 11D) Na/K–Pb hydroxide carbonate, first recognised in the Eureka mine in Catalonia (Spain) and structurally characterised by Ibáñez-Insa et al. (2017). It can include minor quantities of CaO [$Na_{0.96}Ca_{0.04}Pb_{1.98}(CO_3)_2(OH)$] and has a synthetic previously known analogue (Brooker et al. 1983; Krivovichev and Burns 2000; Belokoneva et al. 2002; Bette et al. 2017; Siidra et al. 2018a). Within the lead hydroxycarbonates, the parameters provided by Siidra et al. (2018d) for an unnamed species individuated in Laurion metallurgical slag (Attica, Greece) are also shown in Table 2. This phase has also been found as a reaction product of a cerussite-based pigment (containing 68% cerussite, 6% hydrocerussite and 26% shannonite) treated with Na_2CO_3 and $NaHCO_3$(Kotulanová et al. 2009).

Grootfonteinite is a rare, colourless Pb oxo-carbonate, which has been structurally investigated by Siidra et al. (2018a) (Tables 2 and 3). These last authors pointed out that grootfonteinite is macroscopically very similar to abellaite (as well as to hydrocerussite and plumbonacrite) and that discrimination between grootfonteinite and abellaite is only possible by means of electron microprobe analysis, provided that a preliminary XRD analysis has discriminated these phases from the others.

Somersetite (Tables 2 and 3; Figure 11C) was individuated at the same type locality of plumbonacrite. This is a green or white mineral whose crystallographic structure was resolved by Siidra et al. (2018c).

Plumbonacrite in artwork

Plumbonacrite has been found on the oil painting on canvas *Wheat stack under a cloudy sky* by Vincent van Gogh (Vanmeert et al. 2015).

Plumbonacrite can easily form in water solutions and in rather dry oils at ambient temperature and pressure. As demonstrated by the experiments conducted by Gonzalez et al. (2019a), a mixture of plumbonacrite and hydrocerussite can be observed after having aged PbO particles (litharge) dispersed in heated oil for three months, where PbO was no longer present at the end of the experiment.

Based on the photochemical reaction described by Zhou et al. (2012) and Vanmeert et al. (2015), plumbonacrite can form from the photoactivation of minium (Figure 6), leading to a reduction of Pb^{IV} to Pb^{II}; alternatively, PbO—which can be present as a residue due to the incomplete synthesis of minium—can trigger the transformation. As demonstrated by Kotulanová et al. (2009), both litharge and massicot can lead to the formation of cerussite, hydrocerussite and plumbonacrite due to their instability in humid and alkaline environments (Taylor and Lopata 1984). For the reaction sequence PbO ↔ $Pb_{10}O(OH)_6(CO_3)_6$(plumbonacrite) ↔ $Pb_3(OH)_2(CO_3)_2$(hydrocerussite) ↔ $PbCO_3$ (cerussite), the equilibrium conditions (at ~25 °C) in aqueous carbonate solutions have been investigated by Taylor and Lopata (1984).

With more difficulty, plumbonacrite can also form from lead white (Figure 1); however, being metastable with respect to both PbO and hydrocerussite, it is easily reconverted into hydrocerussite. Other possible origins are limited by the alkaline conditions (pH>10) required for its stability (Gonzalez et al. 2019a). Using a synchrotron radiation technique (μ-XRPD tomography), Janssens and Cotte (2019) identified that plumbonacrite had formed at the interface between minium and degradation products in a painting by Van Gogh.

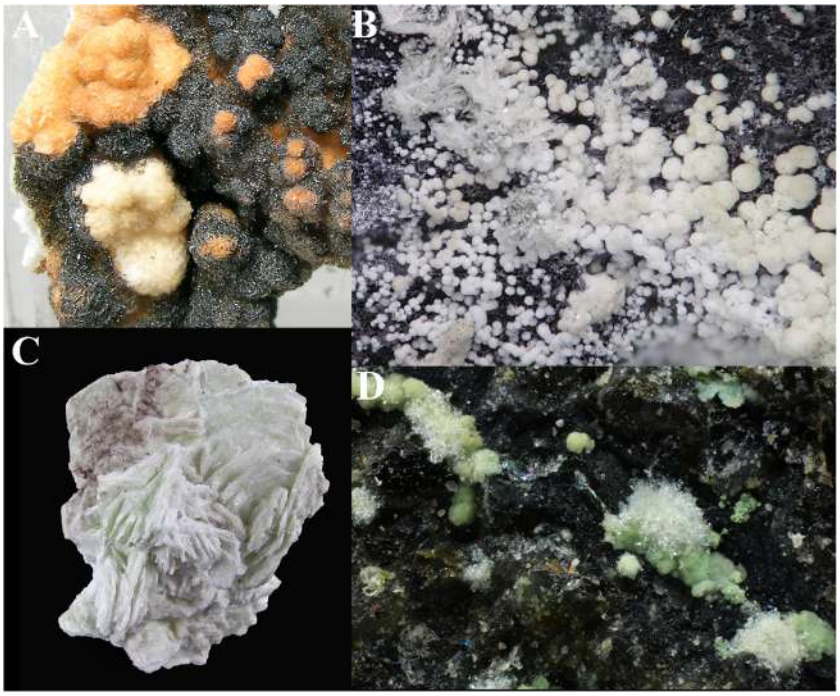

Fig. 11 **A** Plattnerite partially covered by creamy-orange calcite from Preguiça Mine in the Beja District, Portugal [Specimen and photo: fabreminerals.com-Mindat.org Photo ID: 218620]. **B** Plumbonacrite from the Clara Mine at Oberwolfach in the Baden-Württemberg, Germany [Photo credits: Copyright Stephan Wolfsried 2007 -Mindat.org Photo ID: 107026]. **C** Somersetite from the Torr Works Quarry in England, UK [Arkenstone specimens. Photo credits: Rob Lavinsky, irocks.com-Mindat.org Photo ID: 744814]. **D** Abellaite white crystals from the Eureka Mine in Catalonia, Spain [Collection Joan Abellai Creus. Photo credits: Matteo Chinellato – Wikipedia CC BY-SA 4.0]. [**A**–**C** images are subject to copyright owned by the photographers indicated above. The CC-BY licence does not supersede previously copyrighted material. Permission has been obtained for reproduction in this article]

Cotunnite ($PbCl_2$), laurionite (Pb(OH)Cl), blixite ($Pb_8O(OH)_2Cl_4$) and phosgenite ($Pb_2Cl_2(CO)_3$)

Mineralogical phases, structure and occurrence

Cotunnite is a lead chloride forming prismatic, short, or elongated crystals often grouped in radiating aggregates. Granular or massive masses, as well as crusts, are also common (Figure 12A). The crystallographic characteristics of cotunnite (Table 2) have been determined by Sass et al. (1963). This phase occurs both as a primary and secondary mineral, and it is most frequently associated with anglesite, cerussite and hydrocerussite (Table 3). Its stabilisation requires an acidic environment (pH <3) and high chloride activity (Humphreys et al. 1980; Edwards et al. 1992). As cotunnite forms from acid solutions, the increase in pH leads to its transformation into paralaurionite (PbCl(OH)) and, finally, mendipite (Humphreys et al. 1980). Africano et al. (2002) found cotunnite in sublimates deposited by the hot gases (below 325 °C) released by the Satsuma-Iwojima volcano (Japan), Krivovichev et al. (2002) and Pekov et al. (2015) in the incrustations associated with fumaroles of the Tolbachik volcano in the Kamchatka Peninsula (Russia) and Lacroix (1907) in the deposits of the fumaroles of Mt. Vesuvius.

Lacroix (1920), Russel (1920) and Schnorrer-Köhler (1986) reported cotunnite as a natural corrosion product of lead objects placed in marine conditions (*i.e.* in contact with seawater containing chlorine). The Laurion mines in Attica (Greece) are famous for such an environment. Here, a wide range of alteration products, including laurionite, paralaurionite, cotunnite and blixite, had formed naturally by the reaction of seawater with Pb-rich glassy metallurgical slags obtained about 2500 years ago (Siidra et al. 2011). Similarly, Franzini and Perchiazzi (1992) described a rich association of secondary minerals, with cotunnite formed by the interaction of seawater with Etruscan iron slags spread along the Baratti Beach in Tuscany (Italy). Kutzke et al. (1997) mentioned cotunnite, laurionite and phosgenite as corrosion products formed through the prolonged contact of seawater with lead objects from a shipwreck (ca. 80 BC) sunken in the Mediterranean, near the Tunisian coast.

Other occurrences have been reported in Austria, Brazil, Canada, France, India, Iran, Israel, Namibia, New Zealand, Norway, Peru, Poland, Romania, Spain, Tunisia and the USA by Antony et al. (1990).

Laurionite is an orthorhombic lead oxychloride (Tables 2 and 3). It forms colourless or white small crystals, massive masses, or thin crusts (Figure 12B). Its structure was determined by Venetopoulos and Rentzeperis (1975) and Merlino et al. (1993). In its structure, each Pb atom is surrounded by five Cl atoms and three OH groups. The solubility of laurionite in water is low but increases with temperature.

Köchlin (1887) described laurionite, for the first time, in the ancient metallurgical slags corroded by seawater at Laurion, in Greece (hence the name). Here, this phase was associated with other secondary Pb phases, such as anglesite, cotunnite, cerussite and phosgenite (Palache 1934; Katerinopoulos 2010; Periferakis et al. 2019). Scott (1994) also mentioned laurionite at the Endeavor Mine in New South Wales (Australia), where it formed in saline conditions, together with blixite and mendipite. Laurionite, phosgenite, anglesite, paralaurionite and cerussite were further described, by Russell and Hutchinson (1927), from the Wheal Rose Mine in Cornwall (UK). Other occurrences have been listed by Anthony et al. (1990) in Austria, Canada, Czech Republic, France, Germany, Israel, Italy, Mozambique, Norway, South Africa, Tunisia, Turkmenistan and the USA.

Blixite is a lead hydroxychloride, occurring as light green light yellow, yellow–orange, greyish–yellow massive masses and thin crusts (Tables 2 and 3; Figure 12C). It was first described by Gabrielson et al. (1960) from the Långban Mine (Sweden). The structure of the synthetic analogue of blixite has been investigated by Krivovichev and Burns (2006). The authors described it as (OPb_4) oxo-centred tetrahedra, linked by shared Pb…Pb edges to form [O_5Pb_8] sheets parallel to (100). The OH groups are attached to the sheets and form two short OH–Pb bonds. The authors observed: "*it is also possible that blixite exists with differing degrees of order of the* O^{2-} *and* OH^- *anions, which causes different unit-cell parameters*". A blixite + mendipite association was described at the Mendip Hills (UK) by Symes and Embrey (1977). At the Endeavor Mine at Elura (New South Wales, Australia), blixite and laurionite were found in a narrow zone between primary sulfide-bearing assemblages and the overlaying oxidation zone (Scott 1994). At Merehead (now Torr Works) Quarry in Somerset (UK), Edwards et al. (1992) described a deposition sequence starting with blixite→ mendipite → paralaurionite along with the decrease of the pH from ~8 to ~4 and within a temperature range of ~100 °C to a minimum of 30 °C.

Phosgenite is a tetragonal chloride-carbonate of lead (Tables 2 and 3). It forms mainly crusts and masses, with a wide range of colours (Table 1; Figure 12D). In its structure, the (Pb—$2Cl_2$—Pb) layers are connected by COs-groups (Giuseppetti and Tadini 1974). This is a secondary mineral, found mainly in the oxidised zone of lead deposits (Table 3). Köchlin (1887) described phosgenite for the first time from the ancient slags altered by seawater at Laurion (Greece). The type locality for phosgenite is Cromford, near Matlock, in Derbyshire (England), where it occurs together with matlockite (Greg 1851; Bannister 1934). Stanley et al. (1991) mentioned phosgenite and barstowite ($Pb_4Cl_6(CO_3)\cdot H_2O$) in the cavities of lead-antimony veins exposed to the foreshore at Bound Cliffs in Cornwall (UK), where it formed as a result of the action of seawater on a galena assemblage. Phosgenite has also been found at Monteponi Mine in Sardegna (Italy), together with galena, leadhillite, minium, cerussite and anglesite (Guastoni and Pezzotta 2007).

Phosgenite is a mineral which is widespread worldwide and the occurrences listed by the Mindat.orgdatabase—in Argentina, Australia, Austria, Brazil, Chile, China, Czech Republic, France, Germany, Greece, Iran, Ireland, Italy, Mexico, Morocco, Namibia, Norway, Poland, Portugal, Russia, South Africa, Spain, Tunisia, the UK and the USA—are just the best-known ones.

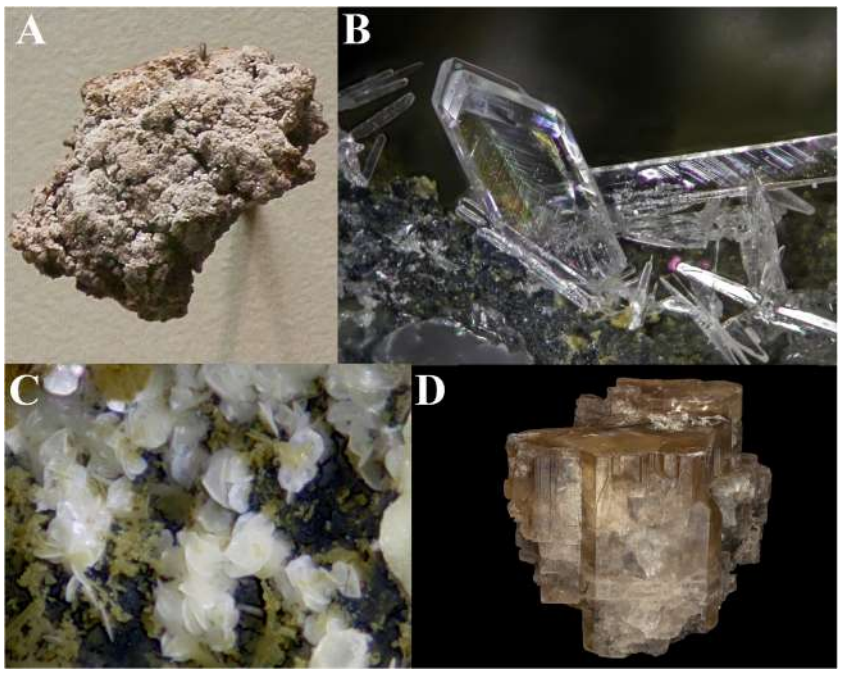

Fig. 12 **A** Cotunnite on display at the New York Museum of Natural History [By Geckzilla - own work, Public Domain, ID=6043437]. **B** Laurionite from the Legrena Cove slag locality in the Lavrion district, Greece [photo credits: Ko Jansen – Mindat.org Photo ID: 677146]. **C** Blixite white/yellowish crystals from the Thorikos Bay slag locality in the Lavrion District, Greece [photo credits: Ko Jansen –Mindat.org Photo ID: 784361]. **D** Phosgenite from Monteponi Mine, Iglesias, Sardinia, Italy [specimen and photo: fabreminerals.com–Mindat.org Photo ID: 935277]. [All images are subject to copyright owned by the photographers indicated above. The CC-BY licence does not supersede previously copyrighted material. Permission has been obtained for reproduction in this article]

Cotunnite, laurionite, blixite and phosgenite in artwork

Cotunnite, lauronite, blixite and phosgenite have been sporadically found in artwork and frequently interpreted as secondary phases. Moreover, the processes that occur in lead objects in contact with seawater (*i.e.* containing chlorine) can provide valuable information for the interpretation of these phases as secondary phases in paintings.

Laurionite (Pb(OH)Cl) and phosgenite ($Pb_2Cl_2(CO)_3$) have been produced starting from litharge, reduced into fine powders and used for cosmetics (Walter et al. 1999). It is also known that laurionite was possibly used as a medicament to treat eye illnesses (Tapsoba et al. 2010). Hence, given the frequent use of the same pigments both for cosmetics and for painting, their use as primary pigments cannot be excluded.

Their occurrences in paintings must be discussed on a case-by-case basis. For example, Ordonez and Twilley (1997) described a thin white cotunnite coating on the blue- and brown-coloured areas of both an oil portrait by Pierre-Auguste Renoir (dated to 1918) and on the painted ceiling of the Powell Library at the University of California (Los Angeles, USA). The authors presumed that cotunnite formed through a reaction between white lead and a Cl-rich fluid; in the second case, originating from the undried plaster.

The white hydrocerussite paint covering a 16th-century terracotta sculpture by Della Robbia showed cotunnite associated with challacolloite KPb_2Cl_5 (Ma and Berrie 2020), where both phases were interpreted as secondary products.

Winter (1981) found that the main white lead-based pigments used for 12th- to 16th-century Japanese paintings was laurionite, while blixite was also present. The author assumed that both laurionite and blixite were most likely artificially produced, probably by precipitation.

A further occurrence of laurionite and/or cotunnite (and possibly of one or more 'other Pb/Cl compounds') has been reported by Salvant et al. (2018), in ~2nd-century AD Roman mummy portraits from Tebtunis in Egypt.

Caledonite ($Cu_2Pb_5(OH)_6CO_3(SO_4)_3$), schulténite ($PbHAsO_4$) and vanadinite ($Pb_5(VO_4)_3Cl$)

Mineralogical phases, structure and occurrence

Caledonite is an orthorhombic lead and copper hydrous carbonate–sulfate (Table 2). It occurs as small prismatic crystals, massive masses and coatings (Figure 13A). The structure consists of CO_3 and SO_4 groups connecting lead polyhedra, and these with chains of CuO_6 square bipyramids. Three independent hydrogen atoms are bound, as hydroxyl groups, to the oxygen atoms at the corners of the CuO_6 bipyramids (Palache and Richmonds 1939; Giacovazzo et al. 1973; Schofield et al. 2009).

Caledonite is a secondary mineral, associated with anglesite, cerussite, leadhillite, linarite, azurite, and malachite, in the oxidation zone of Pb-Cu ore deposits (Table 3). In the oxidised zone of the galena–chalcopyrite deposit at Leadhills, caledonite (+ linarite $PbCu(SO_4)(OH)_2$ or leadhillite) directly replaces anglesite and cerussite. Temple (1956) observed that caledonite and brochantite ($Cu_4(OH)_6(SO_4)$) do not occur together, despite the fact that both minerals (a) are related to oxidised lead-copper ores, (b) are associated with linarite and (c) pseudomorphically replace galena. Caledonite forms from fluids in which lead predominates over copper, whereas brochantite forms from lead-deficient fluids. Thus, the conditions favouring the formation of brochantite inhibit the formation of caledonite and vice versa.

Apart from its occurrence at Leadhills, there are many other places where caledonite has formed, such as the Preobrazhenshy Mine in Sverdlovsk (Russia), Tchah Milleh (Iran), Mammoth Mine in Arizona (USA), Mex-Tex Mine in New Mexico (USA), Cerro Gordo Mine in California (USA), Challacollo Mine (Chile) and the Paddy's River Mine (Australia).

Schulténite is a monoclinic hydrous lead arsenate (pre-IMA species), named in honour of August Benjamin de Schultén (1856–1912), who synthesised the artificial hydrous lead arsenate. It forms small crystals and (sometimes) crusts (Figure 12B). The structure of schulténite (Claringbull 1950; Choudhary 1982; Effenberger and Pertlik 1986b; Wilson et al. 1991; Wilson 1994) involves chains of AsO_4 tetrahedra connected by short hydrogen bonds, where Pb atoms are surrounded by the six nearest oxygen atoms (Table 2).

This is a rare secondary mineral, which forms by the hydrothermal alteration of Pb–As ores (Table 3). At the Tsumeb Mine (Namibia), this phase was found (a) as 'pseudomorphous crusts' and small crystals intermixed with bayldonite, on anglesite (Spencer and Mountain 1926); (b) associated with cuprian adamite and keyite in the lower oxidation zone (Falls et al. 1985); and (c) replaced by bayldonite and duftite (Magalhães et al. 1988). Other occurrences (Mindat.org; Anthony et al. 1990) are at the Schwartzwald Mts. and Black Forrest Mts. (Germany), North Bend (WA, USA), Deer Hills Mine (England) and Michael Mine in Weiler (Germany). An analogue lead arsenate has been synthesised by Effenberger and Pertlik (1986b).

Vanadinite is a hexagonal lead chloride vanadate. It occurs as short prismatic crystals, massive granular masses and crusts (Figure 12C). Its structure has been investigated by Trotter and Barnes (1958), Baker (1966) and Dai and Hughes (1989) (Table 2). The structural unit of vanadinite consists of an octahedron with a Cl atom surrounded by 6 Pb atoms. The octahedra form a continuous chain sharing opposite faces. The VO_4^{3-} groups are isolated as discrete bonding units (Loeffler and Burns 1976), where each vanadium atom is

surrounded by four oxygen atoms at the corners of a tetrahedron. Three oxygen tetrahedra adjoin each of the lead octahedron along the chain (Trotter and Barnes 1958). The red–orange–yellow colour of vanadinite is due to the oxygen (O-II) to metal (VV)charge-transfer within the $(VO_4)^{-II}$ group, which determines a strong absorption of visible light in the violet–green domain (Loeffler and Burns 1976). Vanadinite is a secondary mineral, found in the oxidation zone of lead ore deposits (Table 3). It was first described by von Kobell (1838), and its type locality is Zimapan (Hildalgo, Mexico). Other notable occurrences are (Mindat.org): Tsumeb (Namibia), Bisbee (AZ, USA), Longefay Mine (Rhône, France) and Broken Hill (New South Wales, Australia).

Caledonite, schulténite and vanadinite in artwork

Caledonite has been identified as a decay product of the ultramarine blue paint in 12th- to 13th-century polychrome sculptures of the Parma baptistery and Ferrara Cathedral in Italy (Pinna et al. 2020). The authors discovered it together with gypsum and weddellite and specified that it formed by "*the sulphation process in the presence of […] lead and copper*".

Schulténite (alteration product) was found in the 17th-century oil on canvas still life painting by Jan Davidsz de Heem (1606–1684; De Keyser et al. 2017; Vanmeert et al. 2019).

Vanadinite is rare and, based on the literature available so far, it has not been used as a pigment. A mixture of vanadinite, red ochre and yellow ochre has been determined by Levstik et al. (2019), in the 15th-century orange–yellow paints on the walls of a Gothic church in Koper (Slovenia).

Challacolloite (KPb_2Cl_5) and the dolomite homotype $PbMg(CO_3)_2$

Mineralogical phase, structure and occurrence

Challacolloite is rare chloride, KPb_2Cl_5 (Tables 2 and 3). Its crystal structure has been studied by Schlüter et al. (2005) and Mitolo et al. (2009). As challacolloite is currently synthesised for laser applications, further studies on its structure and properties are available in the literature (see Mitolo et al. 2009 and the references therein). The few recorded occurrences include hydrothermal and volcanic environments, such as the leucotephrite lava produced by the 1855 AD Vesuvius eruption (Italy; Schlüter et al. 2005), the medium-high temperature (T=400 °C) fumaroles at Vulcano in the Aeolian archipelago (Italy; Mitolo et al. 2009), the sublimates of Satsuma-Iwojima volcano in Japan (Africano et al. 2002) and mineralisations in the active fumaroles of the Tolbachik volcano in Kamchatka (Russia; Pekov et al. 2015).

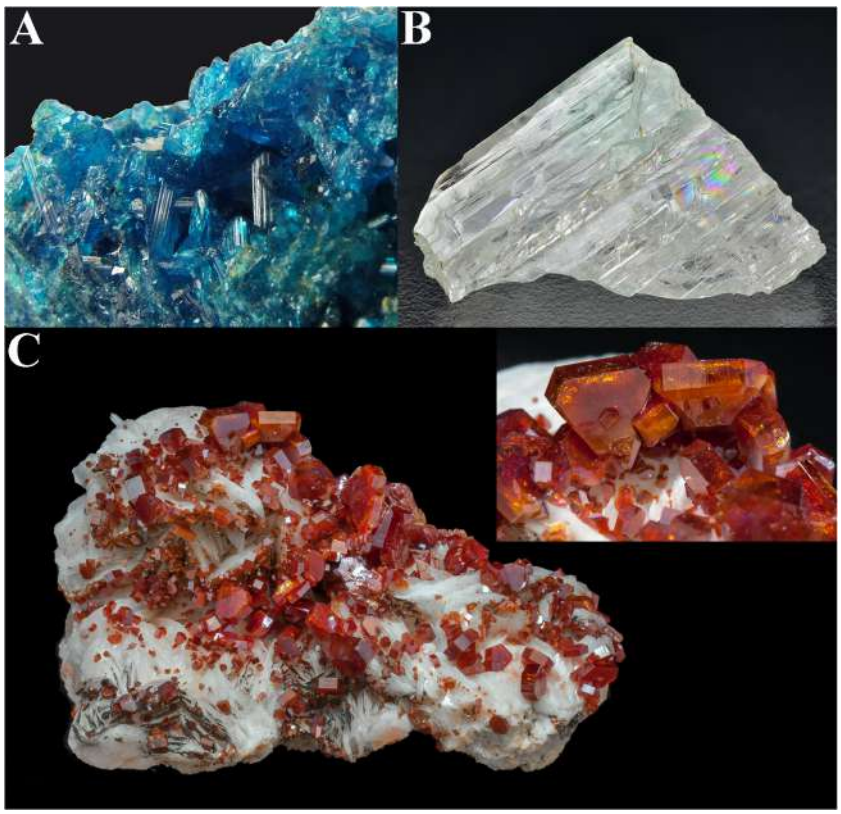

Fig. 13 **A** Caledonite from Mammoth-Saint Anthony Mine, AZ, USA [Arkenstone specimen. Photo credits: Rob Lavinsky, irocks.com–Mindat.org Photo ID: 828378]. **B** Schulténite from Tsumeb Mine, Oshikoto Region, Namibia [collection and photo of Bruce Cairncross –Mindat.org Photo ID: 744912]. **C** Vanadinite on a barite matrix from Mibladen, Midelt, Drâa-Tafilalet Region Morocco [specimen and photo: fabreminerals.com–Mindat.org Photo ID: 862414]. [All images are subject to copyright owned by the photographers indicated above. The CC-BY licence does not supersede previously copyrighted material. Permission has been obtained for reproduction in this article]

The unnamed phase $PbMg(CO_3)_2$ was first studied by Lippmann (1996) who synthesised it by leaving ca. 100 mg of pure lead carbonate ($PbCO_3$) at about 20 °C in a closed vessel with 250 ml of an aqueous solution of 0.01 ml of $MgCl_2$ and 0.02 ml of $NaHCO_3$. After about 6 months, he obtained crystals about 20 μm in size and examined them using XRD. The phase thus studied appeared similar to dolomite and norsethite ($BaMg(CO_3)_2$). Böttcher et al. (1996) investigated this phase using FTIR and Raman spectroscopy while Zheng and Böttcher (2016) studied oxygen and carbon isotope fractionations involving $PbMg(CO_3)_2$. Pimentel and Pina (2015, 2016) obtained this phase from mixing solutions ($Pb(NO_3)_2$, $Mg(NO_3)_2$, Na_2CO_3) at room temperature and observed different sequences of dissolution–crystallisation reactions depending on the Pb:Mg ratios and the overall composition of the slurries. The attention of scholars has mainly focused on norsethite; therefore, this phase has been little studied. However, Kotulanová et al. (2009) performed a series of experiments aimed at simulating the alteration of the wall paintings. They practically repeated Lippmann's experiments starting, however, from red lead instead of lead carbonate. After the same time (6 months), they obtained 26% $PbMg(CO_3)_2$, 51% unconsumed red lead, 13% plattnerite and 10% cerussite.

Challacolloite and $PbMg(CO_3)_2$ in artwork

Challacolloite was first found by Di Stefano and Fuchs (2011) in the middle Ptolemaic Book of the Dead of Amenemhet (papyrus; ROM 978×43.1). The authors interpreted its presence as a secondary product, formed by the interaction of hydrocerussite with the potassium chloride from the earth. A few years later, this phase was found, by Bezur et al. (2015), on a 15th-century Virgin and Child terracotta relief by Michele da Firenze. The authors individuated hydrocerussite as the likely source of lead, and potash lye and hydrochloric acid—possibly used for restoration interventions—as potential sources of potassium and chloride ions. Salvant et al. (2018) found challacolloite in the ~2nd-century AD mummy portraits from Tebtunis (Egypt). The authors found it to be associated with hydrocerussite and suggested its in situ formation from that pigment. The last occurrence was provided by Ma and Berrie (2020), who found challacolloite and cotunnite in the painted decoration of an early 16th-century *Pietà* (terracotta sculpture) by Giovanni della Robbia. As with the previous authors, the formation of this phase was interpreted as a transformation of hydrocerussite under high chloride ion concentrations and/or low pH conditions, following the aqueous solution's evaporation. The possibility of K-leaching by the glaze was considered less likely, given the stability of the glaze.

$PbMg(CO_3)_2$ has been found in a Gallo-Roman (end of 2nd century AD) mural fragment from the Roman villa excavated at Pierre Hardie Street in Metz (France) (Dooryhée et al. 2005). The authors interpreted its presence as a secondary product, due to the interaction of massicot with Mg-containing calcium carbonate. The wall paintings in Kostol'any pod Tribečom (Slovakia) provided a further occurrence, investigated by both Hradil et al. (2013) and Kotulanová et al. (2009). This phase was associated with plattnerite, scrutinyite, cerussite, hydrocerussite and massicot and was interpreted as a secondary phase. Hradil et al. (2013) further claimed that its presence testified the use of dolomitic lime. Kotulanová et al. (2009) suggested that "*Pb^{2+}ions, formed by the disproportionation of red lead, reacted with aqueous magnesium ions in the porous system of the plaster and formed $PbMg(CO_3)_2$*".

Production centres of lead-based pigments

Archaeological evidence of artisanal quarters devoted to the production of the pigments outlined above is small and geographically limited.

The production site individuated in the southern sector of the ancient agora of Kos Island (Greece) is of outstanding importance, as it provides evidence of the close relationship of pigment production with metalworking in the second half of the 1st century BC (Kostomitsopoulou Marketou et al. 2019). The pigments produced onsite (Egyptian blue and red, brown, yellow and green earths) were found, together with litharge rods and lead lumps. The finding of a Fe- and Pb-based red pigment led the authors to hypothesise for this mix either an artificial nature or a natural origin. In the first case, the mix would have represented the product 'of a mixing and calcination process', described by *Plinius* (*Naturalis Historia*, 35, 30, 40) as *sandyx* (rubric and sandarach in 1:1 ratio, calcined with cerussa) and *syricum* (sinopis and sandyx in 1:1 ratio). The second case was suggested by its similarity with a geological sample taken from the 'Metalleio' site on Mt. Dikaios.

Precious information has also been provided by the research project carried out, in an Early to Late Cycladic I (c. 2700–1600 BC) context, at Akrotiri on Santorini Island (Greece). Here, Sotiropoulou et al. (2010) found and analysed raw pigments (in various shapes, ranging from powders to lumps and moulds) and traces of pigments on the surface of stone tools, which were likely used for pigment preparation. In more detail, the authors found the following: (a) a bright-pink layered fragment of minium (4%) mixed with calcite (92%), quartz (3%) and muscovite (1%); (b) various residual lead-based compounds on stone tools (cerussite, hydrocerussite, litharge, caracolite ($Na_3Pb_2(SO_4)_3Cl$), lead sulfate (Pb_2SO_5), lead hydroxide chloride, calcium lead phosphate hydroxide ($Ca_{0.81}Pb_{4.19}(PO_4)_3(OH)$), hydroxylapatite plumboan and drugmanite ($Pb_2(Fe^{3+},Al)H(PO_4)_2(OH)_2$)); and (c) mineral phases not bearing Pb such as hydroxylapatite, clinoptilolite, halite, hematite, calcite, dolomite, kaolinite, illite, albite, labradorite, hornblende and quartz. While the authors were able

to correlate the production of these pigments to the processing of masses of litharge, the use of the pigments remained obscure. The researchers found no evidence of lead-based pigments in the local wall paintings; therefore, pending further discoveries, a likely hypothesis is that they were intended for cosmetics.

In this context, the pigments found in the workshops of artists or stores at Pompei in Italy (see, *e.g.*, Augusti 1967; Giachi et al. 2009; Aliatis et al. 2010), or Delos in Greece (Karydas et al. 2009) provided suitable information for the reconstruction of the production process, as they did not contain binding media. For example, at Pompeii, the cerussite found in a mixture with calcite and quartz in the Egyptian blue powder "*may have been introduced by the painter to fade the blue colour*" (Aliatis et al. 2010); however, it is known that pigments were sold by weight, and therefore, cerussite could be present to increase the weight of the product. Still at Pompeii, the discovery of a powder made of malachite, Egyptian blue, hematite, goethite, cerussite, massicot, albite, calcite, quartz and copper arsenate compound (sample P13 from bowl no. 117364; Aliatis et al. 2009) testifies how different types of pigments were mixed to obtain the desired colours. Conversely, the absence of lead-based pigments in similar contexts, such as at Elephantine Island on the Nile in Egypt (Pagès-Camagna and Raue, 2016) can provide chronologically framed negative evidence of their use.

Finally, underwater findings can help to reconstruct the routes connecting the production centres with the distribution sites. In this regard, the discovery of galena, lead carbonate, minium, metallic objects and raw glass in the shipwreck of Glavat (Mljet/Meleda, Croatia) is very interesting (Auriemma 2018). According to various authors, the origin of the metals and pigments can be traced back to the silver and lead mines located in the Srebrenica area (Bosnia); that is to say, ancient *Argentaria*. The authors observed that the mining area was well-connected with the ports of Salona, Narona and Epidaurus, where the cargo of the sunken ship could have been purchased (Radić Rossi 2009).

Lead-tin yellow I–II, lead-antimony yellow (Naples yellow), lead-tin-antimony yellow and lead chromates

An exhaustive discussion of these pigments would require at least three separate articles. Thus, this section attempts to provide a brief overview, describing the main characteristics of these pigments and indicating the essential bibliographic references from which to start a detailed examination.

For these pigments, it should also be noted that lead stannates and antimonates are common glass colouring and opacifying agents. The intensive study of these phases in the field of ancient glass and ceramic production has created such a body of literature that it cannot be cited here in its entirety. We, therefore, limit ourselves to indicating the texts to be consulted to begin their study: Turner and Rooksby (1959); Hedges and Moorey (1975); Hedges (1976); Henderson and Warren (1983); Mass et al. (1996); Mason and Tite (1997); Freestone and Stapleton (1998); Pernicka et al. (1998); Tite et al. (1998); Molera et al. (1999); Heck and Hoffmann (2000); Mass et al. (2002); Shortland (2002); Tite et al. (2008); Rosi et al. (2011) and Matin (2018).

Lead-tin yellow types I and II

There are conflicting opinions on the terminology and production technology of lead-tin yellow pigment handed down by ancient texts, mainly because all of these pigments (as well as massicot) appeared indiscriminately under the name of *giallorino* or *giallolino*, or using analogous terms such as *zalolin* (*the term zalo* corresponds to modern '*giallo*', meaning yellow). The mentions and recipes handed down since the 15th century are many and, as such, we report only a few examples from the 15th to the 17th century, through which the origin and use of the term are understood (Table 3).

A terminological confusion (at least, as far as today's reader is concerned) persisted in the following centuries, until the analytical research conducted separately by Jacobi and Kühn shed light on the real nature of these pigments, also taking advantage of the studies carried out simultaneously by Turner and Rooksby on opacified glass (Turner and Rooksby 1959, 1963; Rooksby 1964).

Jacobi (1941) first took stock of the conflicting opinions of Raehlmann[13](1910), who claimed to have found Naples yellow on paintings from the Renaissance period, and De Wild (1931), who, having not found it, proposed identification with massicot. He, then, analysed some samples taken from Germano-Gothic artworks of the 15th and early 16th centuries and from Dutch artworks from the 16th and early 17th centuries. The results highlighted the presence of rather high tin levels and allowed him to synthesise the lead-tin yellow 'of the old masters' in various shades. He used a mixture composed of about three parts of lead oxide, red lead or lead dioxide, and one part of metastannic acid for the synthesis process. The mixture was heated at a temperature of 650–800 °C, and different colours were obtained at variable temperatures: orange between 650 and 680 °C, rich yellow at 700 °C and lemon-yellow between 740 and 800 °C.

Kühn (1968) first deduced that "*both the 'giallolino' mentioned in Italian literary sources and the 'massicot' ('masticot') of the northern manuscripts are identical with lead-tin yellow*", based on various elements, including a comparison

[13] Raehlmann was among the first to introduce optical microscopy in the study of works of art. In his text, he identified 'Neapelgelb = antimonsauresBleioxyd' (*i.e.* Naples Yellow = lead oxide antimony).

between Italian and foreign literary sources, the discovery of lead-tin yellow in 154 paintings and 4 polychrome sculptures, the analysis of lead oxides samples from old pharmacies and previous scientific works (Gettens 1967; Coremans et al. 1952; Sneyers and Thissen 1958; Coremans 1961). Secondly, Kühn distinguished between lead-tin yellow I (Pb_2SnO_4) and lead-tin yellow II, the latter being compositionally similar to the yellow lead-tin oxide determined by Rooksby (1964) as a glass opacifier (probably $PbSn_2SiO_7$, Kühn hypothesised). In fact, Rooksby (1964) synthesised this compound at 800–950 °C, starting from a mixture of lead-tin yellow I (Pb_2SnO_4) and silica. Reconstructing the history of this pigment and its studies, Kühn (1968, 1993):

1. suggested that this pigment was "*manufactured in glass furnaces*", based on the connection with the *giallo di vetro* (glass yellow) mentioned in various ancient texts (Table 3);
2. set up a correspondence between lead-tin yellow type I and the *giallolino fino* discussed by Merrifield (1849) as a Flanders origin product;
3. established a correspondence between the lead-tin yellow type II, the *giallo di vetro* (glass yellow) discussed by Merrifield (1849) as a Venetian origin product, and recipe 273 of the Bologna manuscript. Recipe 272 had to represent the first part and was not a recipe in its own right;
4. described the optical characteristics and provided numerous indications of the properties of these pigments, to facilitate their recognition through microchemical tests and instrumental analyses.

Subsequent studies have further clarified the structure of the various compounds and broadened our knowledge about the use of these compounds in painting and glass production. The studies performed by Byström and Westgren (1943), Swanson et al. (1972), Garnier et al. (1976), Gavarri et al. (1981), Gavarri (1982), Vigouroux et al. (1982), Clark et al. (1995) and Spahr et al. (2020) have gradually clarified the characteristics and the thermally induced transformations occurring in the structures.

In artworks, lead-tin yellow types I and II are typically used individually; however, cases in which both phases are used are not unheard of (Penny and Spring 1995; Aloupi et al. 2006; Seccaroni 2006; Borgia et al. 2007; Ricci et al. 2004). Lead-tin yellow type I is more widespread than type II and is almost always associated with lead white and cinnabar. Frequently, it has also been associated with azurite, followed by minium, malachite, ochres/earths, massicot, verdigris and ultramarine.

Lead-tin yellow type I

Walton and Trentelman (2009) argued that this pigment was produced "*out of litharge associated with silver cupellation at the Rio Tinto site*" (Figure 14, 1). Other authors have leaned towards a reconstruction starting from minium, thus synthesising a mixture of Pb_3O_4 and SnO between 650 °C and 900 °C (Figure 14, 2); in this case, it has been demonstrated that, when using higher temperature, the resulting pigment is lighter (Kühn 1968, 1993; Hradil et al. 2007). The hydrothermal synthesis developed by Wu et al. (1999) using lead acetate and sodium stannate (requiring caustic soda or sodium carbonate) has not been attested to in antiquity (Figure 14, 3). Based on Gavarri et al. (1981) and Clark et al. (1995), between 5 and 300 K (~ −268 °C and 27 °C), no phase transition is observed; at temperatures below 800 °C, the reaction is incomplete; and, at temperatures above 900 °C, PbO volatilises and the compound decomposes. Moreover, massicot may be present with an excess of Pb_3O_4.

Modern lead stannate Pb_2SnO_4 (lead-tin yellow type I) is produced by heating $PbCO_3$ and SnO_2 (generally in a 2:1 molar ratio) for a variable time (*e.g.*, 1 week in Swanson et al. 1972; 6–12 h in Hashemi et al. 1992), at temperatures between 750 and 1000 °C. This synthetic phase is characterised by edge-sharing SnO_6-octahedra forming "*chains along the c-direction, interconnected within the (001) planes with* Pb^{2+}*ions*" (Spahr et al. 2020). Its structure was first assigned to the tetragonal space group $P4_2/mbc$ by Byström and Westgren (1943) and Swanson et al. (1972) and then to the orthorhombic space group *Pbam* by Gavarri et al. (1981). Spahr et al. (2020) performed single crystal diffraction at ambient pressure on hydrothermally synthesised Pb_2SnO_4. They demonstrated that, although the *Pbam* space group has to be preferred, this lead stannate can be refined in both $P4_2/mbc$ and *Pbam* space groups.

Regarding the chronology, Clark et al. (1995) claimed a period between 1450 and 1750 for the use of lead-tin yellow type I. In the literature published after their work, this pigment has been found in the following:

- 12^{th}- to 13^{th} (?)-century polychrome sculptures in the porch of the main and south portals of Ferrara cathedral (Pinna et al. 2020);
- 14^{th}-century wood ceilings of the Hall of the Abencerrages and the Hall of the Two Sisters in the Alhambra at Granada (Arjonilla et al. 2019a);
- 14^{th}-century (third quarter) wall paintings of the Dominican Monastery at Ptuj in Slovenia (Gutman et al. 2014)
- 15^{th} (also 16^{th}?)-century manuscripts on parchment (for the 15^{th} century, see, *e.g.*, Chaplin et al. 2005; Duran et al. 2014; Bonizzoni et al. 2016; Carvalho et al. 2018; for a $15^{th}/16^{th}$-century parchment see Vanmeert et al. 2018);
- 15^{th}- to 17^{th}-century panel paintings on wood or walnut (for the 15^{th} century, see, *e.g.*, Martin and Duval 1990, 1998; Dunkerton and Roy, 1996; Hradil et al. 2007;

Bersani et al. 2008; Ricci et al. 2004; Sodo et al. 2019; Gutman Rieppi et al. 2020; for the 16th century, see, *e.g.*, Penny et al. 1996; Higgitt et al. 2003; Roy et al. 2004; Mottin and Laval 2004; Plazzotta et al. 2006 (doubtful); Borgia et al. 2007; Hradil et al. 2007; Dunkerton and Howard 2009; Amadori et al. 2016; Želinska et al. 2018; for the 17th century, see, *e.g.*, Roy 1999; Olszewska-Świetlik et al. 2013);

- 14th- to 17th-century wall paintings (for the 14th and 15th centuries, see, *e.g.*, Perardi et al. 2003; Gutman et al. 2014; Arjonilla et al. 2019a; Levstik et al. 2019; Pinna et al. 2020; for the 17th century, see, *e.g.*, Vlachou-Mogire et al. 2020);
- 17th- and 18th-century oil paintings on canvas (Feller 1973; Hradil et al. 2007; Duran et al. 2010; De Keyser et al. 2017; Vanmeert et al. 2019).

To study the alteration products, Kočí et al. (2019) mixed lead-tin yellow pigment with egg yolk and linseed oil and defined the structure of seven mixed lead carboxylates $[Pb(C16)_{2-x}(C18)_x]$ in model tempera paints. The interactions between lead-tin yellow I and (a) egg yolk, (b) egg yolk and oil emulsion and (c) oil have been further investigated by Švarcová et al. (2019). These authors observed that, while tests containing only oil did not form lead soaps, tests containing the emulsion or egg yolk alone formed lead carboxylates, with a variable ratio of palmitates and stearates.

Lead-tin Type I

$$2PbO + SnO_2 \rightarrow Pb_2SnO_4 \quad [1]$$

$$2Pb_3O_4 + 3SnO_2 \rightarrow 3Pb_2SnO_4 + O_2 \quad [2]$$

$$2(CH_3COO)_2Pb + Na_2SnO_3 + 2NaOH \rightarrow Pb_2SnO_4\downarrow + 4CH_3COONa + H_2O \quad [3]$$

Lead-tin Type II

$$Pb_2SnO_4 + SiO_2 \rightarrow PbSn_{1-x}Si_xO_3 \quad [4]$$

$$6PbO + 3SnO_2 + 2SiO_2 \rightarrow [3PbO\text{-}2SiO_2] + 3[PbSn_{1-x}Si_xO_3] \quad [5]$$

Lead-tin-antimony

$$5PbO + Sb_2S_3 + 2SnO_2 + 6O_2 \rightarrow PbSO_4 + 2Pb_2SbSnO_{6.5} + 2SO_2 \quad [6]$$

$$6PbO + Sb_2S_3 + 2SnO_2 + 6O_2 \rightarrow Pb_2(O)SO_4 + 2Pb_2SbSnO_{6.5} + 2SO_2 \quad [7]$$

Fig. 14 The chemical reactions illustrating the production processes of lead-tin yellow types I and II and lead-tin-antimony yellow. Equations 2 and 4 from Clark et al. (1995); Eq. 3 from Wu et al. (1999); Eqs. 5–7 from Hradil et al. (2007)

Lead-tin yellow type II

The lead stannate $PbSn_{1-x}Si_xO_3$, called lead-tin yellow type II, has been structurally investigated by Morgenstern Badarau and Michel (1971) and Clark et al. (1995). The crystallographic parameters were defined for $PbSnO_3$ by the former and for $PbSn_{0.76}Si_{0.24}O_3$ by the latter. As for the production, lead-tin yellow type I and silica were heated around about 900 °C (Figure 14, 4); being careful not to exceed the temperature of 950 °C, beyond which the basic compounds were obtained (*i.e.* tin oxide, lead oxide and silica). The proportions between the two components could vary within a certain limit, which changed the product's colour and the processing temperature. Based on Clark et al. (1995), an optimum was achieved with a 1:1 ratio. When this ratio was higher or lower, lead-tin yellow types I and II or lead-tin yellow type II and unreacted silica were obtained, respectively. Hradil et al. (2007) have also demonstrated that lead-tin yellow type II can also be obtained by a single-step synthesis, heating the single Pb, Sn and Si oxides at about 850 °C (Figure 14, 5), with a ratio of 6:3:2 of the three components). These authors further noticed that, when using even slightly different ratios, they obtained the following:

(a) PbO forming a glassy phase and unconsumed SnO_2 with a slight excess of SiO_2;
(b) Pb_2SnO_4 with an excess of Pb;
(c) Pb_2SnO_4, $PbSnO_3$ and a glassy phase with equal amounts of PbO and SnO_2 but insufficient SiO_2.

They found the production of this pigment more complicate than that of lead-tin yellow type I and detailed the response in the tendency of lead to form a colourless glassy silicate phase, until a high temperature was reached (800–900 °C).

In artwork, it has been observed from the beginning of the 14th century on panels (Gordon et al. 1985; Martin and Duval 1990; Kühn 1993) and wall paintings (Bandera et al. 2005; Seccaroni 2006). The same use has been attested in the 15th century (Gordon et al. 2002; Borgia et al. 2007; Ricci et al. 2004), 16th century (Kühn 1993; Penny et al. 1996) and the first half of the 17th century (Seccaroni 2006). Accordingly, its diffusion, as indicated by Clark et al. (1995), spans from 1300 to 1650, which is not contradicted by the most recent literature. In this frame, the identification of lead-tin yellow type II, together with yellow chrome, in the rood screen and canopy of St. Mary's decorated by Sir Ninian Comper in 1896–98 for the Church of Our Lady of Egmanton in the UK sounds somewhat out of time (Edwards et al. 2007).

Before moving on to Naples yellow, it is worth noting that, while the chronologies provided for both types of lead-tin yellow likely highlight the period of the greatest diffusion of the pigment, the start and end periods of use may be partially

invalidated by future detailed studies. For example, there already exist several papers that lack type characterisation (for various reasons) and whose dating falls within/outside the indicated chronological range. These latter studies reported the presence of lead-tin yellow pigments on artworks dated from the 6th (Hedegaard et al. 2019) to the 16th (Spring 2007; Espejo Arias et al. 2008; Križnar et al. 2009; Amadori et al. 2013; Franquelo et al. 2015; Aurélie et al. 2016; Martin-Ramos et al. 2017; Doménech-Carbó et al. 2019; Impallaria et al. 2020), 17th (Križnar et al. 2019; Uhlir et al. 2019; Delaney et al. 2020) and 18th (Cortea et al. 2020) centuries. Indeed, more extensive and detailed studies are required, in order to draw an indisputable chronological picture of the use of these pigments.

Lead-antimony yellow (or Naples yellow)

Naples yellow has been also called 'lead antimonate yellow', 'Giallo di Napoli', 'Giallorino' or 'Giallolino di Napoli'. According to Laurenze and Riederer (1982), the term 'Napples yellow' (*Luteolum Romaedicitur Luteolum Napolitanum*) was used for the first time by Pozzo (1698–1702) (see also Table 3).

Naples yellow is an artificial lead–antimony oxide (lead antimonate). Compositionally, it is usually considered as isostructural with bindheimite (Table 2). However, Hålenius and Bosi (2013) recently re-examined old museum specimens collected in the 19th century from the Harstigen Fe-Mn Mine (Sweden) and identified a new mineral species called oxyplumboroméite. This yellow-to-brown phase with the formula $Pb_2Sb_2O_7$ is a valid IMA species, which probably includes two questionable and poorly defined IMA mineral species, monimolite and bindheimite. Chemically, oxyplumboroméite is similar to 'Naples yellow'.

In any case, Naples yellow is generally recognised as an artificial pigment, as the use of natural minerals has never been proven with certainty and the literary sources are not sufficiently clear in tracing the link between Naples yellow and the yellow pigment related to volcanoes (*e.g.*, de Massoul 1797, Marcucci 1816; Merrifield 1846). In detail, Mary Merrifield (1849) mentioned that 'giallorino' (Naples yellow) is sometimes used for fresco painting but should be avoided where the paintings are exposed to the air too much. She also included 'Giallolino di Fornace' and 'Giallolino di Napoli' as alternative names for Naples yellow. According to Merrifield (1846, pp. clxii), there are two types of Naples yellow: (a) a natural mineral related to volcanoes, and which was called giallolino, giallolino di Napoli or jaune de Naples, and (2) an artificial pigment consisting of oxide of lead and antimony, called also 'giallo di Napoli', 'jaune de Naples', or 'Naples yellow' (see also Table 3 on this topic). Merrifield specified that the latter was in use in her times (*i.e.* the middle of the 19th century) but was unknown to the old Italian painters.

The recipes that have been handed down to us directly (literary resources) and indirectly (reconstructed by archaeometric investigations on archaeological artefacts) show different procedures based on the place and chronology (Laurenze and Riederer 1982; Wainwright et al. 1986; Dik et al. 2005; Valeur 2010). For example, Marcucci (1816; p. 66-67) stated that 'giallo di Napoli' (Table 1, MA1) is a "*yellow lead oxide mixed with antimony oxide*", which can be prepared from a mix of white lead, antimony oxide, burnt alum, and ammonium chloride, calcined for 3 h.

Basically, however, all recipes have the calcination of a mixture of lead compounds (*e.g.*, metallic lead, lead monoxide or lead white) and antimony compounds (*e.g.*, metallic antimony, antimony (III) oxide Sb_2O_3, potassium antimonate ($KSbO_3$) and tartar emetic ($K(SbO)C_4H_4O_6 \cdot 1/2H_2O$)) in common (Dik et al. 2002). Two important experimental researches have reconstructed the production process and studied the resulting products. In chronological order, the first was Dik et al. (2005), who estimated temperatures between 700 and 1000 °C for "*historical lead antimonate production*". The second was Hradil et al. (2007), who reproduced different processes, coming to definitively exclude the feasibility of some procedures tested in the past and reaching a significant reconstruction of how the past production could have taken place. In the first case, they showed that heating Pb_3O_4 and Sb_2O_3 without fluxes must reach at least 1000 °C to obtain a mixed product (bindheimite, rosiaite, $Pb_2Sb_2O_7$ and $Pb_{3+x}Sb_2O_{8+x}$). In the second case, they showed that, through the use of 10–20% NaCl (a flux readily available in antiquity), it was possible to obtain a product (single-phase pyrochlore) of better quality than the previous ones at a lower temperature (700–900 °C; even if the elimination of NaCl requires a temperature of 800–850 °C for at least 5–10 h). When repeating the experiment with K_2CO_3 instead of NaCl, the product (pyrochlore with probable K in the structure) did not have the same quality; furthermore, when adding 5–10% silica gel, the product acquired a salmon colour. By replacing Sb_2O_3 with Sb_2S_3 there was no need for a flux.

Historically, lead antimonate has been used both for glass-making, from the 16th to the 14th century BC (see below) and in painting. Clark et al. (1995) indicated the use of this pigment in painting in a period ranging from 1700 to 1850. Detailed accounts of the paintings containing Naples yellow have been given by Wainwright et al. (1986) and Seccaroni (2006).

In addition to the various attestations reported by these authors, further occurrences have been recently reported:

- tempera and oils on panels dated to the 16th (Plesters 1984; Roy and Berrie 1998), 17th (Felici et al. 2004; Moioli and Seccaroni, 2004) and 18th- 19th centuries (Bomford and

Roy 1993; Hradil et al. 2007; Daniilia et al. 2008; Wagner et al. 2019);
- wall paintings from the second half of the 18th century, at Moschopolis in Albania (Pavlidou et al. 2008) and Greece (Malletzidou et al. 2019).

Going back in time, it is undoubtedly worth mentioning the discovery carried out in the wall paintings of the *Domus* below the Basilica of Saints John and Paul on the Caelian Hill in Rome (Italy), dated to the late 1st to 4th centuries (original or retouched unknown).

Considering all these attestations, the period of use of Naples yellow expands from the beginning of the 16th century to, at least, the 19th century (see also Clark et al. 1995; Maggetti et al. 2009; Chiarantini et al. 2015; Yuryeva et al. 2018; Györkös et al., 2020). However, the reconstruction that admitted a complete replacement of lead-tin yellow pigments by Naples yellow at the beginning of the 18th century (Laurenze and Riederer 1982; Lahlil et al. 2011) does not seems completely valid in paintings and was largely undermined by the state-of-the-art of the studies. The versatility of this pigment, both used individually and to obtain green in combination with Prussian blue (Grissom 1986), must have represented one of the advantages that made it so successful.

Lead-tin-antimony yellow

Lead-tin-antimony yellow was mentioned in the Darduin book of recipes (about 1644; Sandalinas and Ruiz-Moreno 2004; Pelosi et al. 2010). Hradil et al. (2007) experimentally reproduced the pigment and obtained $Pb_2Sb_{2-x}Sn_xO_{7-x/2}$ (and traces of unconsumed SnO_2) through heating Pb_3O_4, Sb_2O_3, SnO_2 and 10% NaCl between 700 and 900 °C. The crystallographic structure of the resulting compounds, showing 2:1:1 and 2:1.5:0.5 ratios, was further investigated and found to be consistent with a "*mixture of two pyrochlore structures with different cell sizes*". The same experiment was successfully repeated using Sb_2S_3 instead of Sb_2O_3 (without NaCl) and resulted in the production of the yellow pigment + anglesite at 850 °C (Figure 14, 6) or + lanarkite at 900 °C (Figure 14, 7). Finally, it also worth underlining that these authors provided key indications to facilitate the individuation and discrimination of the various lead, tin and antimony-based pigments.

In artwork, this pigment is sporadically found. As previously observed by Hradil et al. (2007), this pigment "*has not been identified in so many cases as Naples [—] and lead tin [—] yellows because it has not been searched*".

The few occurrences we were able to find can be listed as follows:

- in early 16th-century walls paintings and tempera on panel (Cauzzi 2003; Seccaroni 2006);
- in 17th-century oils on canvas and, to a lesser extent, wall paintings (Garrido Perez 1992; Newman 1993; Ravaud et al. 1998; Roy and Berrie 1998; Santamaria et al. 2000; Leonard et al. 2001; Martin et al. 2003; Ruiz-Moreno et al. 2003; Seccaroni 2006; Pelosi et al. 2007a, b; Howard and Nethersole 2010; Impallaria et al. 2019);
- in 18th- and 19th-century oils on canvas (Hradil et al. 2007; Morrison 2010; Wagner et al. 2019)

Artificial lead chromates—yellow chrome and orange chrome

Artificial lead chromates include a series of yellow ($PbCrO_4$ and $PbCrO_4{\cdot}PbSO_4$) and orange ($PbCrO_4{\cdot}PbO$) pigments. Their production followed the discoveries of 'Siberian red lead' in the Urals (1761 by Johann Gottlob Lehmann; 1770 by Peter Simon Pallas) and, above all, the discovery of chromium—by boiling crocoite with potassium carbonate—byNicolas-Louis Vauquelin in 1797 (Kyle and Shampo 1989). In 1803, Berthollet and Vauquelin (1804) provided evidence of the chromium-based pigment while, in 1809, Vauquelin explained the method for obtaining chromates of potash, ammonia, lime, magnesia, lead, copper, silver metallic chromates and Cr-containing compounds for porcelain. Moreover, he indicated to heat half a part of nitre and one of chromate to decompose iron chromate (*i.e.* chromite, $Fe^{2+}Cr_2O_4$; Table 1, VA1).

These two papers mark the beginning of the production of chromates; therefore, the year 1804 or 1809 is set as the start date for chromium-based pigments in painting. However, lead chromates were immediately used both as a pigment for painting and in leather tanning (discovered and patented in 1884 by Augustus Schultz and Martin Dennis). In the *Nouveau dictionnaire d'histoire naturelle appliquée aux arts* (1818), it is mentioned that Russian painters paid high prices for the lead chromate (*i.e.* crocoite) used for their artworks, thus attesting the very early and widespread use of artificial lead-chromates.

Artificial lead-chromates started to be produced on a large scale only in the second half of the 19th century; however, due to their high price, they were frequently mixed with other substances, such as barite or gypsum (West, 1986).

As for the recipes, the Nouveau dictionnaire (*op. cit.*) reported that it is produced by decomposing potash chromate with lead acetate (Table 1, NO1) and described the main characteristics of the *plomb chromaté* (Table 1, NO2). More recent recipes used lead salts and chromate or bichromate solutions (Hurst 1892) while current technical specifications are provided in the updated version of the standard ASTM D211-67 (2019)[14], including six types of commercial lead chromate pigments (type I—primrose chrome yellow; type II—lemon

[14] Standard specification for chrome yellow and chrome orange pigments

chrome yellow; type III—medium chrome yellow; type IV—light chrome orange; type V—dark chrome orange; and type VI—chrome yellow for green).

For the purposes of this review, it is important to keep in mind two aspects directly related to the production process: (1) the size of the crystals and the amount of lead are responsible for the colour variations, from light yellow to deep orange (Bell et al. 1997) and (2) incomplete reactions, different ratios of the ingredients and variable temperatures produce compounds with different characteristics, and therefore, it is common to find different phases of basic lead chromate within the same pigment (for example, Sansonetti et al. 2010).

As for the individuation of yellow lead chromates, the reader is referred to the section dedicated to crocoite for the yellow $PbCrO_4$. As we have seen, the production process does not give rise to a single phase but, instead, to a group of phases (solid solution) which have, as end members, the monoclinic crocroite and the orthorombic lead (II) sulfate ($PbSO_4$, corresponding to the natural anglesite). "*The $PbCrO_4$-$PbSO_4$ system and its mineralogical significance*" were investigated by X-ray powder diffraction by Crane et al. (2001), who clarified numerous aspects related to the stability of the various phases. The compositional variability of the intermediate compounds is indicated by the chemical formula $PbCr_{1-x}S_xO_4$, where x can range from 0 to 0.8; the structure varies accordingly, from monoclinic to orthorhombic with $x > \sim 0.4$–0.5 (Monico et al. 2019). The different compositions and crystalline structures of these compounds influences their stability in artworks. In this regard, the studies carried out by Monico and co-workers on the photochemical alteration of these pigments are of great importance (Monico et al. 2011, 2014, 2019). In addition to providing numerous reference Raman spectra, these authors demonstrated that the alteration is due to the photoreduction of chromium from the hexavalent to the trivalent state and that the intermediate compounds $PbCr_{1-x}S_xO4$ ($0<x \leq 0.8$) are more unstable than $PbCrO_4$ (in which the S is not present).

Furthermore, they identified the formation of compounds such as viridian ($Cr_2O_3 \cdot 2H_2O$), $Cr_2(SO_4)3 \cdot H_2O$ or $(CH_3CO_2)_7Cr_3(OH)_2$ and experimentally tested the stability of the various compounds in the presence of binders (especially oil and acrylic binders) which had been identified among those responsible for the photoreduction of Cr (VI). A scheme of the reconstructed (photo) reduction mechanism was provided in Monico et al. (2019)

The orange lead chromates correspond to phoenicochroite, $Pb_2O(CrO_4)$, which has been structurally investigated by Williams et al. (1970) (Table 2). It is notable that this lesser-known and -attested phase has been found in 9th to 12th century AD polychrome decorations (carved stucco, wall paintings and terracotta friezes) in Nishapur, Iran, and was deemed to be of local provenance (Holakooei et al. 2018).

In artwork, yellow lead chromates are the most attested, followed by orange and green. Their attestations are all related to the 19th and 20th centuries and include both contemporary works and retouches of older works. To give just a few examples, yellow (mostly) and orange (to a lesser extent) chrome pigments have been found in the following artworks:

- the stuccoes of several Italian churches at Milan (17th-century Guastalla Chapel in the Church of San Fedele), Laino (Church of S. Lorenzo), Campione d'Italia (Church of S. Maria dei Ghirli), Como (Church of S. Maria Assunta at Puria) and Mantova (18th- to 19th-century Church of Sant'Andrea) (Sansonetti et al. 2010, 2020);
- the iconostasis of a small wooden Saint Nicholas Church in Şirineasa (Vâlcea County in Romania), dated to the 18th to 19th centuries (Huică et al. 2020);
- a 19th-century tempera icon from northern Greece (Lazidou et al. 2018);
- the 1812 AD wallpaper *Les Monuments de Paris* by Dufour and Leroy (Paris) (Castro et al. 2004a, b);
- the wall tempera of the Catholicon of the Rila Monastery in Bulgaria, dated to the first half of the 19th century (Stamboliyska et al. 2021);
- the icons kept in the Antim Monastery at Bucharest (Romania) and the One-Wood Monastery in the Valcea County (Romania), dated to the first half of the 19th century (Serafima et al. 2019a);
- a printed Turkish red calico (cotton; Wertz et al. 2019);
- the 19th-century restoration of the wooden polychrome sculptures by Jan Geernaert (1704–1777) (Aliatis et al. 2012);
- the oil on canvas *Battle of Grunwald* by Jan Matejko (1838–1893) (Wagner et al. 2019);
- 1880–1890 Turkish postage stamps (Akyuz and Akyuz 2017);
- the rood screen and canopy by Sir Ninian Comper in the Church of Our Lady of Egmanton in UK (Edwards et al. 2007);
- the 1886–1942 oils on canvas or on cardboard by Pío Collivadino (1869–1945) (Buscaglia et al. 2020);
- the wall paintings by Augusto César Ferrari of the Dome and aisles of the Church of San Miguel at Buenos Aires in Argentina (Tascon et al. 2017);
- the oils on canvas by José María Espinosa (1796–1883) and Epifanio Garay (1849–1903) (Badillo-Sanchez and Baumann 2016);
- the oils on canvas and tin-plated iron sheets by Giorgio Marini (1836–1905) (Bordalo et al. 2016);
- the circa 1900 AD Thai manuscript no. 3 (Burgio et al. 1999).

In the 20th century, its attestations are still numerous; however, they go beyond the chronological limit observed in the

review (*i.e.* up to 19th century) and, therefore, are not cited herein. Conversely, more information about the first uses and early nomenclature can be found in Kühn and Curran (1986). Further occurrences have also been provided by Lei et al. (2017; based on previous literature in Chinese), who reported the finding of this pigment on a Ming Dynasty (1368–1644) sculpture from the Chunyang Temple (Shanxi, China) and in a Qing Dynasty (1644–1912) mural in the West River Site (Zhangqiu, Shandong, China). In these cases, the pigment was deemed to be of European origin.

Finally, it is worth adding that lead chromates represent only the most popular type of Cr-containing pigments. In fact, chromium can also yield yellow pigments when combined with cadmium ($CdCrO_4$), zinc ($K_2O{\cdot}4ZnCrO_4{\cdot}3H_2O$), strontium ($SrCrO_4$) and barium ($BaCrO_4$).

Further notes on the use of lead-based pigments

Binding media and coatings

While the binding media used with lead-based pigments were various, vegetable oils and proteinaceous materials were primarily used, although at varying rates, depending on the period.

Among oils, linseed oil was likely the most popular, followed by walnut oil (in the Middle Ages; see, *e.g.*, Cardell et al. 2009) and poppy oil (from the 17th century) (Gettens et al. 1967). The occurrences of oil media are numerous and span over a long chronological period. To provide just a few examples, in China, they have been attested since the 5th century AD (see, *e.g.*, Liu et al. 2016; Zhou et al. 2020) while in Europe, despite the presence of earlier medieval occurrences (see, *e.g.*, Cardell et al. 2009; Pereira-Pardo et al. 2019; Pinna et al. 2020), they became increasingly popular starting from the 15th to the 16th centuries.

Similarly, egg has had a wide diffusion, both chronologically and geographically. It appears as the preferential medium used to create panel paintings and, especially, icons (see, *e.g.*, Daniilia et al. 2002; Bratu et al. 2015; Lazidou et al. 2018; Serafima et al. 2019a), although there is also no lack of evidence of its use in wall paintings (Daniilia et al. 2008; Malletzidou et al. 2019; Stamboliyska et al. 2021) and woodwork (Cardell et al. 2009; Măruțoiu et al. 2017).

Among other organic binders, animal glues have been frequently attested, especially in Chinese and Japanese paintings (Gettens et al. 1967; Wei et al. 2010; Liu et al. 2016; Luo et al. 2019) and on wooden supports (Arjonilla et al. 2019a; Abdallah et al. 2020; Abdel-Maksoud et al. 2020).

Beeswax has been sporadically reported for artworks ranging from the 2nd century AD onwards (Cardell et al. 2009; Gehad et al. 2015; Salvant et al. 2018; De Meyer et al. 2019a, b), sometimes specifically used as a topcoat (Arjonilla et al. 2019a).

Moving towards (apparently) less-used materials, diterpenic resins (mostly colophony and sandarac) have been sporadically found in 14th- to 17th-century artworks (Cardell et al. 2009; Sansonetti et al. 2010), while terpenic ones have been in 12th- to 19th-century artworks (Stanzani et al. 2016; Abdel-Maksoud et al. 2020; Pinna et al. 2020).

The use of gums (*e.g.*, Arabic gum) has been rarely, but surely, related to either paper/wallpaper (Espejo Arias et al. 2008; Arrizabalaga et al. 2014) or wall paintings (Hradil et al. 2014).

Lastly, it is worth mentioning the use of bovine milk, as a casein-based fixative, in the drawings (1750–1785) of Thomas Gainsborough, in combination with the lead white pigment (Pozzi et al. 2020), as well as the use of heat-bodied tung oil and glue-protein in the 11th-century polychrome statues of the Hua Yan Temple in Datong (Shanxi, China; Wang et al. 2020b).

Diffusion

Lead-based pigments have been used in combination with virtually all known pigments (Supplementary Table S3), from circa the end of the 4th century BC to the 20th century AD. The literature consulted for this review (Supplementary Materials, Appendix 1) has allowed for the collection of archaeometric investigations of artworks found and/or preserved in Albania, Argentina, Austria, Belgium, Bolivia, Brazil, Bulgaria, Cambodia, China, Croatia, Cyprus, Czech Republic, Egypt, Ethiopia, France, Greece, India, Iran, Italy, Malta, The Netherlands, Palestine – Israel, Poland, Romania, Russia, Serbia, Slovakia, Slovenia, Spain, Switzerland, Turkey, the UK, Ukraine and the USA. Among this collection, lead-based pigments from artworks found or preserved in Europe represent the bulk. There are still many countries for which we do not yet have any kind of information solidly based on scientific investigations; however, this does not mean that lead-based pigments did not reach them. The available data do not even allow for the proposal of any type of quantification, as they more reflect the state-of-the-art of the studies than the real diffusion of these pigments.

Despite these limits, it may be interesting to observe how the introduction was geographically diversified. For example, in the ancient 'European' world, lead-based pigments mostly appear as by-products of metalworking. Their use does not seem linked to particular historical-cultural events as to technical-stylistic motivations, linked to markets supply.

In Japan, in contrast, Yamasaki (1967) stated that the introduction of these pigments corresponded to that of Buddhism and, in support of this thesis, reported documentary evidence regarding the monk Koguryo, who introduced new techniques for manufacturing pigments in 610, and that of monk Kansh , who received an award for preparing lead white

in 692. Furthermore, the discovery of 128 paper packages containing red lead powder (for a total of ~ 100 kg) of 'superior', 'medium' and 'low' quality (as written on the packages) in the Shōsōin (*i.e.* the repository of Imperial Treasures at Nara) proves the importance that was attributed to these materials even in the 8th century.

Analytical methods

A plethora of laboratory and portable instruments have been used for the characterisation of pigments and binders.

Based on our survey (Supplementary materials Appendix 1), Raman spectroscopy represents the most-used technique, especially thanks to the development of portable instruments. The possibility of identifying both inorganic and organic compounds is another advantage of this technique and for the study of pictorial works in general. On the other hand, the researcher may encounter two well-known issues. The first difficulty can arise due to fluorescence that produces broad bands and overwhelms the Raman signal. The second difficulty can arise when the compound is mixed and does not seem to allow a certain identification of each component. To solve the first problem, the following measures can be effective: use extremely long/short wavelength lasers, work at large magnifications and apply mathematical corrections to subtract the background fluorescence (Smith and Clark 2004).

The second problem, regarding identifying and quantifying mixed compounds, has been addressed through various approaches. For example, Navas et al. (2010) suggested applying principal component analysis (PCA) to first-derivative Raman spectra. Their experimental work involved the preparation of mixtures with known amounts of both pigments (azurite, chalk, cinnabar, gypsum, lapis lazuli, lead white, minium, raw Sienna and glam) and binders (egg yolk). Their results demonstrated that Raman spectroscopy was able to discriminate the composition of the tests. On the same topic, Pallipurath et al. (2014) proposed a method that combines Fourier transform Raman spectroscopy with multivariate analysis. On one hand, they were able to test the method's effectiveness; on the other hand, they also emphasised the need for suitable reference spectra.

Concerning the use of Raman spectroscopy, it is worth repeating that some lead-based pigments can be converted into other secondary products—and hence damaged—if the analysis is not conducted within certain parameters. For example, the laser wavelength must be kept below a certain threshold, which is not the same for all pigments. In this regard, Burgio et al. (2001) investigated the transformations that can trigger the reaction path $\beta PbO_2 \rightarrow Pb_3O_4 \rightarrow \alpha$-PbO $\rightarrow \beta$PbO when using varying laser power and wavelengths. Similarly, the degradation of plattnerite induced by laser power increase was the subject of the experimental works carried out by Smith et al. (2001), Aze et al. (2008c) and Costantini et al. (2020a). These latter authors used 633 nm and 785 nm laser excitation and temperatures up to 600 °C to test both modern commercial samples of plattnerite and the plattnerite detected in ancient frescoes. They were thus able to observe that the photo/thermal instability of the two types of plattnerite is different (*i.e.* the modern one is more stable) and that the reaction path previously described by Greenwood and Earnshaw (1997) is reversible.

These and other studies investigating the effects of different types of irradiations (see, *e.g.*, Santis et al. 2007; Gourier et al. 2018; She et al. 2020) have provided useful guides for those who want to approach the study of these pigments using this technique.

The second most-used technique is FT-IR spectroscopy. This technique allows for identifying pigments and binders, based on the characteristic absorption bands of both inorganic and organic compounds. Therefore, it can be used in a complementary or substitutive manner to Raman spectroscopy. In comparison, FT-IR does not induce fluorescence but shows a greater scattering intensity of water and hydroxyl groups, thus resulting in less effective results in the presence of species dissolved in aqueous solutions.

The third most common type of technique is represented by microscopy, namely, optical microscopy (OM) and scanning electron microscopy (SEM). The advantage of these techniques is that of observing the morphological characteristics of the pigment grains and their distribution; the disadvantage is that they require sampling in most cases. Some SEMs, such as environmental and field emission SEM, allow for analysis without prior manipulation; however, the sample must be small enough to enter the chamber.

The fourth most common technique is X-ray fluorescence (XRF). The commercialisation of inexpensive handheld XRF equipment has greatly expanded the use of this technique. The most obvious shortcomings are immediately clear when the numerous lead-based compounds found in artworks are listed. Portable or laboratory XRF cannot discriminate cerussite from hydrocerussite or other compounds composed of the same elements. It is, therefore, assumed that a characterisation carried out solely through XRF is not acceptable.

Surprisingly, X-ray diffraction (XRD) is in the fifth position. This technique is indispensable for crystallographic and mineralogical studies; therefore, its effectiveness in discriminating inorganic pigments appears too obvious to be justified. The very structure of this review proved that the investigation of these pigments largely corresponds to the analysis of minerals and that each mineral has a different story to tell. Consequently, only an accurate determination of the phases provides a reliable characterisation of both the primary pigments and their secondary products. Using XRD, the advantage is an unambiguous identification and (possibly) quantification of the phases constituting the pigment, even in the presence of mixtures. The disadvantages are related to the scarce diffusion of portable instruments and the consequent

need for sampling. Even in this case, however, large facilities (*e.g.*, synchrotrons) allow for analysis without manipulating the sample and can also provide spatial distribution maps of the components. In addition, macro XRD (MA-XRD) has been frequently used, as it consists of a mobile scanner that allows the distribution of pigments to be visualised, provided that the artwork has a quasi-flat surface. Indeed, these techniques are not particularly accurate for determining several pigments but have the advantage of providing mineralogical information in a non-destructive way.

Among the remaining techniques, we notably mention:

- all imaging techniques; in particular, hyperspectral imaging reflectance spectroscopy (HSI) has been frequently used, due to its non-invasive and non-destructive nature. It allows for the characterisation of pigments and the results can be modelled when mixtures are present (*e.g.*, deep neural networks, as proposed by Rohani et al. 2019). In this regard, Li et al. (2020a) set up a specific and automatic hyperspectral scanning system (hyperspectral camera + a halogen light source + an automatic scanning platform + data processing software);
- digital radiography (DR) is an X-ray-based imaging technique that provides qualitative information. The lower/higher the atomic number of an element, the darker/lighter the radiographic image will be; however, there may be cases in which gold foils are so thin that they cannot produce a measurable effect (see, *e.g.*, Serafima et al. 2019b);
- μ-computer tomography (μCT), which has been proved to be effective in obtaining virtual cross-sections of the paper (Li et al. 2020c);
- two low-frequency vibrational spectroscopy methods—terahertztime-domain (THz-TDS) and low-frequency Raman (LRS)—which have been proposed as complementary methods for pigment and mixture identification (Kleist and Korter 2020);
- cyclic voltammetry, differential pulse stripping voltammetry and voltammetry of nanoparticles/atomic force microscopy (VNP/AFM), which has been tested on lead-based pigments to assess their reliability in the unambiguous identification of pigments (Doménech-Carbó et al. 2000, 2007);
- several computational methods such as the density functional theory (DFT) and the time-dependent density-functional theory (TDDFT), as well as computer simulations, have been reviewed by Fantacci et al. (2010) and applied to the study of red lead by Amat et al. (2020).

Isotopic analyses have been used to investigate the provenance of lead white—especially for the authentication of artworks—and red lead.

As for lead white, an example is provided by the lead isotope analyses made on lead white samples taken from the *Saint Praxedis* (an oil on canvas with disputed attribution). As stated in the catalogue edited by Christie's for its sale: "*the results placed the lead white squarely in the Dutch/Flemish cluster of samples, establishing with certainty that its origin is north European and entirely consistent with mid-seventeenth century painting in Holland*"[15] (Ragai 2015); however, the attribution left so much perplexity that the painting sold for only US$10,687,160. Further examples have been provided by Keisch and Callahan (1976) and Fortunato et al. (2005). These authors sampled small amounts of lead white pigments (50–200 mg) from several artworks painted by Peter Paul Rubens, Anthony van Dyck, Rembrandt van Rijn, Peter Breughel (Peter Breughel III) and A. Breughel. The authors compared the results obtained with the data available for proven "*Italian paintings*" (L. Giordano, A. Allori, D. Tintoretto, E. Procaccino, GB Caracciolo) and observed that the isotopic values allow for the delineation of a compositional field for the Flemish and Dutch paintings, which was clearly distinguishable from that of Italian painters.

As for red lead, Walton and Trentelman (2009) used inductively coupled plasma time-of-flight mass spectrometry (ICP–TOFMS) and determined the Spanish provenance (Rio Tinto) of the red lead used to paint seven Egyptian mummies (Roman period). Nord et al. (2015) and Nord et al. (2016) investigated 34 samples of minium and plattnerite (as well as one of lead white) through MC-ICP-MS. The samples were taken from different Swedish sites dating between the 12th and early 16th century, where the analyses disclosed the German origin of the pigment (Harz and Erzgebirge). In no case was a correspondence found with the Bergslagen region, representing the principal medieval mining district in Sweden.

In recent years, the application of this method has progressively expanded (see, *e.g.*, Curley et al. 2020), and the analysis of further case studies is fundamental to the growth of the lead isotopes database.

Finally, the dating issue has also been successfully approached using radiocarbon (^{14}C) AMS. First, the oil binders were dated by Hendriks et al. (2018); shortly after, the lead carbonate was subjected to AMS dating by Hendriks et al. (2019). The latter started from the consideration that, in the lead white produced through the stack process, the CO_2 is produced by fermenting organic materials and, therefore, bears atmospheric ^{14}C levels, while in the lead white produced using more recent methods (*e.g.*, the chamber process developed by Herbet in Germany), the CO_2 may come from coal fires, as well as from calcium or potassium carbonates added to vinegar, and therefore, the ^{14}C levels are very low (resulting in radiocarbon ages thousands of years older

[15] https://www.christies.com/presscenter/pdf/2014/CATALOUGE_NOTE_Johannes_Vermeer_Delft_1632_1675_Saint_Praxedis_lot_39.pdf

than the real ones). The authors also pointed out that "*it is not clear if the remineralization of lead carboxylates to lead carbonates will interfere with the ^{14}C dating of the carbonate*"; nevertheless, they (1) suggested the adoption of a two-step method of sample preparation to date both the lead carbonate and the binder and (2) positively assessed the effectiveness of the dating method for lead white produced with the stack process. Finally, they also highlighted that this approach could discriminate between lead whites produced and not produced using the stack method.

Last year, three notable papers were published on this topic. Hendriks et al. (2020) published a new study aimed at combining radiocarbon dating and lead isotope analysis "*to maximise the research output*" from a single sample. They sampled Swiss and British artworks spanning from the 18th to the 20th century and obtained information on both lead white trading (likely from British ores until 1860s, multiple sources after 1860) and the dating of artwork ("*coherent with the signed date*"); however, the authors warned about the possibility of obtaining accurate dates through microsampling when the probable chronological interval ranges between 1700 and 1950.

As for the closely related papers by Messager et al. (2020) and Beck et al. (2020), the former determined the temperature at which lead white samples to be subjected to radiocarbon dating should be heated for C extraction (= 400 °C), while the latter applied the protocol previously established to perform radiocarbon dating on lead white samples taken from two medieval contexts: the 1388–1390 courtly decoration of Margaret of Bavaria's dressing room at the Château de Germolles in Burgundy (France) and the decorations of the destroyed rood screen of the church of the Cordeliers in Fribourg (Switzerland). Among the latter, two groups of paintings were stylistically dated to 1500–1510, while another decoration was tentatively dated between 1340 and 1700. Radiocarbon results placed the French decorations between 1283 and 1419 (with a statistical combination pointing to 1297–1400), the first group of the Swiss ones between 1262 and 1630 (with a statistical combination pointing to 1426–1460) and the second group of the Swiss samples between 1430 and 1666.

Finally, Quarta et al. (2020) deepened the aspect regarding the preparation of the samples, by testing both acid hydrolysis and thermal decomposition. Their results showed that both procedures can be effective, even if thermal decomposition at 500 °C was more effective in eliminating calcium carbonate contamination.

In conclusion, this method is in the midst of its development. The tests carried out appear promising, but limitations have been highlighted in the case of (1) relatively recent samples and (2) the coexistence of other carbon-containing compounds (*e.g.*, contamination from $CaCO_3$). Partially similar problems have been recognised in the study of mortars (see Gliozzo et al. 2021 in this TC for a brief description and the references quoted therein). Apparently, interference due to lead carboxylates is still possible.

Concluding summary of key concepts

This review aimed to provide the tools for an accurate study, without going into numerous details. For this reason, we focused on minerals and pigments and provided some basic information that can help in their recognition and study. The key concepts to be extrapolated from this study are outlined as below.

- **Production and trade**—While archaeological evidence regarding production sites is limited to very few sites, especially in ancient Greece, the discovery of bowls containing lead-based pigments provides valuable information. At present, the state-of-the-art does not allow us to outline an exhaustive picture of the production and trade of lead-based pigments. Lead isotope analyses have proved promising, but the available database is small and strongly biassed towards the almost-modern era.
- **Use**—Despite being known today as toxic products, lead compounds have been used both as paint pigments and as drugs and cosmetics. Red lead has also been used as an anticorrosive paint and a textile paint. The most attested techniques are *a fresco*, *a secco* and tempera, but the former is less frequent when lead white is used. As for binders, there is no evidence of selective use of any particular ones, compared to others. Vegetable oils and proteinaceous materials have been mainly observed in artworks bearing lead-based compounds.
- **Protection**—Lead soaps can deeply affect the visual appearance and integrity of a painting. Different levels of saponification can be observed, depending on the nature of the pigment and binder used, the temperature, the presence of water and the humidity. Overall, lead-based compounds are sensible to humidity, light (photodegradation), heating and chlorine salts. The presence of impurities can trigger/enhance their alterations. All of these factors must be considered for the correct conservation of works of art.
- **Investigation**—Among the analytical techniques, the most often used ones fall in the field of conventional techniques (Raman, FT-IR, XRD, XRF, OM and SEM). While using a single technique always leads to inaccurate and partial results (especially in the case of portable X-ray fluorescence), a combination of techniques is always the best approach. In this case, the combination of destructive and non-destructive techniques also represents a highly suitable choice, able to satisfy the needs for accuracy, completeness and conservation. For example, non-destructive techniques can provide large-scale preliminary analysis and guide targeted sampling for more accurate

destructive analysis. Large facilities, such as synchrotrons, also offer possibilities that cannot be reached with conventional techniques. Notwithstanding the plethora of laboratory and portable instruments that can be used, it is still possible to observe a certain approximation that should be overcome. From a vague determination of lead white, it is necessary to arrive at an accurate qualitative and (possibly) quantitative determination of the cerussite and hydrocerussite ratio. Likewise, it is important to discriminate between litharge and massicot, scrutinyite and plattnerite, or lead-tin yellow types I and II. Finally, as can be seen from the long list of minerals provided, other phases could be present and it is also conceivable that the phases rarely mentioned in the literature are actually not as rare but, instead, simply rarely recognised.

The information available for the main lead-based pigments can be summarised as follows.

- **Cerussite** ($PbCO_3$) and **hydrocerussite** ($2PbCO_3 \cdot Pb(OH)_2$) are colourless to white carbonates constituting the lead white pigment. In nature, the former is more widespread than the latter; however, it is not clear whether natural minerals were used and to what extent or in which period(s). Starting from ancient sources, the use of lead whites produced through lead corrosion likely predominated. The ancient 'Dutch', 'stack', 'chamber' and 'German' methods were at the base of the production processes in different epochs. In artwork, lead white was scarcely observed from the late/final first millennium BC to the 7th century AD. From the 8th century AD, its occurrence increased on every type of support and technique, such as to prepare grounds and gildings, paint in white and lighten other colours. Lead white can transform into several other Pb-based compounds, through heating and/or degradation (leading to colour change and darkening). Recent studies have verified the possibility of dating the production of this pigment through AMS ^{14}C.
- **Red lead—minium** (Pb_3O_4)—is a lead oxide which can be found in nature (relatively infrequently) or artificially produced by roasting lead white and/or litharge. Minium was rare in artworks until the 1st century AD, becoming ever more widespread in the following centuries. Used similarly as lead white, to which it is often associated, minium has also been used to decorate paper currencies and inlays, but less frequently alone or for the preparation of priming layers. The alteration of minium can give rise to whitening or blackening, depending on the degradation product into which it is transformed (lead sulfide or lead carbonates/lead sulfate).
- The red (tetragonal) **litharge** (α-PbO) and the yellow (orthorhombic) **massicot** (β-PbO) can transform into each other through heating (α→β) at a temperature of 489/580 °C, or upon mechanical treatment (β→α). Their occurrences are less frequent than galena but not rare. A typical secondary product of lead cupellation during silver smelting, litharge (*spuma argenti*) has also found applications in medicine and as a building material. In archaeological contexts, litharge may be present in the corrosion crusts of lead objects and paintings. In these, it was likely used as a siccative, rather than an artistic pigment, which is probably why it has rarely been identified in artworks. Massicot is more frequent, generally having been used as a yellow pigment. However, both PbO compounds may be present as deliberately used pigments or impurities derived from red lead. Both litharge and massicot can lead to the formation of cerussite, hydrocerussite, minium and plumbonacrite and may form from scrutinyite and plattnerite.
- **Crocoite** is a lead chromate likely used as a pigment before the end of the 18th century through the beginning of the 19th century, later being substituted by artificial counterparts.
- **Mimetite** is a lead chloroarsenate showing highly variable colours. Its presence is generally interpreted as an alteration product but there exist cases in which it was supposed to be used as a pigment.

The information available for minerals mainly found as alteration phases of the previous pigments is summarised as below.

- **Galena** (PbS) is a widely occurring lead-grey isometric sulfide representing the main raw material for the production of lead. It may contain trace amounts of Mn, Fe, Co, Cu, Zn, Ga, As, Se, Ag, Cd, In, Sn, Sb, Te, Tl, Bi and minor Au and Hg. It is rarely found in artworks, as an alteration product of lead white.
- **Anglesite**, **palmierite** and the associated minerals are natural phases (mainly colourless to white or yellowish) that can be found in the oxidised zones of lead deposits. In artworks, only anglesite has been rarely (if any) used as a white pigment, and most occurrences have denoted its secondary nature. Palmierite has been found as a secondary phase in 17th-century paintings.
- **Scrutinyite** and **plattnerite** are dark mineral phases, generally formed as oxidation products in hydrothermal environments. In artwork, they represent important degradation products of lead white, which can further transform into minium, litharge and massicot. The use of plattnerite as an artistic pigment has been suggested only once, so far.
- **Plumbonacrite** and its associated phases are carbonates (oxohydroxide) related to hydrocerussite, with which they are frequently associated. Unambiguous discrimination between these minerals may not be straightforward, depending on the technique used. In this group, an unnamed

phase was also found in a Laurion metallurgical slag, as a reaction product from a cerussite-based compound. In artwork, plumbonacrite represents an important degradation product: it can easily form in water solutions and in rather dry oils from litharge or massicot or as a product of the photoactivation of minium. Its formation from lead white is more difficult.

- **Cotunnite** and **laurionite** (lead chlorides), **blixite** (oxychloride) and **phosgenite** (chloride-carbonate) occur from rarely to frequently in nature, generally as secondary phases but also primary phases (*e.g.*, cotunnite). Laurionite and phosgenite were produced in antiquity from litharge and used for cosmetics. Laurionite probably also had a pharmaceutical use. Cotunnite, laurionite and blixite have been found on various artwork objects. However, while the formation of cotunnite is generally referred to as a process of alteration of lead white (when in contact with a Cl-rich fluid), deliberate use of the artificially produced pigment has been hypothesised for laurionite and blixite.
- **Caledonite**, **schulténite** and **vanadinite** are lead and copper hydrous carbonate-sulphate, hydrous lead arsenate and lead chloride vanadate, respectively, with highly variable colours. Caledonite has been identified as an alteration product in the presence of ultramarines. The occurrence of vanadinite and schulténite is currently rare and generally associated with that of mimetite.
- **Challacolloite** and the unnamed phase P**bMg(CO$_3$)$_2$**—The first phase is a chloride, which is almost more infrequent in nature than in ancient artefacts. This secondary phase is formed by the interaction of hydrocerussite with potassium chloride from the earth or with potash lye and hydrochloric acid, possibly used in restoration interventions. In any case, high chloride ion concentrations and/or low pH conditions are required for its formation. Regarding the second phase, only research carried out on synthetic materials was found, obtained from lead or red lead carbonate. In artwork, this unnamed phase was found in association with massicot, cerussite, hydrocerussite, plattnerite and scrutinyite.

Finally, the information available for lead-tin yellow types I and II, Naples yellow, lead-tin-antimony yellow and artificial lead chromates can be summarised as follows:

- **Lead-tin yellow type I** is an artificial pigment whose tetragonal/orthorhombic structure can be refined in both $P4_2/mbc$ and *Pbam* space groups. It was produced by heating litharge or minium and SnO to between 650 and 900° C. Different temperatures and component ratios affect the final colour and composition of the pigment (*e.g.*, residual PbO due to incomplete reaction and/or an excess of Pb_3O_4). Its period of use, to the best of our knowledge based on the available literature, ranges from the beginning of the 15th century to, at least, the mid-18th century. Its alteration and degradation are strongly influenced by the presence of organic binders.
- **Lead-tin yellow type II** is a pigment with a cubic structure, which has been less attested than type I. It could have been produced in at least two ways: (1) heating lead-tin yellow type I and silica at ~900 °C. The optimum ratio of the two components was found to be 1:1, while changes in this ratio produced a mixture of lead-tin yellow types I and II or lead-tin yellow type II and unreacted silica, and (2) a single-step synthesis by heating Pb, Sn, and Si oxides at ~850 °C. The optimum ratio of the three components was found to be 6:3:2, while variable changes from this ratio may leave unconsumed $SnO_2$and/or produce an excess of SiO_2 or Pb, mixed products and, especially, a glassy phase. Its period of use known so far ranges from the beginning of the 14th century to the first half of the 17th century. The identification of lead-tin yellow type II in 19th-century paintings requires validation.
- **Lead-antimony yellow** (or Naples yellow) is isostructural with bindheimite and oxyplumboroméite; however, the use of natural minerals has not been proved. The synthesis of the artificial pigment required a mixture of lead and antimony compounds. An experimental reproduction verified that (1) heating Pb_3O_4 and Sb_2O_3 without fluxes requires at least a temperature of 1000 °C to be reached and the final product is a low-quality mixture of several phases; (2) heating the same components with 10–20% NaCl requires lower temperatures (~850 °C) and the final product is a higher quality single-phase; (3) using K_2CO_3 instead of NaCl, the product is of lower quality; (4) adding 5–10% of silica gel, the product becomes salmon-coloured; and (5) when replacing Sb_2O_3 with Sb_2S_3, a flux was not needed. Its period of use known to date (in paintings) ranges from the beginning of the 16th century to, at least, the 19th century AD. The identification of Naples yellow in the late 1st- to 4th-century wall paintings of the *Domus* in Rome may represent the very first attestation of its use or later retouches.
- **Lead-tin-antimony yellow** is an artificial cubic pigment. It may have been produced through heating Pb_3O_4, Sb_2O_3, SnO_2 and 10% NaCl to between 700 and 900 °C. Different ratios of the components affect the colour, composition and processing temperature. By replacing Sb_2O_3 with Sb_2S_3 anglesite (850 °C) or lanarkite (900 °C) were further found. Its period of use known so far ranges from the early 16th to the 19th century.
- **Lead chromates**. The lead chromates are an artificial group of pigments, ranging in composition from crocoite $PbCrO_4$ to $PbCrO_4{\cdot}PbSO_4$. As for the composition, the yellow pigment corresponds to the natural crocoite, while the orange pigment corresponds to phoenicochroite. They

were first produced, in 1804/1809, by decomposing potash chromate with lead acetate; more recently, they have been produced using lead salts and chromates or bichromates. The colour is mainly affected by the amount of lead, while the nature of the final product is determined by the different ingredient ratios and processing temperatures. For this reason, several phases ($PbCr_{1-x}S_xO_4$) can be individuated through analysis of the pigment. The alteration is due to the photoreduction of Cr(VI) to Cr(III), where the intermediate compounds are more unstable than $PbCrO_4$. The binder plays a key role in Cr photoreduction. The period of use known so far ranges from the 14th to the 20th century. The identification of orange lead chromate in a 9th- 12th-century AD polychrome decoration (carved stucco, wall painting and terracotta friezes) in Nishapur, Iran, may represent an early attestation or later retouches.

Supplementary Information The online version contains supplementary material available at https://doi.org/10.1007/s12520-021-01407-z.

Acknowledgements C.I. acknowledges the support of Babeş-Bolyai University Cluj-Napoca through AGC 33504/2020 and AGC 33505/2020 projects. Enrico Bonacina, Bruce Cairncross, Antonio Gamboni, Ko Jansen, Uwe Kolitsch, Stephan Wolfsried, Fabre Minerals and The Arkestone are kindly acknowledged for allowing us to use their magnificent photos of the minerals.

Author contribution EG: anglesite and associated phases, challacolloite, galena, lead chromates, lead-tin yellow I–II, lead white, (cerussite, hydrocerussite), litharge, massicot, palmierite, plattnerite, plumbonacrite and associated phases, red lead, scrutinyite and $PbMg(CO_3)_2$, production centres, binding media and coatings, diffusion, analytical methods, concluding summary. CI: blixite, caledonite, cotunnite, crocoite, laurionite, lead-antimony yellow (Naples yellow), lead-tin-antimony yellow, mimetite, phosgenite, schultenite and vanadinite, funding acquisition and English language revision.

Funding Open access funding provided by Università degli Studi di Bari Aldo Moro within the CRUI-CARE Agreement. Babeş-Bolyai University Cluj-Napoca through AGC 33504/2020 and AGC 33505/2020 projects.

Data availability No new data were created or analysed in this study. The CC-BY licence does not supersede previously copyrighted material; therefore, data and images remain under owner's copyright.

Declarations

Competing interests The authors declare no competing interests.

References

Abdallah M, Abdrabou A, Kamal HM (2020) Multiscientific analytical approach of polychrome greco-roman palette applied on a wooden model naos: case study. Mediter Archaeol Archaeom 20(2):45–65. https://doi.org/10.5281/zenodo.3746942

Abdel-Maksoud G, Ibrahim M, Issa YM, Magdy M (2020) Investigation of painting technique of Coptic icon by integrated analytical methods: imaging, spectroscopic and chemometric methods. J Archaeol Sci Rep 29:102085. https://doi.org/10.1016/j.jasrep.2019.102085

Acero P, Cama J, Ayora C (2007) Rate law for galena dissolution in acidic environment. Chem Geol 245:219–229. https://doi.org/10.1016/j.chemgeo.2007.08.003

Aceto M (2021) The palette of organic colourants in wall paintings. Archaeol Anthropol Sci https://doi.org/10.1007/s12520-021-01392-3

Aceto M, Agostino A, Boccaleri E, Garlanda AC (2008) The Vercelli gospels laid open: an investigation into the inks used to write the oldest gospels in Latin. X-Ray Spectrom 37(4):286–292. https://doi.org/10.1002/xrs.1047

Adams DM, Christy AG, Haines J, Clark SM (1992)Second-order phase transition in PbO and SnO at high pressure: implications for the litharge-massicot phase transformation. Phys Rev B 46(18):11358–11367. https://doi.org/10.1103/PhysRevB.46.11358

Africano F, Van Rompaey G, Bernard A, Le Guern F (2002) Deposition of trace elements from high temperature gases of Satsuma-Iwojima volcano. Earth Planets Space 54:275–286. https://doi.org/10.1186/BF03353027

Aibeo C, Castellucci EM, Matteini M, Sacchi B, Zoppi A, Lofrumento C (2008) A micro-Raman spectroscopy study of the formation of lead dioxide from lead white. In: Kroustallis S, Townsend JH, Bruquetas EC, Stijnman A, San Andres Moya M (eds) Art technology: sources and methods. Proceedings of the second symposium of the Art Technological Source Research Working Group. Archetype Publications, London, pp 138–140

Akyuz T, Akyuz S (2017) Investigations on Empire series postage stamps of Ottomans (printed 1880–1890) by vibrational spectroscopic and energy dispersive X-ray fluorescence techniques. Vib Spectrosc 89:37–43. https://doi.org/10.1016/j.vibspec.2016.12.012

Albertson G, Krekeler A, van Loon A, Gaibor AP, Noble P (2019) The blues of Jan de Bray's Judith and Holofernes: a technical study of two blue pigments and its impact on treatment. J Am Inst Conserv 58(4):217–232. https://doi.org/10.1080/01971360.2019.1643628

Aleksandrov VV, Boldyrev VV, Marusin VV, Morozov VG, Solovjev VS, Rozhentseva TM (1978) Effect of heating rate on the thermal decomposition of lead dioxide. J Therm Anal 13:205–212. https://doi.org/10.1007/BF01912292

Aliatis I, Bersani D, Campani E, Casoli A, Lottici PP, Mantovan S, Marino IG, Ospitali F (2009) Green pigments of the Pompeian artists' palette. Spectrochim Acta A Mol Biomol Spectrosc 73(3):532–538. https://doi.org/10.1016/j.saa.2008.11.009

Aliatis I, Bersani D, Campani E, Casoli A, Lottici PP, Mantovan S, Marino I-G(2010) Pigments used in Roman wall paintings in the Vesuvian area. J Raman Spectrosc 41(11):1537–1542. https://doi.org/10.1002/jrs.2701

Aliatis I, Bersani D, Lottici PP, Marino IG (2012) Raman analysis on 18th century painted wooden statues. ArcheoSciences 36:7–13. https://doi.org/10.4000/archeosciences.3806

Almaviva S, Fantoni R, Colao F, Puiu A, Bisconti F, Fiocchi Nicolai V, Romani M, Cascioli S, Bellagamba S (2018) LIF/Raman/XRF non-invasive microanalysis of frescoes from St. Alexander catacombs in Rome. Spectrochimica Acta - Part A 201(1):207–215. https://doi.org/10.1016/j.saa.2018.04.062

Aloupi, H., Aslani, I., Pachalis, V., Stassinopoulos, S., Karydas, A., Anglos, D., Gionis, V., Chryssikos, J. (2006) Analysis and documentation of The Baptism by Domenicos Theotokopoulos by use of non-destructive physicochemical techniques. Comparison with the Adoration of the Magi of the Benaki Museum. In: International meeting of the special interest icons group. Icons approaches to research, conservation and ethical issues (Athens, 3–7 December 2006)

Amadori ML, Barcelli S, Casoli A, Mazzeo R, Prati S (2013) A scientific approach to the characterization of the painting materials of Fra

Mattia della Robbia polychrome terracotta altarpiece. Appl Phys A: Mater Sci Process 113(4):1055–1064. https://doi.org/10.1007/s00339-013-7748-6

Amadori ML, Poldi G, Barcelli S, Baraldi P, Berzioli M, Casoli A, Marras S, Pojana G, Villa GCF (2016) Lorenzo Lotto's painting materials: an integrated diagnostic approach. Spectrochim Acta A Mol Biomol Spectrosc 164:110–122. https://doi.org/10.1016/j.saa.2016.02.043

Amat A, Rosi F, Miliani C, Sassi P, Paolantoni M, Fantacci S (2020) A combined theoretical and experimental investigation of the electronic and vibrational properties of red lead pigment. J Cult Herit 46: 374–381. https://doi.org/10.1016/j.culher.2020.04.014 in press

Andalo C, Bicchieri M, Bocchini P, Casu G, Galletti GC, Mando PA, Nardone M, Sodo A, Zappalà MP (2001) The beautiful "Trionfod'Amore" attributed to Botticelli: a chemical characterisation by proton-induced X-ray emission and micro-Raman spectroscopy. Anal Chim Acta 429(2):279–286. https://doi.org/10.1016/S0003-2670(00)01292-7

Antao SM (2012) Structural trends for celestite ($SrSO_4$), anglesite ($PbSO_4$), and barite ($BaSO_4$): confirmation of expected variations within the SO_4 groups. Am Mineral 97(4):661–665. https://doi.org/10.2138/am.2012.3905

Antao SM, Hassan I (2009) The orthorhombic structure of $CaCO_3$, $SrCO_3$, $PbCO_3$ and $BaCO_3$: linear structural trends. Can Mineral 47:1245–1255. https://doi.org/10.3749/canmin.47.5.1245

Anthony JW, Bideaux RA, Bladh KW, Nichols MC (1990) Handbook of mineralogy, mineral data publishing. Mineralogical Society of America, Tucson. http://www.handbookofmineralogy.com/

Antunes V, Candeias A, Mirão J, Carvalho ML, Serrão V, Barrocas Dias C, Manhita A, Cardoso A, Manso M (2018) On the origin of Goa Cathedral former altarpiece: material and technical assessment to the work of Garcia Fernandes, Portughese painter from the 16th century Lisbon workshop. Microchem J 138:226–237. https://doi.org/10.1016/j.microc.2018.01.018

Arizzi A, Cultrone G (2021) Mortars and plasters – How to characterise hydraulic mortars. Archaeol Anthropol Sci. https://doi.org/10.1007/s12520-021-01404-2

Arjonilla P, Domínguez-Vidal A, Correa-Gómez E, Domene-Ruiz MJ, Ayora-Cañada MJ (2019a) Raman and Fourier transform infrared microspectroscopies reveal medieval Hispano–Muslim wood painting techniques and provide new insights into red lead production technology. J Raman Spectrosc 50(10):1537–1545. https://doi.org/10.1002/jrs.5660

Arjonilla P, Ayora-Cañada MJ, Rubio Domene R, Correa Gómez E, de la Torre-López MJ, Domínguez-Vidal A (2019b) Romantic restorations in the Alhambra monument: spectroscopic characterization of decorative plasterwork in the Royal Baths of Comares. J Raman Spectrosc 50(2):184–192. https://doi.org/10.1002/jrs.5422

Armenini GB (1856) De' veriprecetti della pittura. Ravenna.

Arrizabalaga I, Gómez-Laserna O, Aramendia J, Arana G, Madariaga JM (2014) Determination of the pigments present in a wallpaper of the middle nineteenth century: the combination of mid-diffuse reflectance and far infrared spectroscopies. Spectrochimica Acta - Part A 124:308–314. https://doi.org/10.1016/j.saa.2014.01.017

Augusti S (1949) Alterazioni della composizione chimica de' colori nei dipinti murali. TipografiaMiccoli, Napoli

Augusti S (1967) I colori pompeiani. De Luca Editore, Roma

Aurélie M, Charlotte D, Floréal D (2016) Material identification of three French medieval illuminations of the XVIth century by hyperspectral imaging (Treasury of Bordeaux Cathedral, France). Color Res Appl 41(3):302–307. https://doi.org/10.1002/col.22042

Auriemma, R. (Ed.) (2018) Nel mare dell'intimità. L'archeologia subacquea racconta l'Adriatico. Exhibition catalogue (Trieste, ex Pescheria-Salone degli Incanti (17th December 2017 - 1st May 2018). Gangemi Editore.

Avvakumov EG, Kosova NV, Aleksandrov VV (1983) Effect of mechanical activation on the decomposition of lead dioxide. Izvestiya Sibirskogo Otdeleniya Akademii Nauk SSSR, Seriya Khimicheskikh Nauk 3(7):25–30 (Russian)

Ayalew E, Janssens K, De Wael K (2016) Unraveling the reactivity of minium toward bicarbonate and the role of lead oxides therein. Anal Chem 88(3):1564–1569. https://doi.org/10.1021/acs.analchem.5b02503

Aze, S. (2005) Alterations chromatiques des pigments au plomb dans les oeuvres du patrimoine- Etude expérimentale des altérations observées. PhD thesis, University de droit, d'economie et des sciences d'Aix-Marseille III, France.

Aze S, Vallet J-M, Baronnet A, Grauby O (2006) The fading of red lead pigment in wall paintings: Tracking the physico-chemical transformations by means of complementary micro-analysis techniques. Eur J Mineral 18(6):835–843. https://doi.org/10.1127/0935-1221/2006/0018

Aze S, Vallet J-M, Pomey M, Baronnet A, Grauby O (2007) Red lead darkening in wall paintings: natural ageing of experimental wall paintings versus artificial ageing tests. Eur J Mineral 19(6):883–890. https://doi.org/10.1127/0935-1221/2007/0019-1771

Aze S, Vallet J-M, Detalle V, Grauby O, Baronnet A (2008a) Chromatic alterations of red lead pigments in artworks: a review. Phase Transit 81(2-3):145–154. https://doi.org/10.1080/01411590701514326

Aze S, Detalle V, Vallet J-M, Pingaud N (2008b) Lead pigment's weathering: study of the red lead and it's reversion feasibility | [L'altération des pigments au plomb: Étude du minium et de sa possible reconversion]. Actual Chim 318:9–15 (French)

Aze S, Delaporte P, Vallet JM, Detalle V, Grauby O, Baronnet A (2008c) Towards the restoration of darkened red lead containing mural paintings: preliminary study of the β-PbO2 to Pb3O4 reversion by laser irradiation. In: Lasers in the Conservation of Artworks. Proceedings of the International Conference LACONA 7 (Madrid, Spain, 17-21 September 2007), pp. 11-13

Badillo-Sanchez D, Baumann W (2016) Comparative palette characterization of oil-on-canvas paintings of two well-known 19th-century Colombian artists by confocal Raman spectroscopy. J Raman Spectrosc 47(12):1540–1547. https://doi.org/10.1002/jrs.5065

Baij L, Hermans JJ, Keune K, Iedema P (2018)Time-dependent ATR-FTIR spectroscopic studies on fatty acid diffusion and the formation of metal soaps in oil paint model systems. AngewandteChemie - International Edition 57(25):7351–7354. https://doi.org/10.1002/anie.201712751

Bajda T (2010) Solubility of mimetite $Pb_5(AsO_4)_3Cl$ at 5–55°C. Environ Chem 7(3):268–278. https://doi.org/10.1071/EN10021

Baker WE (1966) An X-ray diffraction study of synthetic members of the pyromorphite series. Am Mineral 51(11-12):1712–1721

Baleva M, Tuncheva V (1994)Laser-assisted deposition of PbO films. J Mater Sci Lett 13:3–5. https://doi.org/10.1007/BF02352902

Bandera, S., Nicola, A.R., Parodi, V., Frezzato, F., Monni E. (2005) Gli affreschi trecenteschi dell'abbazia di Chiaravalle Milanese: il primo maestro a confronto con il cantiere giottesco, restauro in corso. In: Biscontin, G., Driussi, G. (Eds.) Atti del Convegno Scienza e Beni Culturali XXI, Sulle pitture murali. Riflessioni, conoscenze, interventi (Bressanone 12-15 luglio 2005). Arcadia Ricerche, pp. 793-811.

Bannister FA (1934) The crystal-structure and optical properties of matlockite (PbFCl). Mineralogical Magazine & Journal of the Mineralogical Society 23(146):587–597. https://doi.org/10.1180/minmag.1934.023.146.02

Baraldi C, Toti MP, Van Elslande E, Walter P, Gamberini MC (2020) Phoenicians preferred red pigments: chemical compositions of make-up powders found in archaeological sites from Sicily. Appl Spectrosc 74(3):295–304. https://doi.org/10.1177/0003702819895313

Barriga C, Morales J, Tirado JL (1988) Effect of preliminary mechanical activation on the behaviour of orthorhombic lead dioxide. J Therm Anal 34:1421–1425. https://doi.org/10.1007/BF01914366

Basta NT, McGowen SL (2004) Evaluation of chemical immobilization treatments for reducing heavy metal transport in a smelter-contaminated soil. Environ Pollut 127:73–82. https://doi.org/10.1016/S0269-7491(03)00250-1

Beck L, Messager C, Caffy I, Delqué-Količ E, Perron M, Dumoulin J-P, Moreau C, Degrigny C, Serneels V (2020) Unexpected presence of ^{14}C in inorganic pigment for an absolute dating of paintings. Sci Rep 10(1):9582. https://doi.org/10.1038/s41598-020-65929-7

Becker H (2021) Pigment nomenclature in the ancient Near East, Greece, and Rome. Archaeol Anthropol Sci. https://doi.org/10.1007/s12520-021-01394-1

Bell IM, Clark RJH, Gibbs PJ (1997) Raman spectroscopic library of natural and synthetic pigments (pre- ≈ 1850 AD). Spectrochim Acta A Mol Biomol Spectrosc 53(12):2159–2179. https://doi.org/10.1016/S1386-1425(97)00140-6

Bellanca A (1946) La struttura della palmierite. Periodico di Mineralogia 15(1–3):5–25

Belokoneva EL, Al'-Ama AG, Dimitrova OV, Kurazhkovskaya VS, Stefanovich SY (2002) Synthesis and crystal structure of new carbonate $NaPb_2(CO_3)_2(OH)$. Crystallography Reports 47(2):217–222. https://doi.org/10.1134/1.1466495

Bersani D, Lottici PP, Casoli A, Cauzzi D (2008) Pigments and binders in "Madonna col Bambino e S. Giovannino" by Botticelli investigated by micro-Raman and GC/MS. J Cult Herit 9:97–102. https://doi.org/10.1016/j.culher.2007.05.005

Berthollet M, Vauquelin LN (1804) Rapport fait à la classe des sciences physiques et mathématiques de l'Institut sur un mémoire de M , Godon, intitulé Observations pour servir à l'histoire du chrome. Ann Chim 53:222–229

Bethke PM, Barton PB (1971) Distribution of some minor elements between coexisting sulfide minerals. Econ Geol 66:140–163. https://doi.org/10.2113/gsecongeo.66.1.140

Bette S, Eggert G, Fischer A, Dinnebier RE (2017)Glass-induced lead corrosion of heritage objects: structural characterization of $K(OH)\cdot 2PbCO_3$. Inorg Chem 56(10):5762–5770. https://doi.org/10.1021/acs.inorgchem.7b00391

Beudant FS (1832a) Anglesite, plomb sulfaté. In: Trailé élémentaire de Minéralogie, vol 2, 2nd edn. Verdière, Paris, p 459

Beudant FS (1832b) Mimétèse. In: Trailé élémentaire de Minéralogie, vol 2, 2nd edn. Verdière, Paris, pp 594–595

Bezur A, Kavich G, Stenger J, Torok E, Snow C (2015) Discovery of challacolloite, an uncommon chloride, on a fifteenth-century polychrome terracotta relief by Michele da Firenze. Appl Phys A: Mater Sci Process 121:83–93. https://doi.org/10.1007/s00339-015-9386-7

Bhagat D, Waldiya M, Vanpariya A, Mukhopadhyay I (2018) One pot synthesis of pure micro/nano photoactive α-PbO crystals. In: Ray A., Pati R., Mukhopadhyay I. (Eds.) 1st International Conference on Nanomaterials for Energy Conversion and Storage Applications, NECSA 2018. (Gandhinagar, Gujarat, India 29-31 January 2018). AIP Conference Proceedings, 1961. American Institute of Physics Inc., pp. 030047. DOI: https://doi.org/10.1063/1.5035249

Bilinski H, Schindler P (1982) Solubility and equilibrium constants of lead in carbonate solutions (25°C, I = 0.3 mol dm^{-3}). Geochim Cosmochim Acta 46:921–928. https://doi.org/10.1016/0016-7037(82)90048-5

Bindi L, Menchetti S (2005) Structural changes accompanying the phase transformation between leadhillite and susannite: a structural study by means of in situ high-temperature single-crystal X-ray diffraction. Am Mineral 90(10):1641–1647. https://doi.org/10.2138/am.2005.1808

Bindi L, Nestola F, Kolitsch U, Guastoni A, Zorzi F (2011) Fassinaite, $Pb_2^{2+}(S_2O_3)(CO_3)$, the first mineral with coexisting carbonate and thiosulfate groups: description and crystal structure. Mineral Mag 75:2721–2732. https://doi.org/10.1180/minmag.2011.075.6.2721

Blackburn WH, Schwendeman JF (1977) Trace element substitution in galena. Can Mineral 15:365–377

Blasco-López FJ, Alejandre FJ, Flores-Alés V, Cortés I (2016) Plasterwork in the Ambassadors Hall (Salón de Embajadores) of the Real Alcázar of Seville (Spain): graphic reconstruction of polychrome work by layer characterization. Constr Build Mater 107:332–340. https://doi.org/10.1016/j.conbuildmat.2016.01.021

Boden DP (1998) Improved oxides for production of lead/acid battery plates. J Power Sources 73(1):56–59. https://doi.org/10.1016/s0378-7753(98)00021-4

Bohér P, Garnier P (1984) Influence des impuretés sur la stabilité thermique et la structure dexoxydes de plomb Pb_3O_4 et PbOα. J Solid State Chem (French) 55:245–248. https://doi.org/10.1016/0022-4596(84)90273-1

Boher, P., Garnier, P., Gavarri, J.R., Weigel, D. (1984) Modèle de décomposition thermique des bioxydes de plomb: Rôle des protons, relation avec la structure de l'oxyde pseudocubique $PbO_{1.57}$. J Solid State Chem 55(1): 54-66. https://doi.org/10.1016/0022-4596(84)90247-0

Boher P, Garnier P, Gavarri JR, Hewat AW (1985) Monoxyde quadratique PbO alpha(I): description de la transition structurale ferroelastique Method: neutron Diffraction. J Solid State Chem 57:343–350. https://doi.org/10.1016/0022-4596(85)90197-5

Bomford D, Roy A (1993) Canaletto's 'Stonemason's Yard' and 'San Simeone Piccolo'. National Gallery Technical Bulletin 14:34–41

Bonizzoni L, Bruni S, Galli A, Gargano M, Guglielmi V, Ludwig N, Lodi L, Martini M (2016)Non-invasive in situ analytical techniques working in synergy: the application on graduals held in the Certosa di Pavia. Microchem J 126:172–180. https://doi.org/10.1016/j.microc.2015.12.001

Boon JJ (2006) Processes *inside* paintings that affect the picture: chemical changes *at, near* and *underneath* the paint surface. In: Boon, J.J., Ferreira, E.S.B. (Eds.) Reporting highlights of the De Mayerne Programme: research programme on molecular studies in conservation and technical studies in art history. The Hague: Netherlands Organisation for Scientific Research, pp. 21-32.

Boon JJ, Ferreira ESB (2006) Reporting highlights of the De Mayerne Programme: research programme on molecular studies in conservation and technical studies in art history. Netherlands Organisation for Scientific Research, The Hague, p 134

Boon, J.J., Hoogland, F.H., Keune, K. (2007) Chemical processes in aged oil paints affecting metal soap migration and aggregation. In: Mar Parkin, H. (Ed.) AIC paintings specialty group postprints. 34th annual meeting of the AIC of Historic & Artistic Works providence (Rhode Island, June 16-19, 2006), pp. 16-23.

Bordalo R, Bottaini C, Moricca C, Candeias A (2016) Characterization of a Florentine painter in Portugal in the late 19th century: paintings by Giorgio Marini. Int J Conserv Sci 7(4):967–980

Borgia I, Brunetti BG, Miliani C, Ricci C, Seccaroni C, Sgamellotti A (2007) The combined use of lead-tin yellow type I and II on a canvas painting by Pietro Perugino. J Cult Herit 8:65–68. https://doi.org/10.1016/j.culher.2006.10.006

Boscardin M, Daleffe A, Rocchetti I, Zordan A (2016) Cerussite e sua località tipo. Studi e Ricerche - Associazione Amici del Museo - Museo Civico "G. Zannato"23: 29-34.

Bösiger P (2019) Painted decorations on the Chinese and French lacquers of an eighteenth-century chest of drawers: when one runs over onto the other. Stud Conserv 64:S81–S90. https://doi.org/10.1080/00393630.2018.1563743

Böttcher ME, Gehlken P-L, Reutel C (1996) The vibrational spectra of $PbMg(CO_3)_2$. Neues Jb Mineral Monat 6:241–250

Bottrill RS, Williams PA, Dohnt S, Sorrell S, Kemp NR (2006) Crocoite and associated minerals from Tasmania. Aust J Mineral 12(2):59–90

Bratu I, Măruțoiu C, Moldovan Z, Măruțoiu VC, Trosan L, Pop DT, Sandu ICA (2015) Scientific investigation of the Saint Elijah's icon from Dragus Village, Brasov County for its preservation and restoration. Rev Chim 66(10):1628–1631

Brekoulaki, H. (2006) Le peinture funeraire de Macedonie. Emplis et fonctions de la couleur IVc-IIc s. av. J.-C. I. Texte. *Melethmata* 48, Athens 2006, Diffusion de Boccard Paris, 482 pp.

Bril H, Zainoun K, Puziewicz J, Courtin-Nomade A, Vanaecker M, Bollinger J-C(2008) Secondary phases from the alteration of a pile of zinc-smelting slag as indicators of environmental conditions: an example from Świętochłowice, Upper Silesia, Poland. Can Mineral 46(5):1235–1248. https://doi.org/10.3749/canmin.46.5.1235

Brooker MH, Sunder S, Taylor P, Lopata VJ (1983) Infrared and Raman spectra and X-ray diffraction studies of solid lead(II) carbonates. Can J Chem 61(3):494–502. https://doi.org/10.1139/v83-087

Bruni S, Cariati F, Consolandi L, Galli A, Guglielmi V, Ludwig N, Milazzo M (2002) Field and laboratory spectroscopic methods for the identification of pigments in a northern Italian eleventh century fresco cycle. Appl Spectrosc 56(7):827–833. https://doi.org/10.1366/000370202760171482

Bryan C (1930) The Papyrus Ebers. Geoffrey Bles, London

Buisson N, Burlot D, Eristov H, Eveno M, Sarkis N (2015) The tomb of the three brothers in Palmyra: the use of mimetite, a rare yellow pigment, in a rich decoration. Archaeometry 57(6):1025–1044. https://doi.org/10.1111/arcm.12087

Burgio L (2021) Pigments, dyes and inks – their analysis on manuscripts, scrolls and papyri. Archaeol Anthropol Sci. https://doi.org/10.1007/s12520-021-01403-3

Burgio L, Clark RJH, Gibbs PJ (1999) Pigment identification studies in situ of Javanese, Thai, Korean, Chinese and Uighur manuscripts by Raman microscopy. J Raman Spectrosc 30(3):181–184. https://doi.org/10.1002/(SICI)1097-4555(199903)30:3<181::AID-JRS356>3.0.CO;2-8

Burgio L, Clark RJH, Firth S (2001) Raman spectroscopy as a means for the identification of plattnerite (PbO_2), of lead pigments and of their degradation products. Analyst 126(2):222–227. https://doi.org/10.1039/b008302j

Buscaglia MB, Halac EB, Reinoso M, Marte F (2020) The palette of Pio Collivadino (1869–1945) throughout his career. J Cult Herit 44:27–37. https://doi.org/10.1016/j.culher.2020.02.012

Byström, A., Westgren, A. (1943) The crystal structure of Pb3O4 and SnPb2O4. Arkiv för kemi, mineralogi och geologi, 16B(14). Stockholm Almqvist &Wiksell Berlin Natura.

Caley ER, Richards JF (1956) Theophrastus on stones. Ohio State University Press, Columbus, p 238

Calos NJ, Kennard CHL, Lindsay Davis R (1990) Crystal structure of mimetite, $Pb_5(AsO_4)_3Cl$. Zeitschrift für Kristallographie - Crystalline Materials 191(1-2):125–129. https://doi.org/10.1524/zkri.1990.191.1-2.125

Canepa P, Ugliengo P, Alfredsson M (2012) Elastic and vibrational properties of α- And β-PbO. J Phys Chem C116(40):21514–21522. https://doi.org/10.1021/jp3036988

Cao M, Hu C, Peng G, Qi Y, Wang E (2003)Selected-control synthesis of PbO_2 and Pb_3O_4single-crystalline nanorods. J Am Ceram Soc 125(17):4982–4983. https://doi.org/10.1021/ja029620l

Cardell C, Rodriguez-Simon L, Guerra I, Sanchez-Navas A (2009) Analysis of Nasrid polychrome carpentry at the Hall of the Mexuar Palace, Alhambra complex (Granada, Spain), combining microscopic, chromatographic and spectroscopic methods. Archaeometry 51(4):637–657. https://doi.org/10.1111/j.1475-4754.2008.00438.x

Carlyle L, Townsend JH (1990) An investigation of lead sulfide darkening of nineteenth century painting material. In: Hackney S, Townsend J, Eastaugh N (eds) Dirt and pictures separated: papers given at a conference held jointly by UKIC and the Tate Gallery, January 1990. United Kingdom Institute for Conservation, London, pp 40–43

Caroselli M, Ruffolo SA, Piqué F (2021) Mortars and plasters – how to manage mortars and plasters conservation. Archaeol Anthropol Sci https://doi.org/10.1007/s12520-021-01409-x

Carvalho I, Casanova C, Araújo R, Lemos A (2018) Colour identification, degradation processes and findings in a fifteenth-century Book of Hours: the case study of Cofre n. 31 from Mafra National Palace. Heritage Science 6(1):9. https://doi.org/10.1186/s40494-018-0174-5

Casadio F, Keune K, Noble P, van Loon A, Hendriks E, Centeno SA, Osmond G (Eds.) (2019) Metal Soaps in Art. Conservation and Research. Springer, pp. 424.

Cascales C, Alonso JA, Rasines I (1986) The new pyrochlores $Pb_2(MSb)O_{6.5}$ (M = Ti, Zr, Sn, Hf). J Mater Sci Lett 5:675–677. https://doi.org/10.1007/BF01731548

Castro K, Pérez-Alonso M, Rodríguez-Laso MD, Madariaga JM (2004a) Pigment analysis of a wallpaper from the early 19th century: les Monuments de Paris. J Raman Spectrosc 35(8-9):704–709. https://doi.org/10.1002/jrs.1132

Castro K, Pérez-Alonso M, Rodríguez-Laso MD, Madariaga JM (2004b) Raman fibre optic approach to artwork dating. Spectrochim Acta A Mol Biomol Spectrosc 60(12):2919–2924. https://doi.org/10.1016/j.saa.2004.02.004

Castro K, Pessanha S, Proietti N, Princi E, Capitani D, Carvalho ML, Madariaga JM (2008) Noninvasive and nondestructive NMR, Raman and XRF analysis of a Blaeu coloured map from the seventeenth century. Anal Bioanal Chem 391:433–441. https://doi.org/10.1007/s00216-008-2001-4

Catalano J, Murphy A, Yao Y, Alkan F, Zumbulyadis N, Centeno SA, Dybowski C (2014)^{207}Pb and ^{119}Sn solid-State NMR and relativistic density functional theory studies of the historic pigment lead-tin yellow type I and its reactivity in oil paintings. J Phys Chem A118(36):7952–7958. https://doi.org/10.1021/jp505908j

Cauzzi D (2003) Marco Palmezzano, due Madonne in trono e un giallo…. risolto. Kermes 49:59–63

Cavallo G, Vergani RC, Gianola L, Meregalli A (2012) Archaeological, stylistic and scientific research on 11th-13th century ad painted fragments from the San Giovanni Battista church in Cevio (Switzerland). Archaeometry 54:294–310. https://doi.org/10.1111/j.1475-4754.2011.00613.x

Cavallo G, Riccardi MP (2021) Glass-based pigments in painting. Archaeol Anthropol Sci. https://doi.org/10.1007/s12520-021-01453-7

Chaplin TD, Clark RJH, Jacobs D, Jensen K, Smith GD (2005) The Gutenberg Bibles: analysis of the illuminations and inks using Raman spectroscopy. Anal Chem 77(11):3611–3622. https://doi.org/10.1021/ac050346y

Chen J, Chen Y, Long X, Li Y (2017) DFT study of coadsorption of water and oxygen on galena (PbS) surface: an insight into the oxidation mechanism of galena. Appl Surf Sci 420:714–719. https://doi.org/10.1016/j.apsusc.2017.05.199

Chevrier G, Giester G, Heger G, Jarosch D, Wildner M, Zemann J (1992) Neutron single-crystal refinement of cerussite, $PbCO_3$, and comparison with other aragonite-type carbonates. Z Krist 199:67–74

Chiarantini L, Gallo F, Rimondi V, Benvenuti M, Costagliola P, Dini A (2015) Early Renaissance production recipes for Naples yellow pigment: a mineralogical and lead isotope study of Italian majolica from Montelupo (Florence). Archaeometry 57:879–896. https://doi.org/10.1111/arcm.12146

Choudhary RNP (1982) A neutron diffraction study of ferroelectric $PbHAsO_4$ at room temperature. Pramana 18(4):325–330. https://doi.org/10.1007/bf02879392

Chutas NI, Kress VC, Ghiorso MS, Sack RO (2008) A solution model for high-temperature PbS-$AgSbS_2$-$AgBiS_2$ galena. Am Mineral 93(10):1630–1640. https://doi.org/10.2138/am.2008.2695

Ciomartan DA, Clark RJH, McDonald LJ, Odlyha M (1996) Studies on the thermal decomposition of basic lead(II) carbonate by Fourier-transform Raman spectroscopy, X-ray diffraction and thermal analysis. Dalton Trans 18:3639–3645. https://doi.org/10.1039/DT9960003639

Claringbull G (1950) An X-Ray study of schultenite. Mineral Mag J Mineral Soc 29(211):287–290. https://doi.org/10.1180/minmag.1950.029.211.05

Clark RJH (2002) Pigment identification by spectroscopic means: an arts/science interface. ComptesRendusChimie 5(1):7–20. https://doi.org/10.1016/S1631-0748(02)01341-3

Clark GL, Schieltz NC, Quirke TT (1937) A new study of the preparation and properties of the higher oxides of lead. J Am Chem Soc 59:2305–2308. https://doi.org/10.1021/ja01290a063

Clark RJH, Cridland L, Kariuki BM, Harris KDM, Withnall R (1995) Synthesis, structural characterisation and Raman spectroscopy of the inorganic pigments lead tin yellow types I and II and lead antimonate yellow: their identification on medieval paintings and manuscripts. J Chem Soc Dalton Trans 16:2577–2582. https://doi.org/10.1039/dt9950002577

Clark RJH, Gibbs PJ (1998) Peer reviewed: Raman microscopy of a 13th-century illuminated text. Anal Chem 70(3):99A–104A. https://doi.org/10.1021/ac981719g

Coccato A, Moens L, Vandenabeele P (2017) On the stability of mediaeval inorganic pigments: a literature review of the effect of climate, material selection, biological activity, analysis and conservation treatments. Heritage Science 5(1):12. https://doi.org/10.1186/s40494-017-0125-6

Colombini MP, Giachi G, Modugno F, Pallecchi P, Ribechini E (2003) The characterization of paints and waterproofing materials from the shipwrecks found at the archaeological site of the etruscan and Roman harbour of Pisa (Italy). Archaeometry 45(4):659–674. https://doi.org/10.1046/j.1475-4754.2003.00135.x

Coremans P (1961) Het Calvarie-Drieluik toegeschreven aan Justus van Gent en de bijhorende predella: samenstelling en structuur van verflaag en plamuur. Bulletin Institut Royal du Patrimoine Artistique/Koninklijk Instituut voor het kunstpatrimonium 4:28–31

Coremans P, Thissen L (1962) La descente de croix de Rubens: composition et structure des couches originales. Bulletin de l'Institut royal du patrimoine artistique 5:119–145

Coremans P, Gettens RJ, Thissen J (1952) La technique des "Primitifs flamands". Stud Conserv 1(1):1–29. https://doi.org/10.2307/1504942

Cortea IM, Ghervase L, Ratoiu L, Dinu M, Rădvan R (2020) Uncovering hidden jewels: an investigation of the pictorial layers of an 18th-century Taskin harpsichord. Heritage Science 8(1):55. https://doi.org/10.1186/s40494-020-00401-3

Costa BFO, Lehmann R, Wengerowsky D, Blumers M, Sansano A, Rull F, Schmidt H-J, Dencker F, Niebur A, Klingelhöfer G, Sindelar R, Renz F (2016) Klimt artwork (part II): material investigation by backscattering Fe-57 Mössbauer- and Raman- spectroscopy, SEM and p-XRF. Hyperfine Interactions 237(1):92. https://doi.org/10.1007/s10751-016-1263-z

Costantini I, Lottici PP, Castro K, Madariaga JM (2020a) Use of temperature controlled stage confocal raman microscopy to study phase transition of lead dioxide (Plattnerite). Minerals 10(5):468. https://doi.org/10.3390/min10050468

Costantini I, Lottici PP, Bersani D, Pontiroli D, Casoli A, Castro K, Madariaga JM (2020b) Darkening of lead- and iron-based pigments on late Gothic Italian wall paintings: energy dispersive X-ray fluorescence, μ-Raman, and powder X-ray diffraction analyses for diagnosis: presence of β-PbO_2(plattnerite) and α-PbO_2 (scrutinyite). J Raman Spectrosc 51(4):680–692. https://doi.org/10.1002/jrs.5817

Cotte M, Checroun E, Susini J, Dumas P, Tchoreloff P, Besnard M, Walter P (2006) Kinetics of oil saponification by lead salts in ancient preparations of pharmaceutical lead plasters and painting lead mediums. Talanta 70:1136–1142. https://doi.org/10.1016/j.talanta.2006.03.007

Cotte M, Checroun E, Susini J, Valter P (2007)Micro-analytical study of interactions between oil and lead compounds in paintings. Appl Phys A Mater Sci Process 89:841–848. https://doi.org/10.1007/s00339-007-4213-4

Cotte M, Checroun E, De Nolf W, Taniguchi Y, De Viguerie L, Burghammer M, Walter P, Rivard C, Salomé M, Janssens K, Susini J (2017) Lead soaps in paintings: friends or foes? Stud Conserv 62(1):2–23. https://doi.org/10.1080/00393630.2016.1232529

Crane MJ, Leverett P, Shaddick LR, Williams PA, Kloprogge JTT, Frost RL (2001) The $PbCrO_4$-$PbSO_4$ system and its mineralogical significance. Neues Jahrb Mineral Monatshefte 11:505–519

Criado JM, Gonzalez F, Gonzalez M, Real C (1982) Influence of the grinding of $PbCO_3$ on the texture and structure of the final products of its thermal decomposition. J Mater Sci 17(7):2056–2060. https://doi.org/10.1007/BF00540423

Curley AN, Thibodeau AM, Kaplan E, Howe E, Pearlstein E, Levinson J (2020) Isotopic composition of lead white pigments on qeros: implications for the chronology and production of Andean ritual drinking vessels during the colonial era. Heritage Science 8(1):72. https://doi.org/10.1186/s40494-020-00408-w

Dachille F, Roy R (1960)High-pressure phase transformations in laboratory mechanical mixers and mortars. Nature 186(34):71. https://doi.org/10.1038/186034a0

Dai Y, Hughes JM (1989)Crystal-structure refinements of vanadinite and pyromorphite. Can Mineral 27:189–192

Dai Y, Hughes JM, Moore PB (1991) The crystal of mimetite and clinomimetite, $Pb_5(AsO_4)_3Cl$. Can Mineral 29(2):369–376

Damiani D, Gliozzo E, Turbanti Memmi I (2014) The 'Madonna and Child Enthroned with Saints' of Ambrogio Lorenzetti in the St. Augustine Church (Siena, Italy): Raman microspectroscopy and SEM-EDS characterisation of the pigments. Archaeological-and-Anthropological-Science 6:363–371. https://doi.org/10.1007/s12520-014-0175-6

Daniels V, Thickett D (1992) The reversion of blackened lead white on paper: analytical appendix by T. Baird and N.H. Tennent. In: Fairbrass S (ed) The Institute of Paper Conservation, Conference Papers. Manchester, Institute of Paper Conservation, pp 109–115

Daniilia S, Sotiropoulou S, Bikiaris D, Salpistis C, Karagiannis G, Chryssoulakis Y, Price BA, Carlson JHP (2000) Panselinos' Byzantine wall paintings in the Protaton church, Mount Athos, Greece: a technical examination. J Cult Herit 1:91–110. https://doi.org/10.1016/S1296-2074(00)00164-3

Daniilia S, Bikiaris D, Burgio L, Gavala P, Clark RJH, Chryssoulakis Y (2002) An extensive non-destructive and micro-spectroscopic study of two post-Byzantine overpainted icons of the 16th century. J Raman Spectrosc 33(10): 807-814. DOI: https://doi.org/10.1002/jrs.907

Daniilia S, Minopoulou E, Demosthenous FD, Karagiannis G (2008) A comparative study of wall paintings at the Cypriot monastery of Christ Antiphonitis: one artist or two? J Archaeol Sci 35(6):1695–1707. https://doi.org/10.1016/j.jas.2007.11.011

Daniilia S, Minopoulou E (2009) A study of smalt and red lead discolouration in Antiphonitis wall paintings in Cyprus. Appl Phys A: Mater Sci Process 96(3):701–711. https://doi.org/10.1007/s00339-009-5163-9

D'Antonio P, Santoro A (1980) Powder neutron diffraction study of chemically prepared β-lead dioxide. Acta Crystallographica Section B: Structural Science, Crystal engineering and materials 36: 2394-2397https://doi.org/10.1107/S0567740880008813

De Ferri L, Mazzini F, Vallotto D, Pojana G (2019) In situ non-invasive characterization of pigments and alteration products on the masonry altar of S. Maria ad Undas (Idro, Italy). Archaeol Anthropol Sci 11(2):609–625. https://doi.org/10.1007/s12520-017-0550-1

De Giudici G, Rossi A, Fanfani L, Lattanzi P (2005) Mechanisms of galena dissolution in oxygen-saturated solutions: evaluation of pH effect on apparent activation energies and mineral-water interface. Geochim Cosmochim Acta 69(9):2321–2331. https://doi.org/10.1016/j.gca.2004.12.003

De Keyser N, Van der Snickt G, Van Loon A, Legrand S, Wallert A, Janssens K (2017) Jan Davidsz. de Heem (1606–1684): a technical examination of fruit and flower still lifes combining MA-XRF scanning, cross-section analysis and technical historical sources. Heritage Science 5:38. https://doi.org/10.1186/s40494-017-0151-4

DeLaine J (2021) Production, transport and on-site organisation of Roman mortars and plasters. Archaeol Anthropol Sci https://doi.org/10.1007/s12520-021-01401-5

De la Roja JM, Sancho N, San Andrés M, Baonza VG (2008) Obtención de litargirio a partir de la tostación de blanco de plomo. Caracterizacióncromática de los productosobtenidos [Litharge obtaining from the roasting of lead white. Chromatic characterization of obtained products]. Optica Pura y Aplicada 41(3):245–249 Spanish

De Massoul CM (1797) A treatise on the art of painting and the composition of colours, containing instructions for all the various processes of painting together with observation upon the qualities and ingredients ofcColours. Translated from the French, de Massoul Manufactory London. 242 pp. https://play.google.com/books/reader?id=5HFKAAAAYAAJ&hl=en_GB&pg=GBS.PA7; Accessed 28.01.2021

De Meyer S, Vanmeert F, Vertongen R, Van Loon A, Gonzalez V, Delaney J, Dooley K, Dik J, Van der Snickt G, Vandivere A, Janssens K (2019a) Macroscopic x-ray powder diffraction imaging reveals Vermeer's discriminating use of lead white pigments in Girl with a Pearl Earring. Sci Adv 5(8):eaax1975. https://doi.org/10.1126/sciadv.aax1975

De Meyer S, Vanmeert F, Vertongen R, van Loon A, Gonzalez V, van der Snickt G, Vandivere A, Janssens K (2019b) Imaging secondary reaction products at the surface of Vermeer's Girl with the Pearl Earring by means of macroscopic X-ray powder diffraction scanning. Heritage Science 7(1):67. https://doi.org/10.1186/s40494-019-0309-3

De Viguerie L, Glanville H, Ducouret G, Jacquemot P, Dang PA, Walter P (2018)Re-interpretation of the old masters' practices through optical and rheological investigation: the presence of calcite. ComptesRendus Physique 19(7):543–552. https://doi.org/10.1016/j.crhy.2018.11.003

De Wild AM (1931) Naturwissenschaftliche Gemäldeuntersuchung. München

Delaney JK, Dooley KA, van Loon A, Vandivere A (2020) Mapping the pigment distribution of Vermeer's Girl with a Pearl Earring. Heritage Science 8(1):4. https://doi.org/10.1186/s40494-019-0348-9

Di Stefano LM, Fuchs R (2011) Characterisation of the pigments in a Ptolemaic Egyptian Book of the Dead papyrus. Archaeol Anthropol Sci 3(3):29–244. https://doi.org/10.1007/s12520-011-0054-3

Dietemann P, Higgitt C, Kälin M, Edelmann MJ, Knochenmuss R, Zenobi R (2009) Aging and yellowing of triterpenoid resin varnishes – influence of aging conditions and resin composition. J Cult Herit 10(1):30–40. https://doi.org/10.1016/j.culher.2008.04.007

Dik J, Hermens E, Peschar R, Schenk H (2005) Early production recipes for lead antimonate yellow in Italian art. Archaeometry 47(3):593–607. https://doi.org/10.1111/j.1475-4754.2005.00221.x

Dik J, Tichelaar F, Goubitz K, Peschar R, Schenk H (2002) 19th century Naples yellow re-examined. Zeitschrift für Kunsttechnologie und Konservierung 16(2):291–306

Doménech-Carbó A, Doménech-Carbó MT, Moya-Moreno M, Gimeno-Adelantado JV, Bosch-Reig F (2000) Identification of inorganic pigments from paintings and polychromed sculptures immobilized into polymer film electrodes by stripping differential pulse voltammetry. Anal Chim Acta 407(1-2):275–289. https://doi.org/10.1016/S0003-2670(99)00781-3

Doménech-Carbó MT, Kuckova S, de la Cruz-Cañizares J, Osete-Cortina L (2006) Study of the influencing effect of pigments on the photoageing of terpenoid resins used as pictorial media. J Chromatogr A 1121(2):248–258. https://doi.org/10.1016/j.chroma.2006.04.005

Doménech-Carbó A, Doménech-Carbó MT, Mas-Barberá X (2007) Identification of lead pigments in nanosamples from ancient paintings and polychromed sculptures using voltammetry of nanoparticles/atomic force microscopy. Talanta 71(4):1569–1579. https://doi.org/10.1016/j.talanta.2006.07.053

Doménech-Carbó A, Doménech-Carbó MT, Castelló-Palacios A, Guerola-Blay V, Pérez-Marín E (2019) Electrochemical identification of painters/workshops: the case of Valencian Renaissance-Baroque painters (ca. 1550- ca. 1670). Electrochim Acta 297:685–695. https://doi.org/10.1016/j.electacta.2018.11.212

Domingo Sanz I, Chieli A (2021) Characterising the pigments and paints of prehistoric artists. Archaeol Anthropol Sci. https://doi.org/10.1007/s12520-021-01397-y

Dooryhée E, Anne M, Bardiès I, Hodeau J-L, Martinetto P, Rondot S, Salomon J, Vaughan GBM, Walter P (2005)Non-destructive synchrotron X-ray diffraction mapping of a Roman painting. Appl Phys A Mater Sci Process 81:663–667. https://doi.org/10.1007/s00339-005-3281-6

Dunkerton J, Howard H (2009) Sebastiano del Piombo's 'Raising of Lazarus': a history of change. National Gallery Technical Bulletin 30:26–51

Dunkerton J, Roy A (1996) The materials of a group of late fifteenth-century Florentine panel paintings. National Gallery Technical Bulletin 17:21–31

Duran A, Siguenza MB, Franquelo ML, Jimenez de Haro MC, Justo A, Perez-Rodriguez JL (2010) Murillo's paintings revealed by spectroscopic techniques and dedicated laboratory-made micro X-ray diffraction. Anal Chim Acta 671(1-2):1–8. https://doi.org/10.1016/j.aca.2010.05.004

Duran A, López-Montes A, Castaing J, Espejo T (2014) Analysis of a royal 15th century illuminated parchment using a portable XRF-XRD system and micro-invasive techniques. J Archaeol Sci 45(1):52–58. https://doi.org/10.1016/j.jas.2014.02.011

Eastaugh N, Walsh V, Chaplin T, Siddall R (2004) Pigment compendium: a dictionary and optical microscopy of historic pigments. Elsevier - Butterworth Heinemen, pp. 499.

Edwards R, Gillard RD, Williams PA, Pollard AM (1992) Studies of secondary mineral formation in the PbO-H_2O-HC1 system. Mineral Mag 56(382):53–65. https://doi.org/10.1180/minmag.1992.056.382.07

Edwards HGM, Farwell DW, Newton EM, Perez FR, Villar SJ (2000) Raman spectroscopic studies of a 13th century polychrome statue: identification of a 'forgotten' pigment. J Raman Spectrosc 31(5):407–413. https://doi.org/10.1002/1097-4555(200005)31:5<407::AID-JRS530>3.0.CO;2-Y

Edwards HGM, Rull F, Vandenabeele P, Newton EM, Moens L, Medina J, Garcia C (2001) Mediaeval pigments in the monastery of San Baudelio, Spain: a Raman spectroscopic analysis. Appl Spectrosc 55(1):71–76. https://doi.org/10.1366/0003702011951272

Edwards HGM, Wolstenholme R, Wilkinson DS, Brooke C, Pepper M (2007) Raman spectroscopic analysis of the enigmatic Comper pigments. Anal Bioanal Chem 387(6):2255–2262. https://doi.org/10.1007/s00216-006-1113-y

Effenberger H, Pertlik F (1986a) Four monazite type structures: comparison of $SrCrO_4$, $SrSeO_4$, $PbCrO_4$(crocoite), and $PbSeO_4$. Zeitschrift für Kristallographie - Crystalline Materials 176:75–83

Effenberger H, Pertlik F (1986b) Schultenit, $PbHAsO_4$, und $PbHPO_4$: Synthesen und Kristallstrukturen nebst einer Diskussion zur

Symmetrie. Tschermaks Mineral Petrogr Mitt 35(3):157–166. https://doi.org/10.1007/BF01082083
Embrey PG, Hicks RP (1977) Schultenite from Tsumeb: a note on its morphology. Mineral Rec 8(3):98–99
Ergenç D, Fort R, Varas-Muriel MJ, Alvarez de Buergo M (2021) Mortars and plasters – How to characterise aerial mortars and plasters. Archaeol Anthropol Sci. https://doi.org/10.1007/s12520-021-01398-x
Erhardt D, Tumosa CS, Mecklenburg MF (2000) Natural and accelerated thermal aging of oil paint films. In: Roy, A., Smith, P. (Eds.) Tradition and Innovation: Advances in Conservation, Contributions to the IIC Melbourne Congress. London: International Institute for Conservation of Historic and Artistic Works, pp. 65-69.
Espejo Arias T, López Montes A, García Bueno A, Durán Benito A, Blanc García R (2008) A study about colourants in the Arabic manuscript collection of the Sacromonte Abbey, Granada, Spain. A new methodology for chemical analysis. Restaurator 29(2):76–106. https://doi.org/10.1515/rest.2008.005
Essington ME, Foss JE, Roh Y (2004) The soil mineralogy of lead at Horace's Villa. Soil Sci Soc Am J 68(3):979–993. https://doi.org/10.2136/sssaj2004.9790
Fallon EK, Petersen S, Brooker RA, Scott TB (2017) Oxidative dissolution of hydrothermal mixed-sulfide ore: an assessment of current knowledge in relation to seafloor massive sulfide mining. Ore Geol Rev 86:309–337. https://doi.org/10.1016/j.oregeorev.2017.02.028
Falls R, Cannon B, Mandarino JA (1985) Schultenite from King County, Washington, USA; a second occurrence, and review. Mineral Mag 49(350):65–69. https://doi.org/10.1180/minmag.1985.049.350.08
Fantacci S, Amat A, Sgamellotti A (2010) Computational chemistry meets cultural heritage: challenges and perspectives. Acc Chem Res 43(6):802–813. https://doi.org/10.1021/ar100012b
Felici AC, Fronterotta G, Piacentini M, Nicolais C, Sciuti S, Venditelli M, Vazio C (2004) The wall paintings in the former Refectory of the Trinità dei Monti convent in Rome: relating observations from restoration and archaeometric analyses to Andrea Pozzo's own treatise on the art of mural painting. J Cult Herit 5(1):17–25. https://doi.org/10.1016/j.culher.2003.07.001
Felix VS, Mello UL, Pereira MO, Oliveira AL, Ferreira DS, Carvalho CS, Silva FL, Pimenta AR, Diniz MG, Freitas RP (2018) Analysis of a European cupboard by XRF, Raman and FT-IR. Radiat Phys Chem 151:198–204. https://doi.org/10.1016/j.radphyschem.2018.06.036
Feller RL (1973) Rubens's: The Gerbier Family: technical examination of the pigments and paint layers. Studies in the History of Art5:54–74 http://www.jstor.org/stable/42617886. Accessed February 24, 2021
Feng Q, Zhang X, Ma X (1999) Effects of microbes on color changes of red lead in murals. J Gen Appl Microbiol 45(2):85–88. https://doi.org/10.2323/jgam.45.85
Fioretti G, Raneri S, Pinto D, Mignozzi M, Mauro D (2020) The archaeological site of St. Maria Veterana (Triggiano, Southern Italy): archaeometric study of the wall paintings for the historical reconstruction. J Archaeol Sci Rep 29:102080. https://doi.org/10.1016/j.jasrep.2019.102080
Fiorillo F, Fiorentino S, Montanari M, Roversi Monaco C, Del Bianco A, Vandini M (2020) Learning from the past, intervening in the present: the role of conservation science in the challenging restoration of the wall painting Marriage at Cana by Luca Longhi (Ravenna, Italy). Herit Sci 8(1):10. https://doi.org/10.1186/s40494-020-0354-y
Flemming NJ, Lopata VJ, Sanipelli BL, Taylor P (1984) Thermal decomposition of basic lead carbonates: a comparison of hydrocerussite and plumbonacrite. Thermochim Acta 81(C):1–8. https://doi.org/10.1016/0040-6031(84)85104-7
Foord EE, Shawe DR (1989) Pb-Bi-Ag-Cu-(Hg) chemistry of galena and some associated sulfosalts. A review and some new data from Colorado California and Pennsylvania. Can Mineral 27(3):363–382
Fortunato G, Ritter A, Fabian D (2005) Old Masters' lead white pigments: investigations of paintings from the 16th to the 17th using high precision lead isotope abundance ratios. Analyst 130:898–906. https://doi.org/10.1039/b418105k
Franceschi CM, Costa GA, Franceschi E (2010) Aging of the paint palette of Valerio Castello (1624–1659) in different paintings of the same age (1650–1655). J Therm Anal Calorim 103(1):69–73. https://doi.org/10.1007/s10973-010-1089-x
Franquelo ML, Robador MD, Pérez-Rodríguez JL (2015) Scientific study of the gothic-renaissance altarpiece of Santiago church in Écija (Spain). Eur J Sci Theol 11(2):149–158
Franzini M, Perchiazzi N (1992) I minerali delle scorie ferrifere etrusche di Baratti (Livorno). Atti della Societa Toscana di Scienze Naturali, Memorie A99:43–77
Freestone IC, Stapleton CP (1998) Composition and technology of Islamic enamelled glass of the thirteenth and fourteenth centuries. In: Ward R (ed) Gilded and enamelled glass from the Middle East. British Museum Press, London, pp 122–128
Fu P, Teri G-L, Li J, Li J-X, Li Y-H, Yang H (2020) Investigation of ancient architectural painting from the Taidong tomb in the Western Qing Tombs, Hebei, China. Coatings 10(7):688. https://doi.org/10.3390/coatings10070688
Gabrielson O, Parwel A, Wickman FE (1960) Blixite, a new lead-oxyhalide mineral from Langban. Arkiv foer Mineralogi och Geologi 2:411–415
Garnier P, Calvarin G, Weigel D (1976) Oxydes de plomb: III. Etude par diffraction des rayons X sur poudre des transitions ferroélectrique et ferroélastique de l'oxyde Pb_3O_4. J Solid State Chem 16(1-2):55–62. https://doi.org/10.1016/0022-4596(76)90007-4
Garrappa S, Kočí E, Švarcová S, Bezdička P, Hradil D (2020) Initial stages of metal soaps` formation in model paints: the role of humidity. Microchem J 156:104842. https://doi.org/10.1016/j.microc.2020.104842
Garrido Perez C (1992) Velasquéz. Técnica y evolución. Museo del Prado, Madrid, p 613 Spanish
Gasperin M (1955) Synthese et identification de deux oxydes doubles de tantale et d'etain. Comptes Rendus Hebdomadaires des Seances de l'Academie des Sciences 240:2340–2342
Gavarri JR (1982) Evolution structurale d'oxydes isomorphes Me X_2O_4: Relation entre dilatation, vibrations et rigidite. J Solid State Chem 43(1):12–28. https://doi.org/10.1016/0022-4596(82)90210-9
Gavarri J-R, Weigel D (1975) Oxydes de plomb. I. Structure cristalline du minium Pb_3O_4, à température ambiante (293 K). J Solid State Chem 13(3):252–257. https://doi.org/10.1016/0022-4596(75)90127-9
Gavarri JR, Weigel D, Hewat AW (1978) Oxydes de plomb. IV. Evolution structurale de l'oxyde Pb_3O_4 entre 240 et 5 K et mecanisme de la transition. J Solid State Chem 23(3-4):327–329. https://doi.org/10.1016/0022-4596(78)90081-6
Gavarri JR, Vigouroux JP, Calvarin G, Hewat AW (1981) Structure de $SnPb_2O_4$ à quatre températures: relation entre dilatation et agitation thermiques. J Solid State Chem 36:81–90. https://doi.org/10.1016/0022-4596(81)90194-8
Gebremariam KF, Kvittingen L, Banica F-G(2013) Application of a portable XRF analyzer to investigate the medieval wall paintings of YemrehannaKrestos church, Ethiopia. X-Ray Spectrom 42(6):462–469. https://doi.org/10.1002/xrs.2504
Gehad B, Aly MF, Marey H (2015) Identification of the Byzantine encaustic mural painting in Egypt. Mediter Archaeol Archaeom 15(2):243–256. https://doi.org/10.5281/zenodo.16612
George L, Cook NJ, Ciobanu CL, Wade B (2015) Trace and minor elements in galena: a reconnaissance LA-ICP-MS study. Am Mineral 100:548–569. https://doi.org/10.2138/am-2015-4862
George LL, Cook NJ, Ciobanu CL (2016) Partitioning of trace elements in co-crystallizedsphalerite-galena-chalcopyrite hydrothermal ores. Ore Geol Rev 77:97–116. https://doi.org/10.1016/j.oregeorev.2016.02.009

Gettens RJ, Kühn H, Chase WT (1967) 3. Lead white. Stud Conserv 12(4):125–139. https://doi.org/10.1179/sic.1967.013

Giachi G, De Carolis E, Pallecchi P (2009) Raw materials in Pompeian paintings: characterization of some colors from the archaeological site. Mater Manuf Process 24(9):1015–1022. https://doi.org/10.1080/10426910902982631

Giacovazzo C, Menchetti S, Scordari F (1973) The crystal structure of caledonite, $Cu_2Pb_5(SO_4)_3CO_3(OH)_6$. Acta Crystallogr B 29(9): 1986–1990. https://doi.org/10.1107/S056774087300590X

Giovannoni S, Matteini M, Moles A (1990) Studies and developments concerning the problem of altered lead pigments in wall painting. Stud Conserv 35(1):21–25. https://doi.org/10.1179/sic.1990.35.1.21

Giuseppetti G, Tadini C (1974) Reexamination of the crystal structure of phosgenite, $Pb_2Cl_2(CO_3)$. Tschermaks Mineral Petrogr Mitt 21: 101–109

Giuseppetti G, Mazzi F, Tadini C (1990) The crystal structure of leadhillite: Pb4(SO4)(CO3)2(OH)2. Neues Jahrbuch fur Mineralogie, Monatshefte: 255-268.

Gliozzo E (2021) Pigments –mercury-based red (cinnabar-vermilion) and white (calomel) and their degradation products. Archaeol Anthropol Sci. https://doi.org/10.1007/s12520-021-01402-4

Gliozzo E, Burgio L (2021) Pigments –arsenic-based yellows and reds. Archaeol Anthropol Sci. https://doi.org/10.1007/s12520-021-01431-z

Gliozzo E, Pizzo A, La Russa MF (2021) Mortars, plasters and pigments – research questions and sampling criteria. Archaeol Anthropol Sci. https://doi.org/10.1007/s12520-021-01393-2

Goltz D, McClelland J, Schellenberg A, Attas M, Cloutis E, Collins C (2003) Spectroscopic studies on the darkening of lead white. Appl Spectrosc 57(11):1393–1398. https://doi.org/10.1366/000370203322554563

Gonzalez V, Calligaro T, Wallez G, Eveno M, Toussaint K, Menu M (2016) Composition and microstructure of the lead white pigment in masters paintings using HR synchrotron XRD. Microchem J 125: 43–49. https://doi.org/10.1016/j.microc.2015.11.005

Gonzalez V, Wallez G, Calligaro T, Cotte M, De Nolf W, Eveno M, Ravaud E, Menu M (2017a)Synchrotron-based high angle resolution and high lateral resolution X-ray diffraction: revealing lead white pigment qualities in old masters paintings. Anal Chem 89(24):13203–13211. https://doi.org/10.1021/acs.analchem.7b02949

Gonzalez V, Gourier D, Calligaro T, Toussaint K, Wallez G, Menu M (2017b) Revealing the origin and history of lead-white pigments by their photoluminescence properties. Anal Chem 89(5):2909–2918. https://doi.org/10.1021/acs.analchem.6b04195

Gonzalez V, Cotte M, Wallez G, van Loon A, de Nolf W, Eveno M, Keune K, Noble P, Dik J (2019a) Unraveling the composition of Rembrandt's impasto through the identification of unusual plumbonacrite by multimodal X-ray diffraction analysis. Angew Chem Int Ed 58(17):5619–5622. https://doi.org/10.1002/anie.201813105

Gonzalez V, Wallez G, Calligaro T, Gourier D, Menu M (2019b) Synthesizing lead white pigments by lead corrosion: new insights into the ancient manufacturing processes. Corros Sci 146:10–17. https://doi.org/10.1016/j.corsci.2018.10.033

Gordon D, Bomford D, Plesters J, Roy A (1985) Nardo Di Cione's 'Altarpiece: Three Saints'. National Gallery Technical Bulletin 9: 21–37

Gordon D, Wyld M, Roy A (2002) Fra Angelico's predella for high altarpiece of San Domenico, Fiesole. National Gallery Technical Bulletin 23:4–19

Goryachev BE, Nikolaev A (2012) Galena oxidation mechanism. J Min Sci 48(2):354–362. https://doi.org/10.1134/S1062739148020177

Gourier D, Binet L, Gonzalez V, Vezin H, Touati N, Calligaro T (2018) Effect of analytical proton beam irradiation on lead-white pigments, characterized by EPR spectroscopy. Nucl Instrum Methods Phys Res, Sect B 415:64–71. https://doi.org/10.1016/j.nimb.2017.10.032

Greenwood NN, Earnshaw A (1997) Chemistry of the Elements, 2nd edn. Elsevier Butterworth-Heinemann, Oxford

Greg RP (1851) A description of matlockite, a new oxychloride of lead. The London, Edinburgh, and Dublin Philosophical Magazine and Journal of Science 2(9):120–121. https://doi.org/10.1080/14786445108646841

Grissom CA (1986) Green Earth. In: Feller RL (ed) Artists' Pigments'. A Handbook of their History and Characteristics, vol 1. Natural Gallery of Art Washington & Archetype Publications, London, pp 141–168

Grocholski B, Shim SH, Cottrell E, Prakapenka VB (2014) Crystal structure and compressibility of lead dioxide up to 140 GPa. Am Mineral 99:170–177. https://doi.org/10.2138/am.2014.4596

Gross ST (1943) The crystal structure of Pb_3O_4. J Am Chem Soc 65(5): 1107–1110. https://doi.org/10.1021/ja01246a029

Guastoni A, Pezzotta (2007) Fosgenite di Monteponi: Francesco Mauro e la collezione di fosgeniti del Museo di Storia Naturale di Milano. Rivista Mineralogica Italiana 31(4):248–255

Guillemin C, Prouvost J, Wintenberger M (1955) Sur les variétés fibreuses de mimétite (prixite) et de vanadinite. Bulletin de la Société Française de Minéralogie et de Cristallographie 78(4-6): 301–306. https://doi.org/10.3406/bulmi.1955.5007

Gunn F (1973) The artificial face: a history of cosmetics. Trinity Press, London, p 192

Guo D, Robinson C, Herrera JE (2016) Mechanism of dissolution of minium (Pb_3O_4) in water under depleting chlorine conditions. Corros Sci 103:42–49. https://doi.org/10.1016/j.corsci.2015.10.042

Gutiérrez M, Mickus K, Camacho LM (2016) Abandoned PbZn mining wastes and their mobility as proxy to toxicity: a review. Sci Total Environ 565:392–400. https://doi.org/10.1016/j.scitotenv.2016.04.143

Gutman M, Lesar-Kikelj M, Mladenovič A, Čobal-Sedmak V, Križnar A, Kramar S (2014) Raman microspectroscopic analysis of pigments of the Gothic wall painting from the Dominican Monastery in Ptuj (Slovenia). J Raman Spectrosc 45:1103–1109. https://doi.org/10.1002/jrs.4628

Gutman Rieppi N, Price BA, Sutherland K, Lins AP, Newman R, Wang P, Wang T, Tague TJ Jr (2020) Salvator Mundi: an investigation of the painting's materials and techniques. Heritage Science 8(1):39. https://doi.org/10.1186/s40494-020-00382-3

Györkös D, Bajnóczi B, Szakmány G, Szabó M, Milke R, Aradi EL, Tóth M (2020) Provenance and production technology of late medieval 'Besztercebánya/Banská Bystrica–type' high-quality stove tiles. Archaeol Anthropol Sci 12:284. https://doi.org/10.1007/s12520-020-01221-z

Hålenius U, Bosi F (2013) Oxyplumboroméite, $Pb_2Sb_2O_7$, a new mineral species of the pyrochlore supergroup from Harstigen mine, Värmland, Sweden. Mineral Mag 77(07):2931–2939. https://doi.org/10.1180/minmag.2013.077.7.04

Harada H, Sasa Y, Uda M (1981) Crystal data for β-PbO_2. J Appl Crystallogr 14(2):141–142. https://doi.org/10.1107/S0021889881008959

Hashemi T, Brinkman AW, Wilson MJ (1992) Preparation, sintering and electrical behaviour of di-lead stannate. J Mater Sci Lett 11(10): 666–668. https://doi.org/10.1007/BF00728900

Hazen, R.M., Downs, T., Jones, A.P., Kah, L. (2013) Carbon mineralogy and crystal chemistry. In: Hazen, R.M., Jones, A.P., Baross, J.A. (Eds.) Carbon in Earth. Reviews in Mineralogy and Geochemistry, 75. Mineralogical Society of America, pp. 7-46.

He L, Wang N, Zhao X, Zhou T, Xia Y, Liang J, Rong B (2012) Polychromic structures and pigments in Guangyuan Thousand-Buddha Grotto of the Tang Dynasty (China). J Archaeol Sci 39(6): 1809–1820. https://doi.org/10.1016/j.jas.2012.01.022

Heck M, Hoffmann P (2000) Coloured opaque glass beads of the Merovingians. Archaeometry 42(2):341–357. https://doi.org/10.1111/j.1475-4754.2000.tb00886.x

Hedegaard SB, Delbey T, Brøns C, Rasmussen KL (2019) Painting the Palace of Apries II: ancient pigments of the reliefs from the Palace of Apries, Lower Egypt. Heritage Science 7(1):54. https://doi.org/10.1186/s40494-019-0296-4

Hedges REM (1976)Pre-Islamic glazes in Mesopotamia–Nippur. Archaeometry 18(2):209–213. https://doi.org/10.1111/j.1475-4754.1976.tb00162.x

Hedges REM, Moorey PRS (1975)Pre-Islamic ceramic glazes at Kish and Nineveh in Iraq. Archaeometry 17(1):25–43. https://doi.org/10.1111/J.1475-4754.1975.Tb00113.X

Hédoux A, Grebille D, Garnier P (1989) Structural resolution of the incommensurate phase of α-PbO from X-ray- and neutron-powder-diffraction data. Phys Rev B 40:10653–10656. https://doi.org/10.1103/PhysRevB.40.10653

Hein A, Karatasios I, Mourelatos D (2009) Byzantine wall paintings from Mani (Greece): Microanalytical investigation of pigments and plasters. Anal Bioanal Chem 395(7):2061–2071. https://doi.org/10.1007/s00216-009-2967-6

Henderson, J., Warren, S.E. (1983) Analysis of prehistoric lead glass. In: Aspinall, A., Warren, S.E. (Eds.), Proceedings of the 22nd Symposium on Archaeometry. University of Bradford, pp. 168-180.

Hendriks L, Hajdas I, Ferreira ESB, Scherrer NC, Zumbühl S, Küffner M, Wacker L, Synal H-A, Günther D (2018) Combined ^{14}C analysis of canvas and organic binder for dating a painting. Radiocarbon 60(1):207–218. https://doi.org/10.1017/RDC.2017.107

Hendriks L, Hajdas I, Ferreira ESB, Scherrer NC, Zumbühl S, Küffner M, Carlyle L, Synal H-A, Günther D (2019) Selective dating of paint components: radiocarbon dating of lead white pigment. Radiocarbon 61(2):473–493. https://doi.org/10.1017/RDC.2018.101

Hendriks L, Kradolfer S, Lombardo T, Hubert V, Küffner M, Khandekar N, Hajdas I, Synal H-A, Hattendorf B, Günther D (2020) Dual isotope system analysis of lead white in artworks. Analyst 145(4):1310–1318. https://doi.org/10.1039/c9an02346a

Heraclius (1873) Heraclius von den farben und künsten der Römer - original text und übersetzungmiteinleitung, noten und excursenversehen von Albert Ilg. Wilhelm Braumüller, Wien

Hermans, J.J. (2017) Metal soaps in oil paint: structure, mechanisms and dynamics. PhD thesis - Faculty of Science (FNWI)- University of Amsterdam, pp. 168.

Higgitt C, Spring M, Saunders D (2003)Pigment-medium interactions in oil paint films containing red lead or lead-tin yellow. National Gallery Technical Bulletin 24:75–95

Hill RJ (1985) Refinement of the structure of orthorhombic PbO (massicot) by Rietveld analysis of neutron powder diffraction data. Acta Crystallographica Section C: structural chemistry 41:1281–1284. https://doi.org/10.1107/S0108270185007454

Holakooei P, Karimy A-H(2015) Early Islamic pigments used at the Masjid-iJame of Fahraj, Iran: a possible use of black plattnerite. J Archaeol Sci 54:217–227. https://doi.org/10.1016/j.jas.2014.12.001

Holakooei P, de Lapérouse JF, Rugiadi M, Carò F (2018) Early Islamic pigments at Nishapur, north-eastern Iran: studies on the painted fragments preserved at The Metropolitan Museum of Art. Archaeol Anthropol Sci 10(1):175–195. https://doi.org/10.1007/s12520-016-0347-7

Homburg E, De Vlieger JH (1996) A victory of practice over science. Hist Technol 13:33–52

Howard H, Nethersole S (2010) Two copies of Perugino's 'Baptism of Christ'. National Gallery Technical Bulletin 31:78–95

Hradil D, Grygar T, Hradilová J, Bezdička P, Grunwaldová V, Fogaš I, Miliani C (2007) Microanalytical identification of Pb-Sb-Sn yellow pigment in historical European paintings and its differentiation from lead tin and Naples yellows. J Cult Herit 8(4):377–386. https://doi.org/10.1016/j.culher.2007.07.001

Hradil D, Hradilová J, Kočí E, Švarcová S, Bezdička P, Maříková-Kubková J (2013) Unique pre-romanesque murals in Kostoľany pod Tríbečom, Slovakia: the painting technique and causes of damage. Archaeometry 55(4):691–706. https://doi.org/10.1111/j.1475-4754.2012.00704.x

Hradil D, Hradilová J, Bezdička P, Švarcová S, Čermáková Z, Košařová V, Němec I (2014) Crocoite $PbCrO_4$and mimetite $Pb_5(AsO_4)_3Cl$: rare minerals in highly degraded mediaeval murals in Northern Bohemia. J Raman Spectrosc 45(9):848–858. https://doi.org/10.1002/jrs.4556

Hsieh YH, Huang CP (1989) The dissolution of PbS(s) in dilute aqueous solutions. J Colloid Interface Sci 131(2):537–549. https://doi.org/10.1016/0021-9797(89)90196-3

Huică I, Cortea IM, Ratoiu L, Ghervase L, Rădvan R, Mohanu D (2020) Multidisciplinary approach for time-framing of an overpainted wooden iconostasis from Southern Romania. Microchem J 155:104685. https://doi.org/10.1016/j.microc.2020.104685

Humphreys DA, Thomas JH, Williams PA, Symes RF (1980) The chemical stability of mendipite, diaboleïte, chloroxiphite, and cumengite, and their relationships to other secondary lead(II) minerals. Mineral Mag 43:901–904. https://doi.org/10.1180/minmag.1980.043.331.13

Ibáñez-Insa J, Elvira JJ, Llovet X, Pérez-Cano J, Oriols N, Busquets-Masó M, Hernández S (2017) Abellaite, $NaPb_2(CO_3)_2(OH)$, a new supergene mineral from the Eureka mine, Lleida province, Catalonia, Spain. Eur J Mineral 29(5):915–922. https://doi.org/10.1127/ejm/2017/0029-2630

Hurst GH (1892) Painters' colours, oils, and varnishes: a practical manual. Charles Griffin & Company, London, p 461

Impallaria A, Petrucci F, Bruno S (2019) Judith and Holofernes: reconstructing the history of a painting attributed to Artemisia Gentileschi. Minerals 2:2183–2192. https://doi.org/10.3390/heritage2030132

Impallaria A, Mazzacane S, Petrucci F, Tisato F, Volpe L (2020) Portable X-ray fluorescence device reveals the artistic palette of Carlo Bononi, Baroque artist from Ferrara. X-Ray Spectrom 49(3):442–450. https://doi.org/10.1002/xrs.3139

Jacobi R (1941) Über den in der Malerei verwendeten gelben Farbstoff der alten Meister. Angew Chem 54(1-2):28–29. https://doi.org/10.1002/ange.19410540107

Janssens K, Cotte M (2019) Using synchrotron radiation for characterization of cultural heritage materials. In: Jaeschke, E.J., Khan, S., Schneider, J.R., Hastings, J.B. (Eds.), Synchrotron Light Sources and Free-Electron Lasers, Springer, pp. 1-27. DOI: https://doi.org/10.1007/978-3-319-04507-8_78-1

Jasiński M (2019) Cecco del Caravaggio's Martyrdom of Saint Sebastian. An investigation into Caravaggisti painting technique and technology. Int J Conserv Sci 10(2):271–278

Johnson AW, Gutiérrez M, Gouzie D, McAliley LR (2016) State of remediation and metal toxicity in the Tri-State Mining District, USA. Chemosphere 144:1132–1141. https://doi.org/10.1016/j.chemosphere.2015.09.080

Jussen E (1887)White-lead industry in Austria. Reports from the Consuls of the United States, 83. Government Printing Office, Washington, pp 413–419

Kakoulli I (2002) Late Classical and Hellenistic painting techniques and materials: a review of the technical literature. Stud Conserv 47(Suppl. 1):56–67. https://doi.org/10.1179/sic.2002.47.supplement-1.56

Kameyama N, Fukumoto T (1946) Structures and equilibria of lead oxides. J Soc Chem Ind, Japan 49(10-11):155–157 (Japanese. https://doi.org/10.1246/nikkashi1898.49.154

Kang ZC, Machesky L, Eick HA, Eyring L (1988) The solvolytic disproportionationof mixed-valence compounds: III. Pb_3O_4. J

Solid State Chem 75:52–59. https://doi.org/10.1016/0022-4596(88)90304-0

Kantoglu O, Ergun E, Kirmaz R, Kalayci Y, Zararsiz A, Bayir O (2018) Colour and ink characterization of ottoman diplomatic documents dating from the 13th to the 20th century. Restaurator 39(4):265–288. https://doi.org/10.1515/res-2018-0014

Karydas A, Brecoulaki H, Bourgeois B, Jockey P (2009) In situ X-ray fluorescence analysis of raw pigments and traces of polychromy on Hellenistic sculpture at the archaeological museum of Delos. Bulletin de correspondancehellénique S51:811–829

Katerinopoulos A (2010) The Lavrion Mines. In: Evelpidou N, Figueiredo T, Mauro F, Vassilopoulos A (Eds.). Natural heritage from East to West. Springer Verlag: Berlin. pp. 27–33

Keim MF, Gassmann B, Markl G (2017) Formation of basic lead phases during fire-setting and other natural and man-made processes. Am Mineral 102(7):1482–1500. https://doi.org/10.2138/am-2017-5931

Keim MF, Markl G (2015) Weathering of galena: mineralogical processes, hydrogeochemical fluid path modeling, and estimation of the growth rate of pyromorphite. Am Mineral 100(7):1584–1594. https://doi.org/10.2138/am-2015-5183

Keisch B, Callahan RC (1976) Lead isotope ratios in artists' lead white: a progress report. Archaeometry 18(2):181–193. https://doi.org/10.1111/j.1475-4754.1976.tb00159.x

Keune, K. (2005) Binding medium, pigments and metal soaps characterised and localised in paint cross-sections. PhD thesis Faculty of Science (FNWI), Universiteit van Amsterdam, pp. 182.

Khramchenkova R, Ionescu C, Sitdikov A, Kaplan P, Gál Á, Gareev B (2019) A pXRF*in situ* study of 16th-17th century fresco paints from Sviyazhsk (Tatarstan Republic, Russian Federation). Minerals 9(2):114. https://doi.org/10.3390/min9020114

Kleist EM, Korter TM (2020) Quantitative analysis of minium and vermilion mixtures using low-frequency vibrational spectroscopy. Anal Chem 92(1):1211–1218. https://doi.org/10.1021/acs.analchem.9b04348

Knapp CW, Christidis GE, Venieri D, Gounaki I, Gibney-Vamvakari J, Stillings M, Photos-Jones E (2021) The ecology and bioactivity of some Greco-Roman medicinal minerals: the case of Melos earth pigments. Archaeol Anthropol Sci. https://doi.org/10.1007/s12520-021-01396-z

Köchlin R (1887) Ueber Phosgenit und ein muthmasslich neues Mineral vom Laurion. Ann Naturhist Mus Wien 2(2):185–190

Kočí E, Rohlíček J, Kobera L, Plocek J, Švarcová S, Bezdička P (2019) Mixed lead carboxylates relevant to soap formation in oil and tempera paintings: the study of the crystal structure by complementary XRPD and ssNMR. Dalton Trans 48(33):12531–12540. https://doi.org/10.1039/c9dt02040c

Koller M, Leitner H, Paschinger H (1990) Reconversion of altered lead pigments in alpine mural paintings. Stud Conserv 35(1):15–20. https://doi.org/10.2307/1506277

Kostomitsopoulou Marketou A, Kouzeli K, Facorellis Y (2019) Colourful earth: iron-containing pigments from the Hellenistic pigment production site of the ancient agora of Kos (Greece). J Archaeol Sci Rep 26:101843. https://doi.org/10.1016/j.jasrep.2019.05.008

Kotulanová E, Bezdička P, Hradil D, Hradilová J, Švarcová S, Grygar T (2009) Degradation of lead-based pigments by salt solutions. J Cult Herit 10(3):367–378. https://doi.org/10.1016/j.culher.2008.11.001

Krivovichev SV, Burns PC (2000) Crystal chemistry of basic lead carbonates. II. Crystal structure of 'plumbonacrite', $Pb_5O(OH)_2(CO_3)_3$. Mineral Mag 64:1069–1075. https://doi.org/10.1180/002646100549887

Krivovichev SV, Burns PC (2006) The crystal structure of $Pb_8O_5(OH)_2Cl_4$, a synthetic analogue of blixite? Can Mineral 44(2):512–522. https://doi.org/10.2113/gscanmin.44.2.515

Krivovichev SV, Vergasova LP, Starova GL, Filatov SK, Britvin SN, Roberts AC, Steele IM (2002) Burnsite, $KCdCu_7O_2(SeO_3)_2Cl_9$, a new mineral species from the Tolbachik Volcano, Kamchatka Peninsula, Russia. Can Mineral 40(4):1171–1175. https://doi.org/10.2113/gscanmin.40.4.1171

Križnar A, Muñoz MV, de la Paz F, Respaldiza MA, Vega M (2009) XRF analysis of two terracotta polychrome sculptures by Pietro Torrigiano. X-Ray Spectrom 38(3):169–174. https://doi.org/10.1002/xrs.1135

Križnar A, Ager FJ, Caliri C, Romano FP, Respaldiza MÁ, Gómez-Morón MA, Núñez L, Magdaleno R (2019) Study of two large-dimension Murillo's paintings by means of macro X-ray fluorescence imaging, point X-ray fluorescence analysis, and stratigraphic studies. X-Ray Spectrom 48(5):482–489. https://doi.org/10.1002/xrs.2990

Kucha H (1998) Plattnerite from Kupferschiefer, Poland, and its meaning for mineralizing conditions. *Ann Soc Geol Pol* 68(4):279–285

Kühn H (1968)Lead-tin yellow. Stud Conserv 13(1):7–33

Kühn H, Curran M (1986) Chrome yellow and other chromate pigments. In: Feller RL (ed) Artists' pigments. A handbook of their history and characteristics, vol 1. National Gallery of Art, Washington: Archetype Publications, London, pp 187–200

Kühn H (1993)Lead-Tin Yellow. In: Roy A (ed) Artists Pigments, A Handbook of Their History and Characteristics, vol 2. National Gallery of Art, Washington, pp 101–110

Kutzke H, Barbier B, Becker P, Eggert G (1997) Barstowite as a corrosion product on a lead object from the Mahdia shipwreck. Stud Conserv 42(3):176–180. https://doi.org/10.1179/sic.1997.42.3.176

Kyle RA, Shampo MA (1989)Nicolas-LouisVauquelin—Discoverer of Chromium. Mayo Clin Proc 64(6):643. https://doi.org/10.1016/S0025-6196(12)65341-5

Lacroix A (1907) Les minéraux des fumerolles de l'éruption du Vésuve en avril 1907. Bulletin de la Société française de Minéralogie 30(6):219–266. https://doi.org/10.3406/bulmi.1907.2810 retrieved from https://www.persee.fr/doc/bulmi_0366-3248_1907_num_30_6_2810

Lacroix A (1920) On the occurrence of cotunnite, anglesite, leadhillite, and galena on fused lead from the wreck of the fire-ship 'Firebrand' in Falmouth Harbour, Cornwall. Mineral Mag J Mineral Soc 19(90):64–68. https://doi.org/10.1180/minmag.1920.019.90.02

Lahlil S, Cotte M, Biron I, Szlacheetko J, Menguy N, Susini J (2011) Synthesizing lead antimonate in ancient and modern opaque glass. J Anal At Spectrom 26(5):1040–1050. https://doi.org/10.1039/C0JA00251H

Lancaster LC (2021) Mortars and plasters – how mortars were made. The Literary Sources. Archaeol Anthropol Sci. https://doi.org/10.1007/s12520-021-01395-0

La Russa MF, Ruffolo SA (2021) Mortars and plasters - how to characterise mortars and plasters degradation. Archaeol Anthropol Sci. https://doi.org/10.1007/s12520-021-01405-1

Laurenze C, Riederer J (1982) Die herstellung von Neapelgelb. Berliner Beitraege zur Archaeometrie 7:209–215

Lazidou D, Lampakis D, Karapanagiotis I, Panayiotou C (2018) Investigation of the cross-section stratifications of icons using micro-Raman and micro-Fourier transform infrared (FT-IR) spectroscopy. Appl Spectrosc 72(8):1258–1271. https://doi.org/10.1177/0003702818777772

Lazzari M, Chiantore O (1999) Drying and oxidative degradation of linseed oil. https://doi.org/10.1016/S0141-3910(99)00020-8

Leciejewicz J, Padlo I (1962) Note on the oxygen parameter in tetragonal PbO_2. Naturwissenschaften 49:373–374. https://doi.org/10.1007/BF00629253

Lei Z, Wu W, Shang G, Wu Y, Wang J (2017) Study on colored pattern pigments of a royal Taoist temple beside the Forbidden City (Beijing, China). Vib Spectrosc 92:234–244. https://doi.org/10.1016/j.vibspec.2017.08.005

Leona M (2009) The materiality of art: scientific research in art history and art conservation at the Metropolitan Museum. Metrop Mus Art Bull 67(1):4–11

Leonard M, Khandekar N, Carr DW (2001) Amber Varnish' and Orazio Gentileschi's 'Lot and His Daughters. Burlingt Mag 143(1174):4–10

Levstik MG, Mladenovič A, Križnar A, Kramar S (2019) A Raman microspectroscopy-based comparison of pigments applied in two gothic wall paintings in Slovenia. Periodico di Mineralogia 88(1): 95–104. https://doi.org/10.2451/2019PM778

Li GH, Chen Y, Sun XJ, Duan PQ, Lei Y, Zhang LF (2020a) An automatic hyperspectral scanning system for the technical investigations of Chinese scroll paintings. Microchem J 155:104699. https://doi.org/10.1016/j.microc.2020.104699

Li Z, Wang L, Chen H, Ma Q (2020b) Degradation of emerald green: scientific studies on multi-polychrome Vairocana Statue in Dazu Rock Carvings, Chongqing, China. Herit Sci 8(1):64. https://doi.org/10.1186/s40494-020-00410-2

Li T, Liu C, Wang D (2020c) Applying micro-computed tomography (micro-CT) and Raman spectroscopy for non-invasive characterization of coating and coating pigments on ancient Chinese papers. Herit Sci 8(1):22. https://doi.org/10.1186/s40494-020-00366-3

Lide DR (Ed.) (2008) CRC Handbook of Chemistry and Physics. CRC Press, pp. 2736.

Lin IJ, Nadiv S (1979) Review of the phase transformation and synthesis of inorganic solids obtained by mechanical treatment (mechanochemical reactions). Mater Sci Eng 39:193–209. https://doi.org/10.1016/0025-5416(79)90059-4

Lin IJ, Niedzwiedz S (1973) Kinetics of the massicot-litharge transformation during comminution. J Am Ceram Soc 56(2):62–64. https://doi.org/10.1111/j.1151-2916.1973.tb12358.x

Lippmann F (1966) $PbMg(CO_3)_2$, ein neues rhomboedrisches Doppelcarbonat. Naturwissenschaften 53:701. https://doi.org/10.1007/BF00602722

Liu L, Shen W, Zhang B, Ma Q (2016) Microchemical study of pigments and binders in polychrome relics from maiji mountain grottoes in northwestern China. Microsc Microanal 22(4):845–856. https://doi.org/10.1017/S1431927616011302

Liu L, Gong D, Yao Z, Xu L, Zhu Z, Eckfeld T (2019) Characterization of a MahamayuriVidyarajni Sutra excavated in Lu'an, China. Heritage Science 7(1):77. https://doi.org/10.1186/s40494-019-0320-8

Loeffler BM, Burns RG (1976) Shedding light on the color of gems and minerals: The selective absorption of light according to wavelength—the result of various electronic processes whose energies correspond to certain wavelengths of visible light—gives minerals their distinctive hues. Am Sci 64(6):636–647 https://www.jstor.org/stable/27847555, accessed 23.01.2021

López Cruz O, García Bueno A, Medina Flórez VJ (2011) Evolución del color en el alero de la fachada del rey D. Pedro I, Real Alcázar de Sevilla. Aportaciones del estudio de materiales a la identificación de las intervenciones de restauración a lo largo de su historia. Arqueologia de la Arquitectura 8:163–178. https://doi.org/10.3989/arqarqt.2011.10016

Lukačević I, Ergotić I, Vinaj M (2013)Non-destructive analyses of 16th century printed book "Osorio" with the colorful fore-edge miniatures. Croat Chem Acta 86(2):207–214. https://doi.org/10.5562/cca2040

Luo Y, Chen J, Yang C, Huang Y (2019) Analyzing ancient Chinese handmade Lajian paper exhibiting an orange-red color. Heritage Science 7(1):61. https://doi.org/10.1186/s40494-019-0306-6

Lussier, S.M. (2008) An examination of lead white discoloration and the impact of treatment on paper artifacts: a summary of experimental testing. In: The Book and Paper Group Annual v. 25. American Institute for Conservation of Historic & Artistic Works 34th Annual Meeting (Providence). American Institute for Conservation of Historic & Artistic Works, pp. 9-12.

Lytle DA, Schock MR, Scheckel K (2009) The inhibition of Pb(IV) oxide formation in chlorinated water by orthophosphate. Environ Sci Technol 43:6624–6631. https://doi.org/10.1021/es900399m

Ma X, Berrie BH (2020) Lead chlorides in paint on a Della Robbia terracotta sculpture. Anal Chem 92(7):4935–4942. https://doi.org/10.1021/acs.analchem.9b05045

Macquart LCH (1789) Essai: Ou recueil de memoires sur plusieurs points de mineralogie (1789). Kessinger Publishing (2009), 626 pp., Accessed 23.01.2021

Magalhães MCF, Pedrosa de Jesus JD, Williams PA (1988) The chemistry of formation of some secondary arsenate minerals of Cu(II), Zn(II) and Pb(II). Mineral Mag 52(368):679–690. https://doi.org/10.1180/minmag.1988.052.368.12

Maggetti M, Neururer C, Rosen J (2009) Antimonate opaque glaze colours from the faience manufacture of Le Bois d'Épense (19th century, Northeastern France). Archaeometry 51(5):791–807. https://doi.org/10.1111/j.1475-4754.2008.00442.x

Malletzidou L, Zorba TT, Patsiaoura D, Lampakis D, Beinas P, Touli V, Chrissafis K, Karapanagiotis I, Pavlidou E, Paraskevopoulos KM (2019) Unraveling the materials and techniques of post-Byzantine wall paintings: is there a sole pictorial phase at the catholicon of Stomion, Central Greece? Spectrochimica Acta - Part A 206:328–339. https://doi.org/10.1016/j.saa.2018.07.105

Manzano E, Navas N, Checa-Moreno R, Rodriguez-Simón L, Capitán-Vallvey LF (2009) Preliminary study of UV ageing process of proteinaceous paint binder by FT-IR and principal component analysis. Talanta 77(5):1724–1731. https://doi.org/10.1016/j.talanta.2008.10.014

Marcucci L (1816) Saggio analitico-chimico sopra I colori minerali e mezzi di procurarsi gli artefatti gli smalti e le vernice, 2nd edn. Nella Stamperia di Lino Contendini, Roma, p 264

Maroger J (1948) The secret formulas and techniques of the masters. Studio Publications, New York and London, p 200

Martin E, Duval AR (1990) Les deux varietes de jaune de plomb et d'etain: etude chronologique. Stud Conserv 35(3):117–136. https://doi.org/10.2307/1506164

Martin E, Duval AR (1998) Le jaune de plomb et ses deux varietes. Utilisation en Italie aux XIV et XV sec. In: II Conferenza sulle prove non distruttive. Metodi microanalitici e indagini ambientali per lo studio e la conservazione delle opere d'arte. (Perugia, 17-20 aprile 1988). ICR, pp. 117-136.

Martin É, Jarry A, Jeanne M, Mancuso C, Volle N (2003) Les Muses Baglione: restauration et contexte technique. Techné 17:28–36

Martinetto P, Anne M, Dooryhée E, Walter P, Tsoucaris G (2002) Synthetic hydrocerussite, $2PbCO_3{\cdot}Pb(OH)_2$, by X-ray powder diffraction. Acta Crystallographica Section C: Structural chemistry 58(6):i82–i84. https://doi.org/10.1107/S0108270102006844

Martin-Ramos DJ, Zafra-Gómez A, Vílchez JL (2017)Non-destructive pigment characterization in the painting Little Madonna of Foligno by X-ray powder diffraction. Microchem J 134:343–353. https://doi.org/10.1016/j.microc.2017.07.001

Măruțoiu C, Bratu I, Nemeș OF, Dit I-I, Comes R, Tănăselia C, Falamas A, Miclăuș M, Măruțoiu VC, Moraru R (2017) Instrumental analysis of materials and topology of the Imperial Gates belonging to the Apahida wooden church, Cluj County. Vib Spectrosc 89:131–136. https://doi.org/10.1016/j.vibspec.2017.02.003

Mason RB, Tite MS (1997) The beginnings of tin opacification of pottery glazes. Archaeometry 39(1):41–58. https://doi.org/10.1111/j.1475-4754.1997.tb00789.x

Mass JL, Stone RE, Wypyski MT (1996) An investigation of the antimony-containing minerals used by the Romans to prepare opaque colored glasses. MRS (Materials Research Society) Online Proceedings Library 462:193–204. https://doi.org/10.1557/PROC-462-193

Mass JL, Wypyski MT, Stone RE (2002) Malkata and Lisht glassmaking technologies: towards a specific link between second millennium

BC metallurgists and glassmakers. Archaeometry 44(1):67–82. https://doi.org/10.1111/1475-4754.00043

Mastrotheodoros GP, Beltsios KG, Bassiakos Y (2021) Pigments –iron-based red, yellow and brown ochres. Archaeol Anthropol Sci (forthcoming)

Matin M (2018) On the origins of tin-opacified ceramic glazes: new evidence from early Islamic Egypt, the Levant, Mesopotamia, Iran, and Central Asia. J Archaeol Sci 97:42–66. https://doi.org/10.1016/j.jas.2018.06.011

Mazzeo R, Prati S, Quaranta M, Joseph E, Kendix E, Galeotti M (2008) Attenuated total reflection micro FTIR characterisation of pigment-binder interaction in reconstructed paint films. Anal Bioanal Chem 392(1-2):65–76. https://doi.org/10.1007/s00216-008-2126-5

McFarland MR (1997) The whitening effects of peroxide gels on darkened lead white paint. In: Proceedings of the 25th Annual Meeting of the American Institute for Conservation (San Diego, California June 1997).

Meilunas RJ, Bentsen JG, Steinberg A (1990) Analysis of aged paint binders by FTIR spectroscopy. Stud Conserv 35(1):33–51. https://doi.org/10.2307/1506280

Melo MJ, Araújo R, Castro R, Casanova C (2016) Colour degradation in medieval manuscripts. Microchem J 124:837–844. https://doi.org/10.1016/j.microc.2015.10.014

Mendoza-Flores A, Villalobos M, Pi-Puig T, MartÍNez-Villegas NV (2017) Revised aqueous solubility product constants and a simple laboratory synthesis of the Pb(II) hydroxycarbonates: plumbonacrite and hydrocerussite. Geochem J 51(4):315–328. https://doi.org/10.2343/geochemj.2.0471

Mercy MA, Rock PA, Casey WH, Mokarram MM (1998) Gibbs energies of formation for hydrocerussite $[Pb(OH)_2{\cdot}(PbCO_3)_2(s)]$ and hydrozincite $\{[Zn(OH)_2]_3{\cdot}(ZnCO_3)_2(s)\}$ at 298 K and 1 bar from electrochemical cell measurements. Am Mineral 83:739–745. https://doi.org/10.2138/am-1998-7-806

Merlino S, Pasero M, Perchiazzi N (1993) Crystal structure of paralaurionite and its OD relationships with laurionite. Mineral Mag 57:323–328. https://doi.org/10.1180/minmag.1993.057.387.15

Merrifield MP (1846) The art of fresco painting, as practised by the old Italian and Spanish Masters, with a preliminary inquiry into the nature of the colours used in fresco painting, with observations and notes. Charles Gilpin London & Arthur Wallis Brighton; 134 pp; https://babel.hathitrust.org/cgi/pt?id=uc2.ark:/13960/t1vd6qx6x&view=1up&seq=6; Accessed 27.01.2021

Merrifield MP (1849) Original treatise dating from the XIIth to XVIIth centuries of the arts of painting, in oil, miniature, mosaic, and on glass; of gilding, dyeing, and the preparation of colours and artificial gems. Vol. I, 321 pp. London, John Murray, Albemarle Street, of 134 pp;

Messager C, Beck L, Viguerie LD, Jaber M (2020) Thermal analysis of carbonate pigments and linseed oil to optimize CO_2 extraction for radiocarbon dating of lead white paintings. Microchem J 154:104637. https://doi.org/10.1016/j.microc.2020.104637

Mitolo D, Pinto D, Garavelli A, Bindi L, Vurro F (2009) The role of the minor substitutions in the crystal structure of natural challacolloite, KPb_2Cl_5, and hephaistosite, $TlPb_2Cl_5$, from Vulcano (Aeolian Archipelago, Italy). Mineral Petrol 96:121–128. https://doi.org/10.1007/s00710-008-0041-2

Moioli P, Seccaroni C (2004) I pigmenti degli affreschi del Santuario della Madonna dei Boschi. In: Il Santuario della Madonna dei Boschi di Boves. Ass. Primalpe Costanzo Martini, Cuneo, pp 138–145

Molera J, Pradell T, Salvadó N, Vendrell-Saz M (1999) Evidence of tin oxide recrystallization in opacified lead glazes. J Am Ceram Soc 82(10):2871–2875. https://doi.org/10.1111/j.1151-2916.1999.tb02170.x

Mondillo N, Herrington R, Boyce AJ, Wilkinson C, Santoro L, Rumsey M (2018) Critical elements in non-sulfide Zn deposits: a reanalysis of the Kabwe Zn-Pb ores (central Zambia). Mineralogical Mag 82(S1):S89-S114. https://doi.org/10.1180/minmag.2017.081.038

Monico L, Janssens K, Hendriks E, Brunetti B, Miliani C (2014) Raman study of different crystalline forms of $PbCrO_4$ and $PbCr_{1-x}S_xO_4$ solid solutions for the noninvasive identification of chrome yellows in paintings: a focus on works by Vincent van Gogh†. J Raman Spectrosc 45(11-12):1034–1045. https://doi.org/10.1002/jrs.4548

Monico L, Van der Snickt G, Janssens K, De Nolf W, Miliani C, Verbeeck J, Tian H, Tan H, Dik J, Radepont M, Cotte M (2011) Degradation process of lead chromate in paintings by Vincent van Gogh studied by means of synchrotron X-ray spectromicroscopy and related methods. 1. Artificially aged model samples. Anal Chem 83:1214–1223. https://doi.org/10.1021/ac102424h

Monico L, Sorace L, Cotte M, De Nolf W, Janssens K, Romani A, Miliani C (2019) Disclosing the binding medium effects and the pigment solubility in the (photo)reduction process of chrome yellows ($PbCrO_4$ /$PbCr_{1-x}S_xO_4$). ACS Omega 4(4):6607–6619. https://doi.org/10.1021/acsomega.8b03669

Moore TP, Wilson WE (2012) Major crocoite discoveries at the Adelaide Mine, Tasmania. Mineral Rec 43:651–673

Moreau J, Kiat JM, Garnier P, Calvarin G (1989) Incommensurate phase in lead monoxide α-PbO below 208 K. Phys Rev B 39:10296–10299. https://doi.org/10.1103/PhysRevB.39.10296

Morgan MH (1914) Vitruvius, The Ten Books on Architecture. Harvard University Press, Cambridge

Morgenstern Badarau I, Michel M (1971) Sur un compose de type pyrochlore de formule Pb2Sn2O6(H2O)X. Ann Chim, pp. 109-124.

Morrison R (2010) Mastic and Megilp in Reynolds's "Lord Heathfield of Gibraltar": a challenge for conservation. National Gallery Technical Bulletin 31:112–128

Mottin, B., Laval, E. (2004)Compte-Rendu d'etude C2RMF N° 5109 [RAPHAEL (Raffaello Santi, dit); Urbino 1483 – Rome 1520; La Madone de Lorette; Chantilly, musée Condé, Inv. 40]. Centre de Recherche et de Restauration des musées de France - C2RMF

Mounier A, Schlicht M, Mulliez M, Pacanowski R, Lucat A, Mora P (2020) In search of the lost polychromy of English medieval alabaster panels in the Southwest of France. Color Res Appl 45(3):427–449. https://doi.org/10.1002/col.22482

Moussa AB, Kantiranis N, Voudouris KS, Stratis JA, Ali MF, Christaras V (2009) Diagnosis of weathered Coptic wall paintings in the Wadi El Natrun region, Egypt. J Cult Herit 10(1):152–157. https://doi.org/10.1016/j.culher.2008.09.005

Mugnaini S, Bagnoli A, Bensi P, Droghini F, Scala A, Guasparri G (2006) Thirteenth century wall paintings under the Siena Cathedral (Italy). Mineralogical and petrographic study of materials, painting techniques and state of conservation. J Cult Herit 7(3):171–185. https://doi.org/10.1016/j.culher.2006.04.002

Murat Z (2021) Wall paintings through the ages. The medieval period (Italy, 12th-15th century). Archaeol Anthropol Sci. https://doi.org/10.1007/s12520-021-01410-4

Navas N, Romero-Pastor J, Manzano E, Cardell C (2010) Raman spectroscopic discrimination of pigments and tempera paint modelsamples by principal component analysis on first-derivative spectra. J Raman Spectrosc 41(11):1486–1493. https://doi.org/10.1002/jrs.2646

Negueruela I, González Gallero R, San Claudio M, Méndez A, Presa M, Marín C (2004) Mazarrón-2: el barcofenicio del siglo VII a.C. Campaña de noviembre–1999/marzo 2000. In: Matilla Séiquer, G., Egea Vivancos, A., González Blanco, A. (Eds.) El mundopúnico: religión, antropología y cultura material. Actas II CongresoInternacional del Mundo Púnico (Cartagena, 6–9 April 2000), pp. 453-484.

Newman, R. (1993) Observaciones acerca de los materiales pictóricos de Velázquez. In: McKim-Smith, G., Newman, R. (Eds.) Ciencia e

historia del Arte. Velázquez en el Prado. Spain: Madrid, Museo del Prado/Fundación Central Hispano, pp. 113-147.

Niknejad M, Karimy A-H(2019) Lead white or lead whites? Reconsideration of methods of sefidāb-i-sorb production in Iran. Stud Conserv 64(1):1–9. https://doi.org/10.1080/00393630.2018.1457290

Noda Y, Masumoto K, Ohba S, Saito Y, Toriumi K, Iwata Y, Shibuya I (1987) Temperature dependence of atomic thermal parameters of lead chalcogenides, PbS, PbSe and PbTe. Acta Crystallographica Section C: Structural Chemistry 43:1443–1445. https://doi.org/10.1107/S0108270187091509

Nord AG, Billström K, Tronner K, Björling Olausson K (2015) Lead isotope data for provenancing mediaeval pigments in Swedish mural paintings. J Cult Herit 16(6):856–861. https://doi.org/10.1016/j.culher.2015.02.009

Nord AG, Tronner K, Billström K, Belzacq MG (2016) Pigment traces on medieval stonework in Gotland's churches-examination of seven 12th century baptismal fonts and a limestone pew. Fornvannen 111(1):17–26

Nordenskiöld AE (1877) Mineralogiska meddelanden. Nyaminernlierfrån, Långban. Geologiska Föreningen i Stockholm Förhandlingar 3(12):376–384 (Swedish. https://doi.org/10.1080/11035897709446407

Okuri Y, Ogo Y (1982) Mechanochemical reactions at high pressures. IV. Transformation of lead monoxide. Bull Chem Soc Jpn 55(1):3641–3642. https://doi.org/10.1246/bcsj.55.3641

Olszewska-Świetlik J, Szmelter-Fausek B, Pi ta E, Proniewicz E (2013) Spectroscopic and gas chromatographic studies of pigments and binders in Gdańsk paintings of the 17th century. J Spectrosc 1(1): 187407–187408. https://doi.org/10.1155/2013/187407

Ordonez E, Twilley J (1997) Clarifying the haze: efflorescence on works of art. Anal Chem 69(13):416A–422A. https://doi.org/10.1021/ac9716921

Osbaldeston TA, Wood RP (2000) De materia medica: being an herbal with many other medicinal materials : written in Greek in the first century of the common era : a new indexed version in modern English. IBIDIS, Johannesburg, p 927

Pagès-Camagna S, Raue D (2016) Coloured materials used in elephantine: evolution and continuity from the Old Kingdom to the Roman period. J Archaeol Sci Rep 7:662–667. https://doi.org/10.1016/j.jasrep.2016.02.002

Palache C (1934) The form relations of the lead oxychlorides, laurionite, paralaurionite, and fiedlerite. Mineralogical Magazine & Journal of the Mineralogical Society 23(146):573–586. https://doi.org/10.1180/minmag.1934.023.146.01

Palache C, Richmond WE (1939) Caledonite. Am Mineral 24(7):441–445

Pallipurath A, Vofély RV, Skelton J, Ricciardi P, Bucklow S, Elliott S (2014) Estimating the concentrations of pigments and binders in lead-based paints using FT-Raman spectroscopy and principal component analysis. J Raman Spectrosc 45(11-12):1272–1278. https://doi.org/10.1002/jrs.4525

Paulsen C, Benndorf C, Kösters J, Galéa-Clolus V, Clolus P, Hoffmann R-D, Pöttgen R (2019) Tetravalent lead in nature - Plattnerite crystals from Mine du Pradet (France) and Mount Trevasco (Italy). ZeitschriftfürNaturforschung - Section B Journal of Chemical Sciences 74(5):427–432. https://doi.org/10.1515/znb-2019-0040

Pavlidou E, Civici N, Caushi E, Anastasiou L, Zorba T, Hatzikraniotis E, Paraskevopoulos KM (2008) Study of painting materials and techniques in the 18th century St. Athanasius Church in Moschopolis, Albania. Mater Res Soc Symp Proc 1047:61–69

Pekov IV, Zubkova NV, Yapaskurt VO, Britvin SN, Vigasina MF, Sidorov EG, Pushcharovsky DY (2015) New zinc and potassium chlorides from fumaroles of the Tolbachik volcano, Kamchatka, Russia: mineral data and crystal chemistry. II. Flinteite, K_2ZnCl_4. Eur J Mineral 27(4):581–588. https://doi.org/10.1127/ejm/2015/0027-2459

Pelosi C, Santamaria U, Morresi F, Agresti G, De Santis A, Mattei E (2007a) I gialli di piombo, stagno, antimonio: le opere di Poussin e Saraceni. In: D'Amico C (ed) Atti del IV Congresso Nazionale di Archeometria (Pisa 2-3 febbraio 2006). Bologna, Pàtron Editore, pp 81–94

Pelosi C, Santamaria U, Agresti G, Mattei E, De Santis A (2007b) Production and characterisation of lead, tin and antimony based yellow pigments. In: Townsend JH, Toniolo L, Cappitelli F (eds) Proceedings of the International Conference Conservation Science 2007, Milan 10–11 May, 2007, vol 2008. Archetype Publication, London, pp 187–188

Pelosi C, Agresti G, Santamaria U, Mattei E (2010) Artificial yellow pigments: production and characterization through spectroscopic full paper methods of analysis. In: Maier, M.S. (Ed.) 9th International Conference of the Infrared and Raman Users' Group (Buenos Aires, Argentina, 3-6 March 2010). Morana RTD, pp. 108-115.

Penny N, Spring M (1995) Veronese's paintings in the National Gallery, Technique and Materials: part I. National Gallery Technical Bulletin 16:4–29

Penny N, Roy A, Spring B (1996) Veronese's paintings in the National Gallery. Techniques and materials: part II. National Gallery Technical Bulletin 17:33–55

Perardi A, Appolonia L, Mirti P (2003)Non-destructive in situ determination of pigments in 15th century wall paintings by Raman microscopy. Anal Chim Acta 480:417–425. https://doi.org/10.1016/S0003-2670(02)01660-4

Pereira-Pardo L, Tamburini D, Dyer J (2019) Shedding light on the colours of medieval alabaster sculptures: scientific analysis and digital reconstruction of their original polychromy. Color Res Appl 44(2): 221–233. https://doi.org/10.1002/col.22323

Pérez-Arantegui J (2021) Not only wall paintings – pigments for cosmetics. Archaeol Anthropol Sci. https://doi.org/10.1007/s12520-021-01399-w

Pérez-Rodríguez JL, Maqueda C, Jiménez De Haro MC, Rodríguez-Rubio P (1998) Effect of pollution on polychromed ceramic statues. Atmos Environ 32(6):993–998. https://doi.org/10.1016/S1352-2310(97)00337-3

Periferakis A, Paresoglou I, Paresoglou N (2019) The significance of the Lavrion mines in Greek and European Geoheritage. Eur Geol 48: 23–27

Pernicka E, Rehren T, Schmitt-Strecker S (1998) Late Uruk silver production by cupellation at Habuba Kabira, Syria. In: RehrenTh, Hauptmann A, Muhly J (Eds.), Metallurgica Antiqua. Der Anschnitt 8:123–134

Perry DL, Wilkinson TJ (2007) Synthesis of high-purity α- and β-PbO and possible applications to synthesis and processing of other lead oxide materials. Appl Phys A Mater Sci Process 89(1):77–80. https://doi.org/10.1007/s00339-007-4073-y

Petrova O, Pankin D, Povolotckaia A, Borisov E, Krivul'ko T, Kurganov N, Kurochkin A (2019) Pigment palette study of the XIX century plafond painting by Raman spectroscopy. J Cult Herit 37:233–237. https://doi.org/10.1016/j.culher.2018.11.010

Petushkova JP, Lyalikova NN (1986) Microbiological degradation of lead-containing pigments in mural paintings. Stud Conserv 31(2): 65–69. https://doi.org/10.1179/sic.1986.31.2.65

Photos-Jones E, Bots P, Oikonomou E, Hamilton A, Knapp CW (2020) On metal and 'spoiled' wine: analysing psimythion (synthetic cerussite) pellets (5th–3rd centuries BCE) and hypothesising gas-metal reactions over a fermenting liquid within a Greek pot. Archaeol Anthropol Sci 12(10):243. https://doi.org/10.1007/s12520-020-01184-1

Pimentel C, Pina CM (2015) Síntesis del compuesto homotipo de la dolomita $PbMg(CO_3)_2$ a temperatura ambiente. Revista de la Sociedad Española de Mineralogía 20:117–118

Pimentel C, Pina CM (2016) Reaction pathways towards the formation of dolomite-analogues at ambient conditions. Geochim Cosmochim Acta 178:259–267. https://doi.org/10.1016/j.gca.2015.12.040

Pinna D, Conti C, Mazurek J (2020) Polychrome sculptures of medieval Italian monuments: study of the binding media and pigments. Microchem J 158:105100. https://doi.org/10.1016/j.microc.2020.105100

Pinch WW, Wilson WE (1977) [Tsumeb, Namibia] Minerals: a description list. Mineral Rec 8(3):17–37

Platania E, Streeton NLW, Vila A, Buti D, Caruso F, Uggerud E (2020) Investigation of mineralization products of lead soaps in a late medieval panel painting. Spectrochim Acta A Mol Biomol Spectrosc 228:117844. https://doi.org/10.1016/j.saa.2019.117844

Plater MJ, De Silva B, Gelbrich T, Hursthouse MB, Higgitt CL, Saunders DR (2003) The characterisation of lead fatty acid soaps in "protrusions" in aged traditional oil paint. Polyhedron 22(24):3171–3179. https://doi.org/10.1016/S0277-5387(03)00461-3

Plazzotta C, O'Malley M, Roy A, White R, Wyld M (2006) The Madonna di Loreto: an Alterpiece of Perugino for Santa Maria dei Servi Perugia. National Gallery Technical Bulletin 27:72–95

Plenderleith HJ (1956) The conservation of antiquities and works of art: treatment, repair and restoration. Oxford University Press, London, p 373

Plesters J (1984) Tintoretto's paintings in the National Gallery: part III. National Gallery Technical Bulletin 8:24–35

Poli T, Piccirillo A, Nervo M, Chiantore O (2019) Ageing of natural resins in presence of pigments: metal soaps and oxalates formation. In: Casadio, F., Keune, K., Noble, P., van Loon, A., Hendriks, E., Centeno, S.A., Osmond, G. (Eds.) Metal Soaps in Art. Conservation and Research. Springer, pp. 141-152.

Pozzi F, Arslanoglu J, Galluzzi F, Tokarski C, Snyder R (2020) Mixing, dipping, and fixing: the experimental drawing techniques of Thomas Gainsborough. Heritage Science 8(1):85. https://doi.org/10.1186/s40494-020-00431-x

Pozzo A (1698-1702) Prospettiva de pittori e architetti. Vol. 2.

Prieto AC, Guedes A, Dória A, Noronha F (2005) Characterization of pigments in a limestone sculpture "las tres generaciones" (Cathedral's museum of Santiago de Compostela, Spain) by optical microscopy and micro-raman spectroscopy. Can J Anal Sci Spectrosc 50(2):88–96

Quareni S, de Pieri R (1965) A three-dimensional refinement of the structure of crocoite, $PbCrO_4$. Acta Crystallogr 19:287–289. https://doi.org/10.1107/S0365110X65003304

Quarta G, D'Elia M, Paparella S, Serra A, Calcagnile L (2020) Characterisation of lead carbonate white pigments submitted to AMS radiocarbon dating. J Cult Herit 46:102–107. https://doi.org/10.1016/j.culher.2020.06.006

Rackham, H. (1952) Pliny, Natural History, Volume IX: Books 33-35. Loeb Classical Library no. 394. Cambridge, MA: Harvard University Press.

Radhakrishnan S, Kamalasanan MN, Mehendru PC (1983) Sensitization of photoconductivity in tetragonal lead monoxide. J Mater Sci 18:1912–1916. https://doi.org/10.1007/BF00554982

Radić Rossi I (2009) Il vetro grezzo e le altre materie prime del relitto romano di Mljet (Meleda), Croazia. Quaderni Friulani di Archeologia 19:193–202

Raehlmann E (1910) Über die Maltechnik der Alten: mit besonderer Berücksichtigung der römisch-pompejanischen Wandmalerei, nebst einer Anleitung zur mikroskopischen Untersuchung der Kunstwerke. Berlin: G. Reimer (in German)

Ragai J (2015) The scientist and the forger. Insights into the scientific detection of forgery in paintings. Imperial Colledge Press, UK

Ravaud E, Rioux JP, Loire S (1998) Changement de composition et utilisation d'un pigment jaune peu connu. Techné 7:99–102

Ravindran TR, Arora AK, Ramya S, Subba Rao RV, Raj B (2011) Raman spectroscopic study of medieval Indian art of 17th century. J Raman Spectrosc 42(4):803–807. https://doi.org/10.1002/jrs.2776

Rehren T, Vanhove D, Mussche H, Oikonomakou M (1999) Litharge from Laurion: a medical and metallurgical commodity from south Attica. L'Antiquité Classique 68:299–308. https://doi.org/10.3406/antiq.1999.1348

Renock D, Becker U (2011) A first principles study of coupled substitution in galena. Ore Geol Rev 42:71–83. https://doi.org/10.1016/j.oregeorev.2011.04.001

Renzi M, Montero-Ruiz I, Bode M (2009)Non-ferrous metallurgy from the Phoenician site of La Fonteta (Alicante, Spain): a study of provenance. J Archaeol Sci 36(11):2584–2596. https://doi.org/10.1016/j.jas.2009.07.016

Ricci C, Borgia I, Brunetti BG, Miliani C, Sgamellotti A, Seccaroni C, Passalacqua P (2004) The Perugino's palette: integration of an extended in situ XRF study bu Raman Spectroscopy. J Raman Spectrosc 35:616–621. https://doi.org/10.1002/jrs.1131

Risold D, Nagata J-I, Suzuki R (1998) Thermodynamic description of the Pb-O system. J Phase Equilibria 19:213–233. https://doi.org/10.1361/105497198770342238

Roberts AC, Stirling JAR, Carpenter GJC, Criddle AJ, Jones GC, Birkett TC, Birch WD (1995) Shannonite, Pb_2OCO_3, a new mineral from the Grand Reef Mine, Graham County, Arizona, USA. Mineral Mag 59(2):305–310. https://doi.org/10.1180/minmag.1995.059.395.14

Rohani, N., Pouyet, E., Walton, M., Cossairt, O., Katsaggelos, A.K. (2019) Pigment unmixing of hyperspectral images of paintings using deep neural networks. In: 44th IEEE International Conference on Acoustics, Speech, and Signal Processing, ICASSP 2019. (Brighton, United Kingdom 12-17 May 2019). Institute of Electrical and Electronics Engineers Inc., pp. 3217-3221.

Rooksby HP (1964) Yellow cubic lead-tin oxide opacifier in ancient glasses. Journal of the Society of Glass Technology - Section B: Physics and Chemistry of Glasses 5:20–25

Rosi F, Manuali V, Grygar T, Bezdicka P, Brunetti B, Sgamellotti A, Burgio L, Seccaroni C, Miliani C (2011) Raman scattering features of lead pyroantimonate compounds: implication for the non-invasive identification of yellow pigments on ancient ceramics. Part II. In situ characterisation of Renaissance plates by portable micro-Raman and XRF studies. J Raman Spectrosc 42(3):407–414. https://doi.org/10.1002/jrs.2699

Rouveret A (1998) Un exemple de diffusion des techniques de la peinture hellénistique: les stèles alexandrines du Musée du Louvre. In: L'Italie méridionale et les premières expériences de la peinture hellénistique. Actes de la table ronde de Rome (18 février 1994) organisée par l'École française de Rome. Rome: École Française de Rome, 1998. pp. 175–190. Publications de l'École Française de Rome, no. 244.

Rouveret A, Walter P (1998) Les stèles alexandrines du Musée du Louvre: apport des analyses techniques a l'histoire de la couleur dans la peinture hellénistique. Revue Archéologique 1:216–220

Rowe DJ (2017) Lead manufacturing in Britain: a history. Routledge, London, p 462

Roy A (1993) Artists' pigments. A Handbook of their History and Characteristics, vol 2. National Gallery of Art Washington, Archetype Publications London, p 234

Roy A (1999) Rubens's 'Pax and War'. National Gallery Technical Bulletin 20:89–95

Roy A, Spring M, Plazzota C (2004) Raphael's early in the National Gallery: painting before Rome. National Gallery Technical Bulletin 25:4–35

Roy A, Berrie BH (1998) A new lead-based yellow in the seventeenth century. Stud Conserv 43(Suppl.1):160–165. [Preprints 17th International Congress of the IIC on Painting techniques: history,

materials and studio practice (Dublin, 7-11 September 1998)]. https://doi.org/10.1179/sic.1998.43.Supplement-1.160

Ruby MV, Davis A, Nicholson A (1994) In situ formation of lead phosphates in soils as a method to immobilize lead. Environ Sci Technol 28(4):646–654. https://doi.org/10.1021/es00053a018

Ruiz-Moreno S, Pérez-Pueyo R, Gabaldón A, Soneira M-J, Sandalinas C (2003) Raman laser fibre optic strategy for non-destructive pigment analysis. Identification of a new yellow pigment (Pb, Sn, Sb) from the Italian XVII century painting. J Cult Herit 4(Suppl.1):309–313. https://doi.org/10.1016/S1296-2074(02)01213-X

Rumsey MS, Siidra OI, Krivovichev SV, Spratt J, Stanley CJ, Turner RW (2012a) IMA (11-G): Plumbonacrite is revalidated. Mineralogical Magazine 76: 1288. [In Williams et al. 2012, pp. 1281-1288] https://doi.org/10.1180/minmag.2012.076.5.15

Rumsey MS, Krivovichev SV, Siidra OI, Kirk CA, Stanley CJ, Spratt J (2012b) Rickturnerite, $Pb_7O_4[Mg(OH)_4](OH)Cl_3$, a complex new lead oxychloride mineral. Mineral Mag 76(1):59–73. https://doi.org/10.1180/minmag.2012.076.1.59

Russel A (1920) On the occurrence of cotunnite, anglesite, leadhillite, and galena on fused lead from the wreck of the fire-ship 'Firebrand' in Falmouth Harbour, Cornwall. Mineral Mag J Mineral Soc 19(90): 64–68. https://doi.org/10.1180/minmag.1920.019.90.02

Russell A, Hutchinson A (1927) On laurionite and associated minerals from Cornwall. Mineralogical Magazine & Journal of the Mineralogical Society 21(116):221–228. https://doi.org/10.1180/minmag.1927.021.116.04

Sack SP, Tahk CF, Peters T Jr (1981) A technical examination of an ancient Egyptian painting on canvas. Stud Conserv 26(1):15–23. https://doi.org/10.2307/1505817

Salvadó N, Butí S, Nicholson J, Emerich H, Labrador A, Pradell T (2009) Identification of reaction compounds in micrometric layers from gothic paintings using combined SR-XRD and SR-FTIR. Talanta 79(2):419–428. https://doi.org/10.1016/j.talanta.2009.04.005

Salvadori M, Sbrolli C (2021) Wall paintings through the ages. The Roman period: republic and early empire. Archaeol Anthropol Sci https://doi.org/10.1007/s12520-021-01411-3

Salvant J, Williams J, Ganio M, Casadio F, Daher C, Sutherland K, Monico L, Vanmeert F, De Meyer S, Janssens K, Cartwright C, Walton M (2018) A Roman Egyptian painting workshop: technical investigation of the portraits from Tebtunis, Egypt. Archaeometry 60(4):815–833. https://doi.org/10.1111/arcm.12351

San Andrés, M., De La Roja, J.M., Dornheim, S.D., Baonza, V.G. (2008) Litharge and massicot: thermal decomposition synthetic route for basic lead(II) carbonate and Raman spectroscopy analysis. In: Lasers in the Conservation of Artworks. Proceedings of the International Conference LACONA 7 (Madrid, Spain, 17-21 September 2007). CRC Press, pp. 89-94.

Sánchez-Navas A, López-Cruz O, Velilla N, Vidal I (2013) Crystal growth of lead carbonates: influence of the medium and relationship between structure and habit. J Cryst Growth 376:1–10. https://doi.org/10.1016/j.jcrysgro.2013.04.007

Sandalinas C, Ruiz-Moreno S (2004)Lead-tin-antimony yellow: historical manufacture, molecular characterization and identification in seventeenth-century Italian paintings. Stud Conserv 49(1):41–52

Sansonetti A, Striova J, Biondelli D, Castellucci EM (2010) Colored grounds of gilt stucco surfaces as analyzed by a combined microscopic, spectroscopic and elemental analytical approach. Anal Bioanal Chem 397(7):2667–2676. https://doi.org/10.1007/s00216-010-3491-4

Sansonetti A, Andreotti A, Bertasa M, Bonaduce I, Corti C, Facchin L, La Nasa J, Spiriti A, Rampazzi L (2020) Territory and related artworks: Stuccoworks from the lombard lakes. J Cult Herit 46:38/2–38/3398. https://doi.org/10.1016/j.culher.2020.06.009

Santamaria U, Moioli P, Seccaroni C (2000) Some remarks on lead-tin yellow and Naples yellow. In: Goupye J, Mohen J-P(eds) Actes du congrès Art et chimie, la couleur (Paris, 16-18 septembre 1998). CNRS, Paris, pp 34–38

Santis AD, Mattei E, Pelosi C (2007)Micro-Raman and stratigraphic studies of the paintings on the 'Cembalo' model musical instrument (A.D. 1650) and laser-induced degradation of the detected pigments. J Raman Spectrosc 38(10):1368–1378. https://doi.org/10.1002/jrs.1777

Sass RL, Brackett EB, Bracket TE (1963) The crystal structure of lead chloride. J Phys Chem 67(12):2863–2864. https://doi.org/10.1021/j100806a517

Saunders JA (2000) Pollution and the National Gallery. National Gallery Technical Bulletin 21:77–94

Saunders D, Spring M, Higgitt C (2002) Colour change in red lead-containing paint films. In: ICOM Committee for Conservation 13th Triennial Meeting. (Rio de Janeiro 20-27 September 2002). James & James (Science Publishers) Ltd, pp. 455-463.

Saunders D, Kirby J (2004) The effect of relative humidity on artists' pigments. National Gallery Technical Bulletin 25:62–72

Scaife B, Budd P, McDonnell A, Pollard AM (1999) Lead isotope analysis, oxide ingots and the presentation of scientific data in archaeology. In: Young SMM, Pollard AM, Budd P, Ixer RAF (eds) Metals in Antiquity. BAR International Series, vol 792. Archaeo, Oxford, pp 122–133

Schlüter J, Pohl D, Britvin S (2005) The new mineral challacolloite, KPb_2Cl_5, the natural occurrence of a technically known laser material. Neues Jahrbuch für Mineralogie - Abhandlungen 182(1):95–101. https://doi.org/10.1127/0077-7757/2005/0033

Schnorrer-Köhler G (1986) Mineralogische Notizen III. Aufschluss *37*(*7*):245–254

Schofield PF, Wilson CC, Knight KS, Kirk CA (2009) Proton location and hydrogen bonding in the hydrous lead copper sulfates linarite, $PbCu(SO_4)(OH)_2$, and caledonite, $Pb_5Cu_2(SO_4)_3CO_3(OH)_6$. Can Mineral 47:649–662. https://doi.org/10.3749/canmin.47.3.649-662

Scott KM (1994) Lead oxychlorides at Elura, western NSW, Australia. Mineral Mag 58:336–338

Scott DA, Dennis M, Khandekar N, Keeney J, Carson D, Swartz Dodd L (2003) An Egyptian cartonnage of the Graeco-Roman period: examination and discoveries. Stud Conserv 48(1):41–56

Seccaroni C (2006) Giallorino: Storia dei pigmenti gialli di natura sintetica. De Luca Roma, 399 pp.

Senna M, Kuno H (1971) Polymorphic transformation of PbO by isothermal wet ball-milling. J Am Ceram Soc 54:259–262. https://doi.org/10.1111/j.1151-2916.1971.tb12284.x

Serafima S, Duliu OG, Manea M-M, Vasilica S, Rădulescu C, Constantinescu B, Stan D, Culicov O-A, Zincovscaia I (2019a) Complex investigation of the five19th century Russian-Lipovan icons. Microchem J 150:104126. https://doi.org/10.1016/j.microc.2019.104126

Serafima S, Duliu OG, Manea M-M, Bojar A-V, Costea C, Bîrgăoanu D, Barbu O-C(2019b) An XRF, XRD, FTIR, FT RAMAN, digital radiography and UV photography study of some classical pigments, primers and binders used in panel painting. Rom Rep Phys 71(1):201

Şerifaki K, Böke H, Yalçin Ş, Ipekoğlu B (2009) Characterization of materials used in the execution of historic oil paintings by XRD, SEM-EDS, TGA and LIBS analysis. Mater Charact 60(4):303–311. https://doi.org/10.1016/j.matchar.2008.09.016

She Z, Yang M, Luo T, Feng X, Wei J, Hu X (2020) Lead release and species transformation of commercial minium pigments in aqueous phase under UV-irradiation. Chemosphere 128769:128769. https://doi.org/10.1016/j.chemosphere.2020.128769

Shi J-L, Li T (2013) Technical investigation of 15th and 19th century Chinese paper currencies: fiber use and pigment identification. J Raman Spectrosc 44(6):892–898. https://doi.org/10.1002/jrs.4297

Shortland AJ (2002) The use and origin of antimonate colorants in Early Egyptian glass. Archaeometry 44(4):517–530. https://doi.org/10.1111/1475-4754.t01-1-00083

Siidra OI, Krivovichev SV, Chukanov NV, Pekov IV, Magganas A, Katerinopoulos A, Voudouris P (2011) The crystal structure of $Pb_5(As^{3+}O_3)Cl_7$ from the historic slags of Lavrion, Greece – a novel Pb(II) chloride arsenite. Mineral Mag 75(2):337–345. https://doi.org/10.1180/minmag.2011.075.2.337

Siidra OI, Jonsson E, Chukanov NV, Nekrasova DO, Pekov IV, Depmeier W, Polekhovsky YS, Yapaskurt VO (2018a) Grootfonteinite, $Pb_3O(CO_3)_2$, a new mineral species from the Kombat mine, Namibia, merotypically related to hydrocerussite. Eur J Mineral 30(2):367–373. https://doi.org/10.1127/ejm/2018/0030-2723

Siidra O, Nekrasova D, Depmeier W, Chukanov N, Zaitsev A, Turner R (2018b) Hydrocerussite-related minerals and materials: structural principles, chemical variations and infrared spectroscopy. Acta Crystallogr Sect B: Struct Sci Cryst Eng Mater 74:182–195. https://doi.org/10.1107/S2052520618000768

Siidra OI, Nekrasova DO, Turner R, Zaitsev AN, Chukanov NV, Polekhovsky YS, Spratt J, Rumsey MS (2018c) Somersetite, $Pb_8O(OH)_4(CO_3)_5$, a new complex hydrocerussite-related mineral from the Mendip Hills, England. Mineral Mag 82(5):1211–1224. https://doi.org/10.1180/minmag.2017.081.087

Siidra OI, Nekrasova DO, Chukanov NV, Pekov IV, Yapaskurt VO, Katerinopoulos A, Voudouris P, Magganas A, Zaitsev AN (2018d) The hydrocerussite-related phase, $NaPb_5(CO_3)_4(OH)_3$, from the ancient slags of Lavrion, Greece. Mineral Mag 82(4):809–819. https://doi.org/10.1180/minmag.2017.081.058

Simoen J, De Meyer S, Vanmeert F, de Keyser N, Avranovich E, Van der Snickt G, Van Loon A, Keune K, Janssens K (2019) Combined micro- and macro scale X-ray powder diffraction mapping of degraded orpiment paint in a 17th century still life painting by Martinus Nellius. Heritage Science 7(1):83. https://doi.org/10.1186/s40494-019-0324-4

Smieska LM, Twilley J, Woll AR, Schafer M, MarcereauDeGalan A (2019)Energy-optimized synchrotron XRF mapping of an obscured painting beneath Exit from the Theater, attributed to Honoré Daumier. Microchem J 146:679–691. https://doi.org/10.1016/j.microc.2019.01.058

Smith DC, Barbet A (1999) A preliminary Raman microscopic exploration of pigments in wall paintings in the Roman Tomb discovered at Kertch, Ukraine, in 1891. J Raman Spectrosc 30(4):319–324. https://doi.org/10.1002/(SICI)1097-4555(199904)30:4<319::AID-JRS380>3.0.CO;2-X

Smith GD, Burgio L, Firth S, Clark RJH (2001) Laser-induced degradation of lead pigments with reference toBotticelli'sTrionfod'Amore. Anal Chim Acta 440:185–188. https://doi.org/10.1016/S0003-2670(01)01053-4

Smith GD, Clark RJH (2002a) Note on lead(II) oxide in mediaeval frescoes from the monastery of San Baudelio, Spain. Appl Spectrosc 56(6):804–806. https://doi.org/10.1366/000370202760077577

Smith GD, Clark RJH (2002b) The role of H2S in pigment blackening. J Cult Herit 3(2):101–105. https://doi.org/10.1016/S1296-2074(02)01173-1

Smith GD, Clark RJH (2004) Raman microscopy in archaeological science. J Archaeol Sci 31(8):1137–1160. https://doi.org/10.1016/j.jas.2004.02.008

Smith GD, Derbyshire A, Clark RJH (2002) In situ spectroscopic detection of lead sulphide on a blackened manuscript illumination by Raman microscopy. Stud Conserv 47(4):250–256. https://doi.org/10.1179/sic.2002.47.4.250

Sneyers R, Thissen J (1958) La Justice d'Othon de Thierry Bouts:examen de laboratoire. Bulletin Institut Royal du Patrimoine Artistique/Koninklijk Instituut voor het Kunstpatrimonium 1:49–55

Söderquist R, Dickens B (1967) Studies in solid state chemistry—I.: on a solid-state mechanism for the polymorphic transformation of orthorhombic to tetragonal PbO. J Phys Chem Solids 28(5):823–826. https://doi.org/10.1016/0022-3697(67)90011-X

Sodo A, Tortora L, Biocca P, Casanova Municchia A, Fiorin E, Ricci MA (2019) Raman and time of flight secondary ion mass spectrometry investigation answers specific conservation questions on Bosch painting Saint Wilgefortis Triptych. J Raman Spectrosc 50(2):150–160. https://doi.org/10.1002/jrs.5479

Sotiropoulou S, Perdikatsis V, Apostolaki C, Karydas AG, Devetzi A, Birtacha K (2010) Lead pigments and related tools at Akrotiri, Thera, Greece. Provenance and application techniques. J Archaeol Sci 37(8):1830–1840. https://doi.org/10.1016/j.jas.2010.02.001

Spahr D, Stekiel M, Zimmer D, Bayarjargal L, Bunk K, Morgenroth W, Milman V, Refson K, Jochym D, Byrneeand PJP, Winkler B (2020) Pressure-induced Pb–Pb bonding and phase transition in Pb2SnO4. Acta Crystallographica Section B: Structural Science, Crystal engineering and materials 76:979–991. https://doi.org/10.1107/S205252062001238X

Spencer, L.J., Mountain, E.D. (1926) Schulténite, a new mineral, from South-West Africa. Mineral Mag J Mineral Soc 21(115): 149-155. https://doi.org/10.1180/minmag.1926.021.115.02

Spennemann DHR (2020) Stanislas Sorel's zinc-based paints. Trans Inst Met Finish 98(1):8–13. https://doi.org/10.1080/00202967.2020.1698858

Spring M (2007) Raphael's materials: some new discoveries and their context within early sixteenth-century painting. In: Roy, A., Spring, M. (Eds.) Raphael's painting technique: working practices before Rome. Proceedings of the Eu-ARTECH workshop (National Gallery, London, November 11th 200). Quaderni di Kermes, 4. Florence: Nardini, pp. 77-86.

Stamboliyska B, Tapanov S, Velcheva E, Yancheva D, Rogozherov M, Glavcheva Z, Lalev G, Dimitrov M (2021) The altar wall paintings of the catholicon "The Nativity of the Virgin", Rila Monastery, Bulgaria: identification of the painting materials by means of vibrational spectroscopic techniques complemented by EDX, XRD and TGA analysis. Spectrochimica Acta - Part A 247:119087. https://doi.org/10.1016/j.saa.2020.119087

Stanley CJ, Jones GC, Hart AD, Keller P, Lloyd D (1991) Barstowite, $3PbCl_2.PbCO_3.H_2O$, a new mineral from Bounds Cliff, St Endellion, Cornwall. Mineral Mag 55(378):121–125. https://doi.org/10.1180/minmag.1991.055.378.10

Stanzani E, Bersani D, Lottici PP, Colomban P (2016) Analysis of artist's palette on a 16th century wood panel painting by portable and laboratory Raman instruments. Vib Spectrosc 85:62–70. https://doi.org/10.1016/j.vibspec.2016.03.027

Steele IM, Pluth JJ, Livingstone A (1998) Crystal structure of macphersonite $(Pb_4SO_4(CO_3)_2(OH)_2)$: comparison with leadhillite. Mineral Mag 62(4):451–459. https://doi.org/10.1180/002646198547828

Steele IM, Pluth JJ, Livingstone A (1999) Crystal structure of susannite, $Pb_4SO_4(CO_3)_2(OH)_2$: a trimorph with macphersonite and leadhillite. Eur J Mineral 11(3):493–499. https://doi.org/10.1127/ejm/11/3/0493

Stols-Witlox M (2011) The heaviest and the whitest": lead white quality in north western European documentary sources, 1400-1900. In: Stols-Witlox, M. (Eds.) Studying old master paintings: technology and practice. London: Archetype Publications, pp. 284-294.

Stols-Witlox M, Megens L, Carlyle L (2012) 'To prepare white excellent...': reconstructions investigating the influence of washing, grinding and decanting of stack-process lead white on pigment composition and particle size. In: Eyb-Green, S., Townsend, J.H., Clarke, M., Nadolny, J., Kroustallis, S. (Eds.) The artist's process: technology and interpretation. 4th symposium of the Art Technological Source Research Working Group (Vienna, Austria, 2010). London: Archetype, pp. 112-129.

Stols-Witlox MJN (2014) Historical recipes for preparatory layers for oil paintings in manuals, manuscripts and handbooks in North West Europe, 1550-1900: analysis and reconstructions. PhD thesis-

Faculty of Humanities - Amsterdam School of Historical Studies, The Netherlands, pp. 413.
Švarcová S, Kočí E, Plocek J, Zhankina A, Hradilová J, Bezdička P (2019) Saponification in egg yolk-based tempera paintings with lead-tin yellow type I. J Cult Herit 38:8–19. https://doi.org/10.1016/j.culher.2018.12.004
Švarcová S, Kočí E, Bezdička P, Garrappa S, Kobera L, Plocek J, Brus J, Šťastný M, Hradil D (2020) Uncovering lead formate crystallization in oil-based paintings. Dalton Trans 49(16):5044–5054. https://doi.org/10.1039/d0dt00327a
Švarcová S, Hradil D, Hradilová J, Čermáková Z (2021) Pigments – copper-based greens and blues. Archaeol Anthropol Sci. https://doi.org/10.1007/s12520-021-01406-0
Swanson HE, McMurdie HF, Morris MC, Evans EH, Paretzkin B (1972) Standard X-ray diffraction powder patterns - Section 10-Data for 84 substances. National Bureau of Standards, 25
Symes RF, Embrey PG (1977) Mendipite and other rare oxychloride minerals from the Mendip Hills, Somerset, England. Mineral Rec 8:298–303
Taggart JE, Foord EE, Rosenzweig A, Hanson T (1988) Scrutinyite, natural occurrences of alpha PbO_2 from Bingham, New Mexico, USA, and Mapimi, Mexico. Can Mineral 26:905–910
Tapsoba I, Arbault S, Walter P, Amatore C (2010) Finding out Egyptian Gods' secret using analytical chemistry: biomedical properties of Egyptian black makeup revealed by amperometry at single cells. Anal Chem 82(2):457–460. https://doi.org/10.1021/ac902348g
Tarquini O, Pronti L, Lorenzetti EG, Felici AC (2020) Pigment identification on Campana reliefs from the Palatine Hill and Colosseum Valley in Rome. J Cult Herit 43:294–302. https://doi.org/10.1016/j.culher.2019.07.026
Tascon M, Mastrangelo N, Gallegos D, Marte F (2017) Determination of materials and techniques involved in the mural paintings of San Miguel Church, Argentina. J Raman Spectrosc 48(10):1356–1364. https://doi.org/10.1002/jrs.5223
Taylor P, Lopata VJ (1984) Stability and solubility relationships between some solids in the system PbO–CO_2–H_2O. Can J Chem 62:395–402. https://doi.org/10.1139/v84-070
Temple AK (1956) The Leadhills-Wanlockhead lead and zinc deposits. Trans R Soc Edinburgh 63(01):85–113. https://doi.org/10.1017/s0080456800003021
Thiéry V (2014) Characterization of fibrous mimetite. Microsc Microanal 20(02):596–601. https://doi.org/10.1017/s143192761301413x
Thompson DV (1971)*The materials and techniques of medieval painting*. Dover Publications Inc., New York, p 256
Tissot RG, Rodriguez MA, Sipola DL, Voigt JA (2001)X-ray powder diffraction study of synthetic palmierite, $K_2Pb(SO_4)_2$. Powder Diffract 16:92–97
Tite MS, Freestone IC, Mason R, Molera J, Vendrell-Saz M, Wood N (1998) Lead glazes in Antiquity - methods of production and reasons for use. Archaeometry 40(2):241–260. https://doi.org/10.1111/j.1475-4754.1998.tb00836.x
Tite M, Pradell T, Shortland A (2008) Discovery, production and use of tin-based opacifiers in glasses, enamels and glazes from the Late Iron Age onwards: a reassessment. Archaeometry 50(1):67–84
Toniolo L, Colombo C, Bruni S, Fermo P, Casoli A, Palla G, Bianchi CL (1998) Gilded stuccoes of the Italian baroque. Studies in Conservation 43(4):201–208. https://doi.org/10.1179/sic.1998.43.4.201
Trinquier G, Hoffmann R (1984) Lead monoxide. Electronic structure and bonding. J Phys Chem 88(26):6696–6711. https://doi.org/10.1021/j150670a038
Trinquier J (2013) Cinnabaris et «sang-dragon»: Le «cinabre» des Anciens entre minéral, végétal et animal. Revue Archeologique 56(2):305–346. https://doi.org/10.3917/arch.132.0305
Trotter J, Barnes WH (1958) The structure of vanadinite. Can Mineral 6:161–173
Turner R (2006) A mechanism for the formation of the mineralized Mn deposits at Merehead Quarry, Cranmore, Somerset, England. Mineral Mag 70(6):629–653. https://doi.org/10.1180/0026461067060359
Turner WES, Rooksby HP (1959) A study of the opalising agents in ancient opal glasses throughout 3400 years: Part I. Glastechnische Berichte 32K(VII):17–28
Turner WES, Rooksby HP (1963) A study of the opalising agents in ancient opal glasses throughout 3400 years: part II. In: Matson FR, Rindone GE (eds) Proceedings of the 6th International Congress of Glass. Advances in glass technology (Washington, D.C., U.S.A., July 8-14, 1962). Plenum Press, New York, pp 17–28
Uchida E, Takubo Y, Toyouchi K, Miyata J (2012) Study on the pigments in the cruciform gallery of angkor wat, Cambodia. Archaeometry 54(3):549–564. https://doi.org/10.1111/j.1475-4754.2011.00634.x
Uhlir K, Gironda M, Bombelli L, Eder M, Aresi N, Groschner G, Griesser M (2019) Rembrandt's Old Woman Praying, 1629/30: a look below the surface using X-ray fluorescence mapping. X-Ray Spectrom 48(4):293–302. https://doi.org/10.1002/xrs.2985
Vagnini M, Vivani R, Sgamellotti A, Miliani C (2020) Blackening of lead white: study of model paintings. J Raman Spectrosc 51(7):1118–1126. https://doi.org/10.1002/jrs.5879
Valeur B (2010) La chimie crée sa couleur… sur la palette du peintre. In: Dinh-Audouin MT, Jacquesy RA, Olivier D, Rigny P (eds) La Chimie et l'Art. EDP Sciences, Les Ulis, pp 129–168
van den Brink OF, Ferreira ES, van der Horst J, Boon JJ (2009) A direct temperature-resolved tandem mass spectrometry study of cholesterol oxidation products in light-aged egg tempera paints with examples from works of art. Int J Mass Spectrom 284(1-3):12–21. https://doi.org/10.1016/j.ijms.2008.11.005
Van der Graaf JA (1961) Betekenis en toepassing van "lootwit" en "schelpwit" in de xviie eeuwse nederlandse schilderkunst. Bulletin de l'Institut Royal du Patrimoine Artistique 4:198–201
Van Der Snickt G, Janssens K, Dik J, De Nolf W, Vanmeert F, Jaroszewicz J, Cotte M, Falkenberg G, Van Der Loeff L (2012) Combined use of synchrotron radiation based micro-X-ray fluorescence, micro-X-ray diffraction, micro-X-ray absorption near-edge, and micro-Fourier transform infrared spectroscopies for revealing an alternative degradation pathway of the pigment cadmium yellow in a painting by Van Gogh. Anal Chem 84(23):10221–10228. https://doi.org/10.1021/ac3015627
van der Weerd J, Boon JJ, Geldof M, Heeren RMA, Noble P (2002) Chemical changes in old master paintings: dissolution, metal soap formation and remineralisation processes in lead pigmented paint layers of 17th century paintings. In: Vontobel, R. (Ed.) 13th triennial meeting : ICOM committee for conservation. (Rio de Janeiro 22-27 September 2002). James & James, pp. 36-51.
Van der Weerd J, van Loon A, Boon JJ (2005) FTIR studies of the effects of pigments on the aging of oil. Stud Conserv 50(1):3–22. https://doi.org/10.2307/25487713
van Loon A, Vandivere A, Delaney JK, Dooley KA, De Meyer S, Vanmeert F, Gonzalez V, Janssens K, Leonhardt E, Haswell R, de Groot S, D'Imporzano P, Davies GR (2019) Beauty is skin deep: the skin tones of Vermeer's Girl with a Pearl Earring. Heritage Science 7(1):102. https://doi.org/10.1186/s40494-019-0344-0
Vanmeert F, Van der Snickt G, Janssens K (2015) Plumbonacrite identified by X-ray powder diffraction tomography as a missing link during degradation of red lead in a Van Gogh painting. Angew Chem Int Ed 54(12):3607–3610. https://doi.org/10.1002/anie.201411691
Vanmeert F, De Nolf W, Dik J, Janssens K (2018) Macroscopic X-ray powder diffraction scanning: possibilities for quantitative and depth-selective parchment analysis. Anal Chem 90(11):6445–6452. https://doi.org/10.1021/acs.analchem.8b00241
Vanmeert F, De Keyser N, Van Loon A, Klaassen L, Noble P, Janssens K (2019) Transmission and reflection mode macroscopic X-ray powder

diffraction imaging for the noninvasive visualization of paint degradation in still life paintings by Jan Davidsz de Heem. Anal Chem 91(11):7153–7161. https://doi.org/10.1021/acs.analchem.9b00328

Venetopoulos CC, Rentzeperis PJ (1975) The crystal structure of laurionite, Pb(OH)Cl. Z Krist 141:246–259. https://doi.org/10.1524/zkri.1975.141.16.246

Vidale M, Salviulo G, Zorzi F, Mocchiutti I (2016) Cosmetics and cosmetology at Shahr-I Sokhta. Iran 54(2):1–24. https://doi.org/10.1080/05786967.2016.11879211

Vigouroux JP, Husson E, Calvarin G, Dao NQ (1982) Etude par spectroscopié vibrationnelle des oxydes Pb_3O_4, $SnPb_2O_4$ et $SnPb(Pb_2O_4)_2$. Spectrochim Acta A Mol Biomol Spectrosc 38(4):393–398. https://doi.org/10.1016/0584-8539(82)80013-5

Vitti P (2021) Mortars and masonry - structural lime and gypsum mortars in Antiquity and Middle Ages. Archaeol Anthropol Sci https://doi.org/10.1007/s12520-021-01408-y

Vlachou-Mogire C, Moretti P, Monico L, Chieli A, Iwanicka M, Targowski P, Detalle V, Bourguignon E, Laclavetine K, Mirambet F, Tong T, Pinchin S (2020) A non-invasive multi-technique investigation of Banqueting House Whitehall Rubens ceiling paintings. Microchem J 156:104797. https://doi.org/10.1016/j.microc.2020.104797

von Kobell WF (1838) Grundzüge der Mineralogie. Vanadinit. Johann Leonhard Schrag Nurnberg, pp. 283

Wagner B, Kępa L, Donten M, Wrzosek B, Żukowska GZ, Lewandowska A (2019) Laser ablation inductively coupled plasma mass spectrometry appointed to subserve pigment identification. Microchem J 146:279–285. https://doi.org/10.1016/j.microc.2018.12.061

Wainwright INM, Taylor JM, Harley RD (1986) Lead antimonate yellow. In: Feller RL (ed) Artists' Pigments'. A Handbook of their History and Characteristics, vol 1. Natural Gallery of Art Washington & Archetype Publications, London, pp 219–254

Walter P, Martinetto P, Tsoucaris G, Bréniaux R, Lefebvre MA, Richard G, Talabot J, Dooryhée E (1999) Making make-up in Ancient Egypt. Nature 397(6719):483–484. https://doi.org/10.1038/17240

Walter P, Martinetto P, Tsoucaris G, Lévêque JL (2003) Les formulations cosmétiques a` base de plomb. Memnonia, Cahier supplementaire, Le Caire 1:123–132

Walton MS, Trentelman K (2009)Romano-Egyptian red lead pigment: a subsidiary commodity of Spanish silver mining and refinement. Archaeometry 51(5):845–860. https://doi.org/10.1111/j.1475-4754.2008.00440.x

Wang X, Wang C, Yang J, Chen L, Feng J, Shi M (2004) Study of wall-painting pigments from Feng Hui Tomb by Raman spectroscopy and high-resolution electron microscopy. J Raman Spectrosc 35(4):274–278. https://doi.org/10.1002/jrs.1147

Wang B, Su Y, Tian L, Peng S, Ji R (2020a) Heavy metals in face paints: assessment of the health risks to Chinese opera actors. Sci Total Environ 724:138163. https://doi.org/10.1016/j.scitotenv.2020.138163

Wang X, Zhen G, Hao X, Tong T, Ni F, Wang Z, Jia J, Li L, Tong H (2020b) Spectroscopic investigation and comprehensive analysis of the polychrome clay sculpture of Hua Yan Temple of the Liao Dynasty. Spectrochim Acta A Mol Biomol Spectrosc 240:118574. https://doi.org/10.1016/j.saa.2020.118574

Weast RC (1998) CRC handbook of chemistry and physics. CRC Press, Boca Raton, FL

Wei S, Schreiner M, Guo H, Ma Q (2010) Scientific investigation of the materials in a Chinese ming dynasty wall painting. Int J Conserv Sci 1(2):99–112

Welcomme E, Walter P, Van Elslande E, Tsoucaris G (2006) Investigation of white pigments used as make-up during the Greco-Roman period. Appl Phys A Mater Sci Process 83(4):551–556. https://doi.org/10.1007/s00339-006-3559-3

Wertz JH, Quye A, France D (2019) Turkey red prints: identification of lead chromate, Prussian blue and logwood on Turkey red calico. Conservar Patrimonio 31:31–39. https://doi.org/10.14568/cp2018019

West FitzHugh E (1986) Red lead and minium. In: Feller RL (ed) Artists' Pigments'. A Handbook of their History and Characteristics, vol 1. Natural Gallery of Art Washington & Archetype Publications, London, pp 109–139

White WB, Dachille F, Roy R (1961) High-pressure-high-temperature polymorphism of the oxides of lead. J Am Ceram Soc 44(4):170–174. https://doi.org/10.1111/j.1151-2916.1961.tb13739.x

White JS (1970) New data on plattnerite. Mineral Rec 1(2):75–80

Williams SA (1974) The natural occurring chromates of lead. Bulletin of British Museum (Natural History). Mineralogy 2(8):379–419. https://archive.org/details/bulletinofbritis28brit/page/380/mode/2up. Accessed 18.01.2021

Williams SA, McLean WJ, Anthony JW (1970) A study of phoenicochroite—its structure and properties. Am Mineral 55(5-6):784–792

Williams PA, Hatert F, Pasero M, Mills SJ (2012) IMA Commission on New Minerals, Nomenclature and Classification (CNMNC)-Newsletter 14 - New minerals and nomenclature modifications approved in 2012. Mineral Mag 76(5):1281–1288. https://doi.org/10.1180/minmag.2012.076.5.15

Wilson CC (1994) Structural studies of schultenite in the temperature range 125–324 K by pulsed single crystal neutron diffraction — hydrogen ordering and structural distortions. Mineral Mag 58(393):629–634. https://doi.org/10.1017/minmag.1994.058.393.12

Wilson CC, Cox PJ, Stewart NS (1991) Structure and disorder in schultenite, lead hydrogen arsenate. J Crystallogr Spectrosc Res 21(5):589–593. https://doi.org/10.1007/BF01161081

Winter J (1981) "Lead white" in Japanese paintings. Stud Conserv 26(3):89–101. https://doi.org/10.1179/sic.1981.26.3.89

Wu M, Li X, Shen G, He D, Huang A, Luo Y, Feng S, Xu R (1999) Hydrothermal synthesis of Pb_2SnO_4. Mater Res Bull 34(7):1135–1142. https://doi.org/10.1016/S0025-5408(99)00100-2

Wyckoff RWG (1963) Crystal Structures 1, second edn. Interscience Publishers, New York

Yamasaki K (1967) Pigments employed in old paintings of Japan. In: Levey M (ed) Archaeological Chemistry. University of Pennsylvania Press, Philadelphia, pp 347–368

Ye Y, Smyth JR, Boni P (2012) Crystal structure and thermal expansion of aragonite-group carbonates by single-crystal X-ray diffraction. Am Mineral 97:707–712. https://doi.org/10.2138/am.2012.3923

Yuryeva TV, Morozova EA, Kadikova IF, Uvarov OV, Afanasyev IB, Yapryntsev AD, Lukashova MV, Malykhin SA, Grigorieva IA, Yuryev VA (2018) Microcrystals of antimony compounds in lead-potassium and lead glass and their effect on glass corrosion: a study of historical glass beads using electron microscopy. J Mater Sci 53(15):10692–10717. https://doi.org/10.1007/s10853-018-2332-2

Zaslavskii AI, Tolkachev SS (1952) The structure of the α-modification of lead dioxide. Zhurnal Fizicheskoi Khimii 26:743–452 (Russian)

Zaslavskii AI, Kondrashev YD, Tolkachev SS (1950) The new modification of lead dioxide and the texture of anode sediments. Dokl Akad Nauk SSSR 75:559–561 (in Russian)

Želinska J, Kopecka I, Svobodova E, Milovska S, Hurai V (2018) Stratigraphic EM-EDS, XRF, Raman and FT-IR analysis of multilayer paintings from the main Altar of the St. James Church in Levoča (Slovakia). J Cult Herit 33:90–99. https://doi.org/10.1016/j.culher.2018.03.006

Zha L, Li H, Wang N (2020) Electrochemical study of galena weathering in NaCl solution: kinetics and environmental implications. Minerals 10:416. https://doi.org/10.3390/min10050416

Zhao F, Sun M, Tie F, Wu C, Zhang X, Mu X (2020) Inlaid materials and techniques of an ancient Chinese bronze mirror. Eur Phys J Plus 135(8):666. https://doi.org/10.1140/epjp/s13360-020-00634-y

Zheng Y-F, Böttcher ME (2016) Oxygen isotope fractionation in double carbonates. Isot Environ Health Stud 52(1-2):29–46. https://doi.org/10.1080/10256016.2014.977278

Zhou Y, Lin H, Gu Q, Long J, Wang X (2012) Visible light-induced highly efficient organic pollutant degradation and concomitant CO_2 fixation using red lead. RSC Adv 2:12624–12627. https://doi.org/10.1039/c2ra21660d

Zhou Z, Shen L, Wang N, Ren X, Yang J, Shi Y, Zhang H (2020) Identification of organic materials used in gilding technique in wall paintings of Kizil Grottoes. Chemistry Select 5(2):818–822. https://doi.org/10.1002/slct.201903688

Zyryanov VV, Gusev AA (2001) Mechanochemical reactions in mixtures of lead oxides. Inorg Mater 37(3):257–263. https://doi.org/10.1023/A:1004117414763

WEB PAGES:

International Mineralogical Association (2020) List of Minerals. http://cnmnc.main.jp/. Accessed 31st of December 2020

WebMineral data base (n.d.) http://webmineral.com/

Supplementary materials

Gliozzo, E., Ionescu, C. (2021) *Pigments – Lead-based whites, reds, yellows and oranges and their alteration phases*. Archaeological and Anthropological Sciences

APPENDIX 1. List of consulted papers where lead-based pigments are found or mentioned (parallel or supplementary to the list of references provided in the text).

APPENDIX 2. Excerpts from Jussen, E. (September 1887) *White-lead industry in Austria*. *Reports from the Consuls of the United States*, 83. Washington: Government Printing Office, pp. 413-419

TABLE S1. DMS coordinates (Google maps, MinDat[1], Wiki GeoTemplate[2]) of the localities and places mentioned in the text

TABLE S2. Texts quoted in Table 1 provided in the original language.

TABLE S3. Minerals and pigments occurring in paintings along with lead-based compounds (names as literally reported by Authors) […]

APPENDIX 1. LIST OF CONSULTED PAPERS WHERE LEAD-BASED PIGMENTS ARE FOUND OR MENTIONED (PARALLEL OR SUPPLEMENTARY TO THE LIST OF REFERENCES PROVIDED IN THE TEXT).

Abdallah et al. 2020	Abdallah, M., Abdrabou, A., Kamal, H.M. (2020) Multiscientific analytical approach of polychrome greco-roman palette applied on a wooden model naos: Case study. *Mediterranean Archaeology and Archaeometry* **20**(2): 45-65. DOI: 10.5281/zenodo.3746942
Abdel-Maksoud et al. 2020	Abdel-Maksoud, G., Ibrahim, M., Issa, Y.M., Magdy, M. (2020) Investigation of painting technique of Coptic icon by integrated analytical methods: imaging, spectroscopic and chemometric methods. *Journal of Archaeological Science: Reports* **29**: 102085. DOI: 10.1016/j.jasrep.2019.102085
Aceto et al. 2008	Aceto, M., Agostino, A., Boccaleri, E., Garlanda, A.C. (2008) The Vercelli gospels laid open: An investigation into the inks used to write the oldest Gospels in Latin. *X-Ray Spectrometry* **37**(4): 286-292. DOI: 10.1002/xrs.1047
Aceto et al. 2012	Aceto, M., Agostino, A., Fenoglio, G., Baraldi, P., Zannini, P., Hofmann, C., Gamillscheg, E. (2012) First analytical evidences of precious colourants on Mediterranean illuminated manuscripts. *Spectrochimica Acta - Part A: Molecular and Biomolecular Spectroscopy* **95**: 235-245. DOI: 10.1016/j.saa.2012.04.103
Akyuz et al. 2015	Akyuz, T., Akyuz, S., Gulec, A. (2015) Elemental and spectroscopic characterization of plasters from Fatih Mosque-Istanbul (Turkey) by combined micro-Raman, FTIR and EDXRF techniques. *Spectrochimica Acta - Part A: Molecular and Biomolecular Spectroscopy* **149**: 744-750. DOI: 10.1016/j.saa.2015.05.015
Albertson et al. 2019	Albertson, G., Krekeler, A., van Loon, A., Gaibor, A.P., Noble, P. (2019) The blues of Jan de Bray's Judith and Holofernes: A technical study of two blue pigments and its impact on treatment. *Journal of the American Institute for Conservation* **58**(4): 217-232. DOI: 10.1080/01971360.2019.1643628
Aliatis et al. 2010	Aliatis, I., Bersani, D., Campani, E., Casoli, A., Lottici, P.P., Mantovan, S., Marino, I.-G. (2010) Pigments used in Roman wall paintings in the Vesuvian area. *Journal of Raman Spectroscopy* **41**(11): 1537-1542. DOI: 10.1002/jrs.2701

[1] https://www.mindat.org/; accessed January-February 2021
[2] https://en.wikipedia.org/wiki/Template:GeoTemplate; accessed January-February 2021

Aliatis et al. 2012 — Aliatis, I., Bersani, D., Lottici, P.P., Marino, I.G. (2012) Raman analysis on 18th century painted wooden statues. *ArcheoSciences* **36**: 7-13. DOI: 10.4000/archeosciences.3806

Almaviva et al. 2018 — Almaviva, S., Fantoni, R., Colao, F., Puiu, A., Bisconti, F., Fiocchi Nicolai, V., Romani, M., Cascioli, S., Bellagamba, S. (2018) LIF/Raman/XRF non-invasive microanalysis of frescoes from St. Alexander catacombs in Rome. Spectrochimica Acta - Part A: Molecular and Biomolecular Spectroscopy 201(1): 207-215. DOI: 10.1016/j.saa.2018.04.062

Amadori et al. 2013 — Amadori, M.L., Barcelli, S., Casoli, A., Mazzeo, R., Prati, S. (2013) A scientific approach to the characterization of the painting materials of Fra Mattia della Robbia polychrome terracotta altarpiece. *Applied Physics A: Materials Science and Processing* **113**(4): 1055-1064. DOI: 10.1007/s00339-013-7748-6

Amadori et al. 2016 — Amadori, M.L., Poldi, G., Barcelli, S., Baraldi, P., Berzioli, M., Casoli, A., Marras, S., Pojana, G., Villa, G.C.F. (2016) Lorenzo Lotto's painting materials: An integrated diagnostic approach. Spectrochimica Acta - Part A: Molecular and Biomolecular Spectroscopy 164: 110-122. DOI: 10.1016/j.saa.2016.02.043

Andalo et al. 2001 — Andalo, C., Bicchieri, M., Bocchini, P., Casu, G., Galletti, G.C., Mando, P.A., Nardone, M., Sodo, A., Zappalà, MP. (2001) The beautiful "Trionfo d'Amore" attributed to Botticelli: a chemical characterisation by proton-induced X-ray emission and micro-Raman spectroscopy. Analytica Chimica Acta 429(2): 279-286. DOI: 10.1016/S0003-2670(00)01292-7

Arjonilla et al. 2016 — Arjonilla, P., Domínguez-Vidal, A., de la Torre López, M.J., Rubio-Domene, R., Ayora-Cañada, M.J. (2016) In situ Raman spectroscopic study of marble capitals in the Alhambra monumental ensemble. Applied Physics A: Materials Science and Processing 122(12): 1014. DOI: 10.1007/s00339-016-0537-2

Arjonilla et al. 2019 — Arjonilla, P., Domínguez-Vidal, A., Correa-Gómez, E., Domene-Ruiz, M.J., Ayora-Cañada, M.J. (2019) Raman and Fourier transform infrared microspectroscopies reveal medieval Hispano–Muslim wood painting techniques and provide new insights into red lead production technology. Journal of Raman Spectroscopy 50(10): 1537-1545. DOI: 10.1002/jrs.5660

Arjonilla et al. 2019 — Arjonilla, P., Ayora-Cañada, M.J., Rubio Domene, R., Correa Gómez, E., de la Torre-López, M.J., Domínguez-Vidal, A. (2019) Romantic restorations in the Alhambra monument: Spectroscopic characterization of decorative plasterwork in the Royal Baths of Comares. Journal of Raman Spectroscopy 50(2): 184-192. DOI: 10.1002/jrs.5422

Arrizabalaga et al. 2014 — Arrizabalaga, I., Gómez-Laserna, O., Aramendia, J., Arana, G., Madariaga, J.M. (2014) Determination of the pigments present in a wallpaper of the middle nineteenth century: The combination of mid-diffuse reflectance and far infrared spectroscopies. Spectrochimica Acta - Part A: Molecular and Biomolecular Spectroscopy 124: 308-314. DOI: 10.1016/j.saa.2014.01.017

Aurélie et al. 2016 — Aurélie, M., Charlotte, D., Floréal, D. (2016) Material identification of three French medieval illuminations of the XVIth century by hyperspectral imaging (Treasury of Bordeaux Cathedral, France). *Color Research and Application* **41**(3): 302-307. DOI: 10.1002/col.22042

Avlonitou 2016 — Avlonitou, L. (2016) Pigments and colours: An inside look at the painted decoration of the Macedonian funerary monuments. *Journal of Archaeological Science: Reports* **7**: 668-678. DOI: 10.1016/j.jasrep.2016.03.017

Badillo-Sanchez and Baumann 2016 — Badillo-Sanchez, D., Baumann, W. (2016) Comparative palette characterization of oil-on-canvas paintings of two well-known 19th-century Colombian artists by confocal Raman spectroscopy. *Journal of Raman Spectroscopy* **47**(12): 1540-1547. DOI: 10.1002/jrs.5065

Bagdzevičiene et al. 2009 — Bagdzevičiene, J., Tautkus, S., Senvaitiene, J., Lukšeniene, J. (2009) Investigation of the technique of painting on a tin alloy plate. *Chemija* **20**(2): 93-100.

Barone et al. 2016 — Barone, G., Bersani, D., Coccato, A., Lauwers, D., Mazzoleni, P., Raneri, S., Vandenabeele, P., Manzini, D., Agostino, G., Neri, N.F. (2016) Nondestructive Raman investigation on wall paintings at Sala Vaccarini in Catania (Sicily). *Applied Physics A: Materials Science and Processing* **122**(9): 838. DOI: 10.1007/s00339-016-0370-7

Béarat 1996 — Béarat, H. (1996) Chemical and mineralogical analyses of Gallo-Roman wall painting from Dietikon, Switzerland. *Archaeometry* **38**(1): 81-95. DOI: 10.1111/j.1475-4754.1996.tb00762.x

Blasco-López et al. 2016 — Blasco-López, F.J., Alejandre, F.J., Flores-Alés, V., Cortés, I. (2016) Plasterwork in the Ambassadors Hall (Salón de Embajadores) of the Real Alcázar of Seville (Spain): Graphic reconstruction of polychrome work by layer characterization. Construction and Building Materials 107: 332-340. DOI: 10.1016/j.conbuildmat.2016.01.021

Bonizzoni et al. 2016 — Bonizzoni, L., Bruni, S., Galli, A., Gargano, M., Guglielmi, V., Ludwig, N., Lodi, L., Martini, M. (2016) Non-invasive in situ analytical techniques working in synergy: The application on graduals held in the Certosa di Pavia. *Microchemical Journal* **126**: 172-180. DOI: 10.1016/j.microc.2015.12.001

Bonizzoni et al. 2018 — Bonizzoni, L., Bruni, S., Gargano, M., Guglielmi, V., Zaffino, C., Pezzotta, A., Pilato, A., Auricchio, T., Delvaux, L., Ludwig, N. (2018) Use of integrated non-invasive analyses for pigment characterization and indirect dating of old restorations on one Egyptian coffin of the XXI dynasty. *Microchemical Journal* **138**: 122-131. DOI: 10.1016/j.microc.2018.01.002

Bösiger 2019 — Bösiger, P. (2019) Painted decorations on the Chinese and French lacquers of an eighteenth-century chest of drawers: when one runs over onto the other. Studies in Conservation 64(S1): 881-890. DOI: 10.1080/00393630.2018.1563743

Bracci et al. 2015 — Bracci, S., Caruso, O., Galeotti, M., Iannaccone, R., Magrini, D., Picchi, D., Pinna, D., Porcinai, S. (2015) Multidisciplinary approach for the study of an Egyptian coffin (late 22nd/early 25th dynasty): Combining imaging and spectroscopic techniques. *Spectrochimica Acta - Part A: Molecular and Biomolecular Spectroscopy* **145**: 511-522. DOI: 10.1016/j.saa.2015.02.052

Bratu et al. 2015 — Bratu, I., Marutoiu, C., Moldovan, Z., Marutoiu, V.C., Trosan, L., Pop, D.T., Sandu, I.C.A. (2015) Scientific investigation of the Saint Elijah's icon from Dragus Village, Brasov County for its preservation and restoration. Revista de Chimie 66(10): 1628-1631.

Bratu et al. 2016 — Bratu, I., Paduraru, M., Marutoiu, C., Pop, S.S.F., Kacso, I., Tanaselia, C., Marutoiu, O.F., Sandu, I.C.A. (2016) Multianalytical study on two wooden icons from the beginning of the eighteenth century evaluation of conservation state. *Revista de Chimie* **67**(11): 2383-2388

Bratu et al. 2017 — Bratu, I., Siluan, M., Măruţoiu, C., Kacso, I., Garabagiu, S., Măruţoiu, V.C., Tănăselia, C., Popescu, D., Postolache, D.L., Pop, D. (2017) Science applied for the investigation of Imperial Gate from eighteenth century wooden church of Nicula Monastery. Journal of Spectroscopy: 6167856. DOI: 10.1155/2017/6167856

Brocchieri et al. 2020 — Brocchieri, J., de Viguerie, L., Sabbarese, C., Boyer, M. (2020) Combination of noninvasive imaging techniques to characterize pigments in Buddhist thangka paintings. X-Ray Spectrometry: (in press). DOI: 10.1002/xrs.3189

Bruni et al. 1999 — Bruni, S., Cariati, F., Casadio, F., Toniolo, L. (1999) Identification of pigments on a XV century illuminated parchment by Raman and FTIR microspectroscopies. Spectrochimica Acta - Part A: Molecular and Biomolecular Spectroscopy 55(7-8): 1371-1377. DOI: 10.1016/S1386-1425(98)00300-X

Bruni et al. 2002 — Bruni, S., Cariati, F., Consolandi, L., Galli, A., Guglielmi, V., Ludwig, N., Milazzo, M. (2002) Field and laboratory spectroscopic methods for the identification of pigments in a northern Italian eleventh century fresco cycle. Applied Spectroscopy 56(7): 827-833. DOI: 10.1366/000370202760171482

Burgio et al. 1999 — Burgio, L., Clark, R.J.H., Gibbs, P.J. (1999) Pigment identification studies in situ of Javanese, Thai, Korean, Chinese and Uighur manuscripts by Raman microscopy. Journal of Raman Spectroscopy 30(3): 181-184. DOI: 10.1002/(SICI)1097-4555(199903)30:3<181::AID-JRS356>3.0.CO;2-8

Buscaglia et al. 2020 — Buscaglia, M.B., Halac, E.B., Reinoso, M., Marte, F. (2020) The palette of Pio Collivadino (1869–1945) throughout his career. Journal of Cultural Heritage 44: 27-37. DOI: 10.1016/j.culher.2020.02.012

Calà et al. 2019 — Calà, E., Agostino, A., Fenoglio, G., Capra, V., Porticelli, F., Manzari, F., Fiddyment, S., Aceto, M. (2019) The Messale Rosselli: Scientific investigation on an outstanding 14th century illuminated manuscript from Avignon. *Journal of Archaeological Science: Reports* **23**: 721-730. DOI: 10.1016/j.jasrep.2018.12.001

Campos-Suñol et al. 2009 — Campos-Suñol, M.J., De la torre-Lopez, M.J., Ayora-Cañada, M.J., Dominguez-Vidal, A. (2009) Analytical study of polychromy on exterior sculpted stone. *Journal of Raman Spectroscopy* **40**(12): 2104-2110. DOI: 10.1002/jrs.2379

Cardell et al. 2009 — Cardell, C., Rodriguez-Simon, L., Guerra, I., Sanchez-Navas, A. (2009) Analysis of Nasrid polychrome carpentry at the Hall of the Mexuar Palace, Alhambra complex (Granada, Spain), combining microscopic, chromatographic and spectroscopic methods. Archaeometry 51(4): 637-657. DOI: 10.1111/j.1475-4754.2008.00438.x

Cardell-Fernández and Navarrete-Aguilera 2006 — Cardell-Fernández, C., Navarrete-Aguilera, C. (2006) Pigment and plasterwork analyses of Nasrid polychromed Lacework stucco in the Alhambra (Granada, Spain). *Studies in Conservation* **51**(3): 161-176. DOI: 10.1179/sic.2006.51.3.161

Carter et al. 2016 — Carter, E.A., Perez, F.R., Garcia, J.M., Edwards, H.G.M. (2016) Raman spectroscopic analysis of an important Visigothic historiated manuscript. *Philosophical Transactions of the Royal Society A: Mathematical, Physical and Engineering Sciences* **374**(2082): 20160041. DOI: 10.1098/rsta.2016.0041

Carter et al. 2016 — Carter, E.A., Perez, F.R., Garcia, J.M., Edwards, H.G.M. (2016) Raman spectroscopic analysis of an important Visigothic historiated manuscript. *Philosophical Transactions of the Royal Society A: Mathematical, Physical and Engineering Sciences* **374**(2082): 20160041. DOI: 10.1098/rsta.2016.0041

Carvalho et al. 2018 Carvalho, I., Casanova, C., Araújo, R., Lemos, A. (2018) Colour identification, degradation processes and findings in a fifteenth-century Book of Hours: the case study of Cofre n.º 31 from Mafra National Palace. Heritage Science 6(1): 9. DOI: 10.1186/s40494-018-0174-5

Castro et al. 2004 Castro, K., Pérez-Alonso, M., Rodríguez-Laso, M.D., Madariaga, J.M. (2004) Pigment analysis of a wallpaper from the early 19th century: les Monuments de Paris. Journal of Raman Spectroscopy 35(8-9): 704-709. DOI: 10.1002/jrs.1132

Castro et al. 2004 Castro, K., Pérez-Alonso, M., Rodríguez-Laso, M.D., Madariaga, J.M. (2004) Raman fibre optic approach to artwork dating. Spectrochimica Acta - Part A: Molecular and Biomolecular Spectroscopy 60(12): 2919-2924. DOI: 10.1016/j.saa.2004.02.004

Castro et al. 2008 Castro, K., Pessanha, S., Proietti, N., Princi, E., Capitani, D., Carvalho, M.L., Madariaga, J.M. (2008) Noninvasive and nondestructive NMR, Raman and XRF analysis of a Blaeu coloured map from the seventeenth century. Analytical and Bioanalytical Chemistry 391(1): 433-441. DOI: 10.1007/s00216-008-2001-4

Cavallo et al. 2012 Cavallo, G., Vergani, R.C., Gianola, L., Meregalli, A. (2012) Archaeological, stylistic and scientific research on 11th-13th century ad painted fragments from the San Giovanni Battista church in Cevio (Switzerland). Archaeometry 54(2): 294-310. DOI: 10.1111/j.1475-4754.2011.00613.x

Cavallo et al. 2020 Cavallo, G., Aceto, M., Emmenegger, R., Keller, A.T., Lenz, R., Villa, L., Wörz, S., Cassitti, P. (2020) Preliminary non-invasive study of Carolingian pigments in the churches of St. John at Müstair and St. Benedict at Malles. Archaeological and Anthropological Sciences 12(3): 73. DOI: 10.1007/s12520-020-01024-2

Chaplin et al. 2005 Chaplin, T.D., Clark, R.J.H., Jacobs, D., Jensen, K., Smith, G.D., (2005) The Gutenberg Bibles: Analysis of the illuminations and inks using Raman spectroscopy. *Analytical Chemistry* **77**(11): 3611-3622. DOI: 10.1021/ac050346y

Chaplin et al. 2006 Chaplin, T.D., Clark, R.J.H., McKay, A., Pugh, S. (2006) Raman spectroscopic analysis of selected astronomical and cartographic folios from the early 13th century Islamic 'Book of Curiosities of the Sciences and Marvels for the Eyes'. Journal of Raman Spectroscopy 37(8): 865-877. DOI: 10.1002/jrs.1536

Clark and Gibbs 1997 Clark, R.J.H., Gibbs, P.J. (1997) Identification of lead(II) sulfide and pararealgar on a 13th century manuscript by Raman microscopy. Chemical Communications 11: 1003-1004. DOI: 10.1039/a701837a

Clark and Gibbs 1998 Clark, R.J.H., Gibbs, P.J. (1998) Peer reviewed: Raman microscopy of a 13th-century illuminated text. *Analytical Chemistry* **70**(3): 99A-104A. DOI: 10.1021/ac981719g

Clark and Van Der Weerd 2004 Clark, R.J.H., Van Der Weerd, J. (2004) Identification of pigments and gemstones on the Tours Gospel: the early 9th century Carolingian palette. Journal of Raman Spectroscopy 35(4): 279-283. DOI: 10.1002/jrs.1148

Clarke 2004 Clarke, M. (2004) Anglo-Saxon manuscript pigments. Studies in Conservation 49(4): 231-244. DOI: 10.1179/sic.2004.49.4.231

Colombini et al. 2003 Colombini, M.P., Giachi, G., Modugno, F., Pallecchi, P., Ribechini, E. (2003) The characterization of paints and waterproofing materials from the shipwrecks found at the archaeological site of the etruscan and Roman harbour of Pisa (Italy). Archaeometry 45(4): 659-674. DOI: 10.1046/j.1475-4754.2003.00135.x

Cortea et al. 2020 Cortea, I.M., Ghervase, L., Ratoiu, L., Dinu, M., Rădvan, R. (2020) Uncovering hidden jewels: an investigation of the pictorial layers of an 18th-century Taskin harpsichord. Heritage Science 8(1): 55. DOI: 10.1186/s40494-020-00401-3

Cosano et al. 2019 Cosano, D., Esquivel, D., Costa, C.M., Jiménez-Sanchidrián, C., Ruiz, J.R. (2019) Identification of pigments in the Annunciation sculptural group (Cordoba, Spain) by micro-Raman spectroscopy. Spectrochimica Acta - Part A: Molecular and Biomolecular Spectroscopy 214: 139-145. DOI: 10.1016/j.saa.2019.02.019

Costa et al. 2016 Costa, B.F.O., Lehmann, R., Wengerowsky, D., Blumers, M., Sansano, A., Rull, F., Schmidt, H.-J., Dencker, F., Niebur, A., Klingelhöfer, G., Sindelar, R., Renz, F. (2016) Klimt artwork (Part II): material investigation by backscattering Fe-57 Mössbauer- and Raman- spectroscopy, SEM and p-XRF. *Hyperfine Interactions* **237**(1): 92. DOI: 10.1007/s10751-016-1263-z

Costantini et al. 2020b Costantini, I., Lottici, P.P., Bersani, D., Pontiroli, D., Casoli, A., Castro, K., Madariaga, J.M. (2020) Darkening of lead- and iron-based pigments on late Gothic Italian wall paintings: Energy dispersive X-ray fluorescence, μ-Raman, and powder X-ray diffraction analyses for diagnosis: Presence of β-PbO2 (plattnerite) and α-PbO2 (scrutinyite). Journal of Raman Spectroscopy 51(4): 680-692. DOI: 10.1002/jrs.5817

Damiani et al. 2014 Damiani, D., Gliozzo, E., Turbanti Memmi, I. (2014) The ‘Madonna and Child Enthroned with Saints’ of Ambrogio Lorenzetti in the St. Augustine Church (Siena, Italy): Raman

microspectroscopy and SEM-EDS characterisation of the pigments. *Archaeological-and-Anthropological-Science* **6**: 363-371. DOI: 10.1007/s12520-014-0175-6

Daniilia and Andrikopoulos 2007 — Daniilia, S., Andrikopoulos, K.S. (2007) Issues relating to the common origin of two Byzantine miniatures: In situ examination with Raman spectroscopy and optical microscopy. *Journal of Raman Spectroscopy* **38**(3): 332-343. DOI: 10.1002/jrs.1648

Daniilia and Minopoulou 2009 — Daniilia, S., Minopoulou, E. (2009) A study of smalt and red lead discolouration in Antiphonitis wall paintings in Cyprus. *Applied Physics A: Materials Science and Processing* **96**(3): 701-711. DOI: 10.1007/s00339-009-5163-9

Daniilia et al. 2000 — Daniilia, S., Sotiropoulou, S., Bikiaris, D., Salpistis, C., Karagiannis, G., Chryssoulakis, Y., Price, B.A., Carlson, J.H.P. (2000) Panselinos' Byzantine wall paintings in the Protaton church, Mount Athos, Greece: a technical examination. Journal of Cultural Heritage 1: 91-110. DOI: 10.1016/S1296-2074(00)00164-3

Daniilia et al. 2002 — Daniilia, S., Bikiaris, D., Burgio, L., Gavala, P., Clark, R.J.H., Chryssoulakis, Y. (2002) An extensive non-destructive and micro-spectroscopic study of two post-Byzantine overpainted icons of the 16th century. Journal of Raman Spectroscopy 33(10): 807-814. DOI: 10.1002/jrs.907

Daniilia et al. 2008 — Daniilia, S., Minopoulou, E., Demosthenous, Fr.D., Karagiannis, G. (2008) A comparative study of wall paintings at the Cypriot monastery of Christ Antiphonitis: one artist or two?. Journal of Archaeological Science 35(6): 1695-1707. DOI: 10.1016/j.jas.2007.11.011;

de Ferri et al. 2019 — de Ferri, L., Mazzini, F., Vallotto, D., Pojana, G. (2019) In situ non-invasive characterization of pigments and alteration products on the masonry altar of S. Maria ad Undas (Idro, Italy). Archaeological and Anthropological Sciences 11(2): 609-625. DOI: 10.1007/s12520-017-0550-1

De Keyser et al. 2017 — De Keyser, N., Van der Snickt, G., Van Loon, A., Legrand, S., Wallert, A., Janssens, K. (2017) Jan Davidsz. de Heem (1606–1684): a technical examination of fruit and flower still lifes combining MA-XRF scanning, cross-section analysis and technical historical sources. Heritage Science 5: 38. DOI: 10.1186/s40494-017-0151-4;

De Meyer et al. 2019 — De Meyer, S., Vanmeert, F., Vertongen, R., Van Loon, A., Gonzalez, V., Delaney, J., Dooley, K., Dik, J., Van der Snickt, G., Vandivere, A., Janssens, K. (2019) Macroscopic x-ray powder diffraction imaging reveals Vermeer's discriminating use of lead white pigments in Girl with a Pearl Earring. *Science Advances* **5**(8): eaax1975. DOI: 10.1126/sciadv.aax1975

de Viguerie et al. 2018 — de Viguerie, L., Glanville, H., Ducouret, G., Jacquemot, P., Dang, P.A., Walter, P. (2018) Re-interpretation of the Old Masters' practices through optical and rheological investigation: The presence of calcite. Comptes Rendus Physique 19(7): 543-552. DOI: 10.1016/j.crhy.2018.11.003

Del Monte et al. 1998 — Del Monte, M., Ausset, P., Lefevre, R.A. (1998) Traces of ancient colours on Trajan's column. Archaeometry 40(2): 403-412. DOI: 10.1111/j.1475-4754.1998.tb00846.x

Delaney et al. 2020 — Delaney, J.K., Dooley, K.A., van Loon, A., Vandivere, A. (2020) Mapping the pigment distribution of Vermeer's Girl with a Pearl Earring. Heritage Science 8(1): 4. DOI: 10.1186/s40494-019-0348-9

Doleżyńska-Sewerniak et al. 2020 — Doleżyńska-Sewerniak, E., Jendrzejewski, R., Klisińska-Kopacz, A., Sawczak, M. (2020) Non-invasive spectroscopic methods for the identification of drawing materials used in XVIII century. *Journal of Cultural Heritage* **41**: 34-42. DOI: 10.1016/j.culher.2019.07.008

Doménech-Carbó et al. 2019 — Doménech-Carbó, A., Doménech-Carbó, M.T., Castelló-Palacios, A., Guerola-Blay, V., Pérez-Marín, E. (2019) Electrochemical identification of painters/workshops: The case of Valencian Renaissance-Baroque painters (ca. 1550- ca. 1670). Electrochimica Acta 297: 685-695. DOI: 10.1016/j.electacta.2018.11.212

Dominguez-Vidal et al. 2014 — Dominguez-Vidal, A., De La Torre-López, M.J., Campos-Suñol, M.J., Rubio-Domene, R., Ayora-Cañada, M.J. (2014) Decorated plasterwork in the Alhambra investigated by Raman spectroscopy: Comparative field and laboratory study. Journal of Raman Spectroscopy 45(11-12): 1006-1012. DOI: 10.1002/jrs.4439

Duran et al. 2014 — Duran, A., López-Montes, A., Castaing, J., Espejo, T. (2014) Analysis of a royal 15th century illuminated parchment using a portable XRF-XRD system and micro-invasive techniques. Journal of Archaeological Science 45(1): 52-58. DOI: 10.1016/j.jas.2014.02.011

Edwards et al. 1999 — Edwards, H.G.M., Farwell, D.W., Newton, E.M., Perez, F.R. (1999) Minium; FT-Raman non-destructive analysis applied to an historical controversy. *Analyst* **124**(9): 1323-1326. DOI: 10.1039/a904083h

Edwards et al. 1999 — Edwards, H.G.M., Farwell, D.W., Rull Perez, F., Jorge Villar, S., (1999) Spanish mediaeval frescoes at Basconcillos del Tozo: A fourier transform Raman spectroscopic study. *Journal of Raman Spectroscopy* **30**(4): 307-311. DOI: 10.1002/(SICI)1097-4555(199904)30:4<307::AID-JRS373>3.0.CO;2-W

Edwards et al. 2000 — Edwards, H.G.M., Farwell, D.W., Newton, E.M., Perez, F.R., Villar, S.J. (2000) Raman spectroscopic studies of a 13th century polychrome statue: identification of a 'forgotten' pigment.

Journal of Raman Spectroscopy 31(5): 407-413. DOI: 10.1002/1097-4555(200005)31:5<407::AID-JRS530>3.0.CO;2-Y

Edwards et al. 2001 Edwards, H.G.M., Rull, F., Vandenabeele, P., Newton, E.M., Moens, L., Medina, J., Garcia, C. (2001) Mediaeval pigments in the monastery of San Baudelio, Spain: A Raman spectroscopic analysis. Applied Spectroscopy 55(1): 71-76. DOI: 10.1366/0003702011951272

Edwards et al. 2004 Edwards, H.G.M., Jorge Villar, S.E., Eremin, K.A. (2004) Raman spectroscopic analysis of pigments from dynastic Egyptian funerary artefacts. *Journal of Raman Spectroscopy* **35**(8-9): 786-795. DOI: 10.1002/jrs.1193

Edwards et al. 2005 Edwards, H.G.M., Farwell, D.W., Brooke, C.J. (2005) Raman spectroscopic study of a post-medieval wall painting in need of conservation. *Analytical and Bioanalytical Chemistry* **383**(2): 312-321. DOI: 10.1007/s00216-005-0012-y

Edwards et al. 2007 Edwards, H.G.M., Wolstenholme, R., Wilkinson, D.S., Brooke, C., Pepper, M. (2007) Raman spectroscopic analysis of the enigmatic Comper pigments. Analytical and Bioanalytical Chemistry 387(6): 2255-2262. DOI: 10.1007/s00216-006-1113-y

Edwards et al. 2007 Edwards, H.G.M., Beale, E., Garrington, N.C., Alia, J.-M. (2007) FT-Raman spectroscopy of pigments on a Hindu statue, Kali Walking on Siva. *Journal of Raman Spectroscopy* **38**(3): 316-322. DOI: 10.1002/jrs.1645

Edwards et al. 2010 Edwards, H.G.M., Newton, E.M., O'Connor, S., Evans, D. (2010) FT-Raman spectroscopic analysis of pigments from an Augustinian friary. *Analytical and Bioanalytical Chemistry* **397**: 2685-2691. DOI: 10.1007/s00216-010-3568-0

Egel and Simon 2013 Egel, E., Simon, S. (2013) Investigation of the painting materials in Zhongshan Grottoes (Shaanxi, China). Heritage Science 1: 29. DOI: 10.1186/2050-7445-1-29

Espejo Arias et al. 2008 Espejo Arias, T., López Montes, A., García Bueno, A., Durán Benito, A., Blanc García, R. (2008) A study about colourants in the Arabic manuscript collection of the Sacromonte Abbey, Granada, Spain. A new methodology for chemical analysis. *Restaurator* **29**(2): 76-106. DOI: 10.1515/rest.2008.005

Fermo et al. 2013 Fermo, P., Piazzalunga, A., De Vos, M., Andreoli, M. (2013) A multi-analytical approach for the study of the pigments used in the wall paintings from a building complex on the Caelian Hill (Rome). *Applied Physics A: Materials Science and Processing* **113**(4): 1109-1119. DOI: 10.1007/s00339-013-7754-8

Fioretti et al. 2020 Fioretti, G., Raneri, S., Pinto, D., Mignozzi, M., Mauro, D. (2020) The archaeological site of St. Maria Veterana (Triggiano, Southern Italy): Archaeometric study of the wall paintings for the historical reconstruction. *Journal of Archaeological Science: Reports* **29**: 102080. DOI: 10.1016/j.jasrep.2019.102080

Fiorillo et al. 2020 Fiorillo, F., Fiorentino, S., Montanari, M., Roversi Monaco, C., Del Bianco, A., Vandini, M. (2020) Learning from the past, intervening in the present: the role of conservation science in the challenging restoration of the wall painting Marriage at Cana by Luca Longhi (Ravenna, Italy). Heritage Science 8(1): 10. DOI: 10.1186/s40494-020-0354-y

Franceschi et al. 2010 Franceschi, C.M., Costa, G.A., Franceschi, E. (2010) Aging of the paint palette of Valerio Castello (1624–1659) in different paintings of the same age (1650–1655). Journal of Thermal Analysis and Calorimetry 103(1): 69-73. DOI: 10.1007/s10973-010-1089-x

Franceschi et al. 2011 Franceschi, C.M., Franceschi, E., Nole, D., Vassallo, S., Glozheni, L. (2011) Two Byzantine Albanian icons: A non-destructive archaeometric study. Archaeological and Anthropological Sciences 3(4): 343-355. DOI: 10.1007/s12520-011-0073-0

Franquelo et al. 2015 Franquelo, M.L., Robador, M.D., Pérez-Rodríguez, J.L. (2015) Scientific study of the gothic-renaissance altarpiece of Santiago church in Écija (Spain). *European Journal of Science and Theology* **11**(2): 149-158.

Franquelo et al. 2019 Franquelo, M.L., Duran, A., Perez-Rodriguez, J.L. (2019) Laboratory multi-technique study of Spanish decorated leather from the 12th to 14th centuries. *Spectrochimica Acta - Part A: Molecular and Biomolecular Spectroscopy* **218**: 331-341. DOI: 10.1016/j.saa.2019.04.012

Fu et al. 2020 Fu, P., Teri, G.-L., Li, J., Li, J.-X., Li, Y.-H., Yang, H. (2020) Investigation of ancient architectural painting from the taidong tomb in the Western Qing Tombs, Hebei, China. Coatings 10(7): 688. DOI: 10.3390/coatings10070688

Garrote et al. 2017 Garrote, M.A., Robador, M.D., Perez-Rodriguez, J.L. (2017) Analytical investigation of Mudéjar polychrome on the carpentry in the Casa de Pilatos palace in Seville using non-destructive XRF and complementary techniques. *Spectrochimica Acta - Part A: Molecular and Biomolecular Spectroscopy* **173**: 279-291. DOI: 10.1016/j.saa.2016.09.027

Gebremariam et al. 2013 Gebremariam, K.F., Kvittingen, L., Banica, F.-G. (2013) Application of a portable XRF analyzer to investigate the medieval wall paintings of Yemrehanna Krestos church, Ethiopia. X-Ray Spectrometry 42(6): 462-469. DOI: 10.1002/xrs.2504

Gebremariam et al. 2016 — Gebremariam, K.F., Kvittingen, L., Nicholson, D.G. (2016) Multi-analytical investigation into painting materials and techniques: The wall paintings of Abuna Yemata Guh church. *Heritage Science* **4**(1): 32. DOI: 10.1186/s40494-016-0101-6

Gehad et al. 2015 — Gehad, B., Aly, M.F., Marey, H. (2015) Identification of the Byzantine encaustic mural painting in Egypt. Mediterranean Archaeology and Archaeometry 15(2): 243-256. DOI: 10.5281/zenodo.16612

Gómez-Morón et 2016 — Gómez-Morón, M.A., Ortiz, P., Martín-Ramírez, J.M., Ortiz, R., Castaing, J. (2016) A new insight into the vaults of the kings in the Alhambra (Granada, Spain) by combination of portable XRD and XRF. Microchemical Journal 125: 260-265. DOI: 10.1016/j.microc.2015.11.023

Gómez-Morón et al. 2020 — Gómez-Morón, A., Ortiz, P., Ortiz, R., Colao, F., Fantoni, R., Castaing, J., Becerra, J. (2020) Multi-approach study applied to restoration monitoring of a 16th century wooden paste sculpture. Crystals 10(8): 708. DOI: 10.3390/cryst10080708

Gong et al. 2020 — Gong, Y., Qiao, C., Zhong, B., Zhong, J., Gong, D. (2020) Analysis and characterization of materials used in heritage theatrical figurines. *Heritage Science* **8**(1): 13. DOI: 10.1186/s40494-020-0358-7

Guerra et al. 2016 — Guerra, M., Carvalho, M.L., Le Gac, A., Manso, M., Mortari, C., Longelin, S., Pessanha, S. (2016) New insights into the red and green pigments in the illuminated foral charter of Setubal (1515) by combined use of μ-Raman and X-ray fluorescence spectrometry. Journal of Applied Physics 119(10): 104902. DOI: 10.1063/1.4943617

Gutman et al. 2014 — Gutman, M., Lesar-Kikelj, M., Mladenovič, A., Čobal-Sedmak, V., Križnar, A., Kramar, S. (2014) Raman microspectroscopic analysis of pigments of the Gothic wall painting from the Dominican Monastery in Ptuj (Slovenia). Journal of Raman Spectroscopy 45: 1103-1109. DOI: 10.1002/jrs.4628

Gutman Rieppi et al. 2020 — Gutman Rieppi, N., Price, B.A., Sutherland, K., Lins, A.P., Newman, R., Wang, P., Wang, T., Tague, T.J.Jr. (2020) Salvator Mundi: an investigation of the painting's materials and techniques. *Heritage Science* **8**(1): 39. DOI: 10.1186/s40494-020-00382-3

Ha and Lee 2015 — Ha, J.-W., Lee, S.-J. (2015) Identification of natural inorganic pigments used on 18th century Korean traditional mural paintings by using a portable X-ray fluorescence. *Journal of Industrial and Engineering Chemistry* **28**: 328-333. DOI: 10.1016/j.jiec.2015.03.011

Hayez et al. 2004 — Hayez, V., Denoël, S., Genadry, Z., Gilbert, B. (2004) Identification of pigments on a 16th century Persian manuscript by micro-Raman spectroscopy. *Journal of Raman Spectroscopy* **35**(8-9): 781-785. DOI: 10.1002/jrs.1192

He et al. 2012 — He, L., Wang, N., Zhao, X., Zhou, T., Xia, Y., Liang, J., Rong, B. (2012) Polychromic structures and pigments in Guangyuan Thousand-Buddha Grotto of the Tang Dynasty (China). Journal of Archaeological Science 39(6): 1809-1820. DOI: 10.1016/j.jas.2012.01.022

Hedegaard et al. 2019 — Hedegaard, S.B., Delbey, T., Brøns, C., Rasmussen, K.L. (2019) Painting the Palace of Apries II: ancient pigments of the reliefs from the Palace of Apries, Lower Egypt. *Heritage Science* **7**(1): 54. DOI: 10.1186/s40494-019-0296-4

Hein et al. 2009 — Hein, A., Karatasios, I., Mourelatos, D. (2009) Byzantine wall paintings from Mani (Greece): Microanalytical investigation of pigments and plasters. Analytical and Bioanalytical Chemistry 395(7): 2061-2071. DOI: 10.1007/s00216-009-2967-6

Herrera et al. 2008 — Herrera, L.K., Cotte, M., Jimenez de Haro, M.C., Duran, A., Justo, A., Perez-Rodriguez, J.L. (2008) Characterization of iron oxide-based pigments by synchrotron-based micro X-ray diffraction. Applied Clay Science 42(1-2): 57-62. DOI: 10.1016/j.clay.2008.01.021

Holakooei and Karimy 2015 — Holakooei, P., Karimy, A.-H. (2015) Early Islamic pigments used at the Masjid-i Jame of Fahraj, Iran: A possible use of black plattnerite. Journal of Archaeological Science 54: 217-227. DOI: 10.1016/j.jas.2014.12.001

Holakooei et al. 2020 — Holakooei, P., Karimy, A.-H., Saeidi-Anaraki, F., Vaccaro, C., Sabatini, F., Degano, I., Colombini, M.P. (2020) Colourants on the wall paintings of a mediæval fortress at the mount Sofeh in Isfahan, central Iran. Journal of Archaeological Science: Reports 29: 102065. DOI: 10.1016/j.jasrep.2019.102065

Hradil et al. 2013 — Hradil, D., Hradilová, J., Kočí, E., Švarcová, S., Bezdička, P., Maříková-Kubková, J. (2013) Unique pre-romanesque murals in Kostoľany pod Tríbečom, Slovakia: The painting technique and causes of damage. *Archaeometry* **55**(4): 691-706. DOI: 10.1111/j.1475-4754.2012.00704.x

Hradil et al. 2014 — Hradil, D., Hradilová, J., Bezdička, P., Švarcová, S., Čermáková, Z., Košařová, V., Němec, I. (2014) Crocoite PbCrO4and mimetite Pb5(AsO4)3Cl: Rare minerals in highly degraded mediaeval murals in Northern Bohemia. Journal of Raman Spectroscopy 45(9): 848-858. DOI: 10.1002/jrs.4556

Hu et al. 2013 — Hu, K., Bai, C., Ma, L., Bai, K., Liu, D., Fan, B. (2013) A study on the painting techniques and materials of the murals in the Five Northern Provinces' Assembly Hall, Ziyang, China. *Heritage Science* **1**(1): 18. DOI: 10.1186/2050-7445-1-18

Huică et al. 2020	Huică, I., Cortea, I.M., Ratoiu, L., Ghervase, L., Rădvan, R., Mohanu, D. (2020) Multidisciplinary approach for time-framing of an overpainted wooden iconostasis from Southern Romania. Microchemical Journal 155: 104685. DOI: 10.1016/j.microc.2020.104685
Impallaria et al. 2020	Impallaria, A., Mazzacane, S., Petrucci, F., Tisato, F., Volpe, L. (2020) Portable X-ray fluorescence device reveals the artistic palette of Carlo Bononi, Baroque artist from Ferrara. *X-Ray Spectrometry* 49(3): 442-450. DOI: 10.1002/xrs.3139
Iordanidis et al. 2011	Iordanidis, A., Garcia-Guinea, J., Strati, A., Gkimourtzina, A., Papoulidou, A. (2011) Byzantine wall paintings from Kastoria, northern Greece: Spectroscopic study of pigments and efflorescing salts. Spectrochimica Acta - Part A: Molecular and Biomolecular Spectroscopy 78(2): 874-887. DOI: 10.1016/j.saa.2010.12.055
Jasiński 2019	Jasiński, M. (2019) Cecco del Caravaggio's Martyrdom of Saint Sebastian. An investigation into Caravaggisti painting technique and technology. International Journal of Conservation Science 10(2): 271-278.
Kanth and Singh 2019	Kath, A.P., Singh, M.R. (2019) Vibrational spectroscopy and SEM-EDX analysis of wall painted surfaces, Orchha Fort, India. *Journal of Archaeological Science: Reports* **24**: 434-444. DOI: 10.1016/j.jasrep.2019.02.008
Kantoglu et al. 2018	Kantoglu, O., Ergun, E., Kirmaz, R., Kalayci, Y., Zararsiz, A., Bayir, O. (2018) Colour and ink characterization of ottoman diplomatic documents dating from the 13th to the 20th century. Restaurator 39(4): 265-288. DOI: 10.1515/res-2018-0014
Karapanagiotis et al. 2009	Karapanagiotis, I., Minopoulou, E., Valianou, L., Daniilia, S., Chryssoulakis, Y. (2009) Investigation of the colourants used in icons of the Cretan School of iconography. *Analytica Chimica Acta* **647**(2): 231-242. DOI: 10.1016/j.aca.2009.06.012
Karapanagiotis et al. 2013	Karapanagiotis, I., , Lampakis, D., Kostanta, A., Farmakalidis, H. (2013) Identification of colourants in icons of the Cretan School of iconography using Raman Spectroscopy and liquid chromatography. *Journal of Archaeological Science* **40**: 1471-1478. DOI: 10.1016/j.jas.2012.11.004
Khramchenkova et al. 2018	Khramchenkova, R., Biktagirova, I., Gareev, B., Kaplan, P. (2018) Horse-headed Saint Christopher fresco in the Sviyazhsk Assumption cathedral (16^{th}-17^{th} century, Russia): history and archaeometry. *Mediterranean Archaeology and Archaeometry* **18**(3): 195-207. DOI: 10.5281/zenodo.1476971
Kim et al. 2016	Kim, M., Lee, J., Doh, J.-M., Ahn, H., Kim, H.D., Yang, Y., Lee, Y. (2016) Characterization of ancient Korean pigments by surface analytical techniques. *Surface and Interface Analysis* **48**(7): 409-414. DOI: 10.1002/sia.5975
Kotulanová et al. 2009	Kotulanová, E., Bezdička, P., Hradil, D., Hradilová, J., Švarcová, S., Grygar, T. (2009) Degradation of lead-based pigments by salt solutions. Journal of Cultural Heritage 10(3): 367-378. DOI: 10.1016/j.culher.2008.11.001
Kovala-Demertzi et al. 2012	Kovala-Demertzi, D., Papathanasis, L., Mazzeo, R., Demertzis, M.A., Varella, E.A., Prati, S. (2012) Pigment identification in a Greek icon by optical microscopy and infrared microspectroscopy. Journal of Cultural Heritage 13(1): 107-113. DOI: 10.1016/j.culher.2011.06.003
Kriznar et al. 2008	Kriznar, A., Muñoz, M.V., De La Paz, F., Respaldiza, M.A., Vega, M. (2008) Pigment identification using x-ray fluorescence in a polychromated sculpture by Pedro Millán. *X-Ray Spectrometry* **37**(4): 355-359. DOI: 10.1002/xrs.1020
Križnar et al. 2009	Križnar, A., Muñoz, M.V., de la Paz, F., Respaldiza, M.A., Vega, M. (2009) XRF analysis of two terracotta polychrome sculptures by Pietro Torrigiano. *X-Ray Spectrometry* **38**(3): 169-174. DOI: 10.1002/xrs.1135
Križnar et al. 2019	Križnar, A., Ager, F.J., Caliri, C., Romano, F.P., Respaldiza, M.Á., Gómez-Morón, M.A., Núñez, L., Magdaleno, R. (2019) Study of two large-dimension Murillo's paintings by means of macro X-ray fluorescence imaging, point X-ray fluorescence analysis, and stratigraphic studies. X-Ray Spectrometry 48(5): 482-489. DOI: 10.1002/xrs.2990
Lazidou et al. 2018	Lazidou, D., Lampakis, D., Karapanagiotis, I., Panayiotou, C. (2018) Investigation of the cross-section stratifications of icons using micro-Raman and micro-Fourier Transform Infrared (FT-IR) spectroscopy. Applied Spectroscopy 72(8): 1258-1271. DOI: 10.1177/0003702818777772
Lehmann et al. 2017	Lehmann, R., Wengerowsky, D., Schmidt, H.J., Kumar, M., Niebur, A., Costa, B.F.O., Dencker, F., Klingelhöfer, G., Sindelar, R., Renz, F. (2017) Klimt artwork: red-pigment material investigation by backscattering Fe-57 Mössbauer spectroscopy, SEM and p-XRF. Science and Technology of Archaeological Research 3(2): 450-455. DOI: 10.1080/20548923.2017.1399332
Lei et al. 2017	Lei, Z., Wu, W., Shang, G., Wu, Y., Wang, J. (2017) Study on colored pattern pigments of a royal Taoist temple beside the Forbidden City (Beijing, China). Vibrational Spectroscopy 92: 234-244. DOI: 10.1016/j.vibspec.2017.08.005

Leuzzi et al. 2018 Leuzzi, M.C., Crippa, M., Costa, G.A. (2018) Application of non-destructive techniques. The Madonna del latte case study. *Acta IMEKO* **7**(3): 52-56. DOI: 10.21014/acta_imeko.v7i3.587

Levstik et al. 2019 Levstik, M.G., Mladenovič, A., Križnar, A., Kramar, S. (2019) A Raman microspectroscopy-based comparison of pigments applied in two gothic wall paintings in Slovenia. Periodico di Mineralogia 88(1): 95-104. DOI: 10.2451/2019PM778

Li et al. 2020 Li, G.H., Chen, Y., Sun, X.J., Duan, P.Q., Lei, Y., Zhang, L.F. (2020) An automatic hyperspectral scanning system for the technical investigations of Chinese scroll paintings. *Microchemical Journal* **155**: 104699. DOI: 10.1016/j.microc.2020.104699

Li et al. 2020 Li, Z., Wang, L., Chen, H., Ma, Q. (2020) Degradation of emerald green: scientific studies on multi-polychrome Vairocana Statue in Dazu Rock Carvings, Chongqing, China. *Heritage Science* **8**(1): 64. DOI: 10.1186/s40494-020-00410-2

Li et al. 2020 Li, T., Liu, C., Wang, D. (2020) Applying micro-computed tomography (micro-CT) and Raman spectroscopy for non-invasive characterization of coating and coating pigments on ancient Chinese papers. *Heritage Science* **8**(1): 22. DOI: 10.1186/s40494-020-00366-3

Li et al. 2020 Li, G.H., Chen, Y., Sun, X.J., Duan, P.Q., Lei, Y., Zhang, L.F. (2020) An automatic hyperspectral scanning system for the technical investigations of Chinese scroll paintings. *Microchemical Journal* **155**: 104699. DOI: 10.1016/j.microc.2020.104699

Liu et al. 2016 Liu, L., Shen, W., Zhang, B., Ma, Q. (2016) Microchemical study of pigments and binders in polychrome relics from maiji mountain grottoes in northwestern China. Microscopy and Microanalysis 22(4): 845-856. DOI: 10.1017/S1431927616011302

Liu et al. 2019 Liu, L., Gong, D., Yao, Z., Xu, L., Zhu, Z., Eckfeld, T. (2019) Characterization of a Mahamayuri Vidyarajni Sutra excavated in Lu'an, China. Heritage Science 7(1): 77. DOI: 10.1186/s40494-019-0320-8

López et al. 2011 López Cruz, O., García Bueno, A., Medina Flórez, V.J., (2011) Evolución del color en el alero de la fachada del rey D. Pedro I, Real Alcázar de Sevilla. Aportaciones del estudio de materiales a la identificación de las intervenciones de restauración a lo largo de su historia [The evolution of the colour in the eaves of the façade of the palace of the king Pedro I, Royal Palace of Seville. Contribution of the study of materials to the identification of the conservation works undertaken throughout its history]. *Arqueologia de la Arquitectura* **8**: 163-178. DOI: 10.3989/arqarqt.2011.10016

Lukačević et al. 2013 Lukačević, I., Ergotić, I., Vinaj, M. (2013) Non-destructive analyses of 16th century printed book "Osorio" with the colorful fore-edge miniatures. Croatica Chemica Acta 86(2): 207-214. DOI: 10.5562/cca2040

Luo et al. 2019 Luo, Y., Chen, J., Yang, C., Huang, Y. (2019) Analyzing ancient Chinese handmade Lajian paper exhibiting an orange-red color. Heritage Science 7(1): 61. DOI: 10.1186/s40494-019-0306-6

MacLennan et al. 2019 MacLennan, D., Trentelman, K., Szafran, Y., Woollett, A.T., Delaney, J.K., Janssens, K., Dik, J. (2019) Rembrandt's An old man in military costume: combining hyperspectral and MA-XRF imaging to understand how two paintings were painted on a single panel. *Journal of the American Institute for Conservation* **58**(1-2): 54-68. DOI: 10.1080/01971360.2018.1540245

Malagodi et al. 2014 Malagodi, M., Rovetta, T., Licchelli, M. (2014) Study of materials and techniques in painted ceiling panels from a palace in Cremona (Italy, 15th century). *Heritage Science* **2**(1): 9. DOI: 10.1186/2050-7445-2-9

Malletzidou et al. 2019 Malletzidou, L., Zorba, T.T., Patsiaoura, D., Lampakis, D., Beinas, P., Touli, V., Chrissafis, K., Karapanagiotis, I., Pavlidou, E., Paraskevopoulos, K.M. (2019) Unraveling the materials and techniques of post-Byzantine wall paintings: Is there a sole pictorial phase at the catholicon of Stomion, Central Greece?. Spectrochimica Acta - Part A: Molecular and Biomolecular Spectroscopy 206: 328-339. DOI: 10.1016/j.saa.2018.07.105

Manso et al. 2013 Manso, M., Gac, A.L., Longelin, S., Pessanha, S., Frade, J.C., Guerra, M., Candeias, A.J., Carvalho, M.L. (2013) Spectroscopic characterization of a masterpiece: The Manueline foral charter of Sintra. *Spectrochimica Acta - Part A: Molecular and Biomolecular Spectroscopy* **105**: 288-296. DOI: 10.1016/j.saa.2012.11.110

Manzano et al. 2020 Manzano, E., Rodríguez-Simón, L.R., Navas, N., Capitán-Vallvey, L.F. (2020 in press) Non-invasive and spectroscopic techniques for the study of Alonso Cano's visitation from the golden age of Spain. Studies in Conservation : . DOI: 10.1080/00393630.2020.1830528

Martin-Ramos et al. 2017 Martin-Ramos, D.J., Zafra-Gómez, A., Vílchez, J.L. (2017) Non-destructive pigment characterization in the painting Little Madonna of Foligno by X-ray Powder Diffraction. *Microchemical Journal* **134**: 343-353. DOI: 10.1016/j.microc.2017.07.001

Marutoiu et al. 2017 Marutoiu, C., Bratu, I., Nemes, O.F., Dit, I.-I., Comes, R., Tanaselia, C., Falamas, A., Miclaus, M., Marutoiu, V.C., Moraru, R. (2017) Instrumental analysis of materials and topology of the Imperial Gates belonging to the Apahida wooden church, Cluj County. Vibrational Spectroscopy

89: 131-136. DOI: 10.1016/j.vibspec.2017.02.003

Mazzocchin et al. 2003 — Mazzocchin, G.A. , Agnoli, F., Mazzocchin, S., Colpo, I. (2003) Analysis of pigments from Roman wall paintings found in Vicenza. *Talanta* **61**: 565-572. DOI: 10.1016/S0039-9140(03)00323-0

Miliani et al. 2009 — Miliani, C., Doherty, B., Daveri, A., Loesch, A., Ulbricht, H., Brunetti, B.G., Sgamellotti, A. (2009) In situ non-invasive investigation on the painting techniques of early Meissen Stoneware. *Spectrochimica Acta - Part A: Molecular and Biomolecular Spectroscopy* **73**(4): 587-592. DOI: 10.1016/j.saa.2009.02.003

Molari et al. 2020 — Molari, R., Appoloni, C.R., Rodriguez, S.H. (2020) Non-destructive portable X-ray fluorescence analysis of the Portrait of a Young Man with a Golden Chain (c. 1635) by Rembrandt and/or atelier. Applied Radiation and Isotopes 158: 105100. DOI: 10.1016/j.apradiso.2020.109346

Mounier et al. 2020 — Mounier, A., Schlicht, M., Mulliez, M., Pacanowski, R., Lucat, A., Mora, P. (2020) In search of the lost polychromy of English medieval alabaster panels in the Southwest of France. *Color Research and Application* **45**(3): 427-449. DOI: 10.1002/col.22482

Moussa et al. 2009 — Moussa, A.B., Kantiranis, N., Voudouris, K.S., Stratis, J.A., Ali, M.F., Christaras, V. (2009) Diagnosis of weathered Coptic wall paintings in the Wadi El Natrun region, Egypt. Journal of Cultural Heritage 10(1): 152-157. DOI: 10.1016/j.culher.2008.09.005

Olszewska-Świetlik et al. 2013 — Olszewska-Świetlik, J., Szmelter-Fausek, B., Pięta, E., Proniewicz, E. (2013) Spectroscopic and gas chromatographic studies of pigments and binders in Gdańsk paintings of the 17th century. *Journal of Spectroscopy* **1**(1): 187407. DOI: 10.1155/2013/187407

Papazoglou et al. 2019 — Papazoglou, D., Malletzidou, L., Zorba, T., Beinas, P., Karapanagiotis, I., Pavlidou, E. (2019) Characterization of a two field icon of Virgin Mary "eleousa" (19th century). In: Mishonov T.M., Varonov A.M. (Eds.) 10th Jubilee Conference of the Balkan Physical Union, BPU 2018. (Sofia, Bulgaria, 26-30 August 2018). AIP Conference Proceedings, 2075. American Institute of Physics Inc., pp. 200004.

Pavlidou et al. 2008 — Pavlidou, E., Civici, N., Caushi, E., Anastasiou, L., Zorba, T., Hatzikraniotis, E., Paraskevopoulos, K.M. (2008) Study of painting materials and techniques in the 18th century St. Athanasius Church in Moschopolis, Albania. *Materials Research Society Symposium Proceedings* **1047**: 61-69.

Pelosi et al. 2020 — Pelosi, C., Lo Monaco, A., Bernabei, M., Agresti, G., Colantonio, C., Perri, A., Comelli, D., Valentini, G., Manzoni, C. (2020) Beyond the visible: The Viterbo Crucifixion panel painting attributed to Michelangelo Buonarroti. Microchemical Journal: 104636. DOI: 10.1016/j.microc.2020.104636

Pereira-Pardo et al. 2019 — Pereira-Pardo, L., Tamburini, D., Dyer, J. (2019) Shedding light on the colours of medieval alabaster sculptures: Scientific analysis and digital reconstruction of their original polychromy. Color Research and Application 44(2): 221-233. DOI: 10.1002/col.22323

Pérez-Alonso et al. 2004 — Pérez-Alonso, M., Castro, K., Álvarez, M., Madariaga, J.M. (2004) Scientific analysis versus restorer's expertise for diagnosis prior to a restoration process: The case of Santa Maria Church (Hermo, Asturias, North of Spain). *Analytica Chimica Acta* **524**(1-2): 379-389. DOI: 10.1016/j.aca.2004.06.034

Pérez-Rodríguez et al. 1998 — Pérez-Rodríguez, J.L., Maqueda, C., Jiménez De Haro, M.C., Rodríguez-Rubio, P. (1998) Effect of pollution on polychromed ceramic statues. Atmospheric Environment 32(6): 993-998. DOI: 10.1016/S1352-2310(97)00337-3

Perez-Rodriguez et al. 2014 — Perez-Rodriguez, J.L., Robador, M.D., Centeno, M.A., Siguenza, B., Duran, A. (2014) Wall paintings studied using Raman spectroscopy: A comparative study between various assays of cross sections and external layers. *Spectrochimica Acta - Part A: Molecular and Biomolecular Spectroscopy* **120**: 602-609. DOI: 10.1016/j.saa.2013.10.052

Petrova et al. 2019 — Petrova, O., Pankin, D., Povolotckaia, A., Borisov, E., Krivul'ko, T., Kurganov, N., Kurochkin, A. (2019) Pigment palette study of the XIX century plafond painting by Raman spectroscopy. Journal of Cultural Heritage 37: 233-237. DOI: 10.1016/j.culher.2018.11.010

Pięta et al. 2019 — Pięta, E., Olszewska-Świetlik, J., Paluszkiewicz, C., Zając, A., Kwiatek, W.M. (2019) Application of ATR-FTIR mapping to identification and distribution of pigments, binders and degradation products in a 17th century painting. Vibrational Spectroscopy 103: 102928. DOI: 10.1016/j.vibspec.2019.102928

Pinna et al. 2020 — Pinna, D., Conti, C., Mazurek, J. (2020) Polychrome sculptures of medieval Italian monuments: Study of the binding media and pigments. Microchemical Journal 158: 105100. DOI: 10.1016/j.microc.2020.105100

Pinna et al. 2020 — Pinna, D., Conti, C., Mazurek, J. (2020) Polychrome sculptures of medieval Italian monuments: Study of the binding media and pigments. Microchemical Journal 158: 105100. DOI: 10.1016/j.microc.2020.105100

Porat and Ilani 1998 Porat, N., Ilani, S. (1998) A Roman period palette: composition of pigments from King Herod's palaces in Jericho and Massada, Israel. Israel Journal of Earth Sciences 47(2): 75-85.

Rampazzo and Di Foggia 2018 Rampazzo, M., Di Foggia, M. (2018) The sunk-panel book-binding of a Renaissance Venetian Commissione Dogale: the scientific examination of the decoration materials. Heritage Science 6(1): 14. DOI: 10.1186/s40494-018-0180-7

Ravindran et al. 2011 Ravindran, T.R., Arora, A.K., Ramya, S., Subba Rao, R.V., Raj, B. (2011) Raman spectroscopic study of medieval Indian art of 17th century. Journal of Raman Spectroscopy 42(4): 803-807. DOI: 10.1002/jrs.2776

Refaat et al. 2020 Refaat, F., Mahmoud, H.M., Brania, A. (2020) Uncovering nineteenth-century Rococo-style interior decorations at the National Military Museum of Cairo: the painting materials and restoration approach. *Journal of Architectural Conservation* **26**(1): 87-104. DOI: 10.1080/13556207.2019.1695173

Romero-Pastor et al. 2011 Romero-Pastor, J., Duran, A., Rodríguez-Navarro, A.B., Van Grieken, R., Cardell, C. (2011) Compositional and quantitative microtextural characterization of historic paintings by micro-X-ray diffraction and raman microscopy. *Analytical Chemistry* **83**(22): 8420-8428. DOI: 10.1021/ac201159e

Rull Perez et al. 1999 Rull Perez, F., Edwards, H.G.M., Rivas, A., Drummond, L. (1999) Fourier transform Raman spectroscopic characterization of pigments in the mediaeval frescoes at Convento de la Peregrina, Sahagun, Léon, Spain. Part 1 - Preliminary study. *Journal of Raman Spectroscopy* **30**(4): 301-305. DOI: 10.1002/(SICI)1097-4555(199904)30:4<301::AID-JRS372>3.0.CO;2-G

Sack et al. 1891 Sack, S.P., Tahk, C.F., Peters, T.Jr. (1981) A technical examination of an ancient Egyptian painting on canvas. Studies in Conservation 26(1): 15-23. DOI: 10.2307/1505817

Salvant et al. 2018 Salvant, J., Williams, J., Ganio, M., Casadio, F., Daher, C., Sutherland, K., Monico, L., Vanmeert, F., De Meyer, S. , Janssens, K., Cartwright, C., Walton, M (2018) A Roman Egyptian painting workshop: technical investigation of the portraits from Tebtunis, Egypt. Archaeometry 60(4): 815-833. DOI: 10.1111/arcm.12351

Sansonetti et al. 2010 Sansonetti, A., Striova, J., Biondelli, D., Castellucci, E.M. (2010) Colored grounds of gilt stucco surfaces as analyzed by a combined microscopic, spectroscopic and elemental analytical approach. Analytical and Bioanalytical Chemistry 397(7): 2667-2676. DOI: 10.1007/s00216-010-3491-4

Sansonetti et al. 2020 Sansonetti, A., Striova, J., Biondelli, D., Castellucci, E.M. (2010) Colored grounds of gilt stucco surfaces as analyzed by a combined microscopic, spectroscopic and elemental analytical approach. Analytical and Bioanalytical Chemistry 397(7): 2667-2676. DOI: 10.1007/s00216-010-3491-4

Scott et al. 2003 Scott, D.A., Dennis, M., Khandekar, N., Keeney, J., Carson, D., Swartz Dodd, L. (2003) An Egyptian cartonnage of the Graeco-Roman period: examination and discoveries. Studies in Conservation 48(1): 41-56.

Scott et al. 2004 Scott, D.A., Dodd, L.S., Furihata, J., Tanimoto, S., Keeney, J., Schilling, M.R., Cowan, E. (2004) An ancient Egyptian cartonnage broad collar: Technical examination of pigments and binding media. *Studies in Conservation* **49**(3): 177-192. DOI: 10.1179/sic.2004.49.3.177

Serafima et al. 2019 Serafima, S., Duliu, O.G., Manea, M.-M., Vasilica, S., Radulescu, C., Constantinescu, B., Stan, D., Culicov, O.-A., Zincovscaia, I. (2019) Complex investigation of the five 19th century Russian-Lipovan icons. Microchemical Journal 150: 104126. DOI: 10.1016/j.microc.2019.104126

Shi and Li 2013 Shi, J.-L., Li, T. (2013) Technical investigation of 15th and 19th century Chinese paper currencies: Fiber use and pigment identification. Journal of Raman Spectroscopy 44(6): 892-898. DOI: 10.1002/jrs.4297

Smith and Barbet 1999 Smith, D.C., Barbet, A. (1999) A preliminary Raman microscopic exploration of pigments in wall paintings in the Roman Tomb discovered at Kertch, Ukraine, in 1891. *Journal of Raman Spectroscopy* **30**(4): 319-324. DOI: 10.1002/(SICI)1097-4555(199904)30:4<319::AID-JRS380>3.0.CO;2-X

Smith and Clark 2002 Smith, G.D., Clark, R.J.H. (2002) Note on lead(II) oxide in mediaeval frescoes from the monastery of San Baudelio, Spain. Applied Spectroscopy 56(6): 804-806. DOI: 10.1366/000370202760077577

Sodo et al. 2019 Sodo, A., Tortora, L., Biocca, P., Casanova Municchia, A., Fiorin, E., Ricci, M.A. (2019) Raman and time of flight secondary ion mass spectrometry investigation answers specific conservation questions on Bosch painting Saint Wilgefortis Triptych. Journal of Raman Spectroscopy 50(2): 150-160. DOI: 10.1002/jrs.5479

Sotiropoulou et al. 2016 Sotiropoulou, S., Eirini Papliaka, Z., Vaccari, L. (2016) Micro FTIR imaging for the investigation of deteriorated organic binders in wall painting stratigraphies of different techniques and periods.

Microchemical Journal 124: 559-567. DOI: 10.1016/j.microc.2015.10.002

Stamboliyska et al. 2021 — Stamboliyska, B., Tapanov, S., Velcheva, E., Yancheva, D., Rogozherov, M., Glavcheva, Z., Lalev, G., Dimitrov, M. (2021) The altar wall paintings of the catholicon "The Nativity of the Virgin", Rila Monastery, Bulgaria: Identification of the painting materials by means of vibrational spectroscopic techniques complemented by EDX, XRD and TGA analysis. *Spectrochimica Acta - Part A* **247**: 119087. DOI: 10.1016/j.saa.2020.119087

Stanzani et al. 2016 — Stanzani, E., Bersani, D., Lottici, P.P., Colomban, P. (2016) Analysis of artist's palette on a 16th century wood panel painting by portable and laboratory Raman instruments. Vibrational Spectroscopy 85: 62-70. DOI: 10.1016/j.vibspec.2016.03.027

Stojanović et al. 2015 — Stojanović, S.R., Gajić-Kvaščev, M.D., Damjanović, L.S. (2015) Spectroscopic study of an icon painted on wooden panel | [Spektroskopsko ispitivanje ikone slikane na drvenom nosiocu]. Hemijska Industrija 69(4): 387-393 (Bosnian). DOI: 10.2298/HEMIND140430053S

Striová et al. 2009 — Striová, J., Coccolini, G., Micheli, S., Lofrumento, C., Galeotti, M., Cagnini, A., Castellucci, E.M. (2009) Non-destructive and non-invasive analyses shed light on the realization technique of ancient polychrome prints. *Spectrochimica Acta - Part A: Molecular and Biomolecular Spectroscopy* **73**(3): 539-545. DOI: 10.1016/j.saa.2008.10.031

Szczepanowska and Fitzhugh 1999 — Szczepanowska, H., Fitzhugh, E.W. (1999) Fourteenth-century documents of the Knights of St. John of Jerusalem: Analysis of inks, parchment and seals. The Paper Conservator 23: 36-45. DOI: 10.1080/03094227.1999.9638615

Tarquini et al. 2020 — Tarquini, O., Pronti, L., Lorenzetti, E.G., Felici, A.C. (2020) Pigment identification on Campana reliefs from the Palatine Hill and Colosseum Valley in Rome. Journal of Cultural Heritage 43: 294-302. DOI: 10.1016/j.culher.2019.07.026

Tascon et al. 2017 — Tascon, M., Mastrangelo, N., Gallegos, D., Marte, F. (2017) Determination of materials and techniques involved in the mural paintings of San Miguel Church, Argentina. Journal of Raman Spectroscopy 48(10): 1356-1364. DOI: 10.1002/jrs.5223

Tempesta et al. 2018 — Tempesta, G., Porfido, C., Bellino, M., Monno, A. (2018) The "Exultet 1" of Bari: Multi-methodological approach for the study of a rare medieval parchment roll. Periodico di Mineralogia 87(2): 93-102. DOI: 10.2451/2018PM753

Tomasini et al. 2016 — Tomasini, E.P., Marte, F., Careaga, V.P., Landa, C.R., Siracusano, G., Maier, M.S. (2016) Virtuous colours for Mary. Identification of lapis lazuli, smalt and cochineal in the Andean colonial image of Our Lady of Copacabana (Bolivia). Philosophical Transactions of the Royal Society A: Mathematical, Physical and Engineering Sciences 374(2082): 20160047. DOI: 10.1098/rsta.2016.0047

Tsatsouli and Nikolaou 2017 — Tsatsouli, K., Nikolaou, E. (2017) The ancient Demetrias figurines: new insights on pigments and decoration techniques used on Hellenistic clay figurines. *Science and Technology of Archaeological Research* **3**(2): 341-357. DOI: 10.1080/20548923.2018.1424302

Uchida et al. 2012 — Uchida, E., Takubo, Y., Toyouchi, K., Miyata, J. (2012) Study on the pigments in the cruciform gallery of Angkor Wat, Cambodia. Archaeometry 54(3): 549-564. DOI: 10.1111/j.1475-4754.2011.00634.x

Uhlir et al. 2019 — Uhlir, K., Gironda, M., Bombelli, L., Eder, M., Aresi, N., Groschner, G., Griesser, M. (2019) Rembrandt's Old Woman Praying, 1629/30: A look below the surface using X-ray fluorescence mapping. X-Ray Spectrometry 48(4): 293-302. DOI: 10.1002/xrs.2985

Van Der Snickt et al. 2012 — Van Der Snickt, G., Janssens, K., Dik, J., De Nolf, W., Vanmeert, F., Jaroszewicz, J., Cotte, M., Falkenberg, G., Van Der Loeff, L. (2012) Combined use of Synchrotron Radiation Based Micro-X-ray Fluorescence, Micro-X-ray Diffraction, Micro-X-ray Absorption Near-Edge, and Micro-Fourier Transform Infrared Spectroscopies for Revealing an Alternative Degradation Pathway of the Pigment Cadmium Yellow in a Painting by Van Gogh. Analytical Chemistry 84(23): 10221-10228. DOI: 10.1021/ac3015627

Vanmeert et al. 2015 — Vanmeert, F., Vandersnickt, G., Janssens, K. (2015) Plumbonacrite identified by X-ray powder diffraction tomography as a missing link during degradation of red lead in a Van Gogh painting. Angewandte Chemie - International Edition 54(12): 3607-3610. DOI: 10.1002/anie.201411691

Vanmeert et al. 2018 — Vanmeert, F., De Nolf, W., Dik, J., Janssens, K. (2018) Macroscopic X-ray powder diffraction scanning: possibilities for quantitative and depth-selective parchment analysis. Analytical Chemistry 90(11): 6445-6452. DOI: 10.1021/acs.analchem.8b00241

Vanmeert et al. 2019 — Vanmeert, F., De Keyser, N., Van Loon, A., Klaassen, L., Noble, P., Janssens, K. (2019) Transmission and reflection mode macroscopic X-ray powder diffraction imaging for the noninvasive visualization of paint degradation in still life paintings by Jan Davidsz. de Heem. Analytical Chemistry 91(11): 7153-7161. DOI: 10.1021/acs.analchem.9b00328

Venuti et al. 2020 Venuti, V., Fazzari, B., Crupi, V., Majolino, D., Paladini, G., Morabito, G., Certo, G., Lamberto, S., Giacobbe, L. (2020) In situ diagnostic analysis of the XVIII century Madonna della Lettera panel painting (Messina, Italy). Spectrochimica Acta - Part A: Molecular and Biomolecular Spectroscopy 228: 117822. DOI: 10.1016/j.saa.2019.117822

Vettori et al. 2019 Vettori, S., Bracci, S., Cantisani, E., Conti, C., Ricci, M., Caggia, M.P. (2019) Archaeometric and archaeological study of painted plaster from the Church of St. Philip in Hierapolis of Phrygia (Turkey). Journal of Archaeological Science: Reports 24: 869-878. DOI: 10.1016/j.jasrep.2019.03.008

Vlachou-Mogire et al. 2020 Vlachou-Mogire, C., Moretti, P., Monico, L., Chieli, A., Iwanicka, M., Targowski, P., Detalle, V., Bourguignon, E., Laclavetine, K., Mirambet, F., Tong, T., Pinchin, S. (2020) A non-invasive multi-technique investigation of Banqueting House Whitehall Rubens ceiling paintings. Microchemical Journal 156: 104797. DOI: 10.1016/j.microc.2020.104797

Wagner et al. 2019 Wagner, B., Kępa, L., Donten, M., Wrzosek, B., Żukowska, G.Z., Lewandowska, A. (2019) Laser ablation inductively coupled plasma mass spectrometry appointed to subserve pigment identification. Microchemical Journal 146: 279-285. DOI: 10.1016/j.microc.2018.12.061

Wallert 1995 Wallert, A. (1995) Unusual pigments on a greek marble basin. *Studies in Conservation* **40**(3): 177-188. DOI: 10.1179/sic.1995.40.3.177

Wang et al. 2014 Wang, N., He, L., Egel, E., Simon, S., Rong, B. (2014) Complementary analytical methods in identifying gilding and painting techniques of ancient clay-based polychromic sculptures. Microchemical Journal 114: 125-140. DOI: 10.1016/j.microc.2013.12.011

Wang et al. 2020 Wang, X., Zhen, G., Hao, X., Tong, T., Ni, F., Wang, Z., Jia, J., Li, L., Tong, H. (2020) Spectroscopic investigation and comprehensive analysis of the polychrome clay sculpture of Hua Yan Temple of the Liao Dynasty. Spectrochimica Acta - Part A: Molecular and Biomolecular Spectroscopy 240: 118574. DOI: 10.1016/j.saa.2020.118574

Wei et al. 2010 Wei, S., Schreiner, M., Guo, H., Ma, Q. (2010) Scientific investigation of the materials in a Chinese ming dynasty wall painting. International Journal of Conservation Science 1(2): 99-112.

Wei et al. 2012 Wei, S., Ma, Q., Schreiner, M. (2012) Scientific investigation of the paint and adhesive materials used in the Western Han dynasty polychromy terracotta army, Qingzhou, China. *Journal of Archaeological Science* **39**(5): 1628-1633. DOI: 10.1016/j.jas.2012.01.011

Wertz et al. 2019 Wertz, J.H., Quye, A., France, D. (2019) Turkey red prints: identification of lead chromate, Prussian blue and logwood on Turkey red calico. Conservar Patrimonio 31: 31-39. DOI: 10.14568/cp2018019

Zannini et al. 2012 Zannini, P., Baraldi, P., Aceto, M., Agostino, A., Fenoglio, G., Bersani, D., Canobbio, E., Schiavon, E., Zanichelli, G., De Pasquale, A. (2012) Identification of colorants on XVIII century scientific hand-coloured print volumes. Journal of Raman Spectroscopy 43(11): 1722-1728. DOI: 10.1002/jrs.4119

Želinska et al. 2018 Želinska, J., Kopecka, I., Svobodova, E., Milovska, S., Hurai, V. (2018) Stratigraphic EM-EDS, XRF, Raman and FT-IR analysis of multilayer paintings from the main Altar of the St. James Church in Levoča (Slovakia). Journal of Cultural Heritage 33: 90-99. DOI: 10.1016/j.culher.2018.03.006

Zhao et al. 2020 Zhao, F., Sun, M., Tie, F., Wu, C., Zhang, X., Mu, X. (2020) Inlaid materials and techniques of an ancient Chinese bronze mirror. European Physical Journal Plus 135(8): 666. DOI: 10.1140/epjp/s13360-020-00634-y

Zhou et al. 2020 Zhou, Z., Shen, L., Wang, N., Ren, X., Yang, J., Shi, Y., Zhang, H. (2020) Identification of Organic Materials Used in Gilding Technique in Wall Paintings of Kizil Grottoes. Chemistry Select 5(2): 818-822. DOI: 10.1002/slct.201903688

APPENDIX 2. EXCERPTS FROM JUSSEN, E. (SEPTEMBER 1887) *WHITE-LEAD INDUSTRY IN AUSTRIA. REPORTS FROM THE CONSULS OF THE UNITED STATES*, 83. WASHINGTON: GOVERNMENT PRINTING OFFICE, PP. 413-419

Excerpts from Jussen, E. (September 1887) *White-lead industry in Austria. Reports from the Consuls of the United States*, 83. Washington: Government Printing Office, pp. 413-419.

Page 413 – on the origin of the name.

"(…) *but the best quality of white lead still bears the name of "Kremserweiss." "Cremnitz" weiss, or white, is an appellation unknown to the trade here, and doubtless originated in the similarity of the two names of Krems and Cremnitz (or Kremnitz). Kremnitz (or Cremnitz) is a small city (population, 8,550) in the Bars Comitat in Hungary, and I am informed by Austrian dealers that no white lead whatever is manufactured there. Dr. I Szabo, professor of geology at the University of Budapest, states, in answer to an inquiry made by Consul Sterne, that white lead has never been manufactured at Kremnitz in any quantity whatever. Mr. Henry Sterne, United States consul at Budapest, informs me further that the Hungarian dealers in white lead state that no white lead is manufactured at Kremnitz, and that Kremserweiss, but not Kremnitzerweiss, is known in the Hungarian market. The city of Kremnitz is known for the gold and silver mines situate in the immediate vicinity, and particularly for the so-called Kremnitzer ducats coined at the Kremnitzer mint. Kremnitzer white lead is clearly an American misnomer. Another grade of white lead is called Venetianerweiss (Venetian white) because at some remote period, so remote that no definite recollection or tradition of the exact period exists, an excellent quality of white lead was manufactured at Venice, and a particular grade of the lead still retains the appellation. For a similar reason a certain shade of red is called Venetian red*."

Page 416 – on the quality of different white leads and their adulteration

"*The manufacturers also claim that they do not adulterate their product with other and cheaper white substances, and that they add only the purest sulphate of baryta (Schwerspath) for the purpose of producing the qualities known in the market as Venetian, Holland, and Hamburg white lead. The fact that cheaper qualities of white lead are imported into Austria-Hungary (1,969 meter centners during 1886, as above stated) seems to be strong circumstantial evidence in proof of the honest process of manufacture contended for by Austrian producers. They charge that German manufacturers are in the habit of adulterating their product with all sorts of cheap ingredients—terra alba, for instance—and that for this reason Austrian white lead is in greater and better demand than the German article. This demand is supplied entirely by three white-lead factories situate at Klagenfurth, of which that of Mr. Paul Herbert is the largest. Possibly white lead may be manufactured at other points, but if so, the quantity produced is so very inconsiderable that the Vienna dealers have no knowledge whatever of its existence*."

Page 418 – on the methods and processes used in white lead manufactures.

"*The following methods are also employed in Europe in the manufacture of white lead, viz: Lothman's process or method (see London Journal of Arts, September, 1847, p. 92); Gannal's method; Fourmetier's method; Pattinson's method; Chenot's method; method employed in the white-lead factory of Theodor Lefebre & Co., in Moulins-Lille, Departement du Nord, France; Barreswill's method (see Journal de Pharmacie, October, 1882, p. 291). All of which methods and processes are particularly described in H. Ludwig's Hand-Book for the Manufacture of White Lead and Sugar of Lead, second edition. Weimar, 1854, B. Fred. Voigt, printer and publisher*."

TABLE S1. DMS COORDINATES (GOOGLE MAPS, MINDAT, WIKI GEOTEMPLATE) OF THE LOCALITIES AND PLACES MENTIONED IN THE TEXT

Place/Locality	**County/Country**	**DMS coordinates**
Adelaide Mine	Dundas district, Tasmania (Australia)	41°53'7" S; 145°25'44" E
Akrotiri	Santorini (Thera) Island (Greece)	36°21′5″ N; 25°24′13″ E
Alexandria	Egypt	31°12′0″ N; 29°55′0″ E
Alhambra complex in Granada	Andalusia (Spain)	37°10′37″ N; 3°35′24″ W
Altemannfels	Baden-Württemberg (Germany)	47°47'19" N; 7°40'33" E
Angkor Watcomplex	Cambodia	13°24′45″ N; 103°52′0″ E
Antim Monastery in Bucharest	Romania	44°25′35″ N; 26°5′38″ E
Auguste Victoria mines inHüls	Nordrhein-Westfalen (Germany)	51°22′20″ N; 6°30′40″ E
Baia Mare Mining District	Maramureș (Romania)	47°39′1″ N; 23°35′25″ E
Baratti Beach	Tuscany (Italy)	42°59′53″ N; 10°31′3″ E
Băița Bihor	Bihor County (Romania)	46°29′3″ N; 22°33′41″ E
Basilica of Saints John and Paul on Caelian Hill, in Rome	Italy	41°53′11″ N; 12°29′32″ E
Bisbee	Arizona (USA)	31°26′53″ N; 109°55′42″ W
Bleialf	Rheinland-Pfalz (Germany)	50°14′22″ N; 6°17′11″ E
Bleiberg	Carinthia (Austria)	46°38′0″ N; 13°40′0″ E
Bologna	Italy	44°29′38″ N; 11°20′34″ E
Borieva Mine in the Madan ore field	Bulgaria	41°27'0" N; 24°58'0" E
Bound Cliffs[3]	Cornwall (UK)	50°35'48" N; 4°47'56" W
Broken Hill	New South Wales (Australia)	31°57′24″ S; 141°28′4″ E
Bunker Hill Mine	Idaho (USA)	47°32′28″ N; 116°8′53″ W
Caldbeck Fells	Cumbria (UK)	54°41'25" N; 3°4'37" W
Cerro Gordomines	California (USA)	36°32′16″ N; 117°47′42″ W
Challacollo Mine in Iquique	Atacama Desert (Chile)	20°57'12" S; 69°19'55" W
Champallement	Bourgogne-Franche-Comté (France)	47°13'59" N; 3°29'23" E
Chunyang Temple	Shanxi Province (China)	23°5′16″ N; 113°17′22″ E
Château de Germolles	Burgundy (France)	46°48′21″ N; 4°45′5″ E
Church of the Cordeliers in Fribourg	Switzerland	46°48′26″ N; 7°9′39″ E
Church of Our Lady of Egmanton in Egmanton	York (UK)	53°12′44″ N; 0°53′59″ W
Church of San Fedele in Milan	Italy	45°28′0″ N; 9°11′29″ E
Church of San Miguel (de Arcángel) in Buenos Aires	Argentina	34°36'26" S; 58°22'45" W
Church of S. Lorenzo in Laino	Como Province (Italy)	45°58′59″ N; 9°4′38″ E
Church of S. Maria deiGhirli in Campione d'Italia	Lugano Region (Italy)	45°58'4"N; 8°58'7"E
Church of S. Maria Assunta in Puria	Como Province (Italy)	46°1′58″ N, 9°3′26″ E
Church of Sant'Andrea in Mantua	Italy	45°9′32″ N; 10°47′39″ E
Church of St. Gallus in Kuřívody	Northern Bohemia (Czech Republic)	50°35'10" N; 14°48'12" E
Clara Mine in Oberwolfach, Schwartzwald	Baden-Württemberg (Germany)	48°22′47″ N; 8°13′43″ E
Cromford (near Matlock)	Derbyshire (UK)	53°6′29″ N; 1°33′40″ W
Cucamonga Peak	California (USA)	34°13′22″ N; 117°35′7″ W
Dagaoxuan (Da Gaoxuan) Taoist Temple in Beijing	China	39°55'27" N; 116°23'36" E
DarrehZanjir	Yazd Province (Iran)	31°43'0" N; 54°12'33" E
Darwin	California (USA)	36°16′5″ N; 117°35′30″ W
Dazu Rock Carvings in Chongqing	Chongqing (China)	29°42′4″ N; 105°42′18″ E
Deer Hills Mine, in Caldbeck Fells Mining Region	Cumbria (UK)	54°43'10" N; 3°3'59" W
Delos Island	Cyclades Archipelago (Greece)	37°23′36″ N;25°16′16″ E
Dundas near Zeehan	Zeehan District, Tasmania (Australia)	41°52′31″S; 145°25′15″E
Elephantine Island on Nile	Egypt	24°5′20″ N; 32°53′20″ E
Endeavor Mine in Elura	New South Wales (Australia)	31°24'19" S; 145°47'49" E
Eureka Mine, Castell-Estaó	Catalonia (Spain)	42°23'9" N; 0°57'26" E
Feng Hui (Fenghui) Tomb	Shaanxi Province (China)	34°15'58" N; 108°47'40" E
Ferrara Cathedral in Ferrara	Italy	44°50′8″ N; 11°37′13″ E
Freiberg	Saxony (Germany)	50°54′43″ N; 13°20′34″ E
Friedrichssegen Mine	Rhineland-Pfalz (Germany)	50°18′9″ N; 7°40′38″ E
Genna Zinkhütte	Nordrhein-Westfalen (Germany)	51°21'39" N;7°37'2" E
Glückauf Mineat Sondershausen	Thuringia **(**Germany**)**	51°21'18" N; 10°55'1" E
Goa Cathedral in Old Goa	Goa (India)	15°30′14″ N; 73°54′46″ E
Goiabeira	Minas Gerais (Brazil)	18°58′55″ S; 41°13′22″ W
Grand Deposit Mine	New Mexico (USA)	39°36'55" N; 114°33'34" W

[3]Stanley et al. (1991)

Happy Jack Mine (Lady Bee Mine)	Western Australia (Australia)	29°56'36" S; 121°7'34" E
Harstigen Mine	Värmland County (Sweden)	59°47'7" N, 14°18'50" E
Hua Yan Temple in Datong	Shanxi Province (China)	40°5′56″ N; 113°18′5″ E
Imperial Taidong Tomb	Hebei Province (China)	39°20′0″ N; 115°13′0″ E
Johanngeorgenstadt	Sachsen (Germany)	50°25′52″ N; 12°43′26″ E
Kalushdeposit	Ukraine	49°2′39″ N; 24°21′35″ E
Katowice	Poland	50°15′35″ N; 19°1′18″ E
Klagenfurt	Carinthia (Austria)	46°37′0″ N; 14°18′0″ E
Kombat Mine, in Tsumeb	Oshikoto Region (Namibia)	19°43′0″ S; 17°43′0″ E
Koper	Slovenia	45°33′0″ N; 13°44′0″ E
Kos Island	Dodecanese, South Aegean Sea (Greece)	36°51′0″ N; 27°14′0″ E
Kosminsky Mine	Zeehan District, Tasmania (Australia)	41°52'54" S; 145°26'25" E
Kostol'any pod Tribečom	Nitra Region (Slovakia)	48°25′0″ N; 18°15′0″ E
Kröller-Müller Museum in Otterlo	The Netherlands	52°5′45″ N; 5°49′01″ E
La Cruz smelting in Linares	Andaluzia (Spain)	38°5′0″ N; 3°38′0″ W
Långban Mine	Sweden	59°51′0″ N; 14°15′0″ E
Laurion (Lavrion) mines in Lavrion Mining District	Attica (Greece)	37°46'34" N; 24°2'22" E
Leadhills in Larnakshire	Scotland (UK)	55°25'6" N; 3°45'36" W
Leadville	Colorado (USA)	39°15′0″ N; 106°17′30″ W
Legrena Cove in Lavrion Mining District	Attica (Greece)	37°39'39" N; 23°58'37" E
Les Molérats Mine[4]	Bourgogne (France)	46°58'8" N; 4°2'51" E
Longefay Mine	Rhône (France)	46°7'43" N; 4°30'35" E
Louvre Museum in Paris	France	48°51′40″ N; 2°20′11″ E
Magnet Mine	Dundas District, Tasmania (Australia)	41°26'31"S; 145°26'56" E
Mammoth-Saint Anthony Mine (now Tiger Mine)	Arizona (USA)	32°42′23″ N;110°41′05″ W
Margarita mines at Caracoles	Chile	23°1′12″ S; 69°0′36″ W
Masjid-iJame (Jameh) Mosque in Fahraj	Yazd Province (Iran)	31°45′36″ N; 54°34′48″ E
Matlock	Derbyshire (UK)	53°8′24″ N; 1°33′0″ W
Maui volcano	Hawaii (USA)	20°48′0″ N; 156°20′0″ W
Mauritshuis (museum), in The Hague	The Netherlands	52°4′50″ N; 4°18′52″ E
Mendip Hills	Somerset (UK)	51°18′0″ N; 2°44′0″ W
Merehead (now Torr Works) Quarry	Somerset (UK)	51°11′59″ N; 2°26′16″ W
Mex-Tex Mine	New Mexico (USA)	33°49'29" N; 106°21'57" W
Mežica	Slovenia	46°31′14″ N; 14°51′13″ E
MibladenMinig District	Drâa-Tafilalet Region (Morocco)	32°46'0" N; 4°37'59" W
Michael Mine in Weiler	Baden-Württemberg (Germany)	48°20'23" N; 7°58'6" E
Monteponi Mine, near Iglesias	Sardinia (Italy)	39°18'15" N; 8°30'20" E
MontevecchioMine, near Iglesias	Sardinia (Italy)	39°33′24″ N; 8°34′14″ E
Moschopolis (Voskopoia)	Albania	40°37′59″ N; 20°35′20″ E
Mont Saint-Hilaire	Quebec (Canada)	45°33′8″ N; 73°9′3″ W
Mt. Dikaios in Kos Island	Dodecanese, South Aegean Sea (Greece)	36°50′4″ N; 27°12′25″ E
Mt. Vesuvius	Naples (Italy)	40°49′0″ N; 14°26′0″ E
Royal Alcázars of Seville	Spain	37°23′2″ N; 5°59′29″ W
Nakhlak (Madan-e Nakhlak) Mine	Isfahan Province (Iran)	33°33'47" N; 53°50'42" E
Naples	Italy	40°50′42″ N; 14°15′30″ E
Nerchinsk	Zabaykalsky Krai (Siberia, Russia)	51°59′40″ N; 116°33′20″ E
American Museum of Natural History	Manhattan (New York, USA)	40°46′50″ N; 73°58′25″ W
Niedersachsen Potash Works in Wathlingen	Lower Saxony (Germany)	52°31'29" N; 10°8'16" E
Nishapur	Razavi Khorasan Province (Iran)	36°12′48″ N; 58°47′45″ E
Nontron	Region Nouvelle-Aquitaine (France)	45°31′46″ N; 0°39′43″ E
North Bend	Washington (USA)	47°29'38" N; 121°47'10" W
ObercallenbergQuarry	Saxony (Germany)	50°49′37″ N; 12°38′ 56″ E
Oberhütte	Saxony (Germany)	51°32'57" N; 11°32'47" E
Ojuela Mine near Mapimí	Durango (Mexico)	25°47′37″ N; 103°47′29″ W
One-Wood Monastery in Frâncești	Vâlcea County (Romania)	44°59′57″N; 24°11′23″E
Paddy's River Mine	Australian Capital Territory (Australia)	35°21'29" S; 148°57'13" E
Palatine Hill in Rome	Italy	41°53′18″ N; 12°29′13″ E
Palmyra	Homs Governorate (Syria)	34°33′33″ N; 38°16′25″ E
Parma Baptistery	Parma (Italy)	44°48′11″ N; 10°19′49″ E
Parys Mine (Island of Anglesey)	Wales (UK)	53°22′56″ N; 4°21′9″ W
Phoenixville	Pennsylvania (USA)	40°7′51″ N; 75°31′9″ W
Pierre Hardie Street in Metz	Grand Est Region (France)	49°7'9" N; 6°10'23" E
Pompeii	Italy	40°45′0″ N; 14°29′10″ E

[4]Thyéry (2014)

Powell Library at University of California	Los Angeles (USA)	34°4′18″ N; 118°26′ 32″ W
Preguiça Mine nearSobral da Adiça	Portugal	38°2'35" N; 7°17'45" W
Preobrazhenshy Mine, Berezovskoedeposit	Sverdlovsk Region (Russia)	56°53'59" N; 60°46'59" E
Příbram	Czech Republic	49°41′18″ N; 14°0′34″ E
Punta de Lobos	Tarapacá **(**Chile**)**	21°12'0"S; 70°5'0" W
Red Lead Mine	Dundas district Tasmania (Australia)	41°53'22" S; 145°25'51" E
Rila Monastery in Rila Mts.	Bulgaria	42°8′0″ N; 23°20′25″ E
Rome	Italy	41°53′0″ N; 12°30′0″ E
Royal Palace in Milan	Italy	45°27′48″ N; 9°11′28″ E
Sanctuary of Rho in Milan	Italy	45°32′0″ N; 9°2′0″ E
San Rossore at Pisa	Italy	43°43'28" N; 10°23'15"E
Santiago Church in Écija	Spain	37°32′16″ N; 5°4′46″ W
Sarrabus	Sardinia (Italy)	39°25′12″ N; 9°34′12″ E
Satsuma-Iwojima volcano	Japan	55°49′51″N; 160°19′33″ E
Schwartzwald (Black Forrest) Mountains	Baden-Württemberg (Germany)	~48°0′0″ N; ~8°0′0″ E
Seh-Changi Mine, nearNeyband	Khorassan (Iran)	32°32'50" N; 58°2'55" E
Seville Cathedral	Spain	37°23′9″ N; 5°59′35″ W
Shōsōin (Tōdai-ji) in Nara	Japan	34°41′31″ N; 135°50′19″ E
Siena Cathedral in Siena	Italy	43°19′4″ N; 11°19′44″ E
Silver Peak Marsh	Nevada (USA)	37°46'0" N; 117°35'28" W
Saint Nicholas Church in Şirineasa	Vâlcea County (Romania)	44°56′0″ N; 24°12′0″ E
Smyrna	Turkey	8°25′7″ N; 27°8′21″ E
St. Day	Cornwall (UK)	50°14'20" N; 5°11'2" W
St. George Church at Kostol'any pod Tríbečom	Nitra Region (Czech Republic)	48°24'55" N; 18°14'48" E
Stomio	Thessaly (Greece)	39°52′0″ N; 22°44′0″ E
St. Petersburg	Russia	59°56′15″ N; 30°18′31″ E
St. Stephan Chapel near Bolzano	Sud Tyrol (Italy)	46°36′1″ N; 10°49′30″ E
Strechau Castle	Styria (Austria)	47°31′42″ N; 14°19′3″ E
Sunshine#1 adit (Blanchard Mine), at Bingham	New Mexico (USA)	33°48'42" N; 106°22'30" W
Susanna Mine, at Leadhills in Lanarkshire	Scotland (UK)	55°25'24" N; 3°46'3" W
Swedish Museum of Natural History in Stockholm	Sweden	59°22′8″ N; 18°3′13″ E
Taxiarhis Church on Alibei-Adasi Island	Balikesir Province (Turkey)	39°19′59″ N; 26°39′29″ E
Tebtunis	Egypt	29°7′0″ N; 30°45′0″ E
TchahMilleh (ChahMileh) Mine	Isfahan Province (Iran)	33°25'56" N; 53°48'24" E
The Metropolitan Museum of Art in New York	New York (USA)	40°46′46″ N; 73°57′47″ W
Thorikos Bay, Lavrion Mining District	Attica (Greece)	37°44'12" N; 24°3'30" E
Thousand-Buddha Grotto near Guangyuan	Sichuan (China)	32°26′10″ N; 105°50′38″ E
Tiny-Arenas Mine	Sardinia (Italy)	39°24'30" N; 8°33'40" E
Tolbachik volcano	Kamchatka Peninsula (Russia)	55°49′51″N; 160°19′33″ E
Torr Works (former Merehead) Quarry	Somerset (UK)	51°11′59″ N; 2°26′16″ W
Touissit in Touissit-Bou Beker Mining District	Morocco	34°28'39" N; 1°45'54" W
Tsumeb Mine, in Tsumeb	Oshikoto Region (Namibia)	19°13'37" S; 17°43'39" E
Tsvetnoi Mine, Berezov ore deposit	Ural Mts. (Russia)	63°56′4″ N; 65°2′40″ E
Touissit Mine	Morocco	34°28′0″ N; 1°46′0″ W
Venice	Italy	45°26′15″ N; 12°20′9″ E
Vulcano Island	Aeolian Archipelago (Italy)	8°23′58″ N; 14°57′50″ E
Wadi El Natrun	Egypt	30°35′0″ N; 30°20′0″ E
Wadnaminga mines	South Australia	32°33'13" S; 140°12'28" E
West River Site at Zhangqiu	Shandong Province (China)	~36°41′35″ N; ~117°31′5″ E
Wheal Rose Mine	Cornwall (UK)	50°15′0″ N; 5°12′36″ W
Wolfsberg	Carinthia (Austria)	46°51′0″ N; 14°50′0″ E
Zimapan	Hildalgo (Mexico)	20°44'0" N; 99°23′0″ W

TABLE S2. TEXTS QUOTED IN TABLE 1 PROVIDED IN THE ORIGINAL LANGUAGE.

In text	*REFERENCE*	TEXT
P1	Plinius, *Naturalis Historia*, 33, 31, 95	*excoqui non potest, nisi cum plumbo nigro aut cum vena plumbi — **galenam** vocant —, quae iuxta argenti venas plerumque reperitur. et eodem opere ignium discedit pars in plumbum, argentum autem innatat superne, ut oleum aquis.*
P2	Plinius, *Naturalis Historia*, 33, 35, 106-109	*Fit in isdem metallis et quae vocatur **spuma argenti**. genera eius tria: optima quam chrysitim vocant, sequens quam argyritim, tertia quam molybditim. et plerumque omnes hi colores in isdem tubulis inveniuntur. probatissima est Attica, proxima Hispaniensis. chrysitis ex vena ipsa fit, argyritis ex argento, molybditis e plumbi ipsius fusura — quae fit Puteolis — et inde habet nomen.* *omnis autem fit excocta sua materia ex superiore catino defluens in inferiorem et ex eo sublata vericulis ferreis atque in ipsa flamma convoluta vericulo, ut sit modici ponderis. est autem, ut ex nomine intellegi potest, fervescentis et futurae materiae spuma. distat a scoria quo potest spuma a faece distare: alterum purgantis se materiae, alterum purgatae vitium est.* *quidam duo genera faciunt spumae, quae vocant scirerytida et peumenen, tertium molybdaenum in plumbo dicendam. spuma, ut sit utilis, iterum coquitur confractis tubulis ad magnitudinem anulorum. ita accensa follibus ad separandos carbones cineremque abluitur aceto aut vino simulque restinguitur. quodsi sit argyritis, ut candor ei detur, magnitudine fabae confracta in fictili coqui iubetur ex aqua addito in linteolis tritico et hordeo novis, donec ea purgentur.* *postea VI diebus terunt in mortariis, ter die abluentes aqua frigida et, cum dies desinat, calida, addito sale fossili in libram spumae obolo. novissimo die dein condunt in plumbeo vase. alii cum faba candida et tisana cocunt siccantque sole, alii in lana candida cum faba, donec lanam non denigret. tunc salem fossilem adiciunt subinde aqua mutata siccantque diebus XL calidissimis aestatis. nec non in ventre suillo in aqua coquunt exemptamque nitro fricant et ut supra terunt in mortariis cum sale. sunt qui non coquant, sed cum sale terant et adiecta aqua abluant.*
P3	Plinius, *Naturalis Historia*, 34, 54, 175-176	***Psimithium** quoque, hoc est **cerussam**, plumbariae dant officinae, laudatissimam in Thodo. fit autem ramentis plumbi tenuissimis super vas aceti asperrimi inpositis atque ita destillantibus. quod ex eo cecidit in ipsum acetum, arefactum molitur et cribratur iterumque aceto admixto in pastillos dividitur et in sole siccatur aestate. fit et alio modo, addito in urceos aceti plumbo opturatos per dies X derasoque ceu situ ac rursus reiecto, donec deficiat materia. quod derasum est, teritur et cribratur et coquitur in patinis misceturque rudiculis, donec rufescat et simile sandaracae fiat. dein lavatur dulci aqua, donec nubeculae omnes eluantur. siccatur postea similiter et in pastillos dividitur. vis eius eadem quae supra dictis, lenissima tantum ex omnibus, praeterque ad candorem feminarum. est autem letalis potu sicut spuma argenti. postea cerussa ipsa, si coquatur, rufescit.*
P4	Plinius, *Naturalis Historia*, 35, 19, 37	*Tertius e candidis colos est **cerussa**, cuius rationem in plumbi metallis diximus. fuit et terra per se in Theodoti fundo inventa Zmyrnae, qua veteres ad navium picturas utebantur. nunc omnis ex plumbo et aceto fit, ut diximus.*
P5	Plinius, *Naturalis Historia*, 35, 20, 38	*usta casu reperta est in incendio Piraeei **cerussa** in urceis cremata. hac primum usus est Nicias supra dictus. optima nunc Asiatica habetur, quae et purpurea appellatur. pretium eius in libras VI. fit et Romae cremato sile marmoroso et restincto aceto. sine usta non fiunt umbrae.*

D1	Dioscorides, *De Materia Medica (*Περὶ ὕλης ἰατρικῆς*)*, 5, 87 vel 102	**λιθάργυρος**· ἡ μέν τις ἐκ τῆς μολυβδίτιδος καλουμένης ἄμμου γεννᾶται, χωνευομένης ἄχρι τῆς τελείας ἐκπυρώσεως, ἡ δὲ ἐξ ἀργύρου ἡ δὲ ἐκ μολύβδου. διαφέρει δὲ ἡ Ἀττική, δευτερεύει δὲ ἡ Σπάνη, μεθ' ἃς ἡ ἐν Δικαιαρχίᾳ καὶ Σικελίᾳ· πλείστη γὰρ ἐν τοῖς τόποις ‹τούτοις› γεννᾶται μολυβῶν ἐλασμάτων [2] ἐκφλογουμένων. καλεῖται δὲ ἡ μὲν ξανθὴ καὶ στίλβουσα χρυσῖτις, ἥτις ἐστὶ κρείττων, ἡ δὲ πελιὰ ἀργυρῖτις, ἡ δὲ ἐκ τοῦ ἀργύρου σκαλαυθρῖτις. δύναμιν δὲ ἔχει στυπτικήν, μαλακτικήν, ψυκτικήν, παρεμπλαστικήν, κοιλωμάτων πληρωτικήν, σταλτικὴν τῶν ἐκσαρκούντων καὶ ἀπουλωτικήν. [3] καύσεις δὲ αὐτὴν οὕτως· κατακόψας εἰς καρύων μεγέθη ‹καὶ› ἐπιθεὶς ἐπ' ἄνθρακας, ἐκριπίσας τε ἄχρι πυρώσεως καὶ περιμάξας τὴν περικειμένην ἀκαθαρσίαν ἀποτίθεσο. ἔνιοι δὲ ὄξει ἢ οἴνῳ σβεννύντες αὐτὴν ἐπὶ τρὶς πάλιν καίουσι, καὶ ταῦτα ποιοῦντες ἀποτίθενται. πλύνεται δὲ ὡς ἡ καδμεία. [4] λευκαίνεται δὲ οὕτως· λαβὼν τῆς ἀργυρίτιδος λεγομένης, εἰ δὲ μή γε, τῆς ἄλλης θραῦσον εἰς μεγέθη κυάμων ὅσον χοίνικα Ἀττικήν, βαλών τε εἰς καινὴν χύτραν ἐπίχει ὕδωρ, προσεμβάλλων πυρῶν λευκῶν χοίνικα. καὶ ἰδίᾳ ἐν ὀθονίῳ καθαρῷ ἀραιῷ κριθῶν δράκα ‹δήσας› ἀπὸ τοῦ ὠτὸς τῆς κύθρας κρέμασον, [5] ἕψε τε, ἕως ἂν ῥαγῶσιν αἱ κριθαί. εἶτα κατεράσας πάντα εἰς κρατῆρα πλατύστομον, τοὺς μὲν πυροὺς ῥῖψον χωρίσας, τὴν δὲ λιθάργυρον ἐπιχέας ὕδωρ πλῦνε βιαίως ταῖς χερσὶ προστρίβων ἅμα, εἶτα ἀνελόμενός τε αὐτὴν καὶ ξηράνας τρῖβε ἐν θυίᾳ Θηβαικῇ ἐπιχέων θερμὸν ὕδωρ, ἕως ἂν διαλυθῇ, καὶ ἀπηθήσας τὸ ὕδωρ πάλιν τρῖβε δι' ὅλης τῆς ἡμέρας· εἰς ἑσπέραν δὲ ἐπιχέας ὕδωρ θερμὸν ἔασον, καὶ πρωὶ ἀπηθήσας ἄλλο ἐπίχει καὶ ἀπήθει [6] τῆς ἡμέρας τρίς· τοῦτο ποίει ἐπὶ ἡμέρας ἑπτά. εἶτα μείξας τῇ μνᾷ τῆς λιθαργύρου ἁλῶν ὀρυκτῶν ε΄, θερμόν τε παραχέων λέαινε τρὶς τῆς ἡμέρας, ἀπηθῶν καὶ μειγνὺς ὕδωρ. ὅταν δὲ λευκὴ γένηται, θερμὸν ἐπιχέων τὸ αὐτὸ ποίει, ἄχρι ἂν μηδεμίαν ἔμφασιν ἁλυκότητος ἔχῃ, καὶ ξηράνας ‹ἐν› ὀξυτάτῳ [7] ἡλίῳ προεκβάλλων τὴν ἰκμάδα ἀποτίθεσο. ἢ λαβὼν τῆς ἀργυρίτιδος μνᾶν μίαν λέανον ἐπιμελῶς, καὶ τρίψας μεῖξον ἁλῶν τριπλάσιον λείων ὀρυκτῶν, καὶ βάλε εἰς καινὴν χύτραν, ἐπιχέας τε ὕδωρ ὥστε ὑπερέχειν κίνει ἑκάστης ἡμέρας πρωὶ καὶ δείλης, προσεπιχέας ὕδωρ μηδὲν τοῦ πρώτου ἀποχέων, καὶ ποίει τοῦτο ἐπὶ ἡμέρας τριάκοντα· μὴ κινουμένη γὰρ ἀποστρακοῦται. [8] μετὰ δὲ ταῦτα ἀποχέας πραέως τὴν ἅλμην, ἐν Θηβαικῇ θυίᾳ τὴν λιθάργυρον λέαινε, καὶ βαλὼν αὐτὴν εἰς κεραμεοῦν ἀγγεῖον ἐπιχέας τε ὕδωρ κίνει ταῖς χερσὶν ἐπιμελῶς, ἀποχέων τὸ πρῶτον καὶ ἕτερον ἐπιχέων, ἄχρι οὗ ἂν μηδεμίαν ἔμφασιν τῆς ἁλυκότητος ἔχῃ· εἶτα ἀποχέας τὸ λευκὸν τῆς **λιθαργύρου** εἰς ἄλλο ἀγγεῖον ἀνάπλασσε τροχίσκους καὶ ἀπόθου εἰς μολυβῆν [9] πυξίδα.
D2	*Dioscorides, De Materia Medica (*Περὶ ὕλης ἰατρικῆς*)*, 5, 88 vel 103	**[88] ψιμύθιον** δὲ γίνεται οὕτως· εἰς πιθάκνην πλατύστομον ἢ κεραμεᾶν γάστραν ἐγχέας δριμύτατον ὄξος ἀπέρεισαι μολυβδίνην πλίνθον ἐπὶ τὸ στόμα τοῦ κεραμίου, προυποκειμένου καλαμίνου ῥίπου, ἄνωθέν τε αὐτῆς ἐπίρριψον σκεπάσματα πρὸς τὸ μὴ διαπνεῖσθαι τὸ ὄξος· ὡς δ' ἂν καταρρυεῖσα διαπέσῃ, τὸ μὲν ἐπαιωρούμενον καὶ καθαρὸν ὑγρὸν ἀπηθητέον, τὸ δὲ γλοιῶδες εἰς ἀγγεῖον ἐγχυτέον καὶ ξηραντέον ἐν ἡλίῳ. εἶτα ἀλεστέον ἐν χειρομυλίῳ ἢ λεαντέον ἄλλως καὶ σηστέον, καὶ μετὰ ταῦτα τὸ λοιπὸν τοῦ στερεμνίου λεπτοποιητέον καὶ σηστέον, ἐναλλάξ τε τὰ αὐτὰ καὶ τρίτον καὶ τέταρτον ποιητέον. ἄμεινον δέ ἐστι τὸ πρῶτον ἀποσησθέν, ὃ καὶ εἰς τὰς ὀφθαλμικὰς παραλημπτέον δυνάμεις, δευτερεύει δὲ τὸ ἐχόμενον καὶ κατὰ τάξιν τὰ λοιπά. τινὲς δὲ κατὰ μέσον τὸ ἀγγεῖον κατερείσαντες ‹ξύλον›, τὸν ῥῖπον ἐπιτιθέασιν ὡς μὴ ψαύειν τοῦ ὄξους, τὸ δὲ στόμα αὐτοῦ πωμάσαντες καὶ περιχρίσαντες ἐῶσι καὶ δι‹ὰ ι΄› ἡμερῶν ἀφαιρούμενοι τὸ πῶμα ἐπισκοποῦνται· ὅταν δὲ διαλυθῇ, τὰ ἄλλα ποιοῦσιν ὁμοίως τοῖς προειρημένοις. εἰ δὲ ἀναπλάσαι θέλοι τις αὐτό, ὄξει δριμεῖ φυρατέον καὶ οὕτως ἀναπλαστέον καὶ ξηραντέον ἐν ἡλίῳ. θέρους μέντοι ἐργαστέον τὰ προειρημένα· οὕτως γὰρ λευκὸν καὶ ἐνεργὲς γίνεται. σκευάζεται δὲ καὶ χειμῶνος, τῶν πιθακνῶν ὑπεράνω τῶν ἰπνῶν τῶν βαλανείων τιθεμένων ἢ καμίνων· ἡ γὰρ ἀναφερομένη θερμασία τὸ αὐτὸ δρᾷ τῷ ἡλίῳ. κάλλιστον δὲ ἡγητέον τὸ ἐν Ῥόδῳ σκευασθὲν ἢ ἐν Κορίνθῳ ἢ ἐν Λακεδαίμονι, δευτερεύει δὲ τὸ ἐκ Δικαιαρχίας. ὀπτητέον δὲ αὐτὸ τὸν τρόπον τοῦτον· ἐπ' ἀνθράκων πεπυρωμένων θεὶς ὄστρακον καινόν, μάλιστα Ἀττικόν, ἔμπασον λεῖον τὸ ψιμύθιον καὶ κίνει συνεχῶς· ὅταν δὲ τῇ χρόᾳ ἔνσποδον

		ὑπάρχῃ, ἀνελόμενος ψῦχε καὶ χρῶ. καῦσαι δὲ θέλων εἰς λοπάδα κοίλην λεῖον ἀπόδος, ἐπιθείς τε ἐπὶ τοὺς ἄνθρακας νάρθηκι κίνει, ἕως ἂν τὴν χρόαν ἐοικὸς **σανδαράκῃ** γένηται καὶ ἀνελόμενος χρῶ. τὸ δὲ οὕτως σκευασθὲν σάνδυξ ὑπό τινων προσαγορεύεται. πλύνεται δὲ τὸ ψιμύθιον ὁμοίως ‹τῇ› καδμείᾳ. δύναμιν δὲ ἔχει ψυκτικήν, ἐμπλαστικήν, μαλακτικήν, πληρωτικήν, λεπτυντικήν, ἔτι δὲ πράως κατασταλτικὴν ὑπεροχῶν καὶ κατουλωτικήν, μειγνύμενον κηρωταῖς καὶ λιπαραῖς ἐμπλάστροις καὶ τροχίσκοις· ἔστι δὲ καὶ τῶν ἀναιρετικῶν.
T1	*Theophrastus,* Περὶ λίθων (*De Lapidibus*), 55-57	ταῦτά τε δὴ τέχνῃ γίνεται καὶ ἔτι τὸ **ψιμύθιον**. τίθεται γὰρ μόλυβδος ὑπὲρ ὄξους ἐν πίθοις ἡλίκον πλίνθος. ὅταν δὲ λάβῃ πάχος, λαμβάνει δὲ μάλιστα ἐν ἡμέραις δέκα, τότ’ ἀνοίγουσιν, εἶτ’ ἀποξύουσιν ὥσπερ εὑρῶτά τινα ἀπ’ αὐτοῦ, καὶ πάλιν, ἕως ἂν καταναλώσωσι. τὸ δ’ ἀποξυόμενον ἐν τριπτῆρι τρίβουσι καὶ ἀφηθοῦσιν ἀεί, τὸ δ’ ἔσχατον ὑφιστάμενόν ἐστι τὸ ψιμύθιον. παραπλησίως δὲ καὶ ὁ ἰὸς γίνεται· χαλκὸς γὰρ ἐρυθρὸς ὑπὲρ τρυγὸς τίθεται καὶ ἀποξύεται τὸ ἐπιγινόμενον αὐτῷ, ‹ἐπεὶ› ἐπιφαίνεται γάρ ὁ ἰός.
V1	*Vitruvius, De Architectura,* 7, 12, 1-2	*De **cerussa** aerugineque quam nostri aerucam vocitant non est alienum quemadmodum comparetur dicere. Rhodo enim doliis sarmenta conlocantes aceto suffuso supra sarmenta conlocant plumbeas massas, deinde ea operculis obturant ne spiramentum emittatur. post certum tempus aprientes inveniunt e massis plumbeis cerussam. eadem ratione lamellas aereas conlocantes efficiunt aeruginem quae **aeruca** appellatur. cerussa vero cum in fornace coquitur, mutato colore ad ignem efficitur **sandaraca**. id autem incendio facto ex casu didicerunt homines, et ea multo meliorem usum praestat quam quae de metallis per se nata foditur*.
E1	*(H)Eraclius, De coloribus et de artibus Romanorum,* 1, 36	*Quomodo fit **cerusa**, et de ipsa **rubeum minium**.* *Si vis facere rubeum minium, vel etiam album, qui cerusa dicitur, accipe laminas plumbeas, et mitte in ollam novam, et sic imple illam ollam fortissimo aceto, et cooperi, et mitte in aliquo calido loco, et sie uno mense dimitte; et tunc aperies ollam, et quod inveneris in circuitu laminarum plumbearum mitte in aliam ollam, et pone super ignem, et semper movebis ipsum colorem, donec efficiatur albus sicut nix, et tunc tolles ab igne, et sumes de ipso colore quantum vis, et iste color vocatur cerusa; reliquam partem pone super ignem, et semper movebis donec efficiatur rubeum minium. Propterea moneo ut moveas, quod si non moveris, semper iterum vertetur in album plumbum, et sic tolle ab igne, et ipsam ollam dimitte refrigerari.*
BM1	Bologna Manuscript 2861 (15th century AD) *Segreti per colori*	*Tollj lamine de piombo et metile di / sop(ra) alo vapore de lo acet(o) fortissi(m)o / i(n) uno vaso et cop(ri)lo b(e)n(e) cu(m) luto et / metilo socto lo litamj p(er) doi me / si poi rade la matheria ch(e) e la bia/cha ch(e) trovaraj sop(ra) ale laminj et / fa p(er) lo sop(ra)dito mo(do) p(er) i(n)fino ch(e) son(n)o / (con)su(n)te.*
BM2		*M272. A fare vetrio giallo p(er) patre nostro o ambre.* *Tollj pio(m)bo l(i)br(e) .j. stagno l(i)br(e) doj. et fundi et calcina et fa vetrio p(er) patrenostre.* *M273. A fare zallolino p(er) dipe(n)giare.* *Havve l(i)br(e) doi de q(ue)sto stagno et piombo / calcinat(o) et doi l(i)br(e) de questo vetrio / da patrenostrj et doi l(i)br(e) et ½ de minio / et meza l(i)br(a). de rena de valdarno / sotilme(n)te pista et mecti i(n) fornac(e) et / fa affinare et s(e)ra p(er)fecto.*
PZ1	Andrea Pozzo, *Prospettiva de pittori e architetti*	*Giallolino di fornace* *Chiamasi in Roma giallolino di Napoli. Io l’ho adoprato a fresco, e si è conservato: ma non mi sono mai cimentato di esporlo all’aria* *Colori contrarij alla calce , e che non si possono adoprare nelle pitture a fresco* *Biacca, minio, lacca di Venetia, lacca fine, verde rame, verde azzurro, verde porro, verde in canna, giallo santo, giallolino di Fiandra, orpimento, indico, nero d’osso, biadetto*

MA1	Marcucci (1816)	*il metodo per ottenerlo, e di prendere parti 12 di biacca di Plaiter, e di antimonio diaforetico (o ossido di antimonio bianco per via di nitro) parti due di allume brugiato (ossia solfato di alumina; levatagli una porzione di aqua di cristallizzazione), parte mezza di sale ammoniaco (o muriato di ammoniaca), si fa il tutto in polvere in un mortar di pietra, e posto in vaso di terra, si pone in una furnace per tre ore a calcinarlo; freddo il vaso si macina il giallo, per serbarlo all uso*.
VA1	Vauquelin 1809	*Le procédé pour décomposer le chromate de fer est indiqué avec détail, et consiste principalement à n'employer qu'une demi-partie de nitre contre une de chromate. Pour obtenir l'oxide de chrome bien pur, et d'une très-belle couleur, il suffit de chauffer fortement dans un cornue de grès, bien hutée, le chromate de mercure pur, jusqu'à ce qu'il ne se dégage plus d'oxigène, et de soutenir le feu d'autant plus long - tems que l'on désire obtenir une nuance moins foncée.*
NO1	*Nouveau dictionnaire d'histoire naturelle appliquée aux arts. Tome XXVII*	L'acide chromique et l'oxyde de plomb existent réunis dans la nature. Le chromate de plomb natif est cristallisé et de la couleur rouge-orange la plus éclatante. Le chromate artificiel est dun beau jaune, et sert dans la peinture sur toile, sur porcelaine et sur bois. On l'obtient en décomposant le chromate de potasse par l'acétate de plomb.
NO2		[pp. 67-68] PLOMB CHROMATÉ (*Id.*, Haüy, Delam., Bourn, etc.; *Plomb spathique rouge*, Pallas, Lehmann; *Minera plumbi rubra*, Wall.; *Oxyde de plomb spathique rouge*, de Born; *Plomb rouge et oxyde* ou *chaux de plomb rouge*, Macquart; *Chromate de plomb*, Vauquel ; *Roth bleierz*, Wern., Karst.; *Kallochrom*, Hausm.; *Red Lead ore* ou *chromate of Lead*, James.). Le plomb chromaté, vulgairement nommé *plomb rouge de Sibérie*, est un élégant minéral, remarquable par sa belle couleur rouge orangée ou bien aurore; sa poussière, néanmoins, est d'un jaune citrin ou verdâtre, et quelquefois roussâtre. Il est presque toujours cristallisé en prismes brillans, allongés au sommet, et dont les formes sont extrêmement difficiles à saisir; quelquefois il est en petites masses, en veinules et en incrustations; il est éclatant. Sa cassure est feuilletée dans le sens longitudinal des prismes, et vitreuse dans le sens transversal. Il est translucide et même demi-transparent, ou très-rarement transparent. Il n'est pas dur, et se laisse briser facilement. Sa pesanteur spécifique s'élève à 6,026, selón Brisson , et à 5,750, suivant Bindheim. Exposé au chalumeau, il décrépite et fond en une scorie grise, et colore le verre de borax en vert. On le réduit en partie par le moyen de ce sel. Il ne fait point effervescence avec les acides. D'après MM. Vauquelin et Thénard, il se pose de: 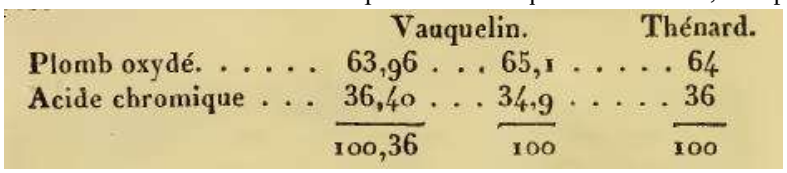 Vauquelin. Thénard. Plomb oxydé. . . . . 63,96 . . . 65,1 . . . . . 64 Acide chromique . . . 36,40 . . . 34,9 . . . . . 36 100,36 100 100

TABLE S3. MINERALS AND PIGMENTS OCCURRING IN PAINTINGS ALONG WITH LEAD-BASED COMPOUNDS (NAMES AS LITERALLY REPORTED BY AUTHORS). (*) indicates organic pigments. Mineral formulae according to IMA List of Minerals[5]. Mineral colours according to WebMineral database (http://webmineral.com/) and Handbook of Mineralogy. For pigments, the chromatic range and composition are based on Baer et al. (1972), Ponting (1973), Azouka et al. (1993), Clark et al. (1995), Kirby and White (1996), Ordonez and Twiley (1997), Eastaugh et al. (2004), Sandalinas and Ruiz-Moreno (2004), Kirby et al. (2005), López-Montalvo et al. (2017), Martin de Fonjaudran et al. (2017), Tamburini et al. (2017, 2018), Ploeger et al. (2019), various websites (Wikipedia; Pigments through Age) and references therein. Valid mineral species are shown in bold, pigments and other substances are shown in italics. This table has been build based on literature information, thus synonymous terms or vague characterisations reflect both the state of the art of the studies in this field and an overall nomenclature that has evolved over time, creating many (misleading) synonyms. [The references are provided below]

Name	Colour/s	Chemical formula and typical composition
	Inorganics	
Albite	White to grey, greenish gray, bluish green, reddish	$Na(AlSi_3O_8)$
Alum	Colorless, white	**K-Alum** $KAl(SO_4)_2{\cdot}12H_2O$
Anatase	Black, brown, reddish brown, grey, yellowish brown, light green, dark blue, grey, light yellow, indigo, light violet, rarely nearly colorless	TiO_2
Anglesite	White, blue, light grey	$Pb(SO_4)$
Anhydrite	Colorless, white, dark grey, grey, light blue, bluish white, mauve, rose, light brown, light violet	$Ca(SO_4)$
Antimony white	White, grey	**Sernamontite** Sb_2O_3
Antlerite	Green, emerald-green, light green, black, blackish green, black green, light green	$Cu^{2+}{}_3(SO_4)(OH)_4$
Aragonite	Colorless, white, yellowish white, grey, light yellow, reddish white, light blue, light violet, light green, light red	$Ca(CO_3)$
Arsenic trioxide	White	**Arsenolite** As_2O_3
Atacamite	Bright green, green, yellowish green, dark emerald-green to blackish green	$Cu_2Cl(OH)_3$
Azurite	Blue, azure-blue, light blue to very dark blue, Berlin-blue	$Cu_3(CO_3)_2(OH)_2$
Baryte (*Barium white, Barium sulphate*)	White, grey, yellowish white, bluish white, greyish white, brownish white, brown, reddish	$Ba(SO_4)$
Blixite	Light green, light yellow, yellow-orange, greyish yellow	$Pb_8O_5(OH)_2Cl_4$
Blue verditer	Blue, azure-blue, light blue to very dark blue	$2Cu(CO_3) + Cu(OH)_2$
Bone black	Black, dark grey	**Calcite**$Ca(CO_3)$ + **Apatite**$Ca_5(PO_4)_3(F,OH)$ + Carbon C
Bone white	White, light grey	**Calcite**$Ca(CO_3)$ + **Apatite** Ca5(PO4)3(F,OH)
Botallackite	Bluish green, green, light green	$Cu_2Cl(OH)_3$
Brochantite	Green, emerald-green, bluish green, light blue, blackish to light green	$Cu_4(SO_4)(OH)_6$
Brown ochre	Brown	**Goethite** FeO(OH) + *Clay (Mudstone)*
Cadmium yellow	Yellow	**Hawleyite** CdS or **Greenockite** CdS
Calcite/*Chalk*	White	$Ca(CO_3)$
Calcium oxalate	White	$Ca(C_2O_4)$
Caledonite	Blue, blue green, green to dark green, pale bluish green	$Cu_2Pb_5(SO_4)_3(CO_3)(OH)_6$
Calomel	White, yellowish grey, grey, brown, yellowish white	Hg_2Cl_2
Caput mortuum	Purple-red	**Hematite** Fe_2O_3
Carbon black	Black, dark grey	*Charcoal or sooth* C± *Potash* $K_2(CO_3)$
Cassiterite	Black, brown, brownish black, grey, colorless to white, green, reddish brown, red, yellow	SnO_2
Celadonite	Green, bluish green	$K(MgFe^{3+}Si_4O_{10}(OH)_2$
Ceruleum	Dark blue, bluish green, sky-blue, deep cyan	$Co(SnO_3)$
Cerussite	White, grey, blue	$Pb(CO_3)$
Challacolloite	Colourless to white	KPb_2Cl_5
Chrome green	Green	*Prussian blue* $Fe^{3+}{}_4[Fe^{2+}(CN)_6]_3$ + *Chrome yellow*
Chrome orange	Orange	$Pb_2(CrO_5)$
Chrome red	Red	$PbO + CrO_3$
Chrome yellow(Canary	Yellow	**Crocoite** ($PbCrO_4$)

[5] International Mineralogical Association, List of Minerals; http://cnmnc.main.jp/; accessed 31st of December 2020

chrome yellow, Chrome lemon, Leipzig yellow, Paris yellow, Lead chromate)		
Clinoatacamite	Green to dark greenish black	$Cu_2Cl(OH)_3$
Cobalt blue	Sky-blue, deep blue	$CoAl_2O_4$
Copper oxalate	Light bluish green, turquise-green, deep blue	$Cu(C_2O_4)$
Copper proteinate	Light bluish green, turquise-green	Cu + *Protein*
Copper resinate	Green	*Verdigris* + *Turpentine*
Coquimbite	Light violet, greenish white to light green, bluish white, yellowish white, brownish white to brownish yellow	$AlFe^{3+}{}_3(SO_4)_6(H_2O)_{12}\cdot 6H_2O$
Cotunnite	Colorless to white, light green, light yellow	$PbCl_2$
Crocoite(*Chrome yellow*)	Hyacinth-red, red, red-orange to orange, yellow	$Pb(CrO_4)$
Diopside	Blue, light blue, white, brown, yellow, light to dark green, grey, colorless, black	$CaMgSi_2O_6$
Dolomite	White, gray, pink, reddish to brownish white, colorless, yellow, brown	$CaMg(CO_3)_2$
Egyptian blue	Blue, azure-blue, blue-green	**Cuprorivaite** $CaCuSi_4O_{10}$
Emerald green (Schweinfurt green, Paris green)	Emerald-green, bluish green	$3Cu(AsO_2)_2 + Cu(CH_3COO)_2$
Galena	Light to dark grey, lead-grey, bluish black	PbS
Glauconite	Green, yellowish green	$K,Na)(Mg,Fe)(Al)Si_4O_{10}(OH)_2$
Goethite	Yellow, brown, reddish to yellowish brown, brownish yellow, blackish brown, ocher yellow	$Fe^{3+}O(OH)$
Green earth	Green, blue-green, yellowish green	**Glauconite**$K,Na)(Mg,Fe)(Al)Si_4O_{10}(OH)_2$ **Celadonite**$K(MgFe^{3+}Si_4O_{10}(OH)_2$
Gypsum	Colorless, white, yellowish white, greenish white, brown, yellow, blue, pink, reddish brown, grey, black	$Ca(SO_4)\cdot 2H_2O$
Han blue	Blue	$BaCuSi_4O_{10}$
Han purple	Purple, dark blue to indigo	$BaCuSi_2O_6$
Hematite	Reddish grey, black, blackish red, steel-grey, dull to bright red, rust-red	Fe_2O_3
Huntite	White, lemon-white	$CaMg_3(CO_3)_4$
Hydrocerussite	White, grey, colorless, greenish	$Pb_3(CO_3)_2(OH)_2$
Hydromagnesite	Colorless, white	$Mg_5(CO_3)_4(OH)_2\cdot 4H_2O$
Hemimorphite	Colorless, Reddish brown, brown, white, greenish gray, yellow-brown	$Zn_4(Si_2O_7)(OH)_2\cdot H_2O$
Ilmenite	Black, iron-black	$Fe^{2+}Ti^{4+}O_3$
Indian yellow (Purree, Snowshoe yellow, Peori, Piuri)	Vivid yellow, orange-yellow	Ca or Mg salts of euxanthic acid: *e.g.*, $MgC_{19}H_{16}O_{11}\cdot 5H_2O$
Iron gall ink	Purple-black, brown-black	Fe gallate (Fe salts + Gallotannic acid)
Iron-based ink	Purple-black, brown-black	Most likely *Iron gall ink*
Ivory black	Black	*Charcoal* C + Ca phosphate
Jarosite	Brown, amber-yellow to dark brown, yellow to light yellow, yellow-brown, reddish yellow	$KFe^{3+}{}_3(SO_4)_2(OH)_6$
Kaolinite	White, yellowish white, brownish white, greyish white, greyish green	$Al_2Si_2O_5(OH)_4$
K-feldspar	Colorless, greenish, yellowish, greyish yellow, white, pink, grey, pale yellow, flesh-red, green, yellowish white, reddish white, bluish green, green, greyish yellow	**Orthoclase**, **Sanidine**, **Microcline** $K(AlSi_3O_8)$
Langite	Blue-green, green-blue, sky-blue, deep blue, greenish blue	$Cu_4(SO_4)(OH)_6\cdot 2H_2O$
Lapislazuli (Ultramarine)	Deep blue, blue, purple	Mixture of minerals, mainly **Lazurite** $Na_3Ca(Si_3Al_3)O_{12}S$
Laurionite	Colorless, white	Pb(OH)Cl
Lavendulan	Bright blue, blue, lavender-blue, greenish blue, lavender	$NaCaCu_5(AsO_4)_4Cl\cdot 5H_2O$
Lazurite	Deep blue, blue, azure, azure-blue, violet-blue, greenish blue	$(Na_3Ca(Si_3Al_3)O_{12}S$
Lead-antimonate yellow (Naples yellow)	Yellow	**Oxyplumboroméite**$Pb_2Sb_2O_7$
Lead carboxylates	White	Pb palmitate/stearate
Leadhillite	Colorless to white, grey, yellowish-white, light green, blue	$Pb_4(SO_4)(CO_3)_2(OH)_2$
Lead sulfate	White, blue, light grey	**Anglesite**$Pb(SO_4)$

Lead white	White	**Hydrocerussite** $Pb_3(CO_3)_2(OH)_2$+ **Cerussite**$Pb(CO_3)$
Lead-magnesium carbonate	White	$PbMg(CO_3)_2$
Lead-tin yellow	Yellow	$PbSnO_4$
Lead-tin yellow type I	Yellow	Pb_2SnO_4
Lead-tin yellow type II	Yellow	$PbSn_{1-x}Si_xO_3$ where x = 0.25
Lead-tin-antimony yellow	Yellow	$Pb_2SnSbO_{6.5}$
Leucite	Colorless, grey to dark grey, yellow grey, white	$K(AlSi_2O_6)$
Lime *(Quicklime)*	Colorless, white	CaO
Litharge	Red, dark red	PbO
Lithopone	White	**Baryte** $BaSO_4$ + **Sphalerite** ZnS
Magnesite	White	$MgCO_3$
Magnetite	Black, grey	Fe_3O_4
Malachite	Bright green, dark green, blackish green	$Cu_2(CO_3)(OH)_2$
Massicot	Yellow, sulfur-yellow to orpiment-yellow, reddish to brownish yellow	PbO
Mimetite	Light to bright yellow, white, orange, yellow-orange, brown, red, colorless, yellowish brown	$Pb_5(AsO_4)_3Cl$
Minium	Red	Pb_3O_4
Montmorillonite	White, light pink, grey-white, yellow to brownish yellow, greenish yellow, red	$(Na,Ca)_{0.3}(Al,Mg)_2Si_4O_{10}(OH)_2 \cdot nH_2O$
Moolooite	Blue, green, turquise-green	$CuC_2O_4 \cdot H_2O$
Mosaic gold (Bronze powder)	Yellow, bronze-yellow	SnS_2
Na-feldspar	White to grey, greenish gray, bluish green, reddish	**Albite** $Na(AlSi_3O_8)$
Naples yellow (Antimony yellow, Lead-antimonate yellow)	Yellow	**(Oxyplumboroméite)** $Pb_2Sb_2O_7$
Natrojarosite	Bright yellow, yellow-brown, ochre-yellow, ochre-brown, golden brown, cinnamon-brown	$NaFe^{3+}_3(SO_4)_2(OH)_6$
Olivenite	Dark green, olive-green, yellowish brown, dirty white, blackish green, liver-brown, greenish brown, brown, greyish green, greyish white	$Cu_2(AsO_4)(OH)$
Orpiment	Deep orange, orange-yellow, lemon-yellow to brownish yellow	As_2S_3
Palmierite	Colorless, white	$K_2Pb(SO_4)_2$
Pararealgar	Bright yellow, orange, yellow-orange, orange-brown	As_4S_4
Paratacamite	Green to dark green, greenish black	$Cu_3(CuZn)Cl_2(OH)_6$
Plattnerite	Brownish black, iron black, dark grey, black	PbO_2
Phosgenite	Colorless, white, light yellow to light brown, yellowith brown, smoky violet, light rose, yellowish grey, light green	$Pb_2(CO_3)Cl_2$
Prussian blue (Berlin blue, Parisian blue,Paris blue)	Deep blue	$Fe^{3+}_4[Fe^{2+}(CN)_6]_3$
Quartz	Colourless, white, greyish, light pink	SiO_2
Realgar	Red, dark red, orange-red, orange-yellow, yellow-orange, reddish orange	AsS
Red lake	Red	K-Alum $KAl(SO_4)_2 \cdot 12H_2O$ + alkali (*e.g.*, lime, chalk, wood ash)
Red ochre	Red	**Hematite** Fe_2O_3 + *Clay*
Romarchite	Black	SnO
Scheele's green (Schloss green)	Yellowish green	Cu arsenites and arsenates
Schultenite	Colorless to white, light yellow	$Pb(AsO_3OH)$
Schweinfurt green (Emerald green)	Deep green	$3Cu(AsO_2)_2 + Cu(CH_3COO)_2$.
Scrutinyite	Translucent red-brown to less translucent clove-brown	α-PbO_2; PbO_2
Sienna ochre	Brownish yellow	**Goethite, Lepidocrocite** $Fe^{3+}O(OH)$ + **Pyrolusite** MnO_2
Smalt (Cobalt glass)	Deep blue	Co oxides or $Co(CO_3)$ + *Glass*SiO_2
Syngenite	Colorless to white, light yellow	$K_2Ca(SO_4)_2 \cdot H_2O$
Ultramarine (Lapislazuli)	Deep blue	**Lazurite** $Na_4Ca_4Al_6Si_6O_{24}S_2$
Umber	Brown, reddish brown	**Goethite, Lepidocrocite** $Fe^{3+}O(OH)$ + **Pyrolusite** MnO_2

Vanadinite	Brown, brownish yellow, brownish red, reddish yellow, colorless	$Pb_5(VO_4)_3Cl$
Verdigris	Bluish green, turquise-green	**Hoganite** $Cu(CH_3COO)_2 \cdot H_2O$ $\pm Cu(OH)_2 \cdot 5H_2O$
Vermillion	Brilliant red, scarlet, brown, brown-pink, lead-grey, grey	**Cinnabar** HgS
Viridian	Green with bluish hues	Hydrous chrome oxide
Vivianite	Blue, grey	$Fe^{2+}_3(PO_4)_2 \cdot 8H_2O$
Weddellite	Colorless, white, dirty white, yellowish brown to brown	$Ca(C_2O_4) \cdot 2H_2O$
Whewellite	Brownish, colorless, grey, yellow, yellow-brown, light yellow, light brown	$Ca(C_2O_4) \cdot H_2O$
Whitlockite	Colorless, grey, greyish white, yellowish white, white	$Ca_9(Mg,Fe^{2+})(PO_3OH)(PO_4)_6$
Yellow ochre (Gold ochre)	Yellow, brown	**Goethite** (+ **Lepidocrocite**) $Fe^{3+}O(OH)$ or **Goethite** $Fe^{3+}O(OH)$ + **Jarosite** $KFe^{3+}_3(SO_4)_2(OH)_6$
Zinc white	White	ZnO
	Organics	
*Brazilwood (*Red lake)	Red	Brazilin $C_{16}H_{14}O_5$
*Carmine lake (*Cochineal lake, *Red lake)	Deep red, carmine-red, bright strawberry-red, magenta-red, blackcurrant-purple	Salt of carminic acid $C_{22}H_{20}O_{13}$
*Cochineal (*Cochineal red lake)	Deep red, carmine-red, bright strawberry-red, magenta-red, blackcurrant-purple	Salt of carminic acid $C_{22}H_{20}O_{13}$
*Gamboge (*Wisteria yellow, *Gummi gatti, *Drop gum, *Camboge, *Cadie gum)	Deep saffron yellow, sunny-yellow, mustard-yellow, bright orange-yellow	Resin (Gambogic acid $C_{38}H_{44}O_8$) + Gum
*Indigo	Deep dark blue	Indigo $C_{16}H_{10}N_2O_2$
*Kermes lake (*Kermesic acid, *Kermesic red lake)	Red	Kermesic acid $C_{16}H_{10}O_8$(1-Methyl-2-carboxy-3,5,6,8-tetrahydroxyanthraquinone)
*Logwood (*Blackwood, *Bluewood, *Natural black)	Violet, grey, black	Haematoxylin + Haematin $C_{16}H_{14}O_6$ or $C_{16}H_{14}O_6 \cdot xH_2O$
*Madder lake (*Garanza lake)	Deep red, pink	Alizarin (1,2-duhydroxyanthraquinone) + Purpurin (1,2,4-trihydroxyanthraquinone)
*Plant black	Black	Charcoal C
*Porpora (Murex) = *Tyrian purple (*Royal purple, *Phoenician red, *Phoenician purple, *Imperial purple, *Imperial dye)	Deep red, purple, violetish red, violet	Organobromide (6,6′-dibromoindigo)
*Purpurine (*Purpurin)	Red, yellow	1,2,4-Trihydroxyanthraquinone
*Red lake	Red	Various organic compositions, *e.g.*, cochineal, kermesic acid, brazilin
*Red laquer	Red	Various organic compositions, *e.g.*, cochineal, kermesic acid, Brazilwood sap
*Sepia (*Cefalopod ink)	Brown, reddish brown	Melanin (or cephalopod ink, from the ink sac of the cuttlefish sepia)
*Shellac	Yellow, light yellow, brown to dark red, red, orange, orange-brown	Mono- and polyesters of e.g., aleuritic acid $C_{16}H_{32}O_5$; shellolic acid $C_{15}H_{20}O_6$; butolic acid; jalaricacid; laccijalaric acids
*Urushi (*Chinese lacquer)	Colorless	Natural resin with urushiol (catechol derivatives) as the main component
*Weld (*Yellow weed)	Yellow	Luteolin$C_{15}H_{10}O_6$ (3′,4′,5,7-Tetrahydroxyflavone)
*Woad (*Isatis tinctoria* L.)	Blue	Indigo$C_{16}H_{10}N_2O_2$
*Yellow lake	Yellow	Kaempferol $C_{15}H_{10}O_6$(3,4′,5,7-tetrahydroxyflavone)

References

Azouka A, Huggett R, Harrison A (1993) The production of shellac and its general and dental uses: a review. J Oral Rehabil 20(4):393–400. https://doi.org/10.1111/j.1365-2842.1993.tb01623.x

Baer NS, Indictor N, Joel A (1972) The chemistry and history of the pigment Indian yellow. Stud Conserv 17(sup1):401–408. https://doi.org/10.1179/sic.1972.17.s1.009

Kirby J, Spring M, Giggitt C (2005) The technology of red lake pigment manufacture: study of the dyestuff substrate. National Gallery Technical Bulletin 26:71–87

Kirby J, White R (1996) The identification of red lake pigment dyestuffs and a discussion of their use. National Gallery Technical Bulletin 17:56–80

López-Montalvo E, Roldán C, Badal E, Murcia-Mascarós S, Villaverde V (2017) Identification of plant cells in black pigments of prehistoric Spanish Levantine rock art by means of a multi-analytical approach. A new method for social identity materialization using chaîne opératoire. PLoS One 12(2):e0172225. https://doi.org/10.1371/journal.pone.0172225

Martin de Fonjaudran C, Acocella A, Accorsi G, Tamburini D, Verri G, Rava A, Whittaker S, Zerbetto F, Saunders D (2017) Optical and theoretical investigation of Indian yellow (euxanthic acid and euxanthone). Dyes Pigments 144:234–241. https://doi.org/10.1016/j.dyepig.2017.05.034

Ploeger R, Shugar A, Smith GD, Chen VJ (2019) Late 19th century accounts of Indian yellow: the analysis of samples from the Royal Botanic Gardens, Kew. Dyes Pigments 160:418–431. https://doi.org/10.1016/j.dyepig.2018.08.014

Ponting KG (1973) Logwood: an interesting dye. J Eur Econ Hist; Rome 2(1):109–119

Tamburini D, Dyer J, Bonaduce I (2017) The characterisation of shellac resin by flow injection and liquid chromatography coupled with electrospray ionisation and mass spectrometry. Sci Rep 7:e14784. https://doi.org/10.1038/s41598-017-14907-7

Tamburini D, Martin De Fonjaudran V, Verri G, Accorsi G, Acocella A, Zerbetto F, Rava A, Whittaker S, Saunders D, Cather S (2018) New insights into the composition of Indian yellow and its use in a Rajasthani wall painting. Microchem J 137:238–249. https://doi.org/10.1016/j.microc.2017.10.022